MOLECULE AND CATALYST DESIGN FOR RECOGNITION AND ACTIVATION OF SMALL MOLECULES

Luis Martinez Rodriguez

Luis Martínez Rodríguez

"Molecular and Catalyst Design for Recognition and Activation of Small Molecules"

Tesis Doctoral

Dirigida por el Prof. Dr. Arjan W. Kleij

Instituto Catalán de Investigación Química

UNIVERSITAT
ROVIRA I VIRGILI

Tarragona

2016

UNIVERSITAT ROVIRA I VIRGILI
MOLECULE AND CATALYST DESIGN FOR RECOGNITION AND ACTIVATION OF SMALL MOLECULES
Luis Martinez Rodriguez

Av. Països Catalanes 16

43007 Tarragona

Tel: +34977920847

E-mail: akleij@iciq.es

HAGO CONSTAR que este trabajo titulado: "Molecular and Catalyst Desing for Recognition and Activation of Small Molecules" que Luis Martínez Rodríguez presenta para la obtención de su título de Doctor, ha sido realizado bajo mi supervisión en el Instituto Catalán de Investigación Química.

Tarragona, 6 de Septiembre de 2016

El director de la tesis doctoral:

Prof. Dr. Arjan W. Kleij

"No, you can't always get what you want.

But if you try sometime you find,

you get what you need"

Sir Michael Philip Jagger

Table of Contents

Chapter IV: Stereoselective Formation of (*Z*)-1,4-but-2-ene Diols using Water as a Nucleophile

List of Relevant Compounds

Conclusions

Acknowledgements

Curriculum Vitae

List of Publications

UNIVERSITAT ROVIRA I VIRGILI
MOLECULE AND CATALYST DESIGN FOR RECOGNITION AND ACTIVATION OF SMALL MOLECULES
Luis Martinez Rodriguez

General Introduction

Chapter I

General Introduction

As a consequence of the increased consumption of fossil fuels and natural resources being limited, new catalytic methods based on general, abundant and renewable feedstocks are needed. Small molecules, such as N_2, O_2, CO_2 and H_2O are naturally present in the atmosphere and oceans and more importantly they are emitted as industrial wastes on a massive scale, which makes their accessibility unlimited. These molecules can be transformed to or coupled with simple substrates to construct more complex compounds.

Chapter I
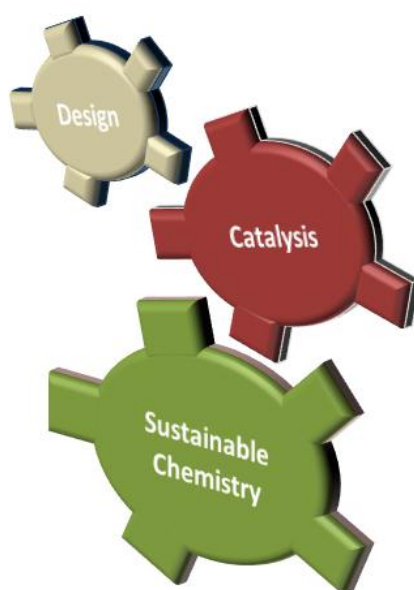
1.1 Small molecule activation

Catalytic methodologies are crucial in the industrial production of valuable chemicals such as fuels, synthetic materials and drugs.[1] Precious metal complexes have been widely studied as powerful catalysts in diverse transformations improving features such as the overall yield, kinetic profile and selectivity for a specific target molecule.[2] By definition, a catalyst increases the rate of a chemical reaction without being consumed during the reaction process.[3] According to this, the catalyst moiety provides a more favoured kinetic pathway in the reaction profile (**Figure 1.1**), without influencing the thermodynamics of the process (ΔG, Gibbs free energy).
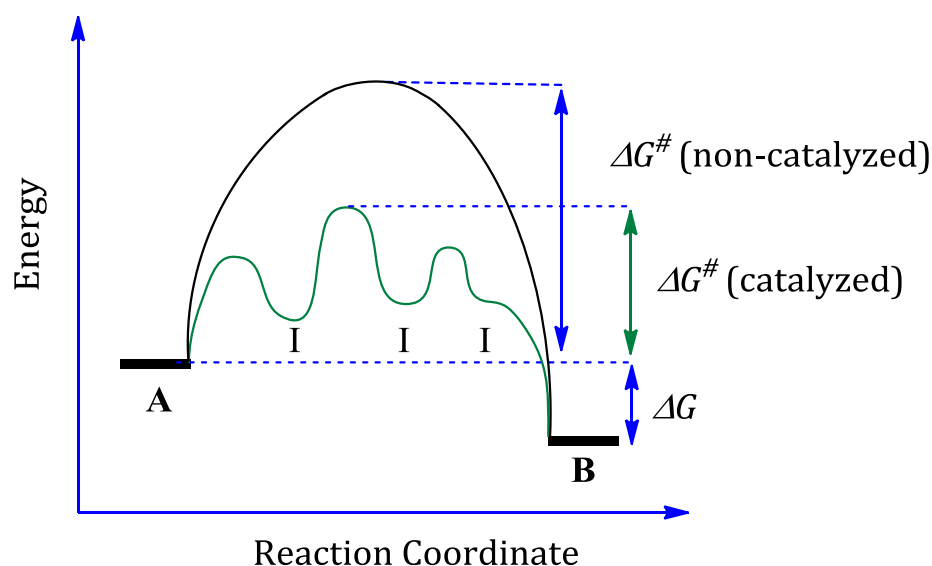
Figure 1.1: Standard reaction profile plot with and without catalyst.

As can be seen in the previous plot, the overall free energy of the process (ΔG) is independent of the presence or absence of catalyst. The energy of the product of the reaction **B** is lower than the starting material **A**, which means that the transformation is exergonic and therefore thermodynamically favoured ($\Delta G < 0$). The free activation energy ($\Delta G^{\ddagger}$) in a particular process is described as the gap between the energy of the reactants in the ground state and the energy of the less stable transition state involved during the reaction. The concerned catalytic system follows a different pathway, lowering the activation energy of the chemical

2

transformation, through the formation of different intermediates **I** until the desired product is formed.

All the species involved in the reaction (starting materials, catalyst, product and the different intermediates) are illustrated in a *catalytic cycle*, and the investigation of the different intermediates facilitates the understanding of the overall process (**Scheme 1.1**). The initial step involves binding of one or more reactants to the active catalyst, forming intermediate species which are lower in energy than the $\Delta G^{\#}$ of the non-catalyzed process. The reaction will evolve towards the formation of the final product and regenerates the catalytic species, thereby closing the *catalytic cycle*. The efficiency of the process is determined by the maximum number of cycles that the catalyst can perform without suffering degradation (TON).[4] To quantify the efficiency in terms of time, the value of the turnover frequency (TOF) is used, which is easily derived from the turnover number during a certain period of time, generally expressed in seconds, minutes or hours.

$$TON = \frac{amount\ product}{catalyst\ loading}$$

$$TOF = \frac{TON}{seconds}$$
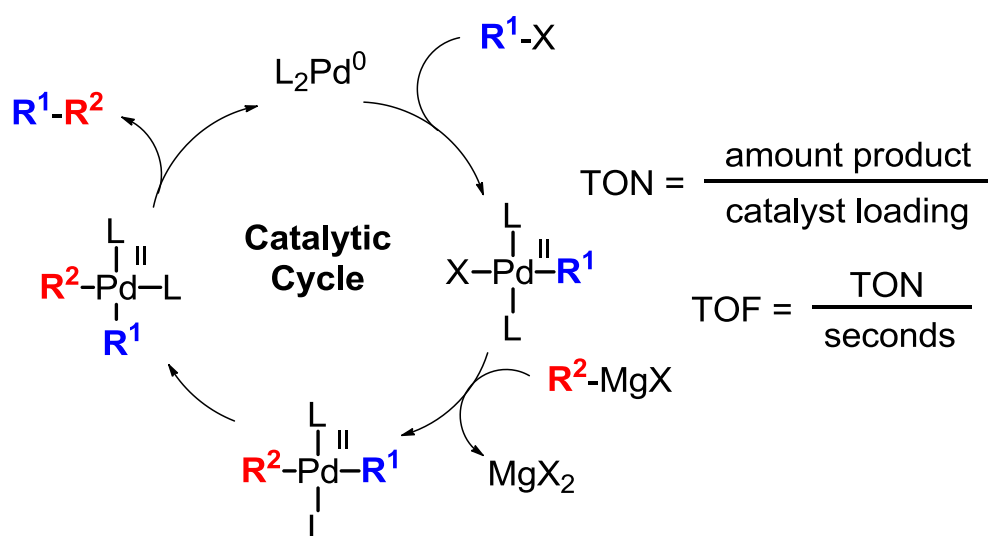
Scheme 1.1: The catalytic cycle for a cross-coupling reaction (left) with TON and TOF equations (right).

The development of new catalysts is of crucial importance in different fields of chemistry.[5] In the search for new and active catalysts, it is necessary to take into account some guidelines: the catalyst must be relative easy to synthesize in terms of time/cost efficiency; the toxicity should be considered especially in areas such

Chapter I

as pharmaceutical drug development and medicinal applications. As highlighted before, high TON/TOF values are also important in order to improve the efficiency, the sustainability and minimize the catalyst loading.[6] Finally, it would be desirable that the catalyst has good air and moisture stability and robustness.

Transition metal complexes are often used as catalysts due to their intrinsic diversity regarding their oxidation state, geometry and coordination number.[7] These features can be readily modulated depending on the nature of the ligands coordinated to the metal; as consequence a proper selection of the appropriate ligand plays an important factor during catalyst screening. Transition metal catalysis has witnessed continuous success in the activation/functionalization of challenging C–X, C–H and other rather unactivated bonds,[8-9] thereby evolving organic synthetic chemistry to a high level of sophistication maximising aspects such as chemo- and stereo-selectivity, and reducing the formation of by-products and number of steps for the targeted molecule. Within catalysis research, small molecule activation has received less attention although it has an important impact on the environment and biosphere.[10-11] Waste gases, such as CO_x or NO_x are generated on a large scale in industrial processes and released into the atmosphere (**Figure 1.2**). Most of these waste molecules are responsible for global warming and associated with negative implications of the greenhouse effect, in particular CO_2 and N_2O. From a sustainable point of view, however, their abundance render these small molecules inexpensive and interesting syntons to construct more complex molecules forming new C–C, C–O or C–X bonds.[12]

On the other hand, simple small molecules including O_2, H_2 or methane are reservoirs of chemical energy,[13-15] which can be used as fuel like nature does in biological systems,[16] or can be incorporated as a building block in order to prepare a certain compound.

UNIVERSITAT ROVIRA I VIRGILI
MOLECULE AND CATALYST DESIGN FOR RECOGNITION AND ACTIVATION OF SMALL MOLECULES
Luis Martinez Rodriguez

General Introduction

Million Tons Emitted
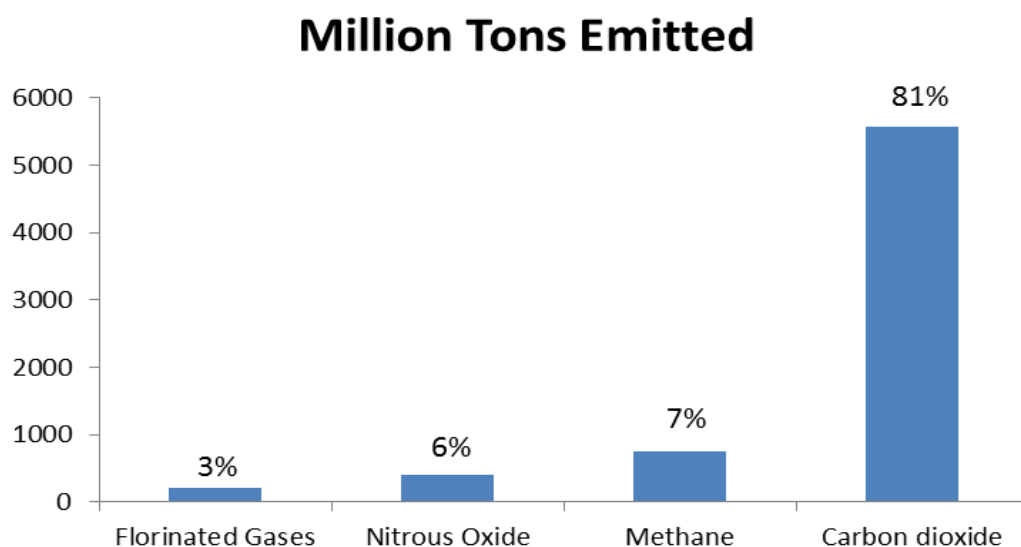
Figure 1.2: Tons of greenhouse effect gases emitted in 2014.

Dioxygen (O_2), in combination with organic matter, generally results in the combustion of the organic framework at high temperature; but O_2 can also be used to oxidize in a chemoselective manner C=C or C–H bonds. Molecular oxygen is among the greenest oxidants for redox reactions at the laboratory scale,[17] due to its abundance and because water is the only by-product.[18] One of the most powerful ways to activate O_2 is the use of metal complexes which can then mediate oxidative chemical transformations. The aerobic oxidation of abundant metal complexes such as Cu,[19-20] Co,[21] or Fe[22] has been widely studied and presents high added value for pharmaceutical and agrochemistry.[23]

Waste gases like CO_x or NO_x incorporate high electron density containing multiple bonds between different heteroatoms, dipolar moments and may give access to different coordination modes upon interacting with a metal.[7] For example, the carbon dioxide molecule presents linear symmetry to minimize the electronic repulsion. In the presence of suitable metal complexes, coordination changes the electronic environment of the carbon dioxide molecule, elongating or contracting the length of the C–O bond and also reducing the O–C–O angle[24-25] activating it for further chemistry with other substrates.

Metal and metal-free Lewis acids can also be used to activate small organic molecules such as epoxides, alcohols, carbonyl compounds among others thus representing an important approach to carry out their conversion within synthetic

methodology.[26-27] These organic molecules are typically quite stable and higher temperatures are required to overcome the activation energy barrier connected to their conversion. Catalysts with powerful Lewis acid or basic sites are used to improve the kinetics of the reaction. Metal-free Lewis acids including DCC (*N,N'*-dicyclohexylcarbodiimide) and DIC (*N,N'*-diisopropylcarbodiimide) are commonly used to catalyse the synthesis of peptides. To synthetize biologically relevant amino acids, amines and carboxylic acids are required as starting materials.[28] The amine group has an intrinsic basic character to perform a nucleophilic attack on the carboxylic acid forming the desired amino acid. Some amines, however, are more electron-deficient to perform the nucleophilic attack and thus the kinetics in these cases are disfavoured. The use of activating agents, such as DCC, favours the overall process by increasing the electrophilicity of the carboxylic acid and turning it into derivatives with a better leaving group.[29] Metal-based Lewis acids can coordinate donor atoms of small molecules, hence activating them and reducing temperature requirement for their conversion.[30] The electron-donating character of O- and N-atoms present in these small molecules have intrinsic Lewis base behaviour. In the specific case of epoxides, an elongation of the carbon-oxygen bond occurs after coordination to an electrophilic metal center, which makes the carbon atom in the α-position more electrophilic favouring the nucleophilic attack (**Scheme 1.2**).
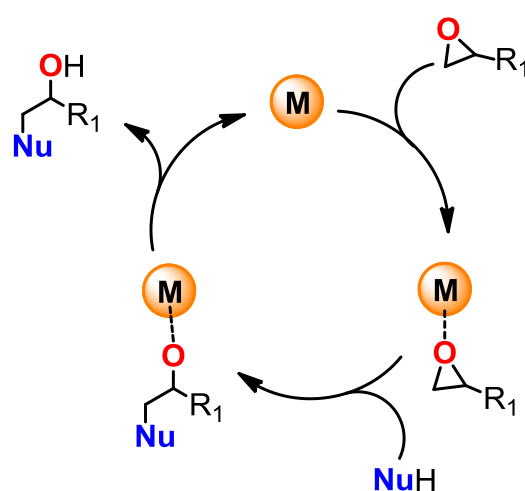
Scheme 1.2: Metal catalyzed nucleophilic ring-opening of epoxides.

UNIVERSITAT ROVIRA I VIRGILI
MOLECULE AND CATALYST DESIGN FOR RECOGNITION AND ACTIVATION OF SMALL MOLECULES
Luis Martinez Rodriguez

General Introduction

1.2 CO_2 valorisation

In other to secure a sustainable future for next generations, our society must put an effort into the rational use of our natural sources. The anthropogenic pollution has been increasing yearly since the first industrial revolution. Around 99% of carbon dioxide emissions are coming from to the use of carbon-based fossil fuels. Although there is no clear evidence for this relationship, the increase of the CO_2 concentration in the atmosphere is likely related to the rise in global energy consumption due an increasing world population (**Figure 1.3**).[31] Carbon dioxide is considered as one of the major contributors to climate change that may be responsible for the extreme weather conditions that are regularly noticed including heat waves, severe floods and hurricanes.
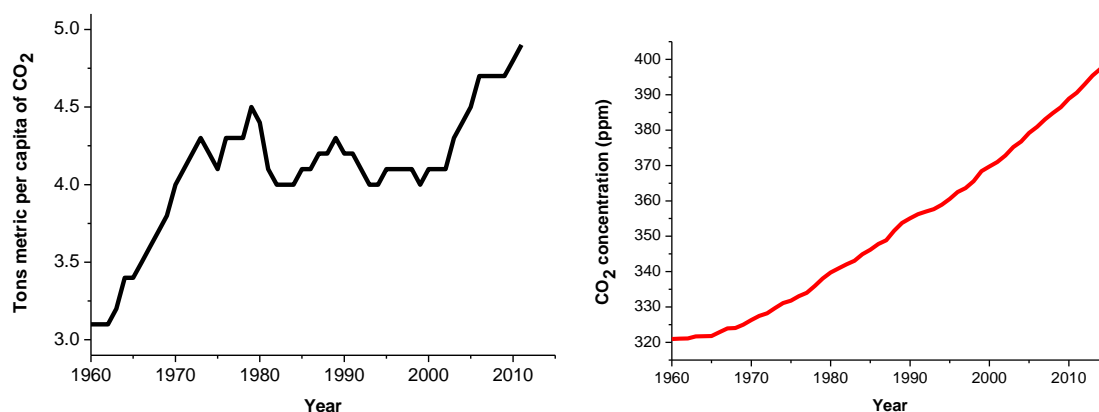
Figure 1.3: Evolution of the CO_2 emission per individual (left) and evolution of the CO_2 concentration in the atmosphere (right).

To keep the CO_2 emission level under control, changes are required regarding our energy demands, reducing our dependence on fossil fuels and finding industrially and synthetically viable processes for CO_2 valorization.[32] Industrial processes such as ammonia production and fermentation generate reasonably pure carbon dioxide at low cost, and can thus be used as feedstock for chemical transformations. However, a mayor part of these CO_2 emissions are generated by power stations, which contain only 14% of CO_2. Its separation from N_2 and especially from SO_x and NO_x is still not very efficient and increases the overall cost of CO_2 production.

Chapter I

Since the first oil crisis, the recycling of CO_2 has become of an ever increasing importance, and some technologies have exploited the use of CO_2 as a raw material at an industrial level such as in the formation of urea (almost 90% of the *recycled* CO_2 is used in this process),[33] salicylic acid,[34] inorganic carbonates[35] and fuels production.[36]

From the molecular point of view, CO_2 is a 16-electron, linear and centrosymmetrical molecule in the ground state. This makes the molecule overall nonpolar, containing two equal polar C=O bonds with opposite dipole directions. Consequently, the symmetrical stretching mode is inactive in the IR spectrum and only the antisymmetric stretching band is observable around 2349 cm^{-1}. This band has a high intensity and is useful for the quantification of the amount of carbon dioxide in the atmosphere.[37] CO_2 is an inert molecule due to its high thermodynamic and kinetic stability with the carbon center in the highest possible oxidation state (+IV) and any transformation will thus require energy. A very promising approach towards reducing the activation energy is the use of transition metal catalysis. The carbon atom (LUMO orbitals) has a Lewis acid character and can be described as an electrophilic center, whereas the oxygen atoms (HOMO orbitals) have poor Lewis base character. As a consequence, carbon dioxide acts predominantly as an electrophile and forms adducts with electron-rich species upon which it transforms from a linear to a more bend structure with an O–C–O angle close to 133º to minimize electron repulsion effects. As a ligand, carbon dioxide principally interacts with electron-rich metal centers through η^1–C coordination especially.[24] Recently, different other coordination modes such as η^1–O (preferred with electron-poor metals) and η^2–C,O chelation have also been demonstrated to be able to activate carbon dioxide.[25] These diverse coordinates modes change the electronic distribution of the CO_2 molecule and the resulting deviations in the molecular angles could be conveniently studied, differentiated and tabulated using IR spectroscopy. All these coordination modes have been confirmed by experimental and theoretical studies, but there are only a few isolated examples of metal complexes binding a CO_2 molecule.[38]

UNIVERSITAT ROVIRA I VIRGILI
MOLECULE AND CATALYST DESIGN FOR RECOGNITION AND ACTIVATION OF SMALL MOLECULES
Luis Martinez Rodriguez

General Introduction
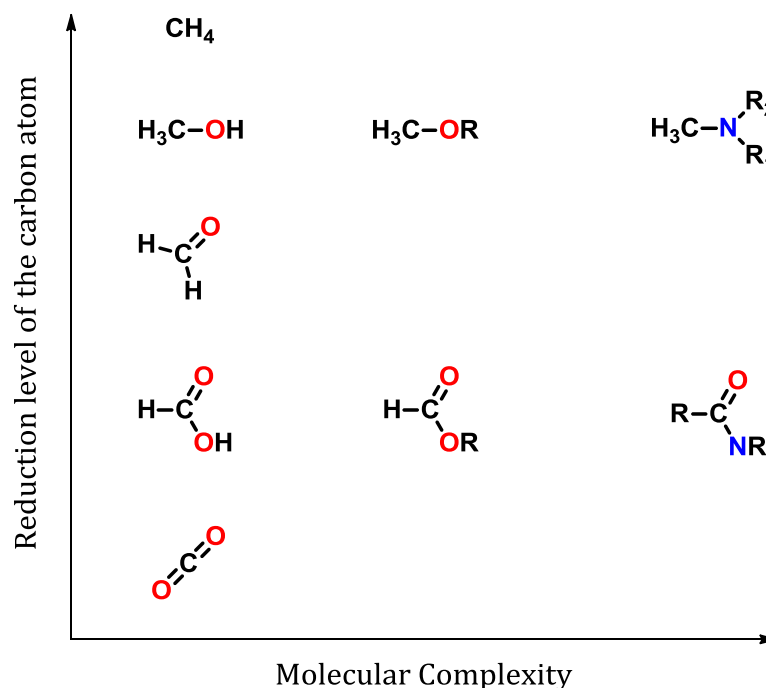
Figure 1.4: CO_2 derived small molecules obtained by reduction.

Once the carbon dioxide molecule is activated, two main different types of chemical transformations can be carried out: a CO_2 insertion reaction (keeping the carbon in the highest oxidation state, *i.e.* +IV) or a chemical reduction of CO_2 that lowers the oxidation state.[39] The reduction reaction has attracted interest from the scientific community since nature can obtain organic matter from carbon dioxide through photosynthesis. Hydrocarbons can also be obtained from CO_2 via this reduction method increasing thereby the H/C ratio compared to the highest oxidation state. In order to achieve this, a hydrogen source is required and the most commonly used one is molecular hydrogen (H_2). The complete hydrogenation of carbon dioxide to obtain methane is known as the Sabatier process and is currently one of the largest challenges in molecular science. This process requires huge amounts of energy (heat, electrochemical or radiation) and harsh pressure conditions. In order to increase the efficiency and sustainability of this process, different studies have been done focusing on the different intermediates that can be obtained from CO_2 while reducing stepwise the formal oxidation state of the carbon center and producing compounds such as formic acid, formaldehyde, methanol and methane (**Figure 1.4**).[40]

Chapter I
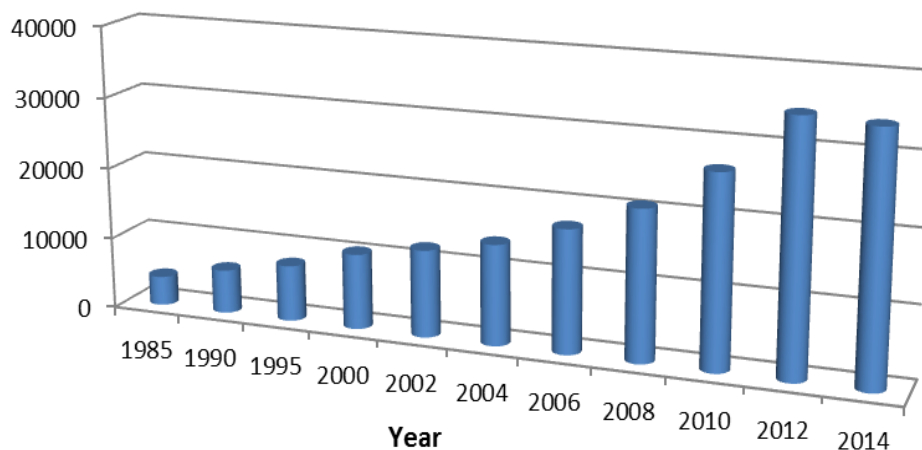
Figure 1.5: Number of peer-reviewed papers published annually concerning CO_2 valorisation.

On the other hand, different transformations can be performed while keeping the carbon atom in the highest oxidation state. The discovery of new methods and protocols to convert carbon dioxide as a chemical feedstock into useful molecules has become a dynamic topic in chemical science, and as a consequence the amount of publications related with CO_2 valorisation has greatly increased over the last decades (**Figure 1.5**). The preparation of valuable building blocks for organic synthesis such as lactones,[41-42] carbamates,[43] nonsymmetric ureas,[44] isocyanates,[45] polyurethanes,[46] polycarbonates[47] and organic carbonates[48] from CO_2 has been studied and can be easily obtained under relatively mild conditions (**Scheme 1.3**).
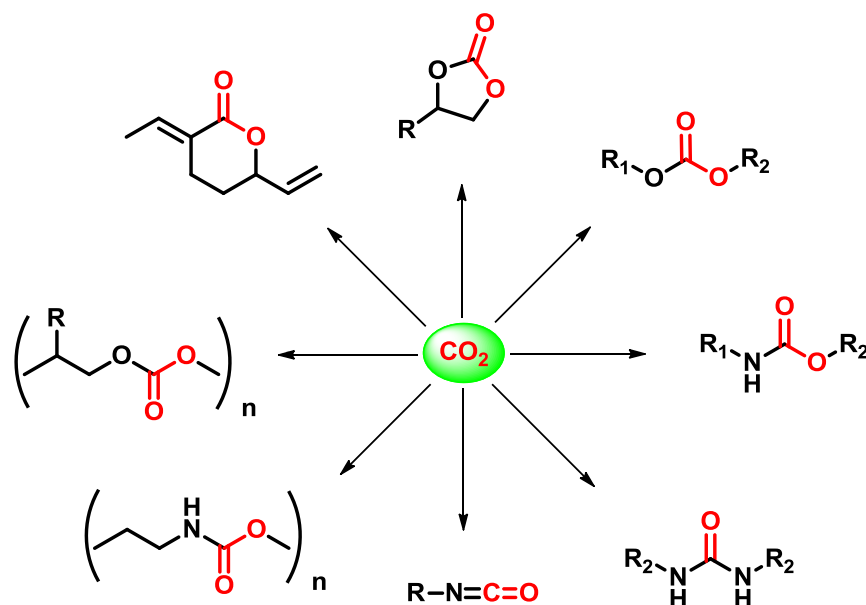
Scheme 1.3: Organic structures that can be obtained by CO_2 conversion processes.

10

UNIVERSITAT ROVIRA I VIRGILI
MOLECULE AND CATALYST DESIGN FOR RECOGNITION AND ACTIVATION OF SMALL MOLECULES
Luis Martinez Rodriguez

General Introduction

The formation of bio-renewable $\gamma-$ and $\delta-$lactones from conjugated dienes and CO_2 can be mediated by palladium catalysis. Starting from a Pd(0) precursor, the first step involves coordination of butadiene to the metal center after which a dimerization process occurs. A bidentate ligand, with weak Pd–N interaction, is required to promote CO_2 insertion forming a Pd–allyl intermediate, that after reductive elimination leads to the formation of the final lactone.[42]

The synthesis of polymers (polyurethanes and polycarbonates) from oxiranes, azetidines or aziridines in combination with CO_2 is a sustainable alternative to the use of toxic phosgene (and its derivatives) at an industrial level.[49] Polyurethane synthesis is of high importance due to wide application potential as thermo-insulators in the construction sector, and as adhesives and foams in many consumer products. On the other hand, polycarbonates are presented as an environmentally friendly alternative for thermoplastic polymers based on bisphenol-A (BPA), which are obtained from fossil fuel derivatives. The polycarbonates based on natural terpenes have received more attention due to their natural abundance (they can be obtained from the peel of fruits) and their high glass transitions (T_g values).[46,50-51] Carbamates are important building blocks in organic synthesis and can be easily obtained from alcohols, amines and CO_2.[52-53] Very recently, the group of Kleij developed a method to obtain multifunctionalized carbamates, controlling the regioselectivity using a Brøndsted base catalyst. Starting from cyclic carbonates and amines, the regio-controlled aminolysis process could be attained by proton-relay transfer using TBD as an organocatalyst.[54]

1.3 Supramolecular chemistry

Nature can be considered as a source of inspiration for synthetic systems that can mimic chemical events that are based on noncovalent interactions between molecules, thereby devising new applications and improved understanding of supramolecular processes and systems. Enzymes belong to a class of compounds that showcase that aggregated, structurally complicated

Chapter I

molecules can act as highly effective biocatalysts that control all the metabolic processes and transformations occurring inside any living organism.[55] This control involves a catalytic effect, *i.e.* accelerating or inhibiting a chemical conversion, and requires a highly specific recognition of a particular substrate which will be converted into the desired target molecule.[56] This specificity is achieved by the presence of so-called binding pockets (the active site) within the enzyme structure that are characterized by complementary shape, charge and using attractive forces optimizing the binding of the substrate. Enzymes are able to distinguish between rather similar substrate molecules in a chemoselective, regioselective and stereospecific manner.[57] The function of the active site is not only substrate recognition, but also mediating the chemical conversion in a (chemo)selective way by lowering the activation energy ($\Delta G^{\ddagger}$). The latter can be achieved in different ways:[58] (a) providing an alternative reaction environment more effective for the catalytic event, (b) destabilizing the substrate ground state, or (c) stabilizing the transition state. The latter stabilization is due to specific interactions between the enzyme and the substrate or, in terms of supramolecular chemistry, between "host" and "guest" molecules.[59] Ribosomes, as an example of enzymes, are responsible for catalyzing important transformations *in vivo*,[60] such as RNA cleavage.[61] The nature of the interactions between a ribozyme and RNA are also important to fully understand the process of self-assembly in a enzymatic complex and to try to effectively reproduce such a process *in vitro*[62] with "artificial enzymes".[63]

Pauling first introduced the theory of enzyme catalysis, where the active site redistributes and stabilizes the electron density around the substrate leading to a lower energetic level of the transition state.[64] More recently, Houk tried to quantify the binding forces between enzymes and substrates by investigating the affinities in artificial host-guest systems in order to extrapolate to *in vivo* systems. The observations done suggest that the sole stabilization of the transition state is not sufficient to explain the high activity of the enzyme, and therefore another features must play an imperative role in the entire process.[65]

Supramolecular chemistry focuses on the study of macromolecular structures (molecular containers, micelles, membranes among others) formed by association of different (smaller) molecular units connected by non-covalent inter-

UNIVERSITAT ROVIRA I VIRGILI
MOLECULE AND CATALYST DESIGN FOR RECOGNITION AND ACTIVATION OF SMALL MOLECULES
Luis Martinez Rodriguez

General Introduction

and intramolecular bonds. Therefore, this domain of chemical research can be considered a bridge between classical chemistry and biologic processes.[66] The involved non-covalent bonding between different molecules or fragments of molecules are typically weak and thus reversible being the essence of supramolecular systems (**Figure 1.6**). Different types of supramolecular interactions can be used to build up macrostructures and the most relevant ones include hydrogen bonding, coordinative interactions between donor ligands and electrophilic metal centers, hydrophobic/hydrophilic interactions, complementary ionic bonding and Van der Waals forces. Due to the liability of these weak interactions, the self-assembly process is reversible and is considered to be dynamic chemistry.[67]
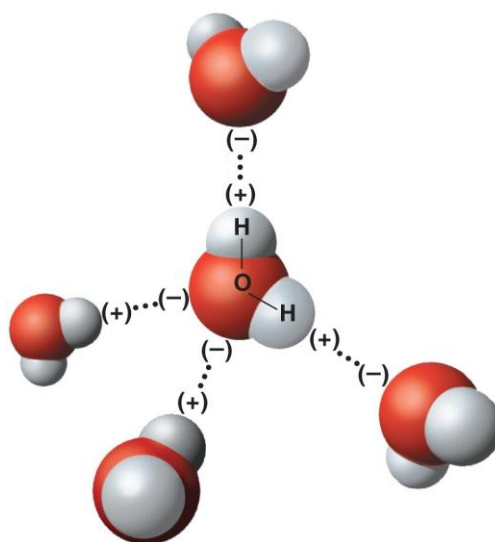
Figure 1.6: Hydrogen bonding interactions between water molecules.

This dynamic feature of any given supramolecular system gives it the capacity to adapt its overall architecture in the presence of appropriate template molecules, which may also involve substrates in catalytic processes. Different small molecules can be used as templates, but metal ions are often used a classical template as a result of their versatility in the available coordination numbers (typically between 3 and 6) and geometrical modes (tetrahedral, square planar, trigonal bipyramidal and octahedral).[7] These templating units can induce a particular rigid orientation and thus controlling and fixing the overall shape of the aggregated structure. One relevant of this templating behaviour was observed in

Chapter I

the case of the calix[4]arene molecule, which in solution is present in two different orientations in dynamic equilibrium, a feature that can be easily recognized by ^{1}H NMR spectroscopy. In the presence of a suitable metal ion, the conformation is fixed (most commonly in the "cone" conformation) since the metal induces and stabilizes a preferred geometry. (**Figure 1.7**).[68]
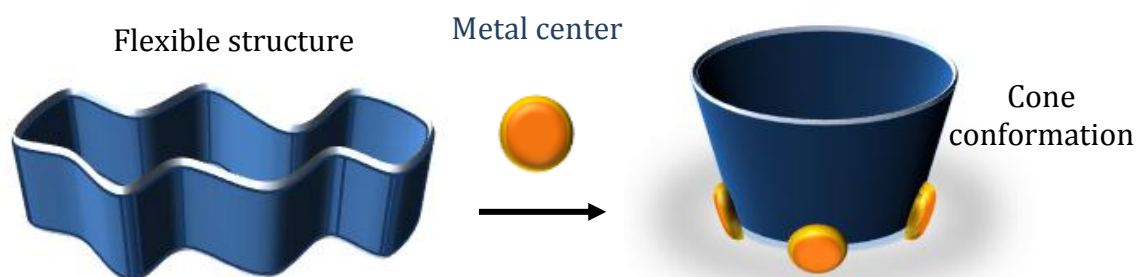
Figure 1.7: Schematic view of a self-assembly process induced by a metal template.

In supramolecular chemistry, molecular host structures which have an *inner cavity* are named molecular containers, cavitands, capsules, molecular vessels or cages. This family of macromolecules have been employed ever since Cram described the first examples of molecular containers based on covalent carcerands (**Figure 1.8**) which can encapsulate solvent molecules in their interior in a non-reversible way.[69-70] Over the last decades, this field (especially using hydrogen and coordinative bonds) has matured significantly resulting in the development of different structures with nanometer-sized cavities.[71] The inner cavity of these containers has a predefined *active site* where a guest molecule can be accommodated thereby playing different potential roles in the host-guest system:[72-73] (a) activating the substrate due to high affinity between the host and the guest, (b) accelerating the rate of the reaction by increasing the concentration of the substrate (*cf.*, effective molarity),[74] or (c) presenting unusual (stereo)selectivity due to a pre-organized orientation in the host-guest system.

14

UNIVERSITAT ROVIRA I VIRGILI
MOLECULE AND CATALYST DESIGN FOR RECOGNITION AND ACTIVATION OF SMALL MOLECULES
Luis Martinez Rodriguez

General Introduction
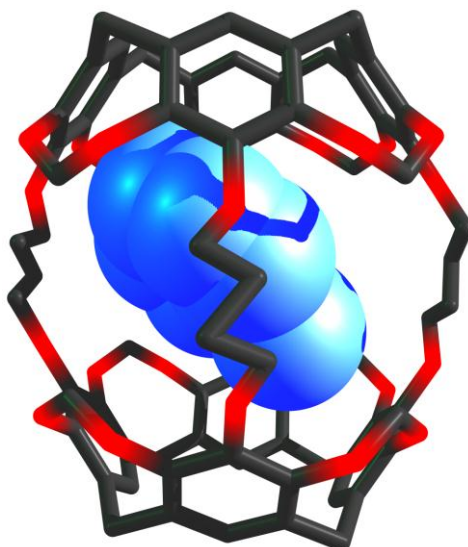
Figure 1.8: A carcerand scaffold encapsulates solvent molecules.

By proper designing and using appropriate building blocks, a great variety of geometrical molecular containers can be obtained such as cubes, pyramides and prisms.[71] As was explained before, the metal centers play a templating role to define the geometry of the cage. Metals ions like Pd(II) and Pt(II) show a strong preference for square-planar coordination geometries which in combination with suitable tritopic amines [1, 3, 5-tris(4-pyridil)triazines] leads to the formation of molecular containers with a closed octahedral capsular structure (**Figure 1.9**). The palladium ions located in the corners of the panel present a 90º *cis* geometry and the tridentate ligand occupies alternate faces of the octahedron providing a large inner cavity.[75-76] The ionic character of the cage (charge +12) increases its solubility in water and the hydrophilic nature of the cavity could potentially be used to incorporate or transport small organic molecules across an aqueous media.
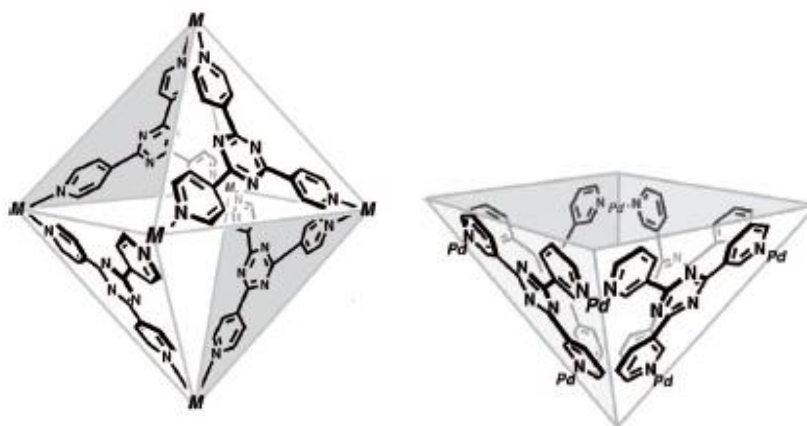
Figure 1.9: Metal-template mediated capsule formation.

Chapter I

In order to obtain metal-free containers, an alternative for metal-templation is to use hydrogen bonds to interconnect different panels of the cage. Rebek and co-workers introduced a bowl-shaped type capsule based on two resorcinarene units with aromatic panels in the *upper rim*, which are interconnected through hydrogen bonding to obtain a cylindrical capsule with an inner space of around 400 Å (**Figure 1.10**).[77] As the presence of heavy (toxic) metals renders capsular systems less attractive from a biological point of view, the formation of organic capsules with a deep cavity and combining water solubility now brings the opportunity of developing new drug delivery systems. The active drug molecule can be included inside the capsule to avoid undesired secondary effects and being transported through living systems and released in a time- and regio-controlled manner. This concept is called "Troyan horse" and is already in use against fighting cancer cells.[78]
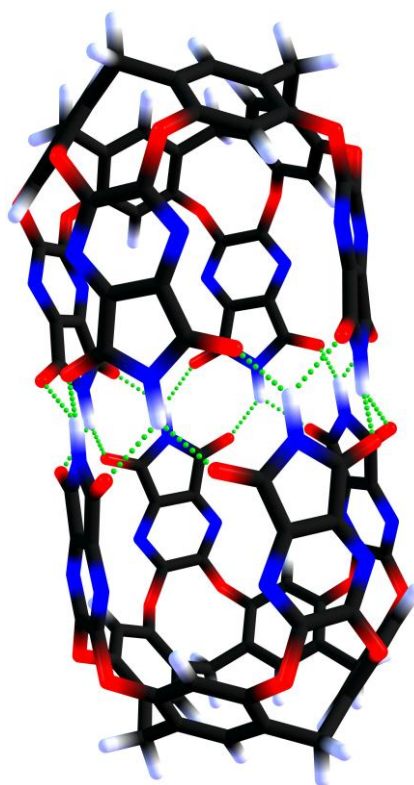
Figure 1.10: Cylindrical capsule reported by Rebek formed *via* multiple hydrogen bonding.

Calix[n]arenes are the most studied bowl-shaped molecules and especially the smaller members of the series (n = 4 and 5) have received a great deal of attention.[79] The classical methodology for their preparation is an acid-catalyzed

UNIVERSITAT ROVIRA I VIRGILI
MOLECULE AND CATALYST DESIGN FOR RECOGNITION AND ACTIVATION OF SMALL MOLECULES
Luis Martinez Rodriguez

General Introduction

condensation of aldehydes (generally folmaldehyde) in the presence of a phenol at high temperature. The reaction starts with an electrophilic aromatic substitution (EAS) followed by elimination of a water molecule and then a second substitution occurs (**Scheme 1.4**). The phenolic groups present in the walls of the macrocycle are joined by a methylene bridge to form the cavitand structure. These calixarenes are symmetrical molecules with some conformational restrictions (especially in the case of calix[4]arenes), and their preferred orientation can be defined as a conical structure, which is commonly described as the "cone" conformation. This predominant orientation is due to hydrogen bonding interactions between hydroxy groups present in the lower rim. The upper rim has *tert*-butyl groups that can be easily removed in order to functionalize and build up a more complex macrocycle.[80] From an application point of view, cavitands scaffolds can be used in different fields of chemistry including molecular recognition,[81] artificial molecular machines[73] and substrate transport.[82-83] Due to the high level of preorganization and potential to study and induce cooperative effects between the cavitand fragments, the calix[4]arenes moieties have been used as ligands in organometallic chemistry to create highly active catalysts,[84] the design of new sensors and in enantioselective synthesis.[85]
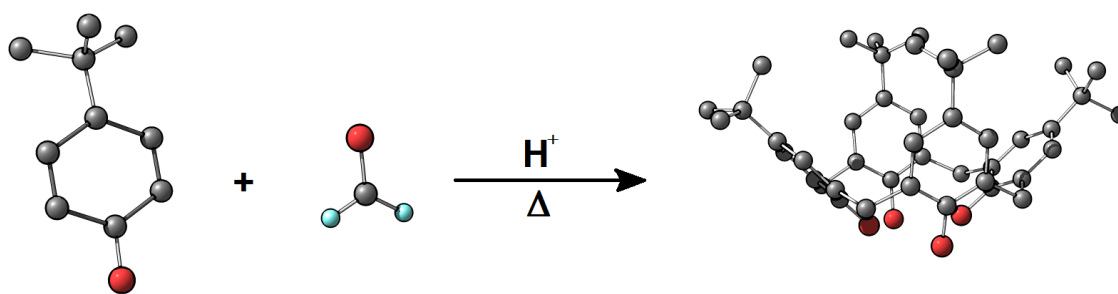
Scheme 1.4: Acid catalyzed the calix[4]arene formation.

In literature the term "cavitand" is used to refer to all kinds of macrocycles which present an inner cavity such as crown-ethers, cyclodextrins, calixarenes, calixpyrrols and resorcinarenes.[86-88] However, according to the original definition of the term cavitand, it refers specifically to compounds which incorporate an enforced cavity; therefore resorcinarenes and calixarenes motifs can be truly considered as cavitands after upper rim functionalization.[89] The upper and lower rims are localized in the peripheral parts of these macrocycles. These parts of the

Chapter I

cavitand can be easily modified maintaining the required inner cavity intact for guest recognition and/or binding. By modifying the upper rim, different functional groups can be included to increase the binding of a potential guest or improve the solubility of the capsule by installing polar/apolar groups.[81] The affinity constant between the host and the guest can be improved by maximizing the complementary of the cavitand in terms of size and shape of the cavity, the electron density and the steric requirements.

1.4 Molecular recognition

Molecular recognition was originally described by the *"lock and key"* model developed by Fischer and described the high selectivity of enzymes for one specific substrate (**Figure 1.11**).[90] In order to mimic enzyme selectivity, a number of artificial sensors have been developed, the first example was presented by Pedersen at the end of the 1960s reporting a family of cryptands that are able to selectively recognize metal cations.[91]
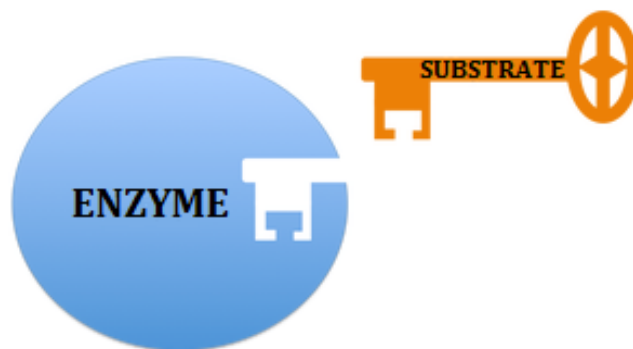
Figure 1.11: The *"lock and key"* model introduced by Fischer.

Cryptands are molecular entities comprising of a cyclic or polycyclic assembly of binding domains that contain three or more binding sites held together by covalent bonds. Overall, this gives rise to a molecular cavity able to bind another molecular entity more strongly compared to individual components. The oxygen atoms of the crown-ethers can encapsulate various metal cations (Li^+, Ca^{+2}, transition metals "TM^{n+}") and even nonmetallic cations such as present in quaternary ammonium salts inside the cavity whereas the counter anion stays

UNIVERSITAT ROVIRA I VIRGILI
MOLECULE AND CATALYST DESIGN FOR RECOGNITION AND ACTIVATION OF SMALL MOLECULES
Luis Martinez Rodriguez

General Introduction

outside of the macrocyclic assembly (**Figure 1.12**). On the other hand, anion recognition has received far less attention despite the fact that biological molecules such us DNA and certain enzymes (*e.g.* carboxypeptidase A)[92] are polyanions.[93-94] The design of the anion receptor must thus be done taking into account the intrinsic nature of the negatively charged molecules: the size of the anions is generally larger than of the cations meaning that they have a lower charge-to-radius ratio, which results in a poorer electrostatic interaction with the receptor.[95]
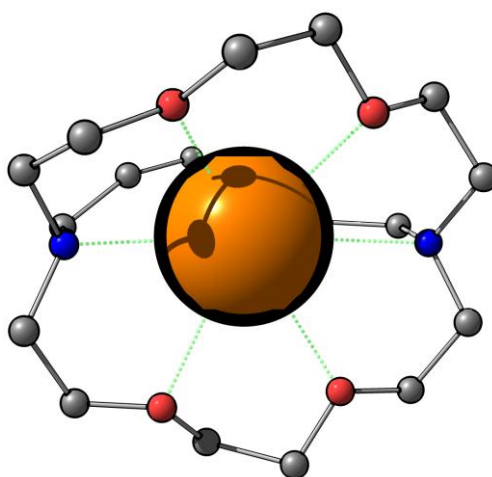
Figure 1.12: A cryptand encapsulating a cation representing a molecular recognition event.

Neutral organic molecules also present challenging guests in the area of substrate recognition. Instead of electrostatic interactions, the molecular container must rely on other weak interactions such as hydrogen bonding or metal coordination in order to increase the guest selectivity (low interference or competition) and sensitivity (low detection limit). High associating constants between the host and the guest render the molecular receptor useful for sensing applications. An excellent example of a selective receptor for carbohydrate recognition was described by Davies and co-workers. They reported a lectin modified with an anthrazene spacer, which has a high selectivity for binding glucose in the presence of other different monosaccharides.[96] The fact that the lectin is bound to two anthrazene groups, which act as fluorophores, allows for detection of the coordination adduct by fluorescence titration (**Figure 1.13**). Due

Chapter I

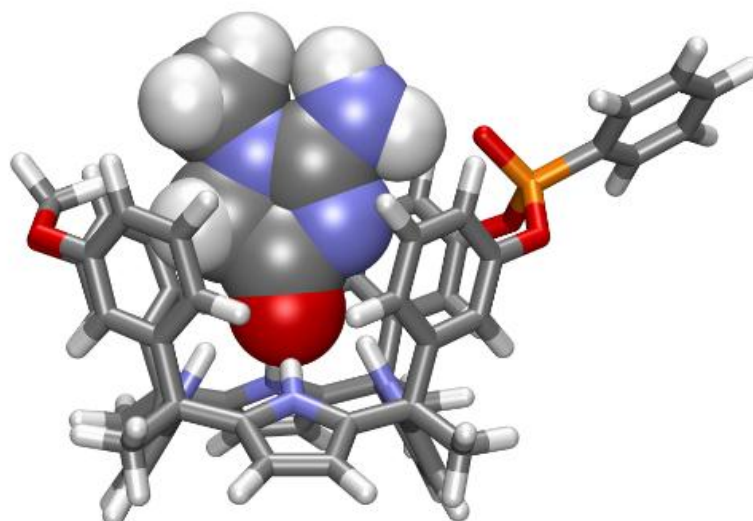to the high selectivity for glucose and the potential it has for quantitative determinations, the system holds promise for blood-glucose tests.
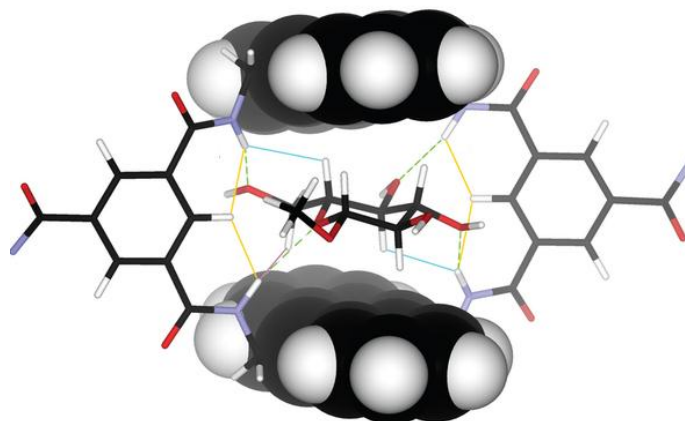
Figure 1.13: Letin based equipped with anthracene units (top and bottom) for selective recognition of glucose.

A practical and applicable sensor should display a specific recognition for a target substrate and also transform the high affinity constant into a physical detectable signal, which represents a technical challenge.[97] Once a useful target molecule has been selected as a potential guest, a complete characterization is required to optimize the design of the corresponding sensor. Understanding the shape, electronic properties and space orientation of the guest and applying this information to improve the synthesis of the host following the "complementary rules", the affinity constant for the host-guest molecule can be optimized. One seminal example of a well-designed receptor was reported by Ballester et al. who focused on the recognition of creatinine using a calix[4]pyrrole motif (**Figure 1.14**) through encapsulation of the substrate inside its cavity.[98] The newly developed method for creatinine recognition presents a huge advantage compared with known methods based on the Jaffe process discovered more than 100 years ago.[99] Their sensor based on a calix[4]pyrrole scaffold provides high sensibility and selectivity for creatinine under biological conditions encountered in urine or plasma. The latter feature makes this an interesting system that could potentially find a practical application in medicinal chemistry.

20

UNIVERSITAT ROVIRA I VIRGILI
MOLECULE AND CATALYST DESIGN FOR RECOGNITION AND ACTIVATION OF SMALL MOLECULES
Luis Martinez Rodriguez

General Introduction

Figure 1.14: A calix[4]pyrrole binding creatinine inside the inner cavity.

From another point of view, the advances made in molecular recognition also has had a huge impact in the field of information technology, applying the sensing principles towards the development of molecular logic gates.[100] Logic gates are the most basic components of electronic digital devices, which immediately (nanoseconds) transform a physical stimuli (input) in an observable signal (output). These responsive signals are codified in a binary system with two possible states: low (0) or high (1). The binary system is used in the computational environment (PCs, smartphones, TVs, toys.) based on silicon-chips. Nowadays, the miniaturization of the components (processors) is limited by physical restrictions.[101-102] The use of supramolecular systems as logic gates has created the opportunity to make computers at the nanometer scale.[103]

1.5 Thesis aims and outline

Small molecule activation opens up new opportunities for the valorisation of waste by-products generated on a large scale in industrial processes, which have undoubtedly their negative influence on the (global) environment. Molecular design plays an important role to successfully trap, recognize and convert these small molecule substrates and to create new opportunities for sustainable

21

Chapter I

chemical transformations. Towards this end, in this thesis different approaches for small molecule recognition and conversion are presented. Different catalysts and receptors have been synthesized and maximizing where possible features such as the cost-effectiveness of the approach and the small molecule recognition/conversion process efficiency under relatively mild conditions.

The aims of the work described in this thesis were: (i) to have a detailed understanding of the self-assembly and recognition process of chiral diamines using modular calix[4]arenes scaffolds and to study the key interactions which control the chiral recognition process (**Chapter 2**); (ii) to develop new methodologies for the synthesis of relevant organic carbonate structures starting from an abundant, cheap and industrial waste: CO_2 (**Chapter 3**). (iii) To extend the knowledge of classical chemical transformations by using a Pd-mediated conversion of vinyl-substituted cyclic carbonates with the aim to provide new synthetic opportunities for useful stereochemical transformations (**Chapter 4**).

The first experimental chapter (Chapter 2) describes the synthesis of a family of cavitands upper rim functionalized with Zn(II) salphen complexes for the chiral recognition of diamines. The self-assembly process between the Zn(II) units and a series of diamine guests was studied in detail revealing a unique binding process that involves both coordinative and other types of interactions. Titration studies and computational analyses indicated the occurrence of an unexpected though highly efficient cooperative encapsulation of the diamine guest by two di-Zn(II)salphen based calix[4]arenes.

In Chapter 3 the focus is on CO_2 valorisation to obtain organic cyclic carbonates from a series of epoxides and CO_2 using an organocatalyst derived from a resorcin[4]arene scaffold. The cavitand scaffold was systematically varied in order to minimize the competitive self-assembly process through hydrogen bonding which inhibits the catalytic activity. The kinetic data and substrate scope for this newly developed organocatalyst are among the best reported to date for metal-free formation of cyclic organic carbonates. As in Chapter 2, the use of cooperative interactions between the cavitand structure and the epoxide substrate increases the overall efficiency and provides a basis for further and improved catalyst design.

UNIVERSITAT ROVIRA I VIRGILI
MOLECULE AND CATALYST DESIGN FOR RECOGNITION AND ACTIVATION OF SMALL MOLECULES
Luis Martinez Rodriguez

General Introduction

In Chapter 4, a new and unprecedented stereoselective synthetic methodology is presented for the formation of (*Z*)-configured 1,4-diols under Pd catalysis. Starting from readily available vinyl cyclic carbonates and using water as nucleophile, synthetically useful 1,4-diols are produced releasing carbon dioxide as the only by-product.

Overall, this thesis summarizes the efforts made in the area of small molecule recognition (Chapter 2) and conversion (Chapters 3 and 4). The importance of cooperativity between different binding sites within a macromolecular host was studied and quantified in two different designs: Zn(salphen) based calix[4]arenes showing unusual binding to chiral diamines and cavitand-based polyphenols that display unprecedented activity for epoxide/CO_2 coupling reactions. Small molecule activation and conversion (CO_2, H_2O) is highlighted in Chapters 3 and 4 to access more complex value-added molecules, illustrating the need to develop new and effective catalytic methods serving the synthetic communities.

1.6 References and notes:

[1]   J. Hagen, *Industrial Catalysis: A Practical Approach*. Weinheim, Germany, Wiley-VCH, **2006**.

[2]   P. W. N. M. van Leeuwen, *Homogeneous Catalysis: Understanding the Art*. Springer, Netherlands, **2004**.

[3]   IUPAC, *Compendium of Chemical Terminology, 2nd ed. (the "Gold Book")*. Ed: A. D. McNaught, A. Wilkinson, Blackwell Scientific Publications, Oxford, **1997**.

[4]   M. Boudart, *Chem. Rev.*, **1995**, *95*, 661.

[5]   A. Behr, P. Neubert, *Applied Homogeneous Catalysis*. Weinheim, Germany, Wiley-VCH, **2012**.

[6]   A. W. Kleij, L. Martínez-Rodríguez, G. Fiorani, C. Martín, *Sustainable Catalysis: Volume 1: Catalysis by Non-Endagered Metals: Chapter 13.* Ed: M. North, RCS, London, **2016**.

[7]   C. Elschenbroich, *Organometallics, 3rd, Completely Revised and Extended Edition.* Weinheim, Germany, Wiley-VCH, **2006**.

[8]   X. Chen, K. M. Engle, D.-H. Wang, J.-Q. Yu, *Angew. Chem. Int. Ed.*, **2009**, *48*, 5094.

[9]   J. Wencel-Delord, T. Dröge, F. Liu, F. Glorius. *Chem. Soc. Rev.,* **2011**, *40*, 4740.

[10]   W. Tolman, *Activation of Small Molecules: Organometallic and Bioinorganic Perspectives*, Weinheim, Germany, Wiley-VCH, **2006**.

Chapter I

[11]   Waste framework Directive 2008/98/EC of the European Parliament and of the Council of 19 November 2008 on waste and repealing certain Directives. In: Official Journal L 312, 22/11/ 2008, pp. 0003–0030. **2008**.

[12]   M. Pradel, T. Pacaud, M. Cariolle. *Waste Biomass Valor.,* **2013,** *4*, 851.

[13]   O. K. Varghese, M. Paulose, T. J. LaTempa, C. A. Grimes, *Nano Lett.*, **2009**, *9*, 731.

[14]   S. Ahmed, M. Krumpelt, *Inter. J. Hydro. Ener.,* **2001**, *26*, 291.

[15]   R. Parsons, T. VanderNoo, *J. Elec. Chem. Inter. Elec.*, **1988**, *257*, 9.

[16]   J. P. Collman, R. Boulatov, C. J. Sunderland, L. Fu, *Chem. Rev.*, **2004**, *104*, 561.

[17]   F. Cavani, J. H. Teles, *ChemSusChem*, **2009**, *2*, 508.

[18]   J. B. Gerken, S. S. Stahl, *ACS Cent. Sci.*, **2015**, *1*, 234.

[19]   E. A. Lewis, W. B. Tolman, *Chem. Rev.*, **2004**, *104*, 1047.

[20]   E. I. Solomon, *Inorg. Chem.*, **2016**, *55*, 6364.

[21]   J. Piera, J.-E. Bäckvall, *Angew. Chem. Int. Ed.*, **2008**, *47*, 3506.

[22]   M. Costas, M. P. Mehn, M. P. Jensen, L. Que, *Chem. Rev.*, **2004**, *104*, 939.

[23]   K. Weissermel, *Industrial Organic Chemistry*. New York, Wiley-VCH, **1997**.

[24]   S. Sakaki, A. Dedieu, *Inorg. Chem.*, **1987**, *26*, 3278.

[25]   J. Mascetti, *Carbon dioxide coordination chemistry and reactivity of coordinated CO$_2$*, Ed: M. Aresta, Wiley-VCH, Weinheim, Germany, **2010**, 55.

[26]   C.-H. Jun, *Chem. Soc. Rev.*, **2004**, *33*, 610.

[27]   P. I. Dalko, L. Moisan, *Angew. Chem. Int. Ed.,* **2004**, *43*, 5138.

[28]   A. El-Faham, F. Albericio, *Chem. Rev.*, **2011**, *111*, 6557.

[29]   J. C. Sheehan, G. P. Hess, *J. Am. Chem. Soc.*, **1955**, *77*, 1067.

[30]   M. North, R. Pasquale, *Angew. Chem. Int. Ed.,* **2009**, *48*, 2946.

[31]   Value obtained from http://www.iea.org/.

[32]   M. Aresta, A. Dibenedetto, A. Angelini, *Chem. Rev.*, **2014**, *114*, 1709.

[33]   The Bosch–Meiser process produces urea from ammonia and CO$_2$. For more information, see: http://boschmeiserprocess.wikispaces.com/.

[34]   H. Kolbe, E. Lautemann, *Annalen,* **1869**, *113*, 125.

[35]   C. Martín, G. Fiorani, A. W. Kleij, *ACS Catal.*, **2015**, *5*, 1353.

[36]   A. Urakawa, J. Sá, *Fuel Production with Heterogeneous Catalysis*, Ed: J. Sá, Taylor & Francis, **2014**, ISBN: 9781482203714.

[37]   A. Chedin, *J. Mol. Spectrosc.*, **1979**, *76*, 430.

[38]   K. Tanaka , D. Ooyama , *Coord. Chem. Rev.*, **2002**, *226*, 211.

[39]   A. M. Appel, J. E. Bercaw, A. B. Bocarsly, H. Dobbek, D. L. DuBois, M. Dupuis, J. G. Ferry, E. Fujita, R. Hille, P. J. A. Kenis, C. A. Kerfeld, R. H. Morris, C. H. F. Peden, A. R. Portis, S. W. Ragsdale, T. B. Rauchfuss, J. N. H. Reek, L. C. Seefeldt, R. K. Thauer, G. L. Waldrop, *Chem. Rev.*, **2013**, *113*, 6621.

[40]   J. Klankermayer, S. Wesselbaum, K. Beydoun, W. Leitner, *Angew. Chem. Int. Ed.*, **2016**, *55*, 7296.

[41]   A. Behr, G. Henze, *Green Chem.*, **2011**, *13*, 25.

[42]   P. Braunstein, D. Matt, D. Nobel, *J. Am. Chem. Soc.*, **1988**, *110*, 3207.

[43]   W. Guo, V. Laserna, E. Martin, E. C. Escudero-Adán, A. W. Kleij, *Chem. Eur. J.*, **2016**, *22*, 1722.

[44]   A. Ion, V. Parvulescu, P. Jacobs, D. De Vos, *Green Chem.*, **2007**, *9*, 158.

[45]   D. Saylik, M. J. Horvath, P. S. Elmes, W. R. Jackson, *J. Org. Chem.*, **1999**, *64*, 3940.

[46]   J. Langanke, A. Wolf, J. Hofmann, K. Böhm, M. A. Subhani, T. E. Müller, W. Leitner, C. Gürtler, *Green Chem.*, **2014**, *16*, 1865.

UNIVERSITAT ROVIRA I VIRGILI
MOLECULE AND CATALYST DESIGN FOR RECOGNITION AND ACTIVATION OF SMALL MOLECULES
Luis Martinez Rodriguez

General Introduction

[47]   L. Peña Carrodeguas, J. González-Fabra, F. Castro-Gómez, C. Bo, A. W. Kleij, *Chem. Eur. J.*, **2015**, *21*, 6115.

[48]   R. Martin, A. W. Kleij, *ChemSusChem*, **2011**, *4*, 1259.

[49]   D. J. Darensbourg, S. J. Wilson, *Green Chem.*, **2012**, *14*, 2665.

[50]   O. Hauenstein, S. Agarwal, A. Greiner, *Nat. Commun.*, **2016**, *7*, 11862.

[51]   F. Auriemma, C. De Rosa, M. R. Di Caprio, R. Di Girolamo, W. C. Ellis, G. W. Coates, *Angew. Chem. Int. Ed.*, **2015**, *54*, 1215.

[52]   A. Ion, C. Van Doorslaer, V. Parvulescu, P. Jacobs, D. De Vos, *Green Chem.*, **2008**, *10*, 111.

[53]   V. Laserna, W. Guo, A. W. Kleij, *Adv. Synth. Catal.*, **2015**, *357*, 2849.

[54]   S. Sopeña, V. Laserna, W. Guo, E. Martin, E. C. Escudero-Adán, A. W. Kleij, *Adv. Synth. Catal.*, **2016**, *358*, 2172.

[55]   W. P. Jencks, *Catalysis in Chemistry and Enzymology*, McGraw-Hill, New York, **1969**.

[56]   A. J. Kirby, *Angew. Chem. Int. Ed.*, **1996**, *35*, 706.

[57]   K. E. Jaeger, T. Eggert, *Curr. Opin. Biotech.*, **2004**, *15*, 305.

[58]   A. R. Fersht, *Enzyme Structure and Mechanism*. 2nd ed. Freeman, New York, **1985**.

[59]   C. J. Pedersen, *J. Am. Chem. Soc.*, **1894**, *27*, 2985.

[60]   D. W. Christianson, W. N. Lipscomb, *Acc. Chem. Res.*, **1989**, *22*, 62.

[61]   R. H. Symons, *Annu. Rev. Biochem.*, **1992**, *61*, 641.

[62]   T. Pan, O. C. Uhlenbeck, *Biochemistry*, **1992**, *31*, 3887.

[63]   J. C. Sherman, D. J. Cram, *J. Am. Chem. Soc.*, **1989**, *111*, 4527.

[64]   L. Pauling, *Nature*, **1948**, *161*, 707.

[65]   K. N. Houk, A. G. Leach, S. P. Kim, X. Y. Zhang, *Angew. Chem. Int. Ed.*, **2003**, *42*, 4872.

[66]   J. M. Lehn, *Acc. Chem. Res.*, **1978**, *11*, 49.

[67]   J.M. Lehn, *Chem. Soc. Rev.*, **2007**, *36*, 151.

[68]   S. Shinkai, *Tetrahedron*, **1993**, *49*, 8933.

[69]   J. R. Moran, S. Karbach, D. J. Cram, *J. Am. Chem. Soc.*, **1982**, *104*, 5826.

[70]   D. J. Cram, S. Karbach, Y. H. Kim, L. Baczynskyj, G. W. Kallemeyn, *J. Am. Chem. Soc.*, **1985**, *107*, 2575.

[71]   M. Fujita, M. Tominaga, A. Hori, B. Therrien, *Acc. Chem. Res.*, **2005**, *38*, 371.

[72]   M. Yoshizawa, J. K. Klosterman, M. Fujita, *Angew. Chem. Int. Ed.*, **2009**, *48*, 3418.

[73]   B. Breiner, J. K. Clegg, J. R. Nitschke, *Chem. Sci.*, **2011**, *2*, 51.

[74]   R. Cacciapaglia, S. Di Stefano, L. Mandolini, *Acc. Chem. Res.*, **2004**, *37*, 113.

[75]   M. Fujita, D. Oguro, M. Miyazawa, H. Oka, K. Yamaguchi, K. Ogura, *Nature*, **1995**, *378*, 469.

[76]   S.-Y. Yu, T. Kusukawa, K. Biradha, M. Fujita, *J. Am. Chem. Soc.*, **2000**, *122*, 2665.

[77]   T. Heinz, D. M. Rudkevich, J. Rebek, *Nature*, **1998**, *394*, 764.

[78]   J. Mattsson, O. Zava, A. K. Renfrew, Y. Sei, K. Yamaguchi, P. J. Dyson, B. Therrien, *Dalton Tans.*, **2010**, *39*, 8248.

[79]   C. D. Gutsche, Calixarenes: *An Introduction, 2nd ed.* Ed: J. F. Stoddart, RCS, Cambridge, **2008**.

[80]   C. D. Gutsche, J. A. Levine, *J. Am. Chem. Soc.*, **1982**, *104*, 2652.

[81]   A. Galan, P. Ballester, *Chem. Soc. Rev.*, **2016**, *45*, 1720.

Chapter I

[82]   K. Wang, Y.-W. Yang, *Annu. Rep. Prog. Chem. Sect. B: Org. Chem.*, **2013**, *109*, 67.

[83]   S. Shimizu, N. Shimada, Y. Sasaki, *Green Chem.*, **2006**, *8*, 608.

[84]   S. Shimizu, S. Shirakawa, Y. Sasaki, C. Hirai, *Angew. Chem. Int. Ed.*, **2000**, *39*, 1256.

[85]   S. J. Wezenberg, A. W. Kleij, *Adv. Synth. Catal.*, **2010**, *352*, 85.

[86]   R. Gramage-Doria, D. Armspach, D. Matt, *Coor. Chem. Rev.*, **2013**, *257*, 776.

[87]   P. Ballester, A. Vidal-Ferran, P. W. N. M. van Leeuwen, Modern Strategies in Supramolecular Catalysis. B. C. Gates, H. Knözinger, Eds: *Advances in Catalysis*, Vol. 54, Burlington: Academic Press, **2011**, pp. 63.

[88]   I. Pochorovski, F. Diederich, *Acc. Chem. Res.*, **2014**, *47*, 2096.

[89]   P. D. Frischmann, M. J. MacLachlan, *Chem. Soc. Rev.*, **2013**, *42*, 871.

[90]   E. Fischer, *Ber. Dt. Chem. Ges.*, **1894**, *27*, 2985.

[91]   C. J. Pedersen, *J. Am. Chem Soc.*, **1967**, *89*, 2495.

[92]   P. D. Beer, P. A. Gale, *Angew. Chem. Int. Ed.*, **2001**, *40*, 486.

[93]   J. Liu. Z. Cao, Y. Lu. *Chem. Rev.*, **2009**, *109,* 1948.

[94]   N. H. Evans, P. D. Beer, *Angew. Chem. Int. Ed.*, **2014**, *53*, 11716.

[95]   R. D. Shannon, *Acta Crystallogr. Sect. A.*, **1976**, *32*, 751.

[96]   C. Ke, H. Destecroix, M. P. Crump, A. P. Davis, *Nature Chem.*, **2012**, *4*, 718.

[97]   C. J. Li, *Chem. Rev.*, **2005**, *105*, 3095.

[98]   T. Guinovart, D. Hernández-Alonso, L. Adriaenssens, P. Blondeau, M. Martínez-Belmonte, F. X. Rius, F. J. Andrade, P. Ballester, *Angew. Chem. Int. Ed.*, **2016**, *55*, 2435.

[99]   J. R. Delanghe, M. M. Speeckaert, *NDT plus*, **2011**, *4*, 83.

[100]   M. A. Reed, J. M. Tour, *Sci. Am.*, **2000**, *282*, 86.

[101]   J. M. Tour, *Acc. Chem. Res.*, **2000**, *33*, 791.

[102]   G. E. Moore, *Electronics*, **1965**, *38*.

[103]   Madhuprasad, M. P. Bhat, H.-Y. Jung, D. Losic, M. D. Kurkuri, *Chem. Eur. J.*, **2016**, *22*, 1.

UNIVERSITAT ROVIRA I VIRGILI
MOLECULE AND CATALYST DESIGN FOR RECOGNITION AND ACTIVATION OF SMALL MOLECULES
Luis Martinez Rodriguez

Chirality Transfer from Diamines Encapsulated within a Calixarene–Salen Host

Chapter II

Chirality Transfer from Diamines Encapsulated within a Calixarene–Salen Host

A calix[4]arene host upper rim functionalized with two zinc(II)salphen complexes presents strong affinity for ditopic guests such as diamines. The use of optically active diamines leads to an efficient chirality transfer to the host confirmed by observation of various Cotton effects by Circular Dichroism (CD) spectroscopy. An unexpected 2:1 ratio between the host and the guest was found and an encapsulation process of the guest was confirmed by detailed titration and DFT studies.
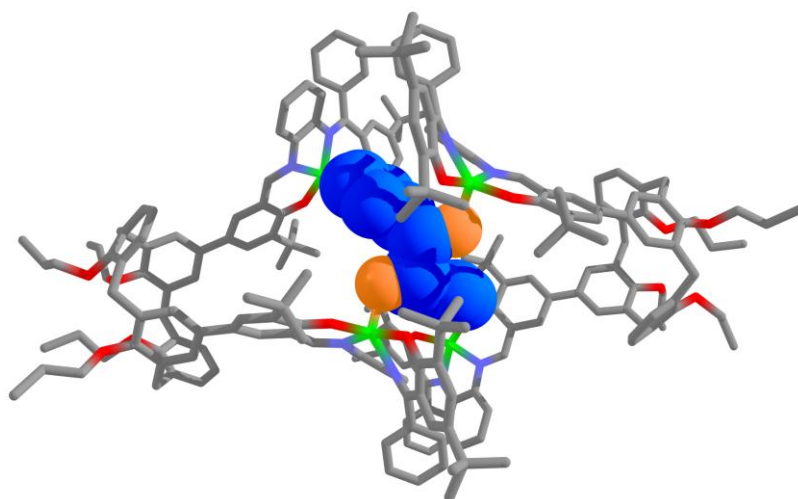
Chapter II

2.1 Chirogenesis and sensoring

The transfer of chirality, also referred to as chirogenesis, plays an important role in nature regarding proteins and other natural systems such as DNA.[1-3] Chiral transmission has also proved to be crucial in asymmetric catalysis processes, where a metal or organic catalyst favors the formation of one preferred chiral product in the enantiocontrolling step.[4-6] Supramolecular chemistry has been used to induce chirality, mimicking the weak interactions of metallo-enzymes present in biological processes.[7-8] Highly efficient methodologies have been designed to create materials with responsive features. Furthermore, smart materials have been developed with predesigned sensing purposes.[9-15]

The field of chirality sensing has rapidly advanced over the last five years with a strong focus on newly designed systems that may facilitate fast and efficient determination of the concentration, absolute configuration, enantiomeric excess, and/or molecular identity of a chiral analyte.[16-22] The transfer of the stereochemical information between molecules is an important approach to develop new chiral transformations, which are based on the use of a pro-chiral precatalyst combined with an enantiomerically pure chiral ligand (often being phosphines, amines and (amino)alcohols) to lead the formation of the desired product with an enantiomeric excess (*e.e.*) (**Scheme 2.1**).
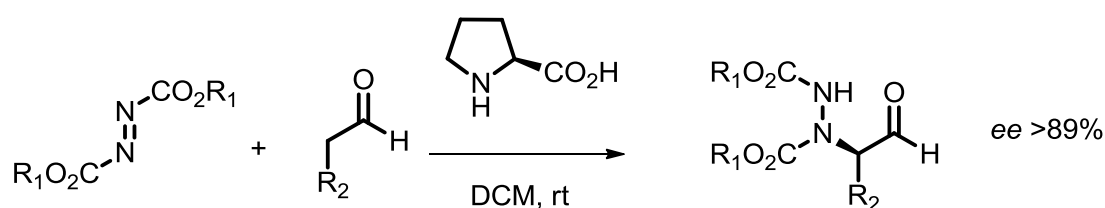
Scheme 2.1: L-Proline inducing chirality in an addition reaction.

Identifying the absolute configuration of organic molecules in asymmetric reactions is of vital importance. Even though two enantiomers have essentially the same physical properties (except for their interaction with polarized light), they can often present distinct chemical activities with significant consequences in biologic processes (*i.e.* talidomide).[23] The absolute configuration of the compound

28

Chirality Transfer from Diamines Encapsulated within a Calixarene–Salen Host

is most commonly confirmed by X-ray diffraction. This technique presents several drawbacks such as the requirement to crystallize the final product, time to obtain the structure and cost and availability of a suitable diffractometer. As an alternative solution, new methods have been developed to identify the absolute configuration using *Circular Dichroism* (CD).[24] The use of sensoring molecules which interact with the chiral guest, absorb light at a specific wavelength (λ) and generate a response by a physical signal (intensity of the Cotton effect in the CD spectrum) can provide an efficient means to determine the absolute configuration of the substrate.

2.2 Metallosalphen complexes

Based on the affinity that metal compounds present to coordinate small molecules containing donor atoms such as nitrogen, oxygen and phosphorus, metal complexes have been widely studied as potential sensors. Focusing on the field of chiral recognition, porphyrins have attracted most attention and still continue to be popular hosts in chirality transfer processes.[25-31] On the contrary, salen complexes have received less attention even though the salen ligands can be easily synthesized, and metallosalen complexes are known with most of the metals from the periodic table. These ligands can be easily obtained from a simple condensation reaction of two equivalents of salicylaldehyde combined with one equivalent of a diamine (**Scheme 2.2**). The flexibility of the salen ligand is controlled by the amine moiety which acts as a linker between the two phenol units generating a *N₂O₂*-tetradentate coordination enviroment.[32] The use of cyclic diamines, especially the aromatic ones, provides planar structures and the salen ligands incorporating a phenyl bridge are commonly named "sal*phen*". By modifying the salicylidene groups and the diamine linker, the electronic and steric environment can be easily modulated. The family of zinc(II) salphen complexes have found many applications such as in the field of homogenous catalysis,[33] self-assembled materials[34-35] and chiral recognition.[36]

The rigidity of the tetracoordinate salphen ligand enforces the zinc ion to reside in a square planar geometry, while zinc(II) ions normally prefer a

Chapter II

tetrahedral coordination. As a consequence, the Zn salphen complexes show axial coordination potential providing square pyramidal geometries with the axial position occupied by electron-donating N– or O–donor molecules[37] or by polar solvent molecules to increase the stability of the complex. In the absence of a polar solvent, the salphen complex can dimerize through a self-assembly process *via* μ-phenyloxo bridges between two zinc salphen units.[38] Sterically crowded pendant groups, like *tert*-butyl, can be installed in the 3 and 3´ positions of the salicylidene units (R_1 in **Scheme 2.2**) of the salphen ligand to minimize or even block the self-assembly process.[39]
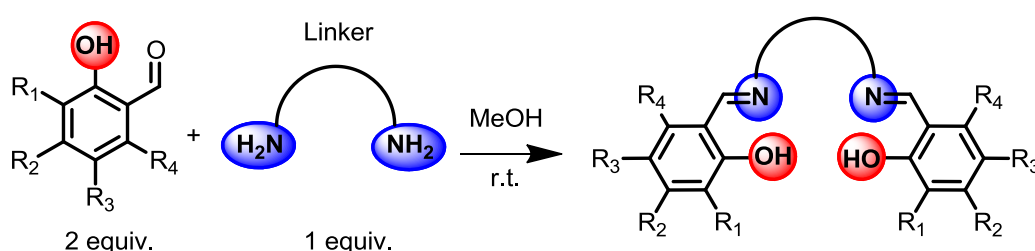
Scheme 2.2: General synthetic route towards salen ligands.

Dinuclear and trinuclear Zn(II)salphen complexes were reported for chiral recognition of carboxylic acids, diamines, aminoalcohols and diols using appropriate host-guest systems.[40] In most of the reported supramolecular host systems to date, transfering of the chiral information by interaction with chiral diamines is hampered by the requirement of a pretreatment of the analyte with additives, the use of a "large" excess of diamine to avoid competitive processes, the requirement of air-sensitive reagents, and/or a relatively low binding constant between the host and guest partners. Owing to these challenges, the quest for an efficient host system that can more efficiently recognize chiral diamines remains an important undertaking.

30

Chirality Transfer from Diamines Encapsulated within a Calixarene–Salen Host
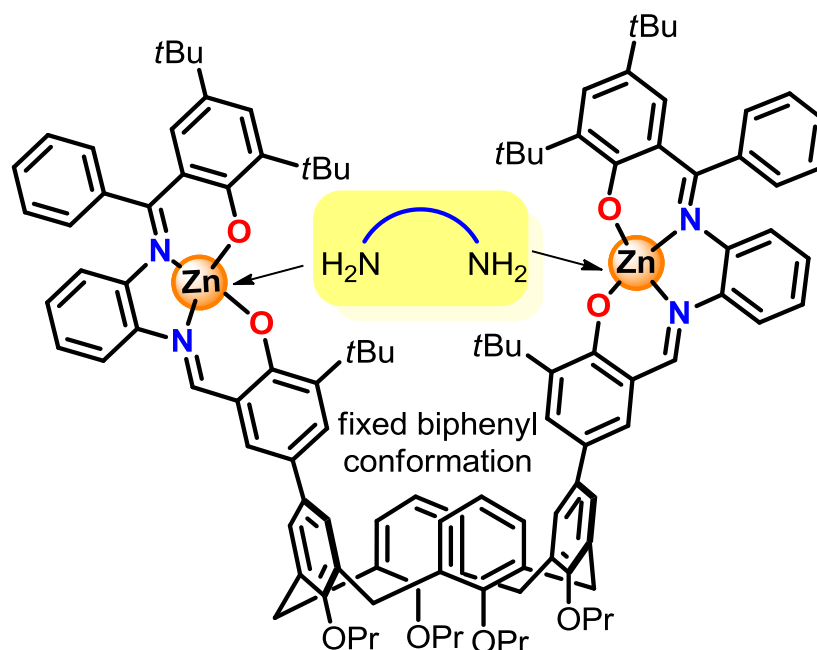
Figure 2.1: Calix[4]arene 5 designed to bind ditopic molecules such as diamines.

For this purpose, the **calix[4]arene 5** scaffold was designed with two co-facially oriented Zn(II)salphen units that should accommodate the binding of suitable chiral diamine guests and block the C_{aryl}-C_{aryl} rotation of the biphenyl units. These salphen complexes are known to form stable aggregates with amine donor ligands in a 1:1 ratio; as a consequence, each molecule of **calix [4]arene 5** would thus bind one molecule of chiral diamine (**Figure 2.1**). The biphenyl groups which connect the calix unit with the salphen complexes are prochiral. This type of chirality is axial like in the case of BINOL and its derivatives.[41] This optical property is also called helepticity and follows the same priority rules as tetrahedral stereocenters (**Figure 2.2**).[42] The *S* isomer is called P (*plus*) and the *R* isomer is named M (*minus*).

Chapter II
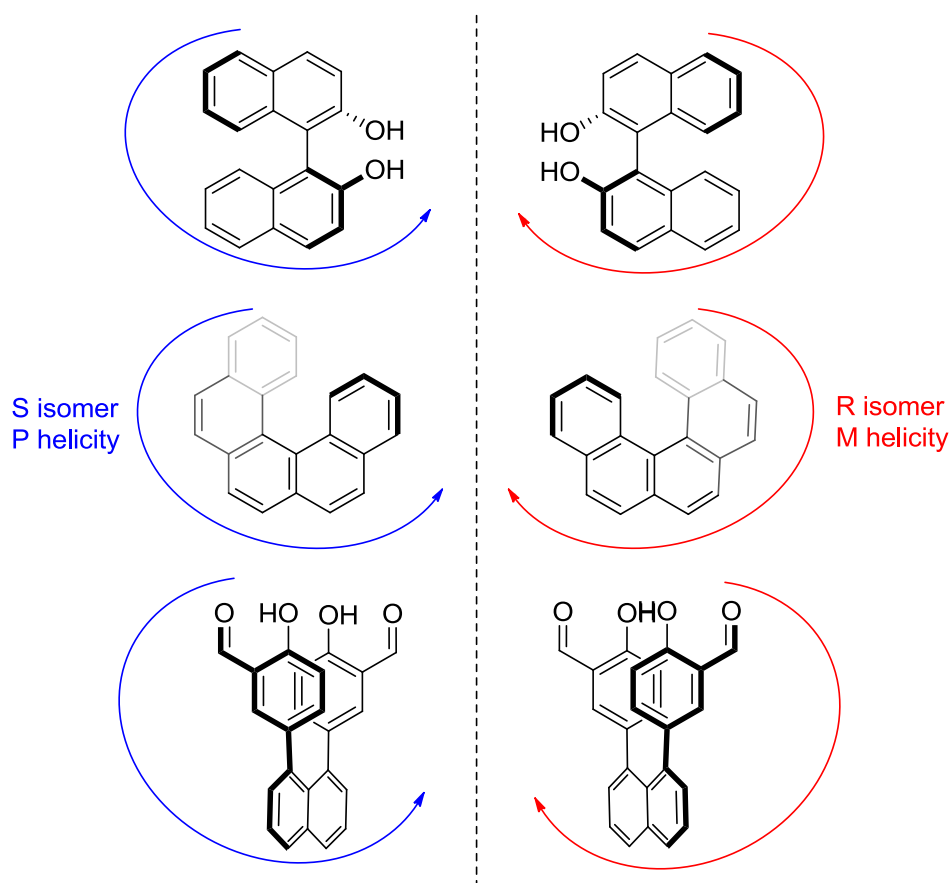
Figure 2.2: Configurations of BINOL (top), heptahelicene (middle) and triaryl units (bottom) following the Cahn-Ingold-Prelog rules.

2.3 Synthesis of calix[4]arenes based on zinc(II) salphen complexes

The design of the molecular host was concluded by taking into account a few important details in order to minimize undesired competitive processes. The presence of *tert*-butyl groups in the 3 and 3′ position of the salicylidene units are necessary to avoid self-assembly between the zinc(II)salphen units.[39] The ketimine groups in the salphen framework will provide more stability and rigidity in the host molecule.[43]

Based on these considerations, the synthesis of bis-Zn(II)salphen **calix[4]arene 5** was carried out and details are provided in **Scheme 2.3**. The host **5** was overall functionalized with two distal Zn(salphen) complexes connected to

Chirality Transfer from Diamines Encapsulated within a Calixarene–Salen Host

the upper rim of the calix[4]arene leading to the formation of two prochiral biphenyl units by rotation of the C_{aryl}-C_{aryl} bonds. At the lower rim, propyl groups were introduced to preserve the cone conformation and increase the solubility in organic solvents.
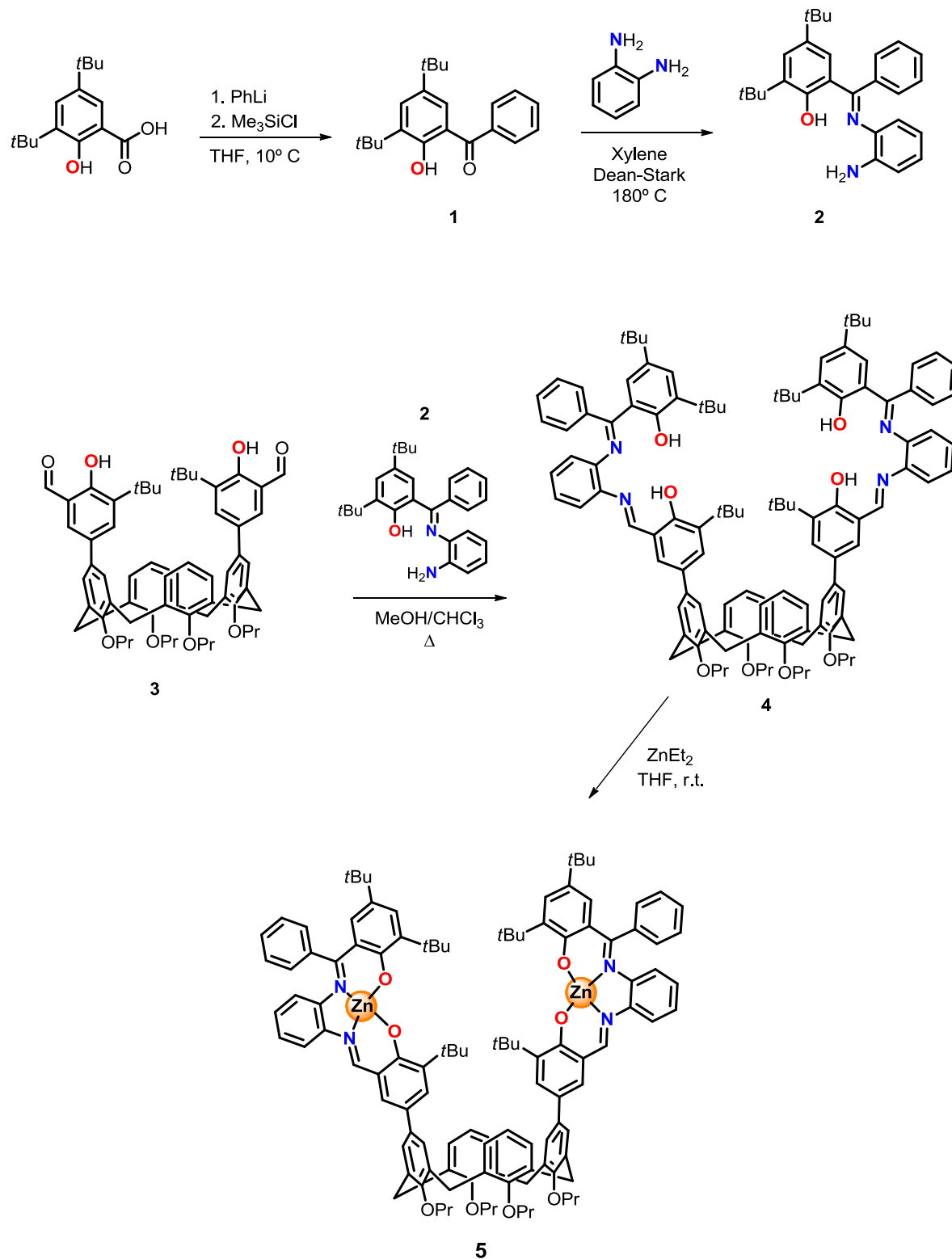
Scheme 2.3: Synthesis of bis-Zn(II)salphen **calix[4]arene 5**.

Chapter II

Starting from the commercially available 3,5-di-*tert*-butylsalicylic acid and the organolithium reagent PhLi, ketone **1** was obtained in 92% yield. Compound **1** gave, in the presence of an excess of *o*-phenylenediamine, the ketimine product **2** through a condensation reaction carried out using a Dean–Stark apparatus (74% yield). Precursor **2** in combination with the previously reported bis-salicyladehyde **3**[44] allowed to prepare the bis-salphen ligand **4** in 70% yield. Bis-ligand **4** can be metalated with a solution of diethylzinc (Et$_2$Zn) to afford the final bis-zinc(II)salphen **calix[4]arene 5** in 83% yield.
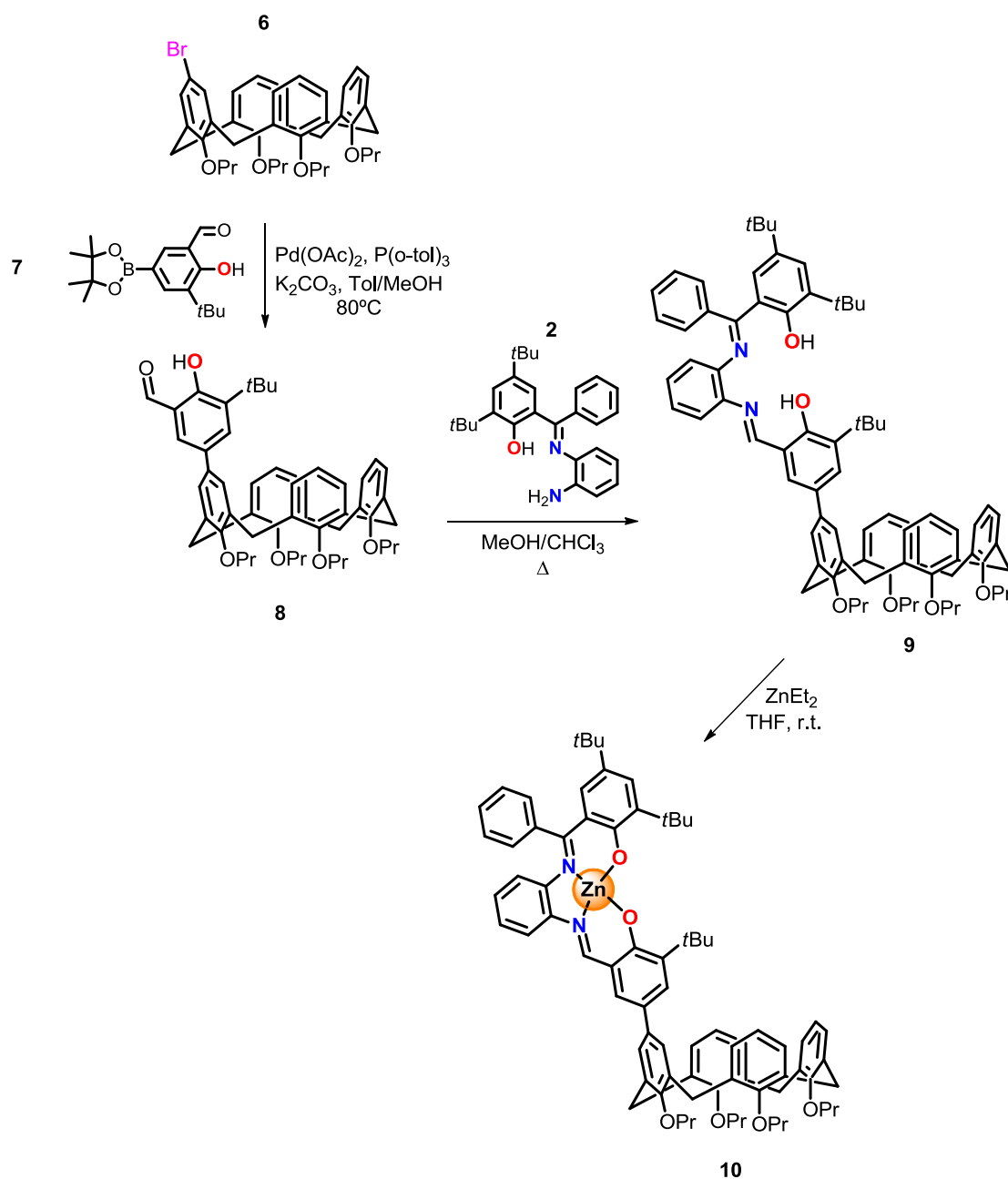
Scheme 2.4. Synthesis of mono-Zn(II)salphen **calix[4]arene 10**.

34

Chirality Transfer from Diamines Encapsulated within a Calixarene–Salen Host

The analogous mono-zinc(II)salphen **calix[4]arene 10** was prepared to perform control experiments and to calculate the association constant as will be discussed below. The synthetic route (**Scheme 2.4**) started from the mono-5-bromotetrapropoxycalix[4]arene (compound **6**) and the reported boronic ester derivative of 3-*tert*-butylsalicyladehyde (compound **7**)[45] which under Suzuki cross-coupling reaction conditions gave access to the mono-salicyladehyde **8** supported by the calix[4]arene scaffold in 71 % yield. The latter was treated with ketimine **2** and afforded the mono-salphen ligand **9** (62% yield). Finally, ligand **9** was metalated by Et$_2$Zn leading to the formation of the desired mono-zinc(II)salphen **calix[4]arene 10** in 99% yield.

2.4 Host-guest assembly formation in the presence of diamines

The characterization of bis-Zn(II)salphen **calix[4]arene 5** by ^{1}H NMR spectroscopy indicated the presence of only type of magnetically equivalent imine protons (9.09 ppm in acetone-d$_6$), which means that the electronic environment of the two imine protons of the host molecule are equal (**Figure 2.3,** bottom, **green**) . The addition of a solution containing a ditopic amine, such as (*R,R*)-diphenylethylenediamine (*R,R*)-**L1**, promoted the coordination of the diamine to the zinc centers blocking thereby the free rotation of the biphenyl units. This coordination process was observed in ^{1}H NMR where the chemical shift of the imine proton changed from 9.09 to 8.64 ppm ($\Delta\delta = -0.45$ ppm) indicating a shielding effect exterted by the (*R,R*)-**L1** molecule (**Figure 2.3,** top, **blue**). Another noteworthy effect is the observation of several imine peaks after addition of diamine, which indicates the formation of different (stereo)isomers.

Chapter II
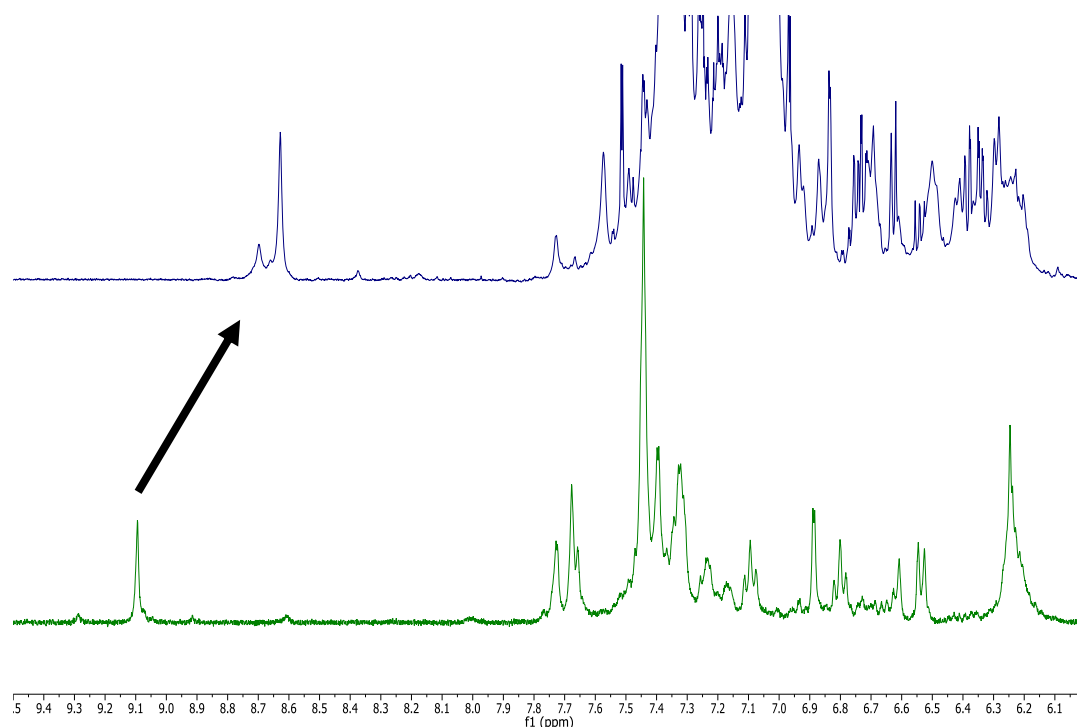
Figure 2.3. ^{1}H NMR spectra of **calix[4]arene 5** host (bottom, **green**) and after the addition of 1 equivalent of (*R,R*)-**L1** (top, **blue**) in acetone-d$_6$ at 50º C.

The host **calix[4]arene 5** can exist as four different atropisomers (P,P; P,M; M,P and M,M) depending on the orientation of the *tert*-butyl groups with respect to the C$_{aryl}$-C$_{aryl}$ bond, as shown in **Scheme 2.5**. The addition of a ditopic ligand to a solution containing **calix[4]arene 5** prospectively blocks the free rotation of the biphenyl groups and stabilizes a particular conformation as a consequence of coordination between the bidentate ligand to the zinc centers. Two of the possible atropisomers are optically active (the P,P and M,M ones) whereas the other two are *meso* forms with the *tert*-butyl groups in *cis* configuration.[46] By using chiral diamines, preferred stereochemically controlled formation of one atropisomer of **calix[4]arene 5** can be induced.

36

Chirality Transfer from Diamines Encapsulated within a Calixarene–Salen Host
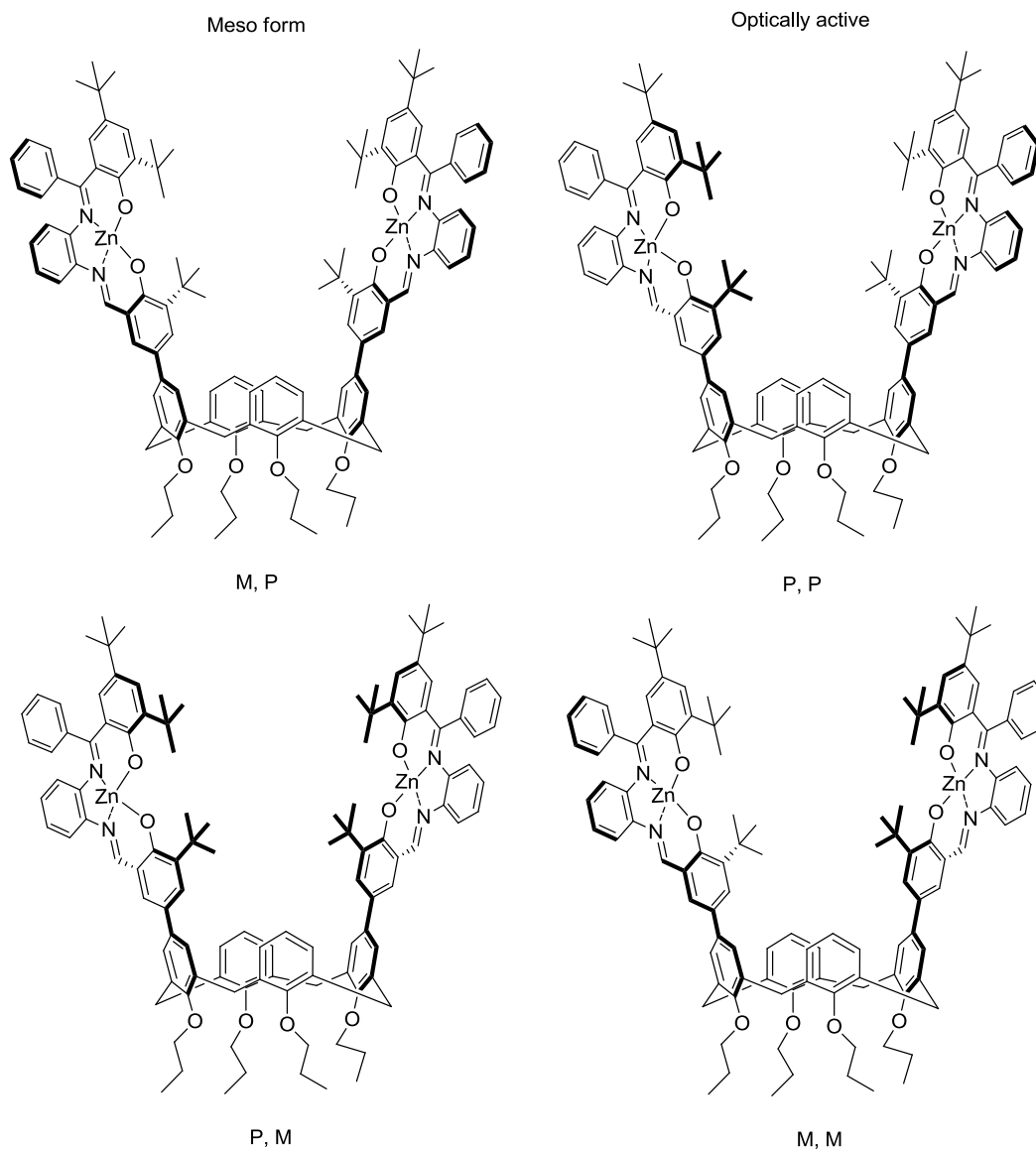
Scheme 2.5. Different atropisomers that can be obtained considering the orientation of the *tert*-butyl and the imine groups in **calix[4]arene 5**.

The potential induction of chirality was thus examined using an optically pure diamine and the host **calix[4]arene 5**. First, an experiment with (*R,R*)-(+)-1,2-diphenylethylenediamine, (*R,R*)-**L1**, was carried out measuring the polarized light by CD spectroscopy and led to the observation of a first positive (+6 *mdeg* at λ = 416 nm) and second negative Cotton effects (−6 *mdeg* at λ = 476 nm) of the corresponding **calix[4]arene 5·**(*R,R*)-**L1** complex (**Figure 2.4**). Consequently, the addition of (*S,S*)-**L1** induced a first negative and second positive Cotton effect which stems from a counterclockwise coupling of electronic transitions and this corresponds to the (M,M)-isomer (**Scheme 2.5**).[36-47] As expected, the CD spectrum

Chapter II

using *rac*-**L1** resulted in non-observable Cotton effects due to the presence of equimolar amounts of both enantiomers (*R,R*) and (*S,S*) of the diamine.
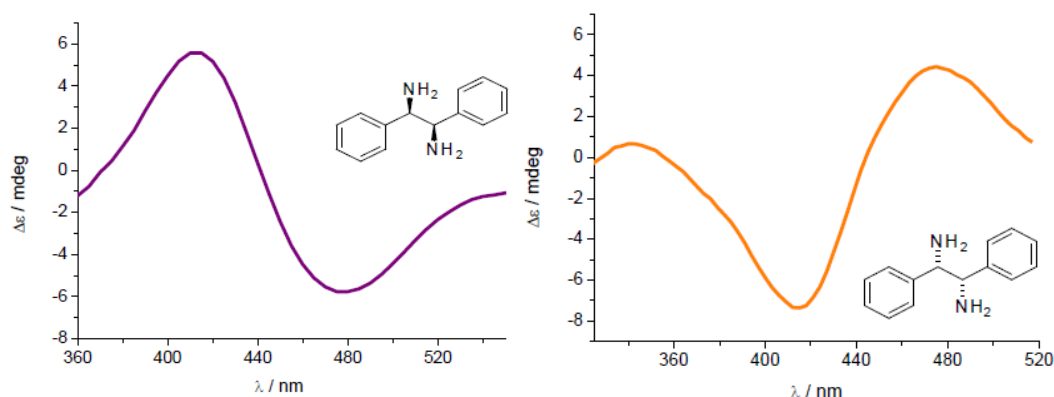
Figure 2.4. CD spectra of **calix[4]arene 5**·(*R,R*)-**L1** (**left**) and **calix[4]arene 5**·(*S,S*)-**L1** (**right**) in CH$_2$Cl$_2$ (2×10^{-5} M).

In order to determine the nature and the stability of the complex generated, different titration studies (UV-vis and CD) were performed. Titration of a solution of **calix[4]arene 5** (CH$_2$Cl$_2$; 6×10^{-5} M) with a solution of the diamine **L1** (CH$_2$Cl$_2$; 6×10^{-4} M) showed typical UV-vis changes for a Zn(salphen) derived complex. A small but detectable bathochromic shift ($\Delta\lambda = 6$ nm) was found together with a significant decrease of the absorption upon addition of higher amounts of diamine **L1** (**Figure 2.5**). Similar types of bathochromic shifts of Zn(II)salphen units were observed in the presence of pyridine donors.[48-49] However, in these cases an increasing absorption was noted at higher concentrations of analyte due to aggregate-to-monomer transitions of these materials. Thus, in the present case it seems that host molecule **5** does not seem to be in an aggregated state rendering it useful for interaction with suitable ditopic substrates such as diamine **L1**.

38

Chirality Transfer from Diamines Encapsulated within a Calixarene–Salen Host
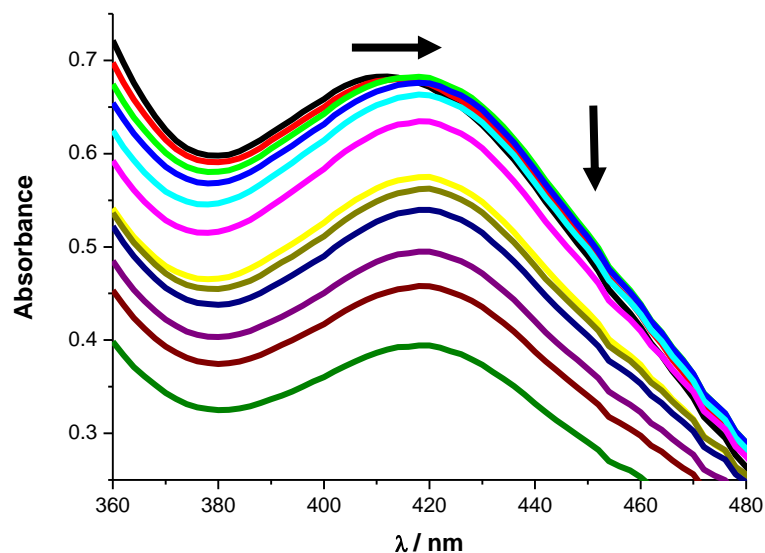
Figure 2.5. a) Zoom of the UV-vis spectrum for **5** (6×10^{-5} M; CH_2Cl_2) in the presence of increasing amounts of diamine (*R,R*)-**L1** (0-to-100 eq).

Titration studies using CD spectroscopy showed that the amplitudes of the Cotton effects were increasing with the amount of chiral amine added. Interestingly, an unexpected saturation point was obtained after the addition of only 0.5 equiv. of optically pure diamine **L1** (**Figure 2.6** and **2.7**). These results suggest the formation of a complex with a 2:1 host-guest ratio where two molecules of **calix[4]arene 5** preferentially interact with one molecule of chiral diamine, and not the expected formation of a 1:1 complex is observed as was envisioned in **Figure 2.1**.
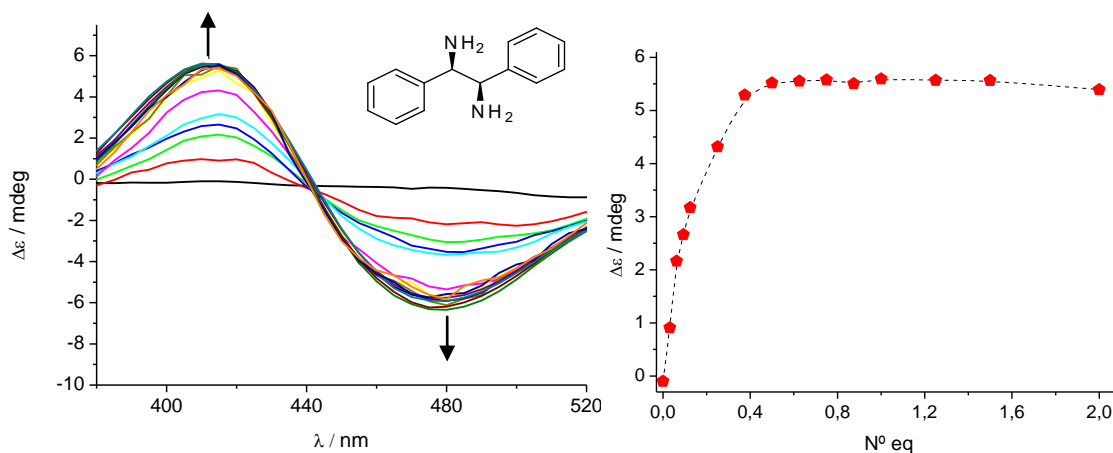

Figure 2.6: Titration plot and curve ($\lambda = 412$ nm) of host **5** (6×10^{-5} M; CH_2Cl_2) with (*R,R*)-**L1** (added equiv. 0, 0.03, 0.06, 0.09, 0.12, 0.25, 0.37, 0.5, 0.62, 0.75, 0.87, 1, 1.25, 1.5, 2).

Chapter II
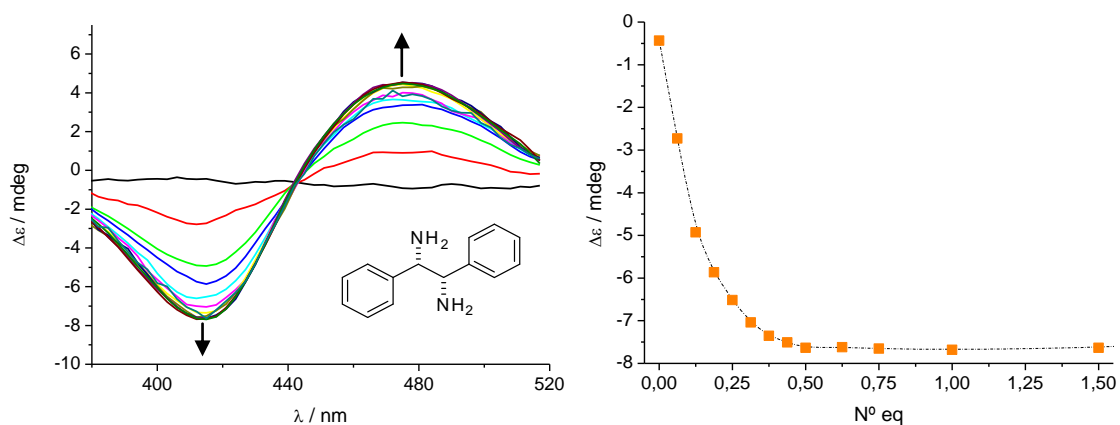
Figure 2.7: Titration plot and curve (λ = 412 nm) of host **5** (6×10^{-5} M; CH_2Cl_2) with (*S,S*)-**L1** (added equiv. 0, 0.03, 0.06, 0.09, 0.12, 0.25, 0.37, 0.5, 0.62, 0.75, 0.87, 1, 1.25, 1.5, 2).

The assembled structure **calix[4]arene 5·(*R,R*)-L1** proved to be rather stable in solution as a large excess of 40 equiv. of the diamine guest are required to fully disrupt the 2:1 assembly (**Figure 2.8**). The underlying reasons for this unusual observation have been investigated in detail using various experimental and computational methods (*vide infra*).
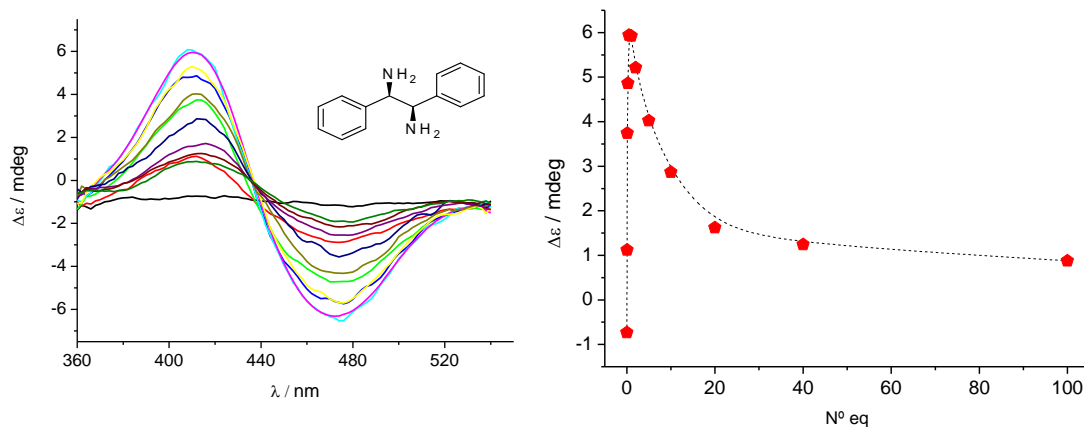
Figure 2.8: Titration plot and curve (λ = 416 nm) of host **5** (6×10^{-5} M; CH_2Cl_2), showing the decay upon addition of a large amount of (*R,R*)-**L1** (added equiv. 0, 0.06, 0.12, 0.25, 0.5, 1, 5, 10, 20, 40, 100).

Thus, the unusual formation of 2:1 host–guest assembly, where two molecules of **calix[4]arene 5** interact with only one diamine molecule. To prove if the formation of this unexpected 2:1 complex only occurs with this particular

40

Chirality Transfer from Diamines Encapsulated within a Calixarene–Salen Host

diamine **L1**, a bulkier diamine **L2**, containing naphthyl groups, was used in the same titration studies (**Figure 2.9**). Gratifyingly, similar Cotton effects were observed (comparing with (*S*,*S*)-**L1**) when (*S*,*S*)-1,2-Bis-(1-naphthyl)-ethylenediamine (*S*,*S*)-**L2** was tested; the saturation point was reached after the addition of 0.5 equivalents of the ditopic ligand, confirming that the assembly process is independent of the nature of the diamine. However, a lower $\Delta\varepsilon$ value obtained with (S,S)-**L2** was noticed, and this effect may be explained by a poorer binding affinity between the zinc centers and the nitrogen donor atoms being under steric control.[24]
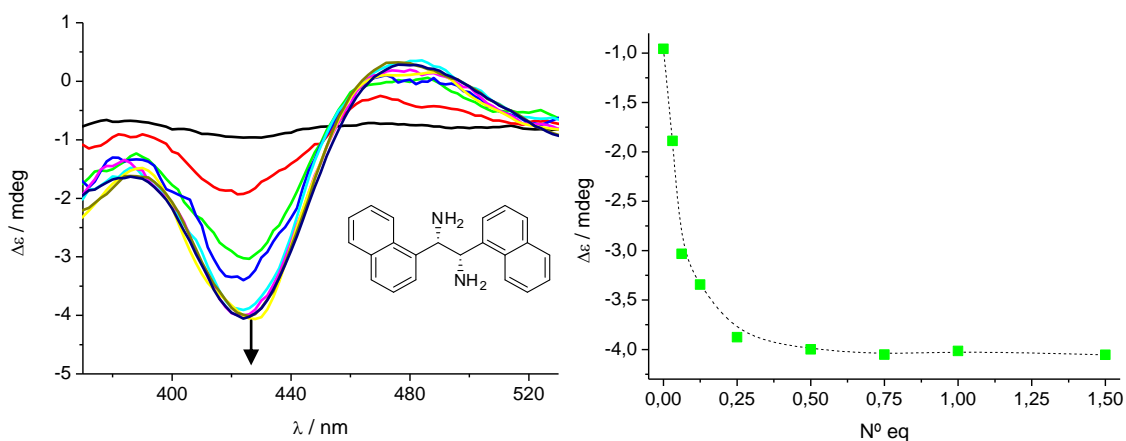
Figure 2.9: Titration plot and curve (λ = 426 nm) of host **5** (6×10^{-5} M; CH_2Cl_2) with (*S*,*S*)-**L2** (added equiv. 0, 0.03, 0.06, 0.125, 0.25, 0.5, 0.75, 1, 1.5) to a solution of **5** (6×10^{-5} M; CH_2Cl_2).

To further investigate the structure of this self-assembled complex, DFT calculations were performed (**Figures 2.10-14**). The computed structures based on the complexes with **calix[4]arene 5** (**Figure 2.10**) and diamine (*S*,*S*)-**L1** (**Figure 2.11**) in a ratio 1:1 and 2:1 with their respective and relative energies were generated and fully optimized using a ONIOM protocol. Interestingly, the 1:1 host-guest complex shows a higher degree of distortion within each Zn(salphen) unit as a consequence of the ditopic binding of diamine **L1**, increasing the overall energy of that complex (**Figure 2.12**).

41

Chapter II
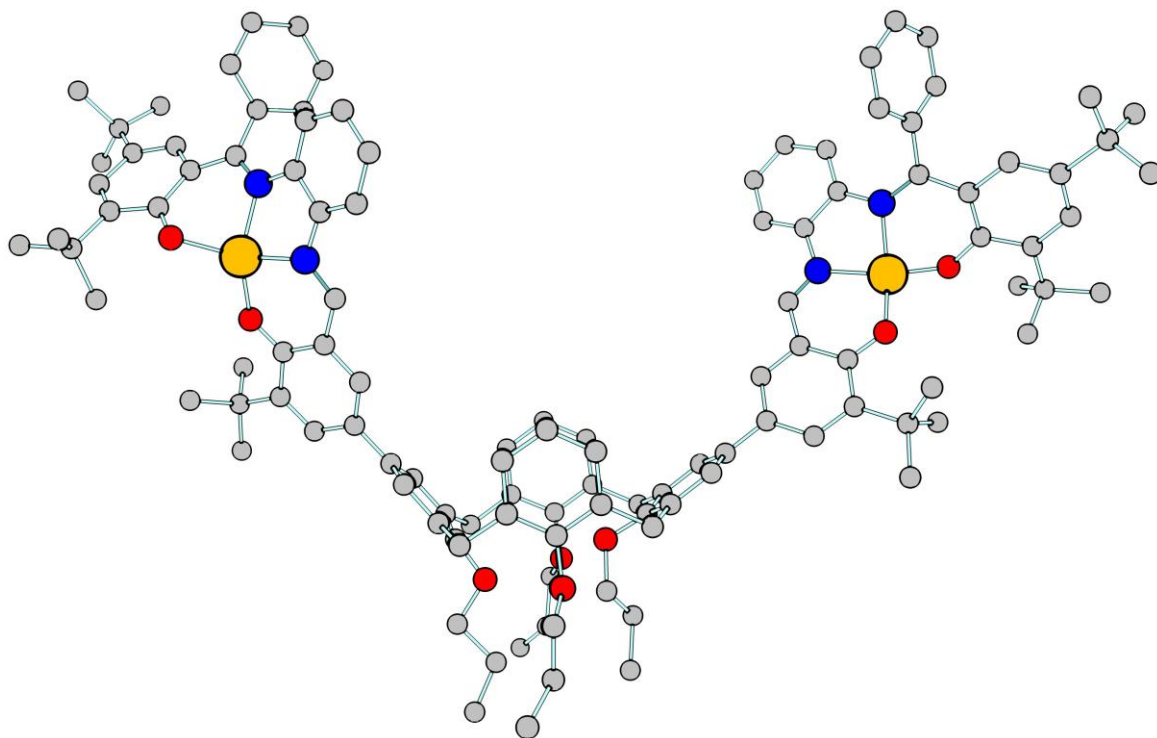
Figure 2.10: ONIOM-minimized structure of the **calix[4]arene 5** host. The hydrogen atoms have been omitted for clarity.
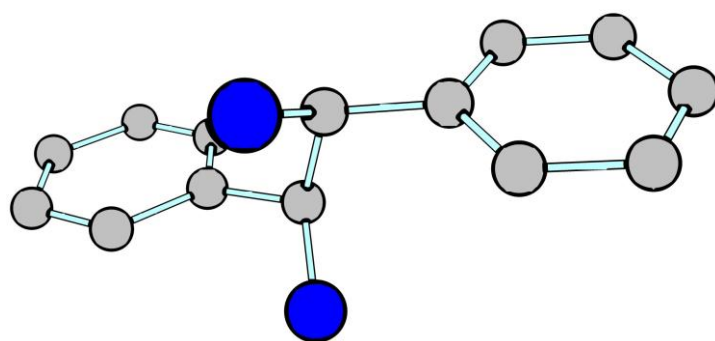
Figure 2.11: ONIOM-minimized structure of the enantiopure diamine (*S,S*)-**L1**. The hydrogen atoms have been omitted for clarity.

Chirality Transfer from Diamines Encapsulated within a Calixarene–Salen Host
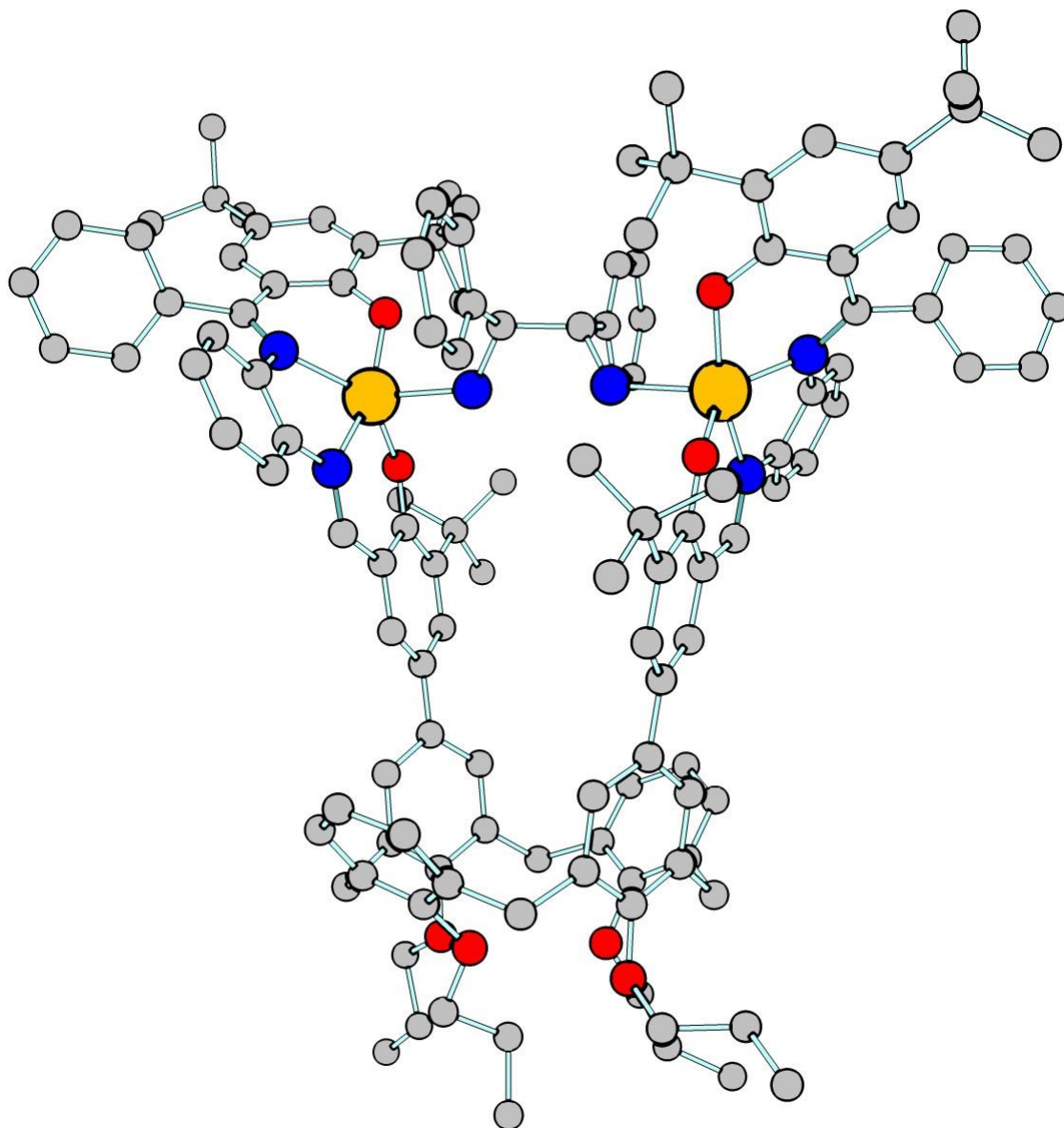
Figure 2.12: ONIOM-minimized structure of the monomer (M,M)-**calix[4]arene 5**·(*S,S*)-**L1** complex with the host and guest present in a 1:1 ratio. The hydrogen atoms have been omitted for clarity.
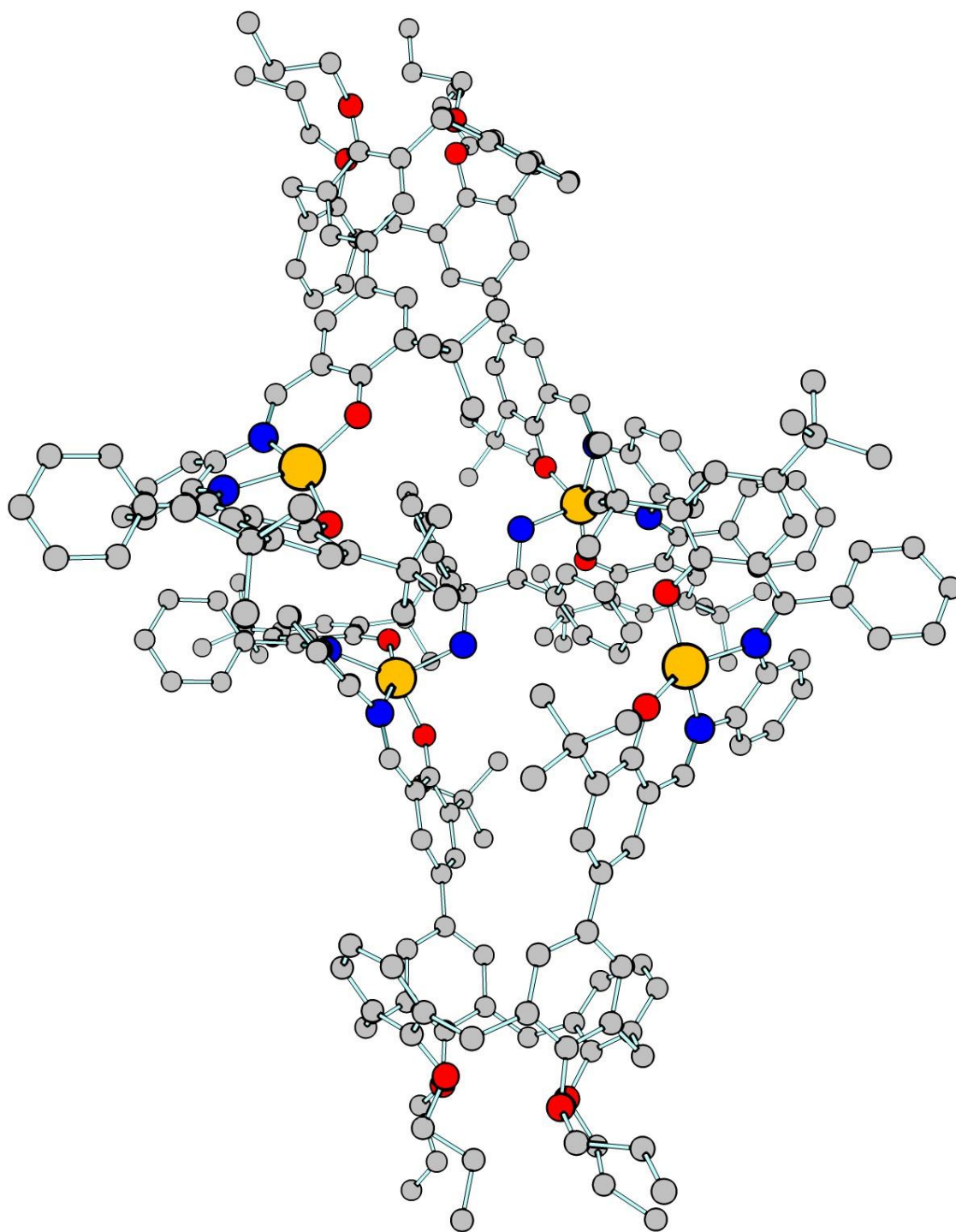
Chapter II

Figure 2.13: ONIOM-minimized structure of the capsule (M,M)-**calix[4]arene 5**·(*S,S*)-**L1** complex with the host and guest present in a 2:1 ratio. The hydrogen atoms have been omitted for clarity.

Chirality Transfer from Diamines Encapsulated within a Calixarene–Salen Host
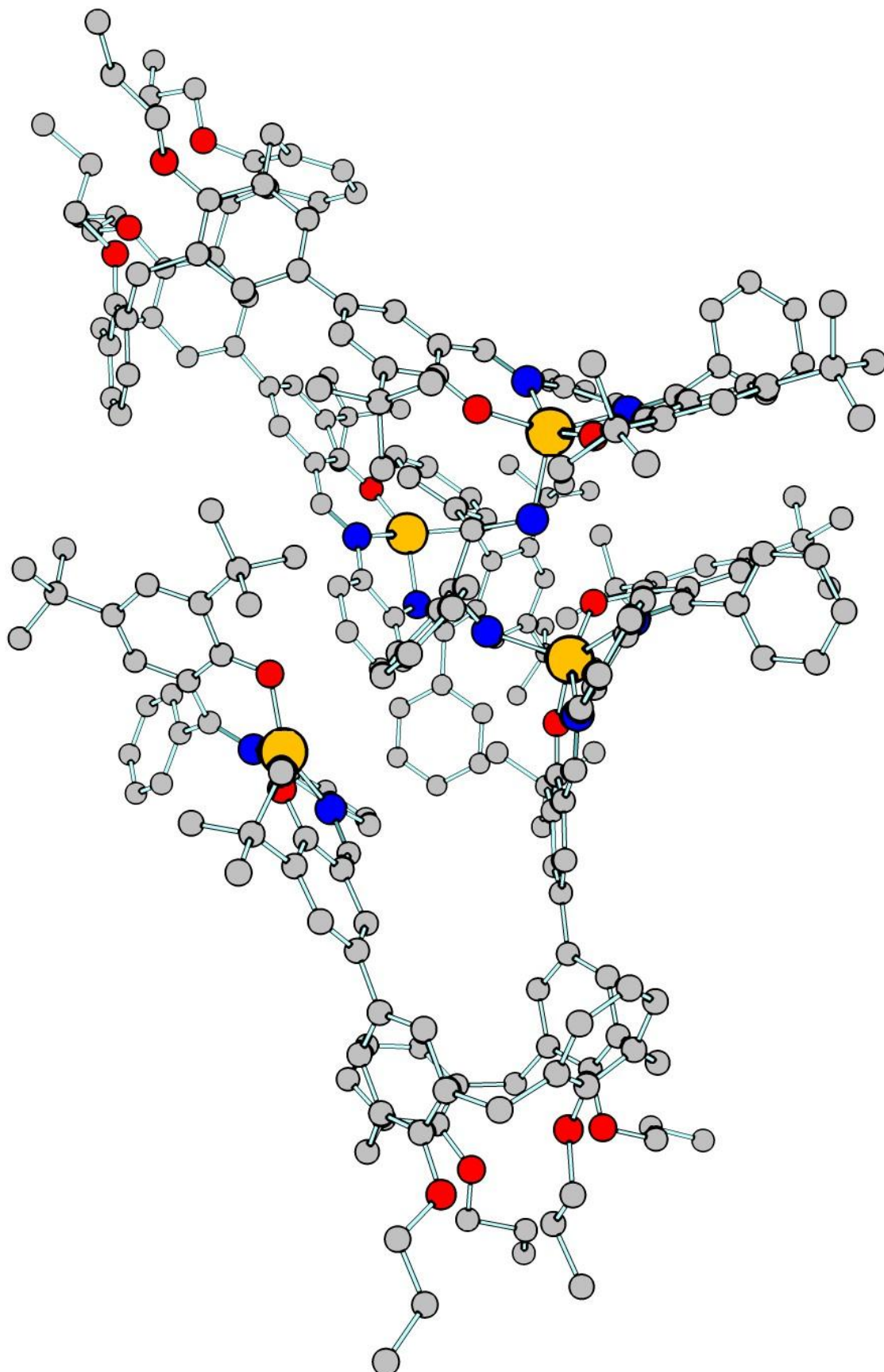
Figure 2.14: ONIOM-minimized structure of the capsule (P,P)-**calix[4]arene 5**·(*S,S*)-**L1** complex with the host and guest present in a 2:1 ratio. The hydrogen atoms have been omitted for clarity.

Chapter II

Table 2.1: Relative energies calculated for the ONIOM-minimized structure of the capsule (M,M)-**calix[4]arene 5**·(*S,S*)-**L1** complex with host/guest ratios 1:1 and 2:1.

Chiral diamine	Atropisomers	Host/ guest ratio	Energy/kcalmol^{-1}
(S,S)-DPEN	M,M	1:1	-27.3
(S,S)-DPEN	M,M	2:1	-34.9

Two key features can be observed from the calculated structures (**Table 2.1** and **Figure 2.15**). The first one is the fact that the calculated energy for the 2:1 complex is 7.6 kcal/mol lower than for the 1:1 complex (−34.9 versus −27.3 kcal/mol). The second feature is the presence of multiple π–π stacking interactions in the host-guest system, which is not observed in the 1:1 complex (**Figure 2.12**). These interactions between the phenyl groups of the guest and those of the Zn(II)salphen units likely stabilize the assembled 2:1 complex.
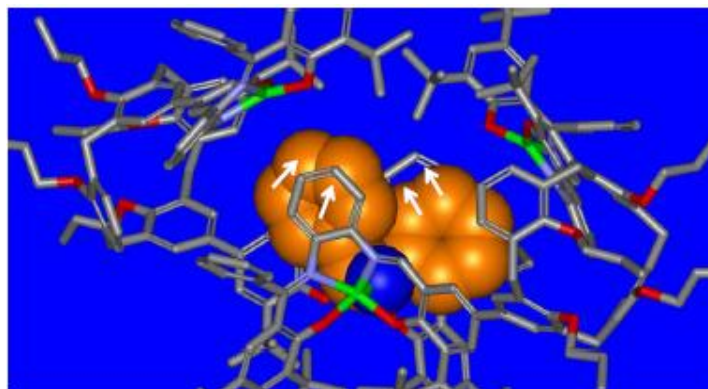
Figure 2.15: Selected zoom of the π–π stacking interactions between the aromatic fragments of the chiral diamine (*S,S*)-**L1** (space-filled) and the calixarene host **5**.

With the computed structures in hand and observing that the formation of the 2:1 complex is favoured over the 1:1, the theoretical CD spectra for both optically active stereoisomers (P,P and M,M) were computed to compare with the experimental spectrum. The calculated CD spectrum for (M,M)-**calix[4]arene 5**·(*S,S*)-**L1** showed a remarkable resemblance with the experimental one, confirming that this isomer should be the predominant species observed in solution which is in concordance with the experimental results (**Figure 2.16**). The

Chirality Transfer from Diamines Encapsulated within a Calixarene–Salen Host

large resemblance of the experimental and calculated CD traces for the 2:1 assembly is further support of a selective encapsulation process.
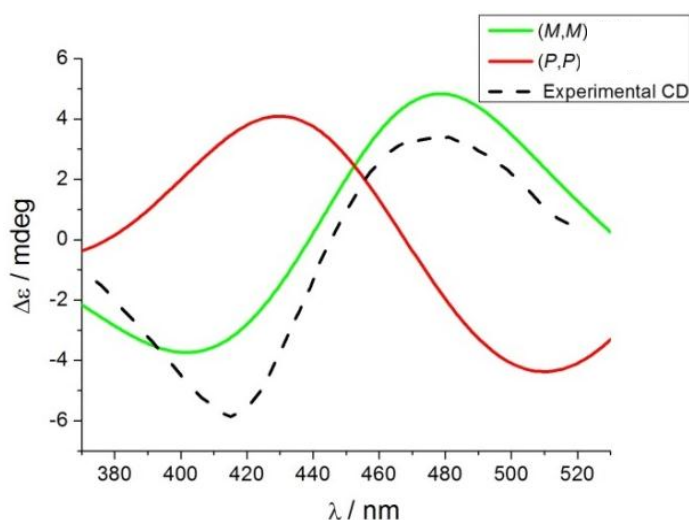
Figure 2.16: Comparison between the computed CD spectra for isomeric assemblies (P,P)-**calix[4]arene 5**·(*S,S*)-**L1** (**red** trace) and (M,M)- **calix[4]arene 5**·(*R,R*)-**L1** (**green** trace), and the experimentally observed one (**dashed** trace).

In order to obtain more information about the assembly process, DOSY NMR experiments were carried out. The diffusion coefficient value (*D*) of the capsular molecule could be obtained via ^{1}H DOSY NMR analysis using an apolar solvent (CD$_2$Cl$_2$) at room temperature, (**Figure 2.17**).
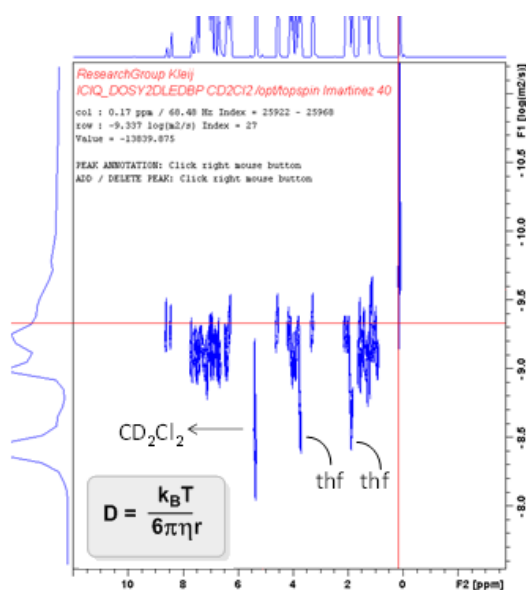
Figure 2.17: [1]H DOSY spectrum for **calix[4]arene 5**·(*S,S*)-**L1** in CD$_2$Cl$_2$**.**

Chapter II

Using the Stokes-Einstein equation for the diffusion of spherical particles,[50] the hydrodynamic radius (r) of the capsule could be estimated. The Boltzmann constant (k_B), the solvent viscosity (η = 0.43 cP for CH_2Cl_2) and the temperature (T = 298 K) are known values. The diffusion coefficient value obtained in this case for the **calix[4]arene 5·**(*S,S*)-**L1 complex,** was D = 4.60 × 10^{-10} m^2/s (log D = -9.337, **Figure 2.17**). The calculation provided a molecular radius of 11.0 Å which is close to the value (11.4 Å) obtained by averaging the radius (= diameter/2) for the height (d = 26.4 Å), width (d = 20.4 Å) and depth (d = 22.8 Å) of the ONIOM-minimized structure calculated by DFT (**Figure 2.13**).
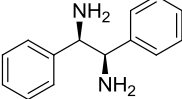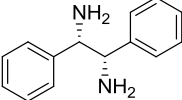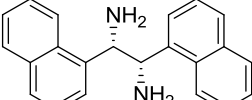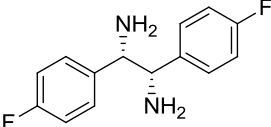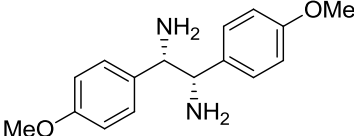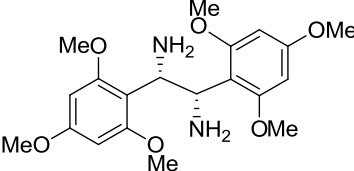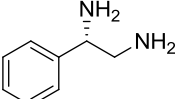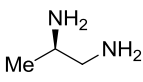
In order to further investigate the scope in diamine substrates, a series of other potentially ditopic substrates (**Table 2.2**) were then combined with host molecule **5** and recording their CD spectra. The other diamine substrates having a (*S,S*) configuration (**L2–L5**) showed similar Cotton effects as (*S,S*)-**L1** suggesting that host **5** could indeed be useful to determine the absolute configuration of chiral diamines. The presence of electron-withdrawing groups in the aromatic system, reduces the nucleophilicity of the diamines, and as consequence, lower $\Delta\varepsilon$ values are recorded in the CD spectrum (Entry 4). On the other hand electron-donating groups increase the amplitude of the Cotton effects (Entries 5 and 6).[24] Interestingly, when chiral diamines with only one chiral centre were used **L6–L7** (Entries 7 and 8), similar CD behaviour was noted as observed for (*S,S*)-**L1–L5**, and therefore the presence of only one chiral centre in the diamine substrate seems to be required for effective chirality transfer. A more rigid diamine such as **L8** did not lead to any observable chirality transfer. The rigidity of the diamine **L8** does not allow for productive complexation as noted for **L1–L7**. The fact that O–donor based amino-alcohol **L9**, amide-based **L10** and diol **L11** did not produce any useful CD output is in line with previous work on the coordination behaviour of Zn(salphen)s that prefer N–donor over alcohol ligands (**Scheme 2.6**). [51-53]

(S,S)-**L8**   (R,S)-**L9**   (S)-**L10**   (R,R)-**L11**
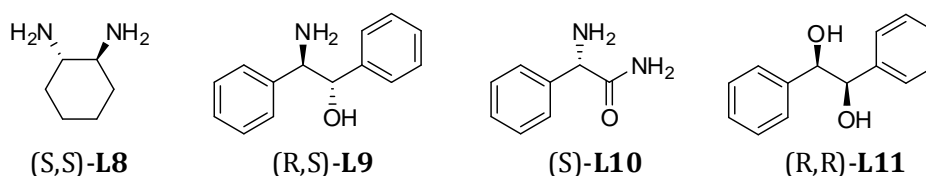
Scheme 2.6. Ditopic ligands which do not result in observable Cotton effects in the CD spectra recorded in the presence of **calixarene host 5**.

48

Chirality Transfer from Diamines Encapsulated within a Calixarene–Salen Host

Table 2.2. Chiral diamines tested in the presence of the host **5** measured after the addition of 1 equiv. of ditopic ligand to **calix[4]arene 5** in CH_2Cl_2 at 6×10^{-5} M.

Entry	Ligand	Structure	λ (nm)	Δε [M⁻¹·cm⁻¹]
1	(*R,R*)-**L1**		416 476	+5.6 −6.4
2	(*S,S*)-**L1**		416 476	−5.4 +6.6
3	(*S,S*)-**L2**		426 475	−4.0 +0.3
4	(*S,S*)-**L3**		420 484	−3.2 +1.2
5	(*S,S*)-**L4**		413 476	-9.5 +6.3
6	(*S,S*)-**L5**		424 481	-6.4 +3.0
7	(*S*)-**L6**		424 480	−1.8 0
8	(*R*)-**L7**		420 480	−2.3 0

Various ratios of (*R,R*)-**L1** and (*S,S*)-**L1** in the presence of host **5** were analysed by CD spectroscopy and the amplitude of their Cotton effects compared with the actual *e.e.* of the diamine samples (**Table 2.3**). The amplitude of the

Chapter II

Cotton effects had a linear correlation with the enantiomeric excess of the sample and the calibration showed low absolute errors in the *e.e.* determinations (around 1%), meaning that this **calix[4]arene 5** could potentially be used to measure the enantiomeric excess of diamine samples with good precision at very low concentrations (10^{-5} to 10^{-6} M) (**Figure 2.18**).
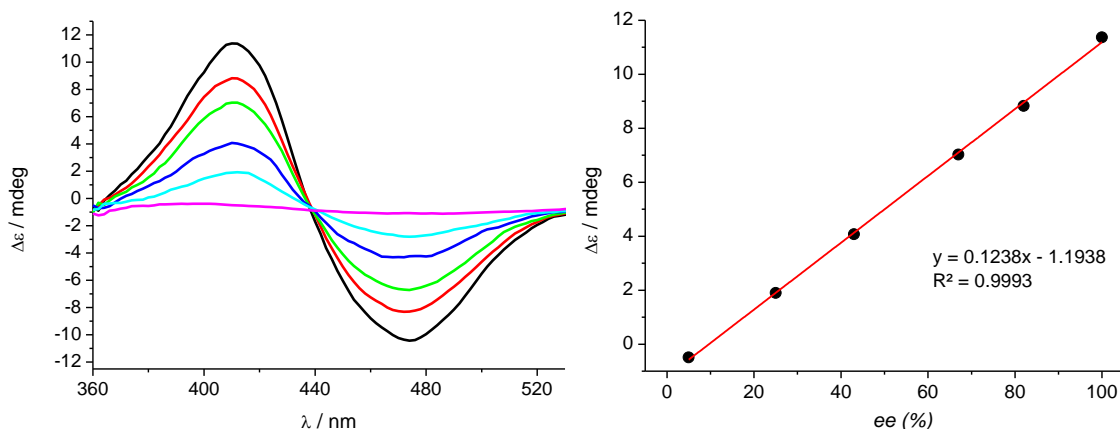
**Figure 2.18:** Calibration plot using different ratios of enantiomerically pure (*S,S*)-**L1** and (*R,R*)-**L1**.

Table 2.3: Data of the calibration plot and linear regression for chiral recognition of unknown analytes.

ee exp.	*ee* calcd.	absolute error
5	6	1%
25	25	<1%
43	43	<1%
67	66	1%
82	81	1%
100	101	1%

2.5 Binding constant and cooperativity factor

Based on the computed encapsulation mode presented in **Figure 2.13** two coordination steps may be involved. The first one is coordination of the nitrogen atom of the diamine ligand to a zinc(salphen) complex of the **calix[4]arene 5**, followed by a second coordination step to a second bis-Zn(salphen) calix host **5** (**Scheme 2.7**).

Chirality Transfer from Diamines Encapsulated within a Calixarene–Salen Host
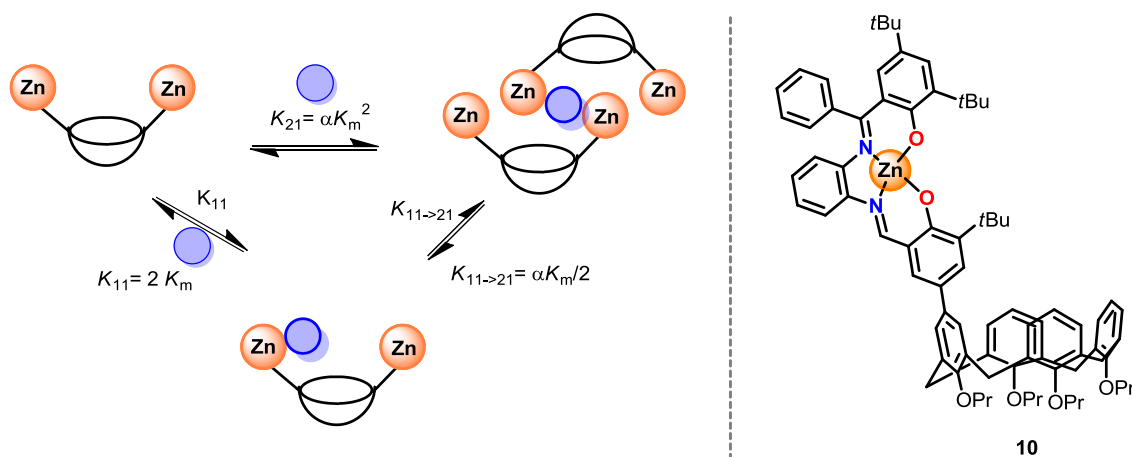
Scheme 2.7: Schematic representation of the possible interaction modes of a diamine (blue) with the calix host **5**. On the right, reference mono-nuclear calixarene **10**.

The encapsulation process is determined by the binding constant $K_{2,1}$ which represents the binding of one diamine with two equiv. of **calix[4]arene 5**. If this binding process is cooperative (*i.e.*, $K_{1,1} < K_{1,1 \to 2,1}$) then $K_{2,1} = \alpha K_M^2$ where α is the cooperativity factor and K_m represents the microscopic binding constant. The K_m value can be derived from the equation $K_{1,1} = 2K_m$ with two possible and identical binding sites for the amine. To evaluate possible cooperative effects in the formation of the **calix[4]arene 5·(L1)** capsule spectroscopic studies (UV-vis) were performed. To determine K_m the mononuclear zinc(salphen) **calix[4]arene 10** was thus prepared and titrated with a monoamine (benzylamine). The **calix[4]arene 10** was dissolved in CH_2Cl_2 (1.25×10^{-5} M) and was titrated with a solution of benzylamine in CH_2Cl_2 (2.5×10^{-2} M) adding 0, 1, 1.5, 2, 3, 6, 10 and 20 equivalents and recording the UV-vis spectra in each case. The titration plot was performed and the data was imported into SPECFIT /32 in order to get $K_{1,1}$ and gave a value of 3.14×10^5 M^{-1}. As a consequence, the association constant K_m was determined to have a value of 1.568×10^5 M^{-1}.

Chapter II
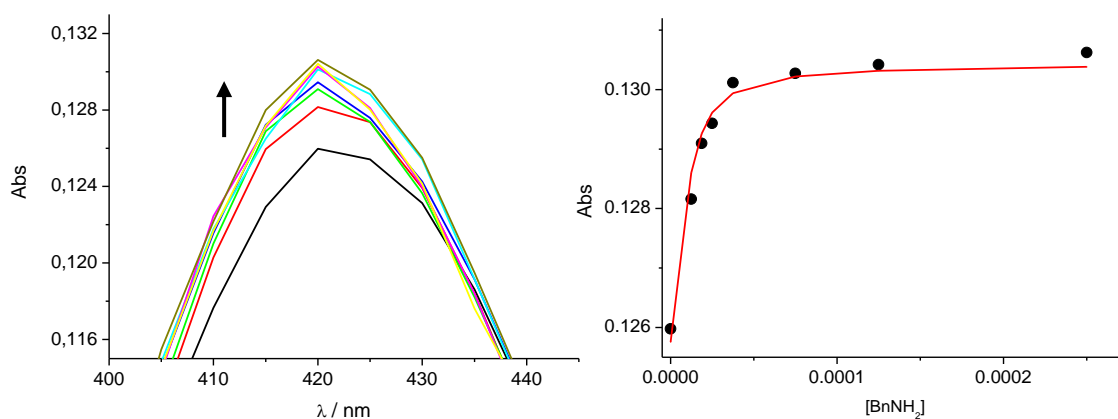
Figure 2.19: UV-vis plot of the titration of reference complex **10** (1.25×10^{-5} M; CH_2Cl_2). Adding different amounts (0, 1, 1.5, 2, 3, 6, 10, 20 equiv.) of benzylamine (2.5×10^{-2} M; CH_2Cl_2). Data fit was done at $\lambda = 556$ nm using SPECFIT/32.

Following **Scheme 2.7**, in order to get $K_{2,1}$ a titration of host **5** was performed using fluorescence spectroscopy. It is known that the sensitivity of fluorescence spectroscopy is higher than that of UV-vis and CD. Therefore, since zinc(salphen) complexes are fluorescence active, to determine $K_{2,1}$, a fluorescence titration of host **5** with (*R,R*)-**L1** as titrant was performed monitoring the changes at $\lambda = 416$ nm upon excitation. The analytical data was imported into SPECFIT/32 and the constant $K_{2,1}$ was determined (**Figure 2.20**). Surprisingly, it was found to be very high ($1.59 \pm 0.14 \times 10^{11}$ M^{-2}) supporting a high stability of the encapsulated system.
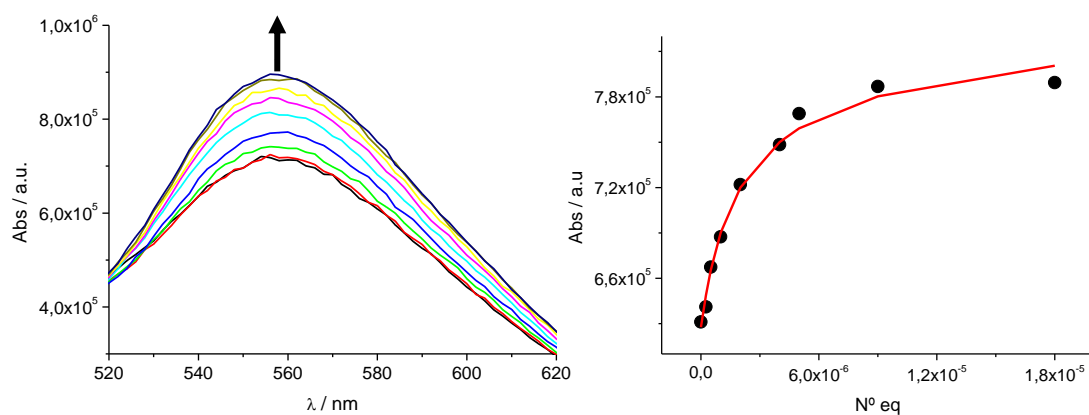
Figure 2.20: Titration of **5** (2×10^{-6} M) with (*R,R*)-**L1** (2×10^{-4} M) in dry CH_2Cl_2 (added equiv: 0, 0.125, 0.25, 0.5, 1.0, 2.0, 3.0, 5.0, 10). Data fit was done at $\lambda = 556$ nm using SPECFIT/32.

52

Chirality Transfer from Diamines Encapsulated within a Calixarene–Salen Host

Once K_m and K_{21} were determined, the cooperative constant value α (6.4) was calculated following **Scheme 2.7**, revealing that the diamine encapsulation process occurs with a high degree of cooperativity.

$$K_{21} = 1.585 \times 10^{11} \pm 0.1359 \text{ M}^{-2}.$$

$$K_m = 1.568 \times 10^5 \text{ M}^{-1}.$$

$$K_{21} = \alpha K_m^{\,2} \longrightarrow \alpha = \frac{(K_{21})^{1/2}}{(K_{11})^{1/2}}$$

$$\boxed{\alpha = 1.585 \times 10^{11} / \, 2.460 \times 10^{10} = \mathbf{6.4}.}$$

2.6 Conclusions and outlook

The design of a calix[4]arene containing two upper-rim positioned Zn(II)salphen complexes has been described. The synthetic route used to prepare host **5** was optimized to minimize undesired self-assembly between the individual Zn(salphen) units and to increase the stability of the calixarene complex. This calixarene-salphen hybrid host was then applied as molecular receptor for chiral diamines revealing an unexpected binding motif between the host and the guest; two molecules of **calix[4]arene 5** (host) bind one diamine guest to form an unusual encapsulated system with effective chirality transfer from guest to the host as supported by CD experiments. The high stability of this new host-guest system determined by various titration studies prospectively allows for the determination of low concentrations of chiral diamines, their absolute configuration and their enantiomeric excess as reported in this chapter.

Chapter II

2.7 Experimental section

Gereral methods and materials: Compound **3**,[44] mono-5-bromo-tetrapropoxycalix[4]arene **6**,[54] 3-(*tert*-butyl)-2-hydroxy-5-(4,4,5,5-tetra-methyl-1,3,2-dioxaborolan-2-yl)benzaldehyde **7**,[45] (*S*)-1-phenylethane-1,2-diamine (*S*)-**L6**,[55] and (*S*)-2-amino-2-phenylacetamine (*S*)-**L10**[56] were prepared as reported previously. All others chemicals are commercial available in Aldrich or TCI and used as received. ^{1}H NMR and ^{13}C NMR spectra were recorded on Bruker Avance 500 NMR spectrometers at 297 K. Chemical shifts are reported in ppm relative to the residual solvent peaks in CDCl$_3$ (δ = 7.26 ppm) and DMSO-d_6 (δ = 2.50 ppm). Mass analyses were carried out by the High Resolution Mass Spectrometry Unit at the ICIQ in Tarragona, Spain. UV/Vis and CD spectra were recorded on an Applied Photophysics Circular Dichroism Chirascan Spectrophotometer.

Synthesis of precursor (3,5-Di-*tert*-butyl-2-hydroxyphenyl)(phenyl)-methanone, 1: Under an argon atmosphere, 3,5-di-*tert*-butylsalicylic acid (1.0 g, 4 mmol) was dissolved in dry THF (30 ml). A phenyllithium solution (1.8 M, 13 ml, 25 mmol) was added drop-wise at 0ºC. The solution was then stirred at 10ºC for 18 h. Then, freshly distillated Me$_3$SiCl (7 ml, 56 mmol) was added, and the reaction mixture was stirred for 1 h. Diluted HCl (3 M, 30 ml) was then added, and the organic phase was extracted with diethyl ether and the combined extracts dried over Na$_2$SO$_4$. The product **1** was purified by column chromatography (5/95 up to 10/90 v/v ethyl acetate/hexane) to give a yellow solid. Yield: 92%. ^{1}H NMR (500 MHz, CDCl$_3$): δ = 1.25 (s, 9H), 1.49 (s, 9H), 7.44 (d, *J* = 2.4 Hz, 2H), 7.71-7.48 (m, 5H), 12.71 (s, 1H); ^{13}C NMR (125 MHz, CDCl$_3$): δ = 29.6, 31.4, 34.4, 35.4, 118.2, 128.0, 128.3, 129.4, 131.4, 131.7, 138.0, 138.9, 140.0, 160.1, 202.7. HRMS (ESI+, MeOH): calcd for C$_{21}$H$_{26}$O$_2$Na [M + Na]$^+$: 333.1825; found: 333.1828.

Synthesis of precursor (*E*)-2-((2-Aminophenyl)imino)-(phenyl)methyl)-4,6-di-*tert*-butylphenol, 2: Compound **1** (273 mg, 0.88 mmol) was dissolved in toluene (20 ml) and *o*-phenylenediamine (191 mg, 1.76 mmol) and *p*-toluenesulfonic acid (8 mg, 0.09 mmol) was added to the mixture. The reaction was performed using a Dean-Stark apparatus (180ºC) for 30 h. Then, the reaction was

54

Chirality Transfer from Diamines Encapsulated within a Calixarene–Salen Host

cooled down and the precipitated solid was filtered off and washed with MeOH to obtain **2** as a yellow solid. Yield: 74%. ^{1}H NMR (500 MHz, CDCl$_3$): δ = 1.15 (s, 9H), 1.51 (s, 9H), 3.84 (s, 2H), 6.27 (dd, J = 1.5; 8.0 Hz, 1H), 6.40 (td, J = 1.4; 7.6 Hz, 1H), 6.67 (dd, J = 1.4; 8.0 Hz, 1H), 6.81 (td, J = 1.5; 7.6 Hz, 1H), 6.96 (d, J = 2.5, 1H), 7.17-7.23 (m, 2H), 7.30-7.34 (m, 3H), 7.46 (d, J = 2.5 Hz, 1H), 14.90 (s, 1H). ^{13}C NMR (125 MHz, CDCl$_3$): δ = 29.7, 31.4, 34.3, 35.4, 115.2, 118.1, 119.0, 122.2, 125.6, 127.0, 128.1, 128.3, 128.5, 129.1, 134.2, 135.1, 136.7, 137.4, 139.1, 139.4, 159.9, 176.2. HRMS (ESI+, MeOH): calcd for C$_{27}$H$_{33}$ON$_2$ [M + H]$^+$: 401.2587; found: 401.2584.

Synthesis of precursor Bis-(4,6-di-*tert*-butylphenol-salphen)calix[4]arene ligand, 4: Compounds **3** (150 mg, 0.16 mmol) and **2** (134 mg, 0.33 mmol) were dissolved in a 50/50 v/v MeOH/CHCl$_3$ (10 ml). The mixture was kept at reflux temperature for 48 h (until all the aldehyde was consumed as followed by TLC). Then the solvent was evaporated to afford a yellow solid, which was washed and triturated with MeOH. Yield: 70%. ^{1}H NMR (500 MHz, CDCl$_3$): δ = 0.88-1.00 (m, 12H), 1.11 (s, 18H), 1.36 (s, 18H), 1.53 (s, 18H), 1.84-2.03 (m, 8H), 3.23 (d, J = 13.5 Hz, 4H), 3.66-3.80 (m, 4H), 3.99-4.12 (m, 4H), 4.52 (d, J = 13.0 Hz, 4H), 6.16-6.35 (m, 8H), 6.86-6.92 (m, 2H), 7.03-7.33 (m, 18H), 7.46 (d, J = 9.5 Hz, 4H), 7.63 (s, 2H), 8.53 (s, 2H), 13.88 (s, 2H), 14.70 (s, 2H). ^{13}C NMR (125 MHz, CDCl$_3$): δ = 10.0, 11.0, 23.2, 23.7, 29.4, 29.8, 31.1, 31.4, 34.2, 35.2, 35.4, 76.6, 77.4, 118.4, 118.5, 119.3, 122.3, 123.6, 125.3, 126.8, 127.0, 127.7, 128.3, 128.4, 128.8, 129.3, 131.2, 133.2, 134.4, 135.6, 137.4, 138.2, 138.7, 139.5, 142.1, 155.4, 157.4, 160.0, 160.3, 162.8, 176.0. HRMS (ESI+, MeOH): calcd for C$_{116}$H$_{133}$O$_8$N$_4$ [M + H]$^+$: 1710.0118; found: 1710.0064.

Synthesis of Bis-(4,6-di-*tert*-butylphenol-salphen)calix[4]arene zinc complex, 5: Under an argon atmosphere, compound **4** (100 mg, 0.059 mmol) was dissolved in dry THF (10 ml), and then a solution of ZnEt$_2$ (1M, 0.12 ml, 0.118 mmol) was added drop-wise and the reaction mixture was stirred for 4 h. Then, the solvent was evaporated to afford a bright orange solid. Yield: 83%. ^{1}H NMR (500 MHz, DMSO-d_6): δ = 0.91 (t, J = 7.5 Hz, 6H), 1.02 (s, 18H), 1.09-1.15 (m, 24H), 1.45 (s, 18H), 1.83-1.90 (m, 4H), 1.95-2.03 (m, 4H), 3.22-3.26 (m, 4H), 3.62-3.68

Chapter II

(m, 4H), 4.01-4.07 (m, 4H), 4.38-4.45 (m, 4H), 4.94 (s, 4H), 6.21-6.28 (m, 8H), 6.33 (d, J = 6.7 Hz, 2H), 6.48 (d, J = 7.9 Hz, 2H), 6.57-6.81 (m, 4H), 7.07 (t, J = 8.0 Hz, 2H), 7.23-7.28 (m, 4H), 7.37-7.45 (m, 10H), 7.56-7.69 (m, 4H), 9.04 (s, 2H). ^{13}C NMR (125 MHz, DMSO-d_6): δ = 10.0, 11.0, 22.8, 23.3, 29.6, 29.8, 30.3, 31.3, 33.6, 35.0, 35.3, 35.6, 76.1, 77.0, 114.7, 115.9, 119.1, 119.7, 121.9, 125.5, 126.0, 126.4, 127.3, 127.6, 128.0, 128.2, 128.5, 129.0, 132.0, 132.9, 134.9, 136.5, 136.8, 140.2, 140.3, 140.7, 141.2, 141.7, 155.0, 156.0, 159.6, 162.9, 170.1, 171.4, 174.2, 175.8. HRMS (MALDI+, dctb): calcd for $C_{116}H_{130}O_8N_4Zn_2$ [M + Na]$^+$: 1836.8628; found: 1836.8772.

Synthesis of precursor 5-Mono-[1-(3-*tert*-butyl-2-hydroxy-1-formylphenyl)]-25,26,27,26-tetra-propoxy-calix[4]arene, 8: Under an argon atmosphere, Pd(OAc)$_2$ (10 mg, 0.045 mmol) and P(o-tol)$_3$ (27 mg, 0.089 mmol) were dissolved in previously deoxygenated toluene (25 ml). After stirring the mixture for 30 min, mono-5-bromo-tetrapropoxycalix[4]arene **6** (500 mg, 0.74 mmol)[53] and 3-(*tert*-butyl)-2-hydroxy-5-(4,4,5,5-tetramethyl-1,3,2-dioxaborolan-2-yl)-benzaldehyde (268 mg, 0.88 mmol)[43] were dissolved in deoxygenated MeOH (5 ml) and added to the mixture with an aqueous solution of K$_2$CO$_3$ (2 M, 5 mL). After 40 h stirring at 65º C, the reaction mixture was cooled down and water (10 mL) and HCl (1 M, 5 mL) were added. The crude product was filtered through Celite and extracted three times with ethyl acetate. The organic phases were combined and dried over Na$_2$SO$_4$. The solvent was evaporated and the white solid obtained further triturated with MeOH. Yield: 71%. ^{1}H NMR (500 MHz, CDCl$_3$): δ = 0.95 (t, J = 7.4 Hz, 6H), 1.04 (t, J = 7.4 Hz, 3H), 1.07 (t, J = 7.4 Hz, 3H), 1.40 (s, 9H), 1.86-2.01 (m, 8H), 3.15 (d, J = 13.4 Hz, 2H), 3.20 (d, J = 13.4 Hz, 2H), 3.76 (t, J = 7.1 Hz, 2H), 3.81 (t, J = 7.1 Hz, 2H), 3.91-3.98 (m, 4H), 4.46 (d, J = 13.4 Hz, 2H), 4.50 (d, J = 13.4 Hz, 2H), 6.06 (t, J = 7.5 Hz, 1H), 6.31 (d, J = 7.5 Hz, 2H), 6.51 (s, 2H), 6.74 (t, J = 7.5 Hz, 2H), 6.85 (d, J = 7.5 Hz, 2H), 6.89 (d, J = 7.5 Hz, 2H), 7.22 (d, J = 7.5 Hz, 2H), 9.86 (s, 1H), 11.65 (s. 1H). ^{13}C NMR (125 MHz, CDCl$_3$): δ = 10.3, 10.7, 23.3, 23.5, 23.6, 29.4, 29.8, 31.1, 31.3, 35.0, 77.0, 77.1, 77.4, 120.6, 121.8, 122.0, 126.2, 127.7, 128.7, 128.8, 129.7, 132.9, 133.4, 133.7, 134.4, 134.9, 136.0, 136.3, 138.0, 155.8, 156.1, 157.4, 160.0, 197.5. HRMS (ESI+, MeOH): calcd for $C_{51}H_{60}O_6Na$ [M + Na]$^+$: 791.4282; found: 791.4281.

Chirality Transfer from Diamines Encapsulated within a Calixarene–Salen Host

Synthesis of precursor 5-Mono-(4,6-di-*tert*-butylphenol-salphen)calix[4] arene ligand, 9: Compounds **8** (100 mg, 0.13 mmol) and **2** (78 mg, 0.20 mmol) were dissolved in a 1:1 v/v MeOH/CHCl$_3$ (5 ml). The mixture was stirred and kept at reflux temperature for 30 h, and showed then full consumption of the aldehyde reagent by TLC. Then the solvent was evaporated to afford a yellow solid, which was triturated with MeOH. Yield: 62%. ^{1}H NMR (500 MHz, CDCl$_3$): δ = 0.96 (t, J = 7.4 Hz, 6H), 1.01-1.06 (m, 6H), 1.09 (s, 9H), 1.27 (s, 9H), 1.51 (s, 9H), 1.86-1.98 (m, 8H), 3.17 (dd, J = 6.7; 13.5 Hz, 4H), 3.78 (t, J = 7.3 Hz, 2H), 3.83 (t, J = 7.3 Hz, 2H), 3.92 (t, J = 7.5 Hz, 4H), 4.47 (t, J = 13.5 Hz, 4H), 6.15 (t, J = 7.5 Hz, 1H), 6.38 (d, J = 7.5 Hz, 2H), 6.58 (s, 2H), 6.69 (t, J = 7.5 Hz, 2H), 6.76-6.91 (m, 6H), 7.00-7.13 (m, 8H), 7.20 (t, J = 7.3 Hz, 2H), 7.42 (d, J = 2.3 Hz, 1H), 8.31 (s, 1H), 13.72 (s, 1H), 16.64 (s, 1H). ^{13}C NMR (125 MHz, CDCl$_3$): δ = 10.3, 10.6, 10.7, 23.3, 23.5, 23.6, 29.3, 29.8, 31.1, 31.3, 31.4, 34.1, 35.0, 35.4, 118.2, 118.5, 119.1, 122.0, 123.6, 125.2, 126.3, 126.7, 127.6, 128.8, 128.2, 128.6, 128.7, 128.8, 128.9, 129.6, 131.5, 134.5, 134.6, 134.9, 135.6, 135.8, 136.0, 137.4, 137.6, 138.7, 139.6, 142.1, 155.6, 156.2, 157.3, 159.7, 160.2, 162.8, 175.9. HRMS (ESI+, MeOH): calcd for C$_{78}$H$_{91}$N$_2$O$_6$ [M + H]$^+$: 1151.6872; found: 1151.6850.

Synthesis of 5-Mono-(4,6-di-*tert*-butylphenol-salphen)calix[4]arene Zinc complex, 10: Under an argon atmosphere, precursor compound **9** (100 mg, 0.086 mmol) was dissolved in dry THF (10 ml) and then a solution of ZnEt$_2$ (1 M, 0.09 ml, 0.09 mmol) was added drop-wise, and the mixture was further stirred for 4 h. The solvent was evaporated to afford a bright orange solid. Yield: 99%. ^{1}H NMR (500 MHz, DMSO-d_6): δ = 0.96 (t, J = 7.5 Hz, 6H), 0.99-1.05 (m, 15H), 1.39 (s, 9H), 1.52 (s, 9H), 1.87 (dt, J = 7.3; 14.3 Hz, 8H), 3.14-3.24 (m, 4H), 3.70-3.88 (m, 4H), 4.30-4.42 (m, 4H), 6.04 (t, J = 7.7 Hz, 1H), 6.33 (d, J = 7.5 Hz, 2H), 6.57 (s, 2H), 6.68 (t, J = 7.3 Hz, 2H), 6.76-6.88 (m, 6H), 6.96 (s, 1H), 7.03-7.42 (m, 14H), 8.88 (s, 1H). ^{13}C NMR (125 MHz, DMSO-d_6): δ = 10.2, 10.4, 10.5, 22.8, 22.9, 23.0, 29.4, 29.5, 29.7, 30.2, 30.4, 30.7, 31.0, 31.1, 33.5, 34.6, 34.9, 35.0, 35.4, 76.3, 116.4, 118.9, 119.1, 121.5, 121.6, 121.8, 124.6, 124.7, 125.2, 125.3, 125.7, 126.5, 127.5, 128.0, 128.2, 128.3, 128.9, 129.7, 131.3, 131.8, 134.2, 134.4, 134.6, 135.1, 136.2, 137.8, 139.9, 140.0, 141.0, 154.3, 155.8, 155.9, 156.3, 156.6, 162.6, 170.9, 171.0, 174.0. HRMS (MALDI+, dctb): calcd for C$_{78}$H$_{88}$N$_2$O$_6$Zn [M]$^+$: 1212.5934; found: 1212.5929.

Chapter II

Obtaining UV/CD spectra: To obtain a typical spectrum data, **calix[4]arene 5** was dissolved at a concentration of 6×10^{-5} M in CH_2Cl_2. 0.5 mL of this solution was transferred into a cuvet and 1.0 equivalent of the corresponding ditopic ligand (6×10^{-3} M) in CH_2Cl_2 was added. The mixture was mixed thoroughly and the UV/CD-spectra recorded subsequently. Typically, the Cotton effects were noted around 380 to 520 nm. Eighth different chiral diamines, one aminoalcohol, one aminoamide and one diol were used as potential ditopic guests (**Scheme 2.6** and **Table 2.2**).

UV-vis/CD/fluorescence titration studies: To determine the binding constant between the host and guest, titration studies were performed using complex **5** as host and (R,R)-**L1** or (S,S)-**L1** as chiral guest to obtain the titration data and corresponding titration curve. The host **5** was dissolved in CH_2Cl_2 (6×10^{-5} M) and 0.5 mL of this solution was transferred to an UV-cuvet. The guest (R,R)-**L1** was dissolved in CH_2Cl_2 (6×10^{-3} M and 6×10^{-4} M solutions were prepared). Different amounts of the guest solution were added and the UV-vis (360-480 nm) and CD spectra (380-520 nm) were recorded. The amount of guest used were 0, 0.06, 0.12, 0.18, 0.25, 0.31, 0.37, 0.43, 0.50, 0.62, 0.75, 1.00, 1.50 equivalents. The titration curve at λ = 416 nm was then determined.

DFT calculations: The DFT calculations were performed in collaboration with the group of Carles Bo (ICIQ). The Gaussian 09 software package[57] was used in a two tier (ONIOM2) approach.[58] The high layer was constituted of the simpler [Zn(salphen)] moiety and the bridging diamine whereas the remainder of the organic framework was modelled as the low layer. The high layer was described with the density functional approach, namely the B3LYP gradient-corrected hybrid three parameter functional[59-60] built upon the Slater local exchange,[61] and the Vosko, Wilk and Nusair's local[62] correlation (VWN formula 3) functionals. The basis set was of the Pople, type contracted 6–31G(d,p) split-valence basis set for all elements. The low layer was described through the semi-empirical parametric model 6 (PM6) of Stewart[63] employing valence-only Slater-type orbitals approximated by a primitive set of six Gaussian functions (STO-6G) on all the atoms. The layer interface was composed of hydrogen link atoms. The total energy

58

Chirality Transfer from Diamines Encapsulated within a Calixarene–Salen Host

of the system can thus be computed[58] as: E(ONIOM2)=$E_{\text{high layer}}$ (subsystem)+$E_{\text{low layer}}$ (full system)− $E_{\text{low layer}}$ (subsystem). The geometries were optimized without any constraints until the default convergence criteria were met. The electronic circular dichroism (ECD) rotatory strength values of the dinuclear complexes were computed with time dependent density functional theory (TDDFT)[64-65] as implemented in Gaussian 09 selecting thirty singlet to singlet transitions in an all electron single point calculation. The computed intensities were broadened by a Gaussian function to be comparable to the experimentally determined spectrum. For the tetranuclear complexes, the calculation of ECD spectra in Gaussian 09 was exceedingly demanding, as it involves a very large number of excitations, so it was opted to compute these ECD transitions with the ADF[66] program, in which a single-point calculation was performed on the previously optimized ONIOM geometry. A double-zeta basis set was employed on all the light atoms while employing a triple-zeta basis set on zinc. One advantage in favor of expediting this demanding calculation was the inclusion of [He] and [Ne] frozen cores on the light elements (apart from hydrogen) and zinc, respectively. The basis sets were further augmented with one polarization d function for C, N, and O and a p function for Zn. A total of three hundred singlet-to-singlet excitations were calculated to reproduce the excitation spectra of the tetranuclear zinc complexes. The GGA class BLYP functional was employed rather than the aforementioned B3LYP used in Gaussian to eschew the computation of exact exchange integrals.

2.8 References and notes:

[1] G. A. Hembury, V. V. Borovkov, Y. Inoue, *Chem. Rev.*, **2008**, *108*, 1.
[2] *Biochemistry*, 2nd ed. Ed: D. Voet, J. G. Voet, John Wiley & Sons, New York, **1995**.
[3] M. R. Ringenberg, T. R. Ward, *Chem. Commun.*, **2011**, *47*, 8470.
[4] P. Dydio, C. Rubay, T. Gadzikwa, M. Lutz, J. N. H. Reek, *J. Am. Chem. Soc.*, **2011**, *133*, 17176.
[5] A. J. Boersma, J. E. Klijn, B. L. Feringa, G. Roelfes, *J. Am. Chem. Soc.,* **2008**, *130*, 11783.
[6] C. J. Brown, R. G. Bergman, K. N. Raymond, *J. Am. Chem. Soc.*, **2009**, *131*, 17530.

Chapter II

[7]   S. Vazquez-Campos, M. Crego-Calama, D. N. Reinhoudt, *Supramol. Chem.*, **2007**, *19*, 95.

[8]   G. Seeber, B. E. F. Tiedemann, K. N. Raymond, *Top. Curr. Chem.*, **2006**, *265*, 147.

[9]   H. Qiu, Y. Inoue, S. Che, *Angew. Chem. Int. Ed.*, **2009**, *48*, 3069.

[10]   J. Wang, B. L. Feringa, *Science*, **2011**, *331*, 1429.

[11]   N. Liu, G. R. Darling, R. Raval, *Chem. Commun.*, **2011**, *47*, 11324.

[12]   G. Haberhauer, *Angew. Chem. Int. Ed.*, **2010**, *49*, 9286.

[13]   P. K. Hashim, N. Tamaoki, *Angew. Chem. Int. Ed.*, **2011**, *50*, 11729.

[14]   K. Rijeesh, P. K. Hashim, S.-I. Noro, N. Tamaoki, *Chem. Sci.*, **2015**, *6*, 973.

[15]   H. Hayasaka, T. Miyashita, M. Nakayama, K. Kuwada, K. Akagi, *J. Am. Chem. Soc.*, **2012**, *134*, 3758.

[16]   K. W. Bentley, Y. G. Nam, J. M. Murphy, C. Wolf, *J. Am. Chem. Soc.*, **2013**, *135*, 18052.

[17]   L. A. Joyce, M. S. Maynor, J. M. Dragna, G. M. da Cruz, V. M. Lynch, J. W. Canary, E. V. Anslyn, *J. Am. Chem. Soc.*, **2011**, *133*, 13746.

[18]   L. You, G. Pescitelli, E. V. Anslyn, L. Di Bari, *J. Am. Chem. Soc.*, **2012**, *134*, 7117.

[19]   M. Anyika, H. Gholami, K. D. Ashtekar, R. Acho, B. Borhan, *J. Am. Chem. Soc.*, **2014**, *136*, 550.

[20]   S. Nieto, V. M. Lynch, E. V. Anslyn, H. Kim, J. Chin, *J. Am. Chem. Soc.*, **2008**, *130*, 9232.

[21]   M. Yamamura, T. Saito, T. Nabeshima, *J. Am. Chem. Soc.*, **2014**, *136*, 14299.

[22]   M. Balaz, A. E. Holmes, M. Benedetti, P. C. Rodriguez, N. Berova, K. Nakanishi, G. Proni, *J. Am. Chem. Soc.*, **2005**, *127*, 4172.

[23]   J. Cheymol , *Revista da Associacao Medica Brasileira*, **1965**, *11*, 123.

[24]   K. Nakanishi, N. Berova, R. W. Woody, *Circular Dichroism, Principles and Applications*, VCH, New York, **1994**.

[25]   V. V. Borovkov, G. A. Hembury, Y. Inoue, *Acc. Chem. Res.*, **2004**, *37*, 449.

[26]   J. Etxebarria, A. Vidal-Ferran, P. Ballester, *Chem. Commun.*, **2008**, 5939.

[27]   V. V. Borovkov, I. Fujii, A. Muranaka, G. A. Hembury, T. Tanaka, A. Ceulemans, N. Kobayashi, Y. Inoue, *Angew. Chem. Int. Ed.*, **2004**, *43*, 5481.

[28]   V. V. Borovkov, G. A. Hembury, Y. Inoue, *Angew. Chem. Int. Ed.*, **2003**, *42*, 5310.

[29]   M. Siczek, P. J. Chmielewski, *Angew. Chem. Int. Ed.*, **2007**, *46*, 7432.

[30]   I. C. Pintre, S. Pierrefixe, A. Hamilton, V. Valderrey, C. Bo, P. Ballester, *Inorg. Chem.*, **2012**, *51*, 4620.

[31]   X. Huang, N. Fujioka, G. Pescitelli, F. E. Koehn, R. T. Williamson, K. Nakanishi, N. Berova, *J. Am. Chem. Soc.*, **2002**, *124*, 10320.

[32]   A. W. Kleij, *Chem. Eur. J.*, **2008**, *14*, 10520.

[33]   E. N. Jacobsen, *Comprehensive Organometallic Chemistry II, Vol. 12*, Ed: E. W. Abel, F. G. A. Stone, E. Willinson, pp. 1097, Pergamon, New York, **1995**.

[34]   S. J. Wezenberg, A. W. Kleij, *Angew. Chem. Int. Ed.*, **2008**, *47*, 2354.

[35]   A. W. Kleij, *Dalton Trans.*, **2009**, 4635.

[36]   S. J. Wezenberg, G. Salassa, E. C. Escudero-Adán, J. Benet-Buchholz, A. W. Kleij, *Angew. Chem. Int. Ed.*, **2011**, *50*, 713.

[37]   C. J. Whiteoak, G. Salassa, A. W. Kleij, *Chem. Soc. Rev.*, **2012**, 41, 622.

[38]   G. Salassa, M. J. J. Coenen, S. J. Wezenberg, B. L. M. Hendriksen, S. Speller, J. A. A. W. Elemans, A. W. Kleij, *J. Am. Chem. Soc.*, **2012**, *134*, 7186.

Chirality Transfer from Diamines Encapsulated within a Calixarene–Salen Host

[39] A. W. Kleij, M. Kuil, M. Luts, D. M. Tooke, A. L. Spek, P. C. J. Kamer, P. W. N. M. van Leeuwen, J. N. H. Reek, *Inor. Chim. Acta*, **2006**, *359*, 1807.

[40] M. V. Escarcega-Bobadilla, G. Salassa, M. Martinez-Belmonte, E. C. Escudero-Adan, A. W. Kleij, *Chem. Eur. J.*, **2012**, *18*, 6805.

[41] L. Qiu, F. Y. Kwong, J. Wu, W. H. Lam, S. Chan, W.-Y. Yu, Y.-M. Li, R. Guo, Z. Zhou, A. S. C. Chan, *J. Am. Chem. Soc.*, **2006**, *128*, 5955.

[42] M. Albrecht, *Chem. Rev.*, **2001**, *101*, 3457.

[43] M. V. Escárcega-Bobadilla, G. A. Zelada-Guillén, S. V. Pyrlin, M. Wegrzyn, M. M.D. Ramos, E. Giménez, A. Stewart, G. Maier, A. W. Kleij, *Nat. Commun.*, **2013**, *4*, 2648.

[44] S. J. Wezenberg, A. W. Kleij, *Adv. Synth. Catal.*, **2010**, *352*, 85.

[45] J. Y. Jang, D. G. Nocera, *J. Am. Chem. Soc.*, **2007**, *129*, 8192.

[46] M. W. Ghosn, C. Wolf, *J. Org. Chem.*, **2011**, *76*, 3888.

[47] J. Etxebarria, H. Degenbeck, A.-S. Felten, S. Serres, N. Nieto, A. Vidal-Ferran, *J. Org. Chem.*, **2009**, *74*, 8794.

[48] M. Martínez-Belmonte, S. J. Wezenberg, R. M. Haak, D. Anselmo, E. C. Escudero-Adan, J. Benet-Buchholz, A. W. Kleij, *Dalton Trans.*, **2010**, *39*, 4541.

[49] J. A. A. W. Elemans, S. J. Wezenberg, M. J. J. Coenen, E. C. Escudero-Adan, J. Benet-Buchholz, D. den Boer, S. Speller, A. W. Kleij, S. De Feyter, *Chem. Commun.*, **2010**, *46*, 2548.

[50] P. Timmerman, J.-L. Wiedmann, K. A. Jolliffe, L. J. Prins, D. N. Reinhoudt, S. Shinkai, L. Frish, Y. Cohen, *J. Chem. Soc. Perkin Trans.*, **2000**, *2*, 2077.

[51] A. W. Kleij, D. M. Tooke, M. Kuil, M. Lutz, A. L. Spek, J. N. H. Reek, *Chem. Eur. J.*, **2005**, *11*, 4743.

[52] S. J. Wezenberg, E. C. Escudero-Adán, J. Benet-Buchholz, A. W. Kleij, *Inorg. Chem.,* **2008**, *47*, 2925.

[53] E. Martin, M. Martínez Belmonte, E. C. Escudero-Adán, A. W. Kleij, *Eur. J. Inorg. Chem.*, **2014**, 4632.

[54] M. Cavazzini, A. Manfredi, F. Montanari, S. Quici, G. Pozzi, *Eur. J. Org. Chem.*, **2001**, 4639.

[55] Y. Hsiao, L. S. Hegedus, *J. Org. Chem.*, **1997**, *62*, 3586.

[56] K. Lin, Z. Cai, W. Zhou, *Zhongguo Yiyao Gongye Zazhi*, **2009**, *40*, 334.

[57] M. J. Frisch, G. W. Trucks, H. B. Schlegel, G. E. Scuseria, M. A. Robb, J. R. Cheeseman, G. Scalmani, V. Barone, B. Mennucci, G. A. Petersson, H. Nakatsuji, M. Caricato, X. Li, H. P. Hratchian, A. F. Izmaylov, J. Bloino, G. Zheng, J. L. Sonnenberg, M. Hada, M. Ehara, K. Toyota, R. Fukuda, J. Hasegawa, M. Ishida, T. Nakajima, Y. Honda, O. Kitao, H. Nakai, T. Vreven, J. A. Montgomery, J. E. Peralta, F. Ogliaro, M. Bearpark, J. J. Heyd, E. Brothers, K. N. Kudin, V. N. Staroverov, R. Kobayashi, J. Normand, K. Raghavachari, A. Rendell, J. C. Burant, S. S. Iyengar, J. Tomasi, M. Cossi, N. Rega, N. J. Millam, M. Klene, J. E. Knox, J. B. Cross, V. Bakken, C. Adamo, J. Jaramillo, R. Gomperts, R. E. Stratmann, O. Yazyev, A. J. Austin, R. Cammi, C. Pomelli, J. W. Ochterski, R. L. Martin, K. Morokuma, V. Zakrzewski, G. A. Voth, P. Salvador, J. J. Dannenberg, S. Dapprich, A. D. Daniels, O. Farkas, J. B. Foresman, J. V. Ortiz, J. Cioslowski, D. J. Fox, *Gaussian 09*, revision D.01; Gaussian, Inc.: Wallingford, CT, **2009**.

[58] M. Svensson, S. Humbel, R. D. J. Froese, T. Matsubara, S. Sieber, K. Morokuma, *J. Phys. Chem.*, **1996**, *100*, 19357.

[59] A. D. Becke, *J. Chem. Phys.*, **1993**, *98*, 5648.

Chapter II

[60]   C. Lee, W. Yang, R. G. Parr, *Phys. Rev. B*, **1988**, *37*, 785.

[61]   J. C. Slater, *Phys. Rev.*, **1951**, *81*, 385.

[62]   S. H. Vosko, L. Wilk, M. Nusair, *Can. J. Phys.*, **1980**, *58*, 1200.

[63]   J. Stewart, *J. Mol. Model.*, **2007**, *13*, 1173.

[64]   C. Adamo, D. Jacquemin, *Chem. Soc. Rev.*, **2013**, *42*, 845.

[65]   A. Rosa, G. Ricciardi, O. V. Gritsenko, E. J. Baerends, *Struct. Bonding (Berlin)*, **2004**, *112*, 49.

[66]   E. J. Baerends, J. Autschbach, A. Bérces, C. Bo, P. M. Boerrigter, L. Cavallo, D. P. Chong, L. Deng, R. M. Dickson, D. E. Ellis, M. van Faassen, L. Fan, T. H. Fischer, C. F. Guerra, S. J. A. van Gisbergen, J. A. Groeneveld, O. V. Gritsenko, M. Grìning, F. E. Harris, P. v. d. Hoek, H. Jacobsen, L. Jensen, G. van Kessel, F. Kootstra, E. van Lenthe, D. A. McCormack, A. Michalak, V. P. Osinga, S. Patchkovskii, P. H. T. Philipsen, D. Post, C. C. Pye, W. Ravenek, P. Ros, P. R. T. Schipper, G. Schreckenbach, J. G. Snijders, M. Sola, M. Swart, D. Swerhone, G. te Velde, P. Vernooijs, L. Versluis, O. Visser, F. Wang, E. van Wezenbeek, G. Wiesenekker, S. K. Wolff, T. K. Woo, A. L. Yakovlev, T. Ziegler, *ADF*, revision ADF-2013.01, http://www.scm.com, Scientific Computing and Modelling NV: Amsterdam, the Netherlands, **2013**.

UNIVERSITAT ROVIRA I VIRGILI
MOLECULE AND CATALYST DESIGN FOR RECOGNITION AND ACTIVATION OF SMALL MOLECULES
Luis Martinez Rodriguez

Cavitand Scaffolds as active Organocatalysts for Carbon Dioxide Conversion

Chapter III

Cavitand Scaffolds as active Organocatalysts for Carbon Dioxide Conversion

The use of cavitand scaffolds based on polyphenols as organocatalysts for carbon dioxide valorization into useful organic cyclic carbonates is discussed in the context of sustainable catalysis. The preorganization of the phenolic units allows for intra- and intermolecular hydrogen bond (HB) networks affecting the reactivity and stability of these cavitand catalysts. These resorcin[4]arenes show cooperative catalysis behavior compared to parent resorcinol in the catalytic coupling of epoxides and CO_2 with significantly higher turnover numbers and frequencies.
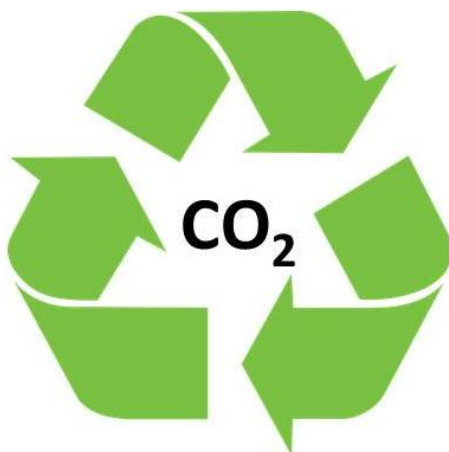
Chapter III

3.1 Cyclic carbonates

One of the biggest challenges associated with carbon dioxide valorization is the design of appropriate catalytic systems that show improved reactivity and selectivity behavior.[1-6] From a sustainable point of view, carbon dioxide is a renewable reagent with high abundance being a by-product from many industrial processes such as the synthesis of ammonia, fermentation processes and the combustion of fossil fuels or organic matter. Since carbon dioxide represents a kinetically and thermodynamically stable molecule, its conversion into useful products involves a large energy barrier. Up to date, most of the attention in the area of CO_2 catalysis has been based on metal complexes of various kinds showing in a few cases high reactivity and unusual scope and/or selectivity.[7-11] Metal catalysts based on abundant metals such as Zn,[12-20] Fe,[21-27] Al,[28-35] and Co[36-40] have by far received most of the attention allowing for significant evolution in both catalyst design as well as improving the product portfolio that can be accessed from CO_2 representing a cheap carbon feedstock for chemical synthesis (**Scheme 3.1**).

One of the most widely studied non-reductive CO_2 valorization processes is the preparation of cyclic organic carbonates.[41-43] They have obtained increasing relevance in the field of material science and organic synthesis due to their intrinsic character as aprotic polar solvents, electrolyte solvents for lithium batteries and as intermediates in organic synthesis.[44-47]
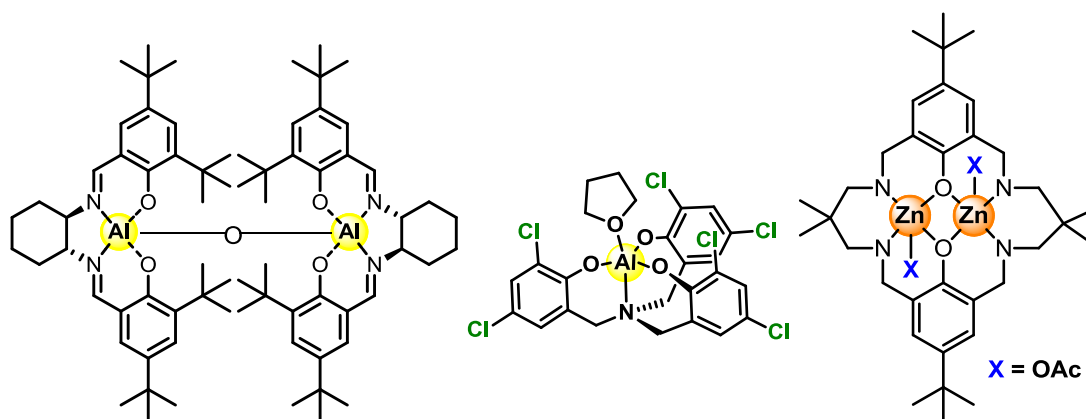
Scheme 3.1: Highly active metal catalysts for CO_2 conversion reactions: North catalyst (left), Kleij catalyst (middle) and Williams catalyst (right).

Cavitand Scaffolds as active Organocatalysts for Carbon Dioxide Conversion

Using these organometallic catalysts as Lewis acids in the direct coupling between CO_2 and oxiranes leads the selectively formation of organic carbonates and represents an atom-efficient transformation from inexpensive and readily available starting materials. The Lewis acid complex alone does not show any activity to perform the CO_2 insertion reaction; a binary/bifunctional catalytic system is required to perform this reaction.[48] By the combination of a Lewis acid and a nucleophile, the activation energy is lowered to mediate the conversion of epoxide and CO_2 to finally form the cyclic organic carbonate. As was stablished previously by DFT studies, the presence of a Lewis acid complex to convert propylene oxide into the corresponding cyclic carbonate may reduce the activation barrier of the overall process by more than 20 kcal/mol in the case of a zinc(salphen) complex, and by more than 25 kcal/mol in the presence of an aluminium triphenolate complex.[49-50]

The mechanism for this transformation has been well explored through control experiments in combination with DFT calculations (**Scheme 3.2**).[51-53] Traditionally, Lewis acid metal complexes are used to coordinate/activate the oxiranes (**SM**) through a metal–oxygen interaction changing the electronic environment of the epoxide, increasing the electrophilicity of the carbon atom in the α-position to the oxygen atom (**I1**). Then a nucleophile is required to ring open the oxirane typically by attack on the least hindered carbon center (halide salts such as tetrabuthylammonium iodide or bromide are the most common nucleophiles used) forming an alkoxide intermediate (**I2**) which is stabilized by coordination to the metal central. No product is observed in the reaction mixture in the absence of the nucleophile, showing the crucial role of the nucleophile during the CO_2 conversion process. Bimetallic catalytic systems, such as the bis-aluminium(salphen) complex reported by North (**Scheme 3.1**), plays a double role during the reaction presenting a different mechanistic pathway.[54] The bis-aluminium(salphen) complex has the ability to activate the epoxide and also the carbon dioxide in a preorganized manner for intramolecular coupling. This effect is rather unique and explains its catalytic activity for the CO_2 insertion reaction at room temperature.

Chapter III
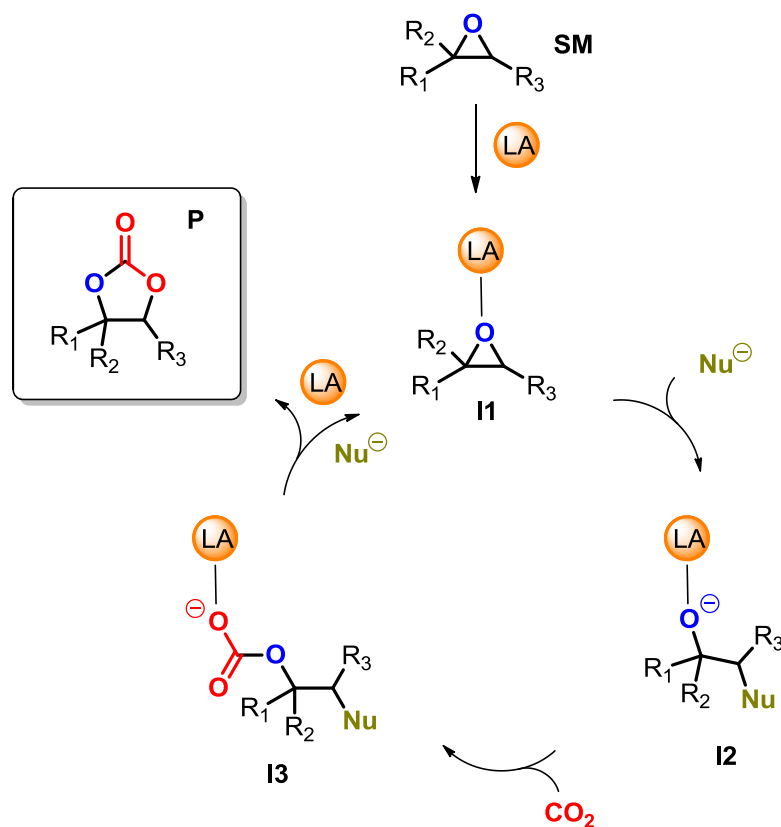
Scheme 3.2: Catalytic cycle for the coupling of epoxides and CO_2 using a binary catalyst based on a Lewis acid and accompanying nucleophile.

After formation of the alkoxide intermediate a molecule of CO_2, which is partially dissolved in the solvent or in the epoxide (under neat conditions) is inserted into the metal-alkoxide bond forming a linear metal-carbonate complex (**I3**). This step involves the formation of a new C–O and M–O bond. The linear carbonate intermediate undergoes an intramolecular ring-closure releasing the nucleophile and Lewis acid, and leading to the formation of the desired five-membered ring carbonate (**P**). The ring-closure process can proceed with inversion or retention of the configuration *via* S_N2 or S_N1 mechanisms (**Scheme 3.3**). The S_N1 process is favored when using highly substituted epoxides which contain electro-donating groups that can stabilize the carbocation intermediate generated in the first step of the S_N1 process (left side **Scheme 3.3**). The nature and amount of the nucleophile used as co-catalyst can also play an important role in the stereochemical divergence of the final product. [52-53]

66

Cavitand Scaffolds as active Organocatalysts for Carbon Dioxide Conversion
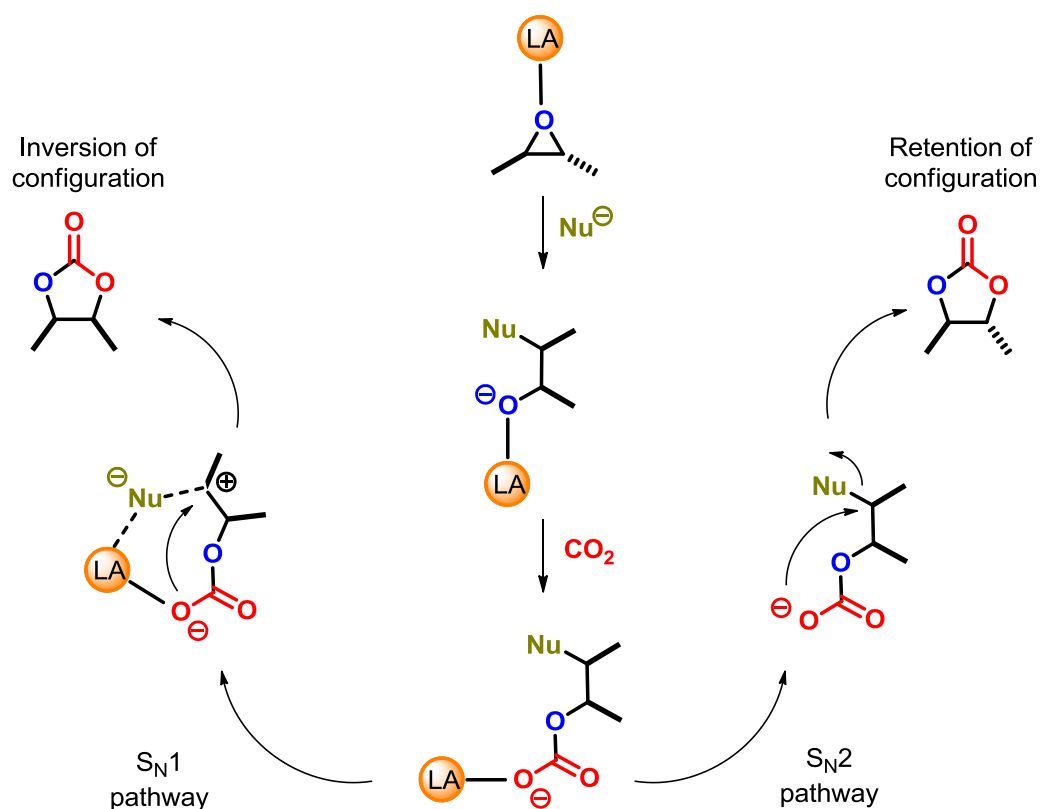
Scheme 3.3: Proposal ring-closure mechanism with two stereochemical pathways: *via* S_N1 (left) and S_N2 based ring-closure (right).

In other to avoid potential toxicity issues related with the use of metal complexes as catalyst components, organocatalysis has recently appeared on the radar of synthetic chemists representing a viable and more sustainable alternative in CO_2 valorization reactions.[55-57] In particular, the catalytic coupling of epoxides and CO_2 has been studied extensively and can be regarded as a benchmark process for a new catalyst development in non-reductive CO_2 couplings. Progress in this area has been considerable with the development of efficient catalyst systems based on binary or bifunctional systems comprising of azaphosphatranes,[58-59] polyphenols,[60-62] phosphonium or ammonium alcohols,[63-65] silanediols[66] and fluorinated alcohols (**Scheme 3.4**).[67-68] All of these catalytic systems are based on the capacity of the catalyst molecules to form hydrogen bonding interactions with the epoxide. The use of molecules that contain amine and/or alcohols motifs have become of high interest for the conversion of epoxides through hydrogen bond (HB) activation. The HB network that arises upon activation of the epoxide towards the formation of key intermediates consequently lowers the kinetic

Chapter III

barrier allowing for either lower temperature conditions (45ºC)[61-62] or the use of a reduced amount of the catalyst loading for higher effective catalytic turnover.

11: X = H; resorcinol
12: X = OH; pyrogallol

Tannic acid
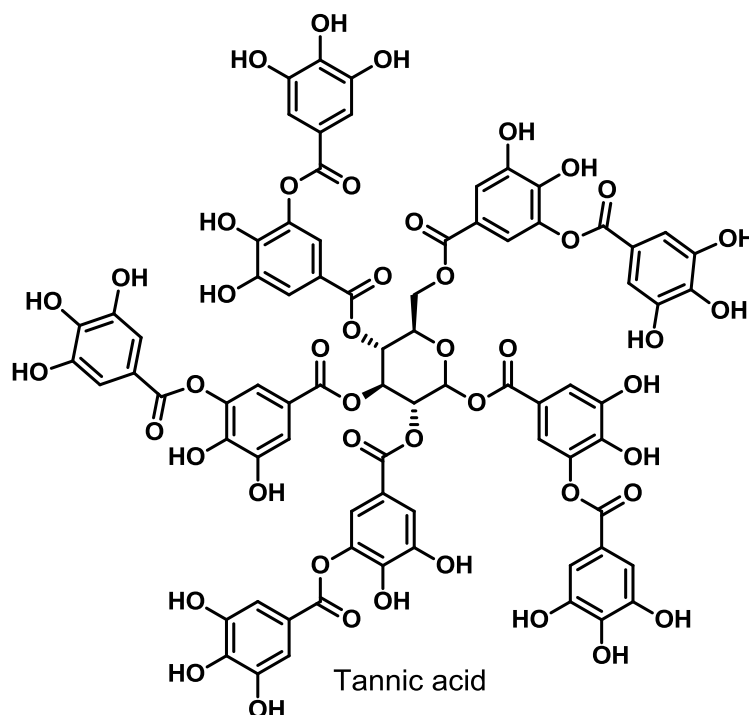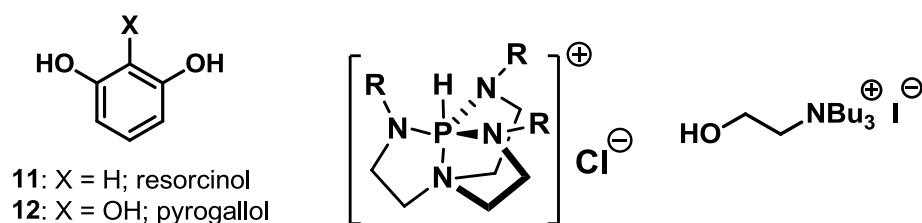
Scheme 3.4: Organocatalysts used for HB activation of epoxides and their coupling with CO_2.

The catalytic activity of polyphenols presents a relation with the Brøndsted acidity of these molecules. Polyphenols containing electron-withdrawing groups in the aromatic unit (which have lower pK_a values than phenol) show higher activity in the formation of organic carbonates from epoxides and CO_2, and also present more attractive kinetic profiles than polyphenols containing electron-donating groups.[62] This effect can be explained as consequence of a better stabilization of the negative charge generated at the alkoxide stage (**I2** in **Scheme 3.2**) after initial nucleophilic attack.

Cavitand Scaffolds as active Organocatalysts for Carbon Dioxide Conversion

The concentration of hydroxy groups in the phenol unit also can help to delocalize better the negative charge and decrease the activation energy of the overall process.[60-62] Nonetheless, there are still challenges to be met regarding the stability of the catalyst based on polyphenols and specifically upon using such systems at higher reaction temperatures (*i.e.,* 80ºC). At these elevated temperatures, some catalyst degradation through deprotonation and formation of inactive phenolate groups cannot be fully avoided preventing the efficient recycling of these phenolic additives and thus restricts the total turnover number (TON).[62]

Parallel to the development of these latter catalytic systems and based on another interesting concept, metal-free cavitand scaffolds have also been reported to increase the nucleophilic character of halide salts by molecular recognition of the cation.[69] These catalyst systems thus act as supramolecular hosts having appropriate binding pockets based on phosphorus ylides[70] or hydroxy-functionalized mono- and bisimidazolium bromides[71] for selective recognition and encapsulation of the ammonium cation, thereby separating the ion pair and activating the nucleophilic anion to perform the ring opening the epoxide.

Therefore, combining the use of preorganized scaffolds such as cavitands and the presence of polyphenol units, and unifying these two features within one structure should provide a new powerful catalyst design with high catalytic activity in the conversion of oxiranes into cyclic organic carbonates under metal-free conditions.

3.2 Resorcin[4]arenes as organocatalysts

Inspired by previous research using polyphenols as organocatalysts for CO_2 conversion into cyclic carbonates,[62] and observing that pyrogallol (**Scheme 3.4** upper left: **12**, polyphenol unit with three hydroxy groups) mediates the formation of the organic cyclic carbonates in higher yields than catechol (1,2-dihydroxybenzene; **11**) or phenol (**13**), the design of supramolecular cavitand structures incorporating polyphenol units was considered. This cavitand "design" was taken into account to develop thermally more robust metal-free catalysts

Chapter III

while maintaining high reactivity and privileged substrate scope.[72-73] The original resorcin[4]arenes scaffolds were developed by Hoegberg[74] and have been fully explored by Cram giving rise to pre-organized supramolecular structures[75] that often form hexameric capsules in solution and in the solid state through *inter*-molecular water-assisted hydrogen bonding interactions (see **Figure 3.1**).[76-78]

The structure of the bowl-shaped *monomeric* cavitand molecules is also controlled through the intramolecular HBs between adjacent resorcinol/pyrogallol units typically expressed in solvent media such as alcohols and acetonitrile.[75] These latter, intramolecular HB patterns suggest a similar potential for catalytic activation of epoxides compared to pyrogallol/tannic acid with stabilization of key intermediate transition states through multiple HB interactions being more efficient than in the absence of such HB donors.[79] It will be demonstrated that cavitand based polyphenols units are excellent HB activators in the formation of cyclic carbonates from epoxides and CO_2 with unprecedented turnover numbers and frequencies (*cf.*, **Table 3.1**).
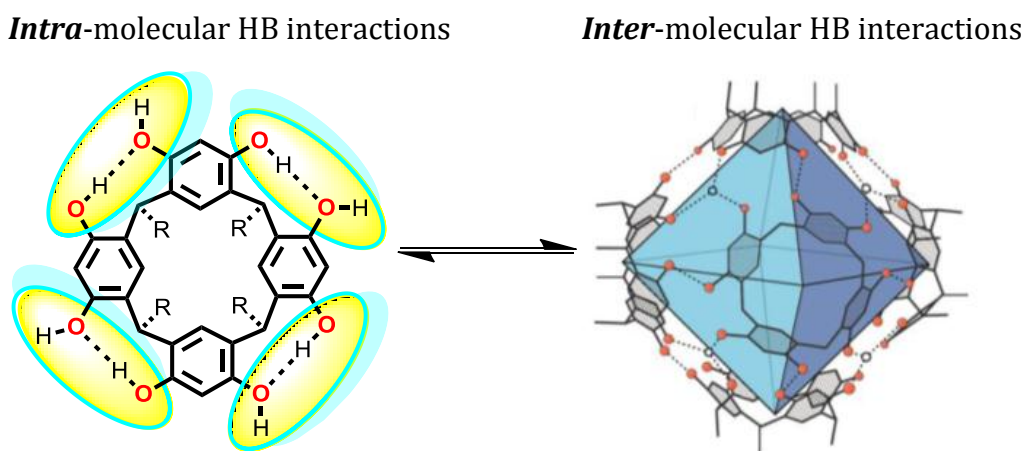
Figure 3.1: *Intra*- and *inter*-molecular hydrogen-bonding networks in cavitand based structures.

The *inter*-molecular hydrogen bonding interactions which lead to the formation of the hexameric capsules can compete with the activation of the oxiranes, and thus inhibit the CO_2 conversion process. By modifying the upper and the lower rim of the resorcin[4]arene scaffold the catalytic activity can be (potentially) fine-tuned minimizing undesired self-assembly process. The resorcin[4]arene systems can be easily prepared by combination of an aldehyde with a polyphenol unit under acidic conditions (**Scheme 3.5**).[74-75]

Cavitand Scaffolds as active Organocatalysts for Carbon Dioxide Conversion

Combining the easy access of these modular and cheap polyphenolic structures with their catalytic potential, these cavitands represent a new and powerful type of organocatalyst for the conversion of CO_2 into value added chemicals as will be detailed in this chapter.
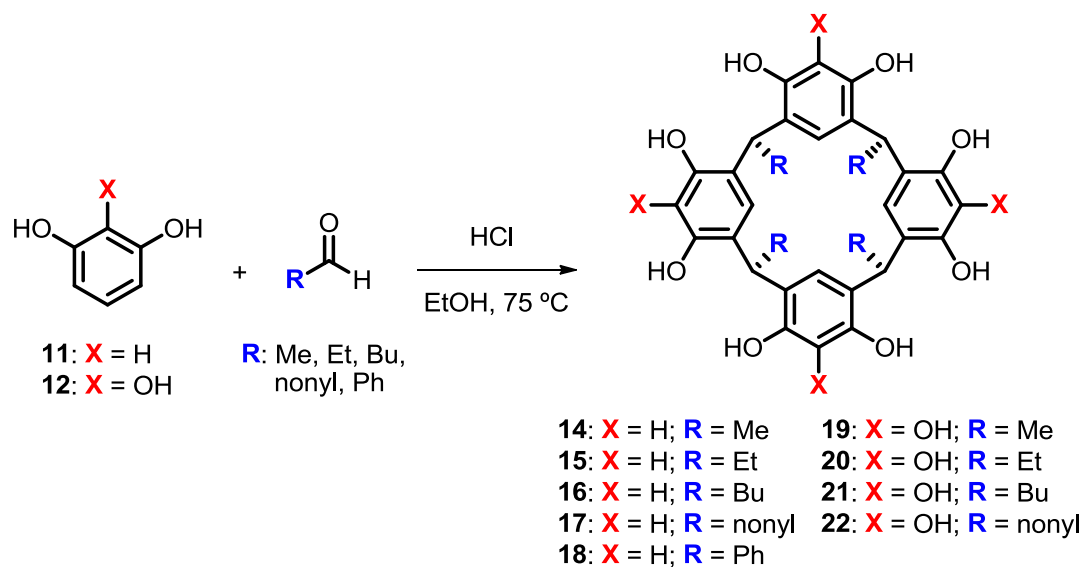
Scheme 3.5: Classical synthesis of resorcin[4]arene scaffolds by acid catalysis.

Initially the resorcin[4]arene **15** (**Scheme 3.5**) was synthesized and tested under relative mild catalytic conditions, and the results compared with the basic monomer units resorcinol (**11**) and pyrogallol (**12**). 1,2-Epoxyhexane was selected as model substrate using further 1.5 mol% of catalyst **15**, 5.0 mol% of the corresponding halide salt, and relative mild reaction conditions (45ºC, 10 bar, MEK = methylethyl ketone as solvent; **Table 3.1**). In order to facilitate comparison of the catalytic results, the catalyst loading was adjusted with respect to the amount of phenolic groups. The yields were calculated using mesitylene as internal standard and the selectivity in all the cases was >99% for the formation of the cyclic carbonate.

The initial experiments using resorcin[4]arene **15**/NBu$_4$I as a binary catalyst showed at 45ºC a NMR yield of 81% (entry 1). Raising the temperature to 50ºC increased this yield to 91% (entry 2). Dilution of the reaction mixture by increasing the amount of solvent (entry 3) gave poorer kinetics leading to lower yields of the desired cyclic carbonate. Different nucleophiles were then tested (I,

Chapter III

Br, Cl) and the iodide based salt gave the best result as was expected, as iodide is a better leaving group than the others halides (entries 4 and 5).

Table 3.1: Screening of the catalytic conditions using polyphenol/TBAX (X = Cl, Br, I) binary catalytic systems in the coupling of CO_2 with 1,2-epoxyhexane in MEK. Yields were determined by ^{1}H NMR using mesitylene as internal standard.
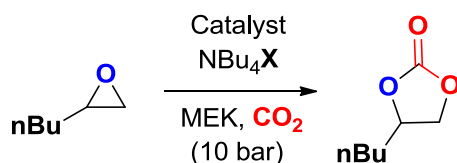
Entry	Catalyst	mol %	NBu4X (mol%)	T (ºC)	MEK (mL)	% Yield
1	15	1.5	I, 5.0	45	2.5	81
2	15	1.5	I, 5.0	50	2.5	91
3	15	1.5	I, 5.0	50	5.0	65
4	15	1.5	Cl, 5.0	50	2.5	31
5	15	1.5	Br, 5.0	50	2.5	65
6	-	0	I, 5.0	50	2.5	4
7	15	1.5	-	50	2.5	0
8	11	6.0	I, 5.0	50	2.5	47
9	11	6.0	I, 5.0	50	5.0	24
10	12	4.0	I, 5.0	50	2.5	99

The background reaction performed in the absence of polyphenol catalyst (entry 6) leads to the formation of the cyclic carbonate in only 4% yield, confirming that the cavitand scaffolds present a significant improvement in the activation of oxiranes under the conditions tested. On the other hand, in the absence of any nucleophile in the media (entry 7), no conversion of the epoxide substrate was noted showing the imperative role of both catalyst components in this coupling reaction. Comparison of the efficiency of resorcin[4]arene **15** (entry 2) with that of the parent building unit resorcinol **11** (entry 7) showed a much higher yield of carbonate for the cavitand based system despite the use of a similar concentration of phenol groups. This effect was maintained under more dilute conditions (*cf.*, entries 3 and 9). The remarkable yield of the cyclic carbonate in the presence of resorcin[4]arene **15** suggests a cooperative effect between the 1,3-

Cavitand Scaffolds as active Organocatalysts for Carbon Dioxide Conversion

diphenol sites in the catalytic activation of the epoxide and/or more efficient stabilization of the intermediates of the carbonate formation reaction.

The use of the cavitand scaffold **15** as organocatalyst presents comparable (though slightly lower) activity compared with pyrogallol **12**, which is the most powerful organocatalyst for CO_2 fixation reported in literature under these conditions (entry 10).[62] Changing the lower and upper rim cavitand functionalization, this catalytic activity could be markedly improved. For this purpose, a series of different resorcin[4]arenes and pyrogallol[4]arenes were synthetized and tested under the same conditions reaction (**Scheme 3.5** and **Table 3.2**). The yields were calculated using mesitylene as internal standard and the selectivity in all the cases was >99% for the formation of the cyclic carbonate.

Table 3.2: Screening of various cavitands scaffolds using polyphenol/TBAI binary catalytic system in the coupling of CO_2 with 1,2-epoxyhexane. Reaction conditions: 1,2-epoxyhexane (1.0 mmol), $p(CO_2)^\circ$ = 10 bars, 18 h, MEK (2.5 mL).
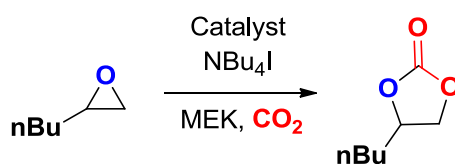
Entry	Catalyst	mol %	NBu$_4$I (mol%)	T (ºC)	R	% Yield
1	14	1.5	5.0	50	Methyl	93
2	15	1.5	5.0	50	Ethyl	91
3	16	1.5	5.0	50	Butyl	94
4	17	1.5	5.0	50	Nonyl	98
5	18	1.5	5.0	50	Phenyl	27
6	19	1.0	5.0	50	Methyl	78
7	20	1.0	5.0	50	Ethyl	84
8	21	1.0	5.0	50	Butyl	87
9	22	1.0	5.0	50	Nonyl	93

The results presented in **Table 3.2** show two different intrinsic features of these catalytic studies: (1) the role of the pendant R groups in the cavitand scaffolds on the overall activity, and (2) the competitive effect of the *intra-molecular* hydrogen bonding network in the cavitand scaffold on the overall catalyst performance. Within the series of resorcin[4]arenes **14–18** where the R

Chapter III

group was increased from methyl to nonyl (entries 1–5), the highest yield was achieved with **17** (R = nonyl), a trend that was also observed within the series of pyrogallol[4]arenes **19–22** (entries 6–9). The cavitand equipped with phenyl substituents (**18**) showed poor catalytic activity due to a poorer solubility in the solvent (MEK) in the reaction medium thereby affecting catalytic turnover. Larger R groups are known to influence the preorganization of these cavitand scaffolds due to steric effects, being thus beneficial for the formation of preorganized cavities. These effects are in particularly well-studied for related calix[4]arenes examples, and most recently in the work from Dufaud et al.[69] where it was reported that extended cavitands can engage with tetraalkyl ammonium halides.

The best-performing nonyl-substituted polyphenols **17** and **22** were then more closely examined and compared with the parent resorcinol **11** and pyrogallol **12** and for each binary system (upon combining with NBu₄I) the kinetic profiles were determined in order to examine their relative catalytic activities (**Figure 3.2**).
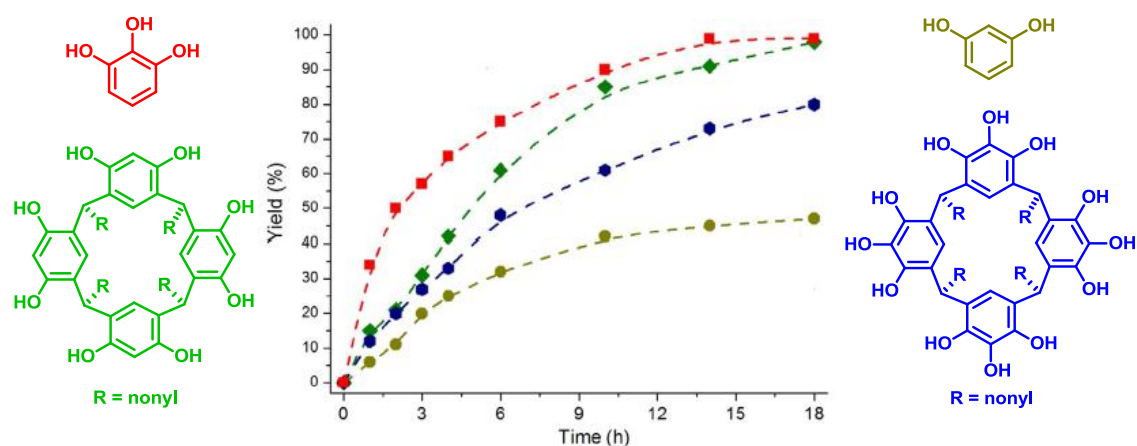
Figure 3.2: Kinetic profiles of pyrogallol **12** (**red**), resorcin[4]arene **17** (**green**), pyrogallol[4]arene **22** (**blue**) and resorcinol **11** (**gold**) at 50 ºC.

Interestingly, the resorcin[4]arene **17** presents much higher catalytic activity during the entire time span in comparison with its parent resorcinol unit **11**. After 18 h (99% vs 46% yield) this rather huge difference in catalytic activity between these two polyphenol based molecules is a consequence of the cooperativity effect between the phenol groups present in the different panels of

Cavitand Scaffolds as active Organocatalysts for Carbon Dioxide Conversion

the resorcin[4]arene **17** (**Figure 3.3**), and such a level of preorganization is not possible with the parent resorcinol **11**.

■ cooperative effect
■ higher phenol acidity
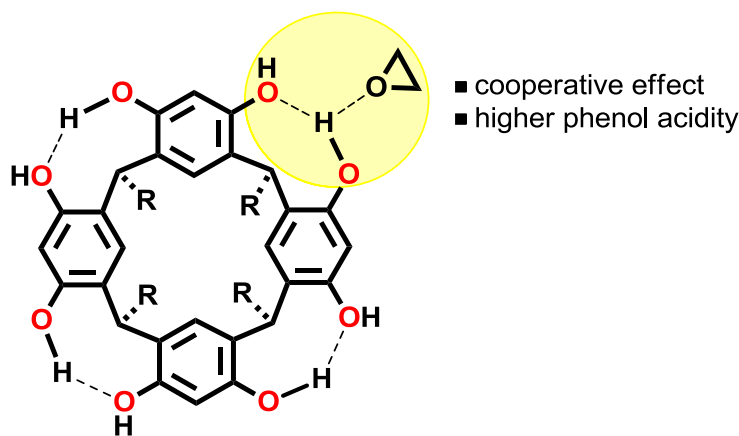
Figure 3.3: Cooperative effect between the polyphenol units present in the resorcin[4]arene.

The kinetic profile of the pyrogallol[4]arene **22** (**blue** line, **Figure 3.2**) shows inferior catalytic performance with respect to resorcin[4]arene **17**. The reason for this behavior is likely the competing self-assembly of the individual cavitand molecules of **22** into larger aggregates (*i.e.* hexamers as in **Figure 3.1**). Cohen *et al.* compared the stability of undecyl-substituted resorcin[4]arenes and pyrogallol[4]arenes by simple titration of these aggregates with polar solvents like methanol or DMSO.[80] These studies involving cavitand molecules demonstrated that upon increasing the polarity of the medium by adding CD_3OD to a solution of the cavitand in $CDCl_3$, the hexameric aggregated state was fully disrupted for both types of cavitand. However, essentially much lower amounts of CD_3OD were required in the case of the resorcin[4]arene in line with a stronger self-assembly behaviour of the pyrogallol[4]arene. Therefore, under the reaction conditions reported in **Table 3.2** and **Figure 3.2**, the poorer performance of pyrogallol[4]arene scaffolds **19–22** compared to the resorcin[4]arene series **14–17** is thus explained in terms of a stronger competing self-assembly. This behaviour competes with hydrogen bonding between the epoxide and the phenolic groups, and thus slows down the reaction. In order to further support the view that competitive HB interactions can slow down the catalytic reaction, the

Chapter III

octahydroxypyridine[4]arene cavitand **23** (**Scheme 3.6**) was prepared[81] and tested under the optimized conditions.

R: nonyl
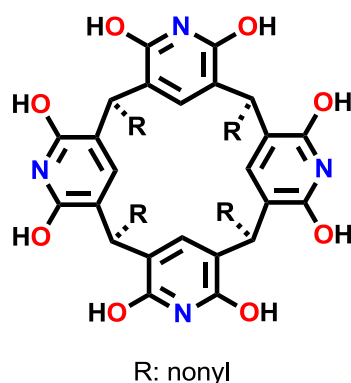
Scheme 3.6: Octahydroxypyridine[4]arene **23** based on 2,6-dihydroxypyridine units.

The 2,6-dihydroxypyridine subunits in **23** are known to induce intramolecular N···HO hydrogen bonds, and the significant lower yield after 18 h (1.5 mol%, 60%) than observed for resorcin[4]arene **17** (1.5 mol%, 98%) is a clear testament of competitive H–bonding. Thus, the best catalytic performance among the cavitand structures at 50 ºC is noted for **17**. Comparing all the polyphenol catalyst tested in the **Figure 3.2**, the best kinetic profile at 50 ºC was obtained with pyrogallol **12**, due to a strong intramolecular hydrogen-bonding interaction between the three hydroxy groups.[62]

In order to investigate the temperature effect on the catalytic performance of the polyphenol systems, the coupling of 1,2-epoxyhexane and CO_2 was carried out at 80 ºC using resorcin[4]arene **17**, pyrogallol[4]arene **22** and pyrogallol **12** as organocatalysts (**Table 3.3**). Under these conditions the nucleophilic additive NBu_4I alone produces poor catalysis (entry 1, 17% yield). Various combinations of cavitand/nucleophile were probed (entries 2–5) while maintaining a similar ratio between both catalyst components (ratio NBu_4I/[OH] groups ~ 3.3). For the resorcin[4]arene **17** based catalyst, the conditions reported in entry 3 revealed quantitative yield of the cyclic carbonate, whereas further lowering the amount of catalyst to 0.25 mol% **17**/ 0.8 mol% NBu_4I showed a modest decrease in yield to 80% (entry 4). For comparison, upon using a similar amount of catalyst derived from pyrogallol[4]arene **22** (*cf.*, entries 3 and 5), a very high though not quantitative yield was noted. Remarkably, under these latter conditions, the

76

Cavitand Scaffolds as active Organocatalysts for Carbon Dioxide Conversion

pyrogallol **12** based catalyst produced a markedly lower yield (77%; *cf.* entries 3 and 7) showing thus a superior performance of the resorcin[4]- and pyrogallol[4]arene based catalysts at 80 ºC.

Table 3.3: Screening of the conditions using polyphenol/TBAI binary catalytic systems in the coupling of CO_2 and 1,2-epoxyhexane. Reaction conditions: 1,2-epoxyhexane 1.0 mmol, $p(CO_2)^\circ = 10$ bar, 18 h, MEK (2.5 mL).
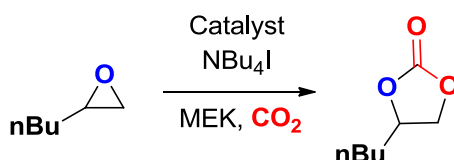
Entry	Catalyst	mol %	NBu$_4$I (mol%)	T (ºC)	% Yield
1	-	0	1.6	80	17
2	**17**	0.75	2.5	80	99
3	**17**	0.50	1.6	80	99
4	**17**	0.25	0.8	80	80
5	**22**	0.33	1.6	80	93
6	**12**	2.00	3.2	80	99
7	**12**	1.30	1.6	80	77
8	**12**	0.66	0.8	80	55

To investigate these observations in more detail, the full kinetic profiles for each of the catalyst systems reported in entries 3, 5 and 7 (**Table 3.3**) were determined (**Figure 3.4**). The pyrogallol catalyst system reaches a plateau conversion of around 70% after 6 h which hereafter barely increases. This is in line with the previous results reported for either pyrogallol **12** or tannic acid (**Scheme 3.4**) as catalysts components; both systems show inferior stability at this elevated temperature causing side-reactions that involve the deprotonation of the polyphenolic unit and replacement thereof by NBu$_4$, inhibiting the CO_2 fixation.[61-62]

The formation of these phenolate groups causes a decrease in the ability to form extended HB networks as to stabilize catalytic intermediates, which results in higher kinetic barriers and thus slower reactions. Consequently, both the nucleophile and polyphenol concentration is negatively affected and the catalysis is shut down in the case of pyrogallol **12**.

Chapter III
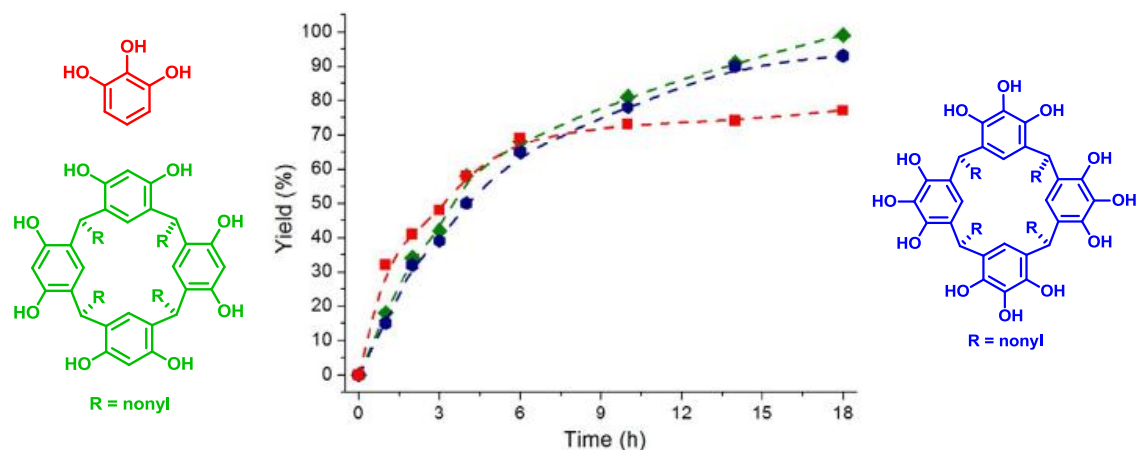
Figure 3.4: Kinetic profiles determined for pyrogallol **12** (**red**), resorcin[4]arene **17** (**green**), and pyrogallol[4]arene **22** (**blue**) at 80 ºC.

On the contrary, both cavitand based catalysts **17** and **22** retain catalytic activity after prolonged use and therefore are more effective systems for cyclic carbonate preparation under elevated temperature conditions with **17** performing slightly better than **22** in the reported time span. Importantly, comparing the pK_a values of resorcinol **11** (9.20)[82] and pyrogallol **12** (9.01)[83-84] shows that the pyrogallol unit is more acidic and likely to undergo de-protonation more facilely. This is causing a shorter lifetime of the catalyst whereas the resorcin[4]arene based system **17** shows comparatively a longer lifetime. This results in better potential for obtaining higher turnover numbers at elevated reaction temperatures. Interestingly, the preorganization of less active resorcinol units in the cavitand significantly increases their catalytic potential as compared with the pyrogallol based one underlining the importance of the catalyst structure for effective turnover.

The influence of the time frame on the performance (turnover numbers/frequencies) of the polyphenol to act as an efficient HB donor in the activation of epoxides was carried out with resorcin[4]arene **17** and pyrogallol **12** in the synthesis of the butyl-substituted carbonate from 1,2-epoxyhexane and CO_2 (**Table 3.4**).

78

Cavitand Scaffolds as active Organocatalysts for Carbon Dioxide Conversion

Table 3.4: Stability studies using polyphenol/TBAI binary catalytic system in the coupling of CO_2 and 1,2-epoxyhexane. Reaction conditions: 1,2-epoxyhexane 10 mmol, $p(CO_2)^o$ = 10 bar, 80 ºC, neat conditions. The amount of polyphenol catalyst used was normalized with respect to the amount of phenol groups. TON = total turnover number, TOF is turnover number per time unit expressed in turnover/h.
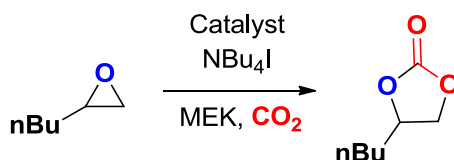
Entry	Catalyst	mol %	mol% OH units	t (h)	% Yield	TON	TOF
1	-	-	-	1	7	-	-
2	-	-	-	18	32	-	-
3	17	0.010	0.080	1	46	575	575
4	17	0.010	0.080	18	74	925	51
5	17	0.010	0.080	30	98	1225	41
6	12	0.026	0.080	18	60	750	42
7	12	1.30	0.080	30	66	825	28

Solventless (neat) conditions were employed to favor the kinetics and the use of nucleophile alone again showed considerably lower yield (entries 1 and 2; 7 and 32%, respectively) compared with the use of both **17** and NBu$_4$I combined (entries 2 and 4; 46 and 74%, respectively). Under these conditions, the TON based on the total of phenol active sites amounted to beyond 1200. Higher turnover numbers were simply achieved by prolonging the reaction (entries 5) showing virtually full conversion after 30 h. The pyrogallol based catalyst (entries 6 and 7) showed lower efficiencies with only a modest increase in the TON after 18 h further confirming the favorable stability features of the cavitand structure **17** at elevated temperatures. Thus the combination of the cooperative action of the resorcinol units in **17** with a higher chemical stability compared to pyrogallol **12** makes this system among the most efficient organocatalyst reported to date with very high TON and TOF values.

Chapter III

3.3 Cyclic carbonate scope under cavitand/NBu₄X catalysis

Motivated by the results obtained with 1,2-epoxyhexane as substrate and with the optimized conditions in hand (1.5 mol% of **17** in combination with 5.0 mol% of NBu₄I in MEK) a wide scope of terminal epoxide substrates were examined in the formation of the cyclic carbonates **24–36**. The temperature and pressure conditions are comparatively very mild considering the use of an organocatalyst system and the presence of solvent was in some cases warranted to prevent solidification of the reaction mixture and incomplete conversion of the substrate. At 50 ºC and 1.0 MPa (10 bar) of pressure, all terminal epoxides were smoothly converted into their carbonates **24–36** in high conversion (>99%) and isolated yields (92–99%), most of could be simply isolated after filtration through silica path (**Scheme 3.7**).
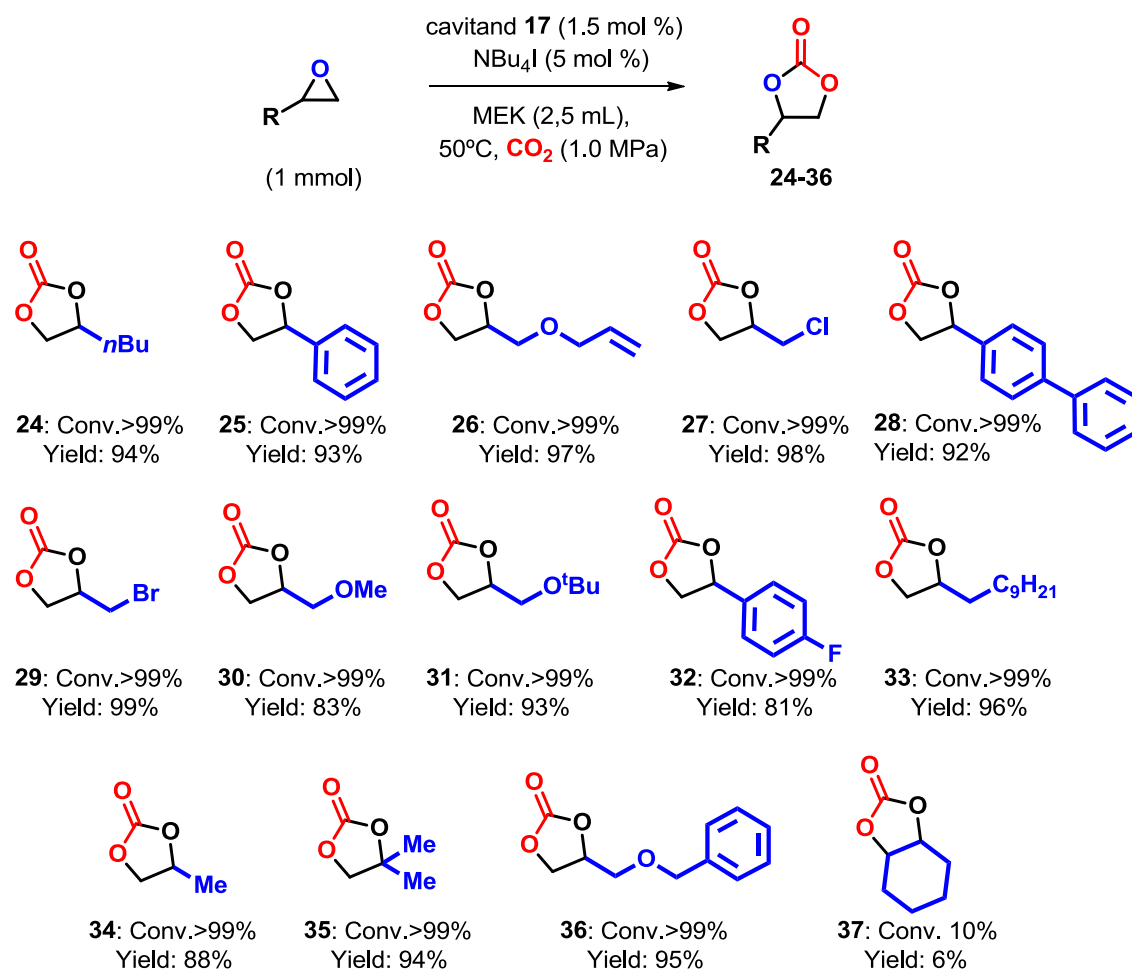
Scheme 3.7: Substrate scope in the conversion of epoxides into the desired cyclic carbonates **24-37**.

80

Cavitand Scaffolds as active Organocatalysts for Carbon Dioxide Conversion

The reaction proceeded with excellent results tolerating electron-withdrawing (**25**, **27** and **29**) or donating groups (**24**, **26**, **30**, **31**, **33**, **34**, **35** and **36**) as substituents in the α-position of the epoxide. Also different aryl-based epoxides were conveniently converted without losing catalytic activity or selectivity (**25**, **28** and **32**). The limitation of this methodology using cavitand scaffolds as organocatalysts was found when internal oxiranes, like cyclohexene oxide, were probed under these mild temperature conditions (50ºC) in the synthesis of organic cyclic carbonate **37**. Under these conditions, cyclic carbonate **37** was only produced to a minor extent (6% yield). This expected result is in line the previous reports present in the literature,[60-62] that indicate that internal epoxide conversion generally requires metal catalysts (*cf.*, **Scheme 3.1**) and elevanted temperatures.[34,42,48, 85]

In the area of organocatalytic formation of cyclic carbonates such reactivity is more unusual even under harsh conditions (>100ºC) due to a weak stability of these high temperatures and weaker substrate activation potential.[55-63] Based on the stability studies of cavitand scaffolds obtained with the kinetic profiles at 80ºC (**Figure 3.4**), we set out to use the cavitand based organocatalysts at 80ºC to examine the more challenging internal epoxides as reaction partners. To date limited progress has been achieved using such epoxide substrates in organocatalytic approaches. One promising example was recently reported by Tassaing et al.[68] using a fluorinated alcohol as HB donor and achieved at 100 ºC and 2 MPa a conversion of 73% of cyclohexene oxide (CHO) after 5 h. Werner et al. reported on the use of bifunctional phosphonium salts that were effective for internal epoxide conversion at temperatures in the range 90−120ºC and 1 MPa.[65] For CHO specifically, the best results in terms of yield were obtained at 120 ºC and 4 MPa (40 bar) producing the carbonate in 69% yield after 6 h.

We were pleased to find that upon increasing the temperature to 80ºC and using 3 mol% of cavitand **17** the conversion of CHO could be significantly increased to 89% (isolated yield of **37**: 85%) using neat conditions. As a control experiment, the reaction in the absence of **17** was also carried out and gave only 8% yield (duplo experiment) showing the importance of the cavitand **17** to achieve a high yield under experimentally similar conditions. Other internal epoxides were then also subjected to these latter conditions including cyclic and acyclic

substrates (*cf.*, synthesis of **38–42**, **Scheme 3.8**). Whereas the 3,4-epoxyfuran was converted into **42** in high conversion (84%) and yield (79%), the corresponding cyclopentene oxide gave a much lower yield (**39**: 38%). Acyclic epoxides could also be converted into their respective carbonates **38** and **41** showing the more general potential of **17**/NBu$_4$I as a binary organocatalyst in the conversion of more challenging internal epoxides. All epoxides were converted with full retention of configuration (*cis* >99% for **37**, **39** and **42**, and *trans* >99% for **41**) except for **38** (*cis/trans* = 85:15). Such loss of stereo-chemical information with this substrate in the formation of its carbonate product in the presence of CO_2 has been observed before,[26,86] and may be related to a (partial) S_N1 character of the nucleophilic attack of the linear carbonate intermediate onto the C–Br bond initially formed in the ring-opening of the epoxide by NBu$_4$Br as illustrated in **Scheme 3.3**.
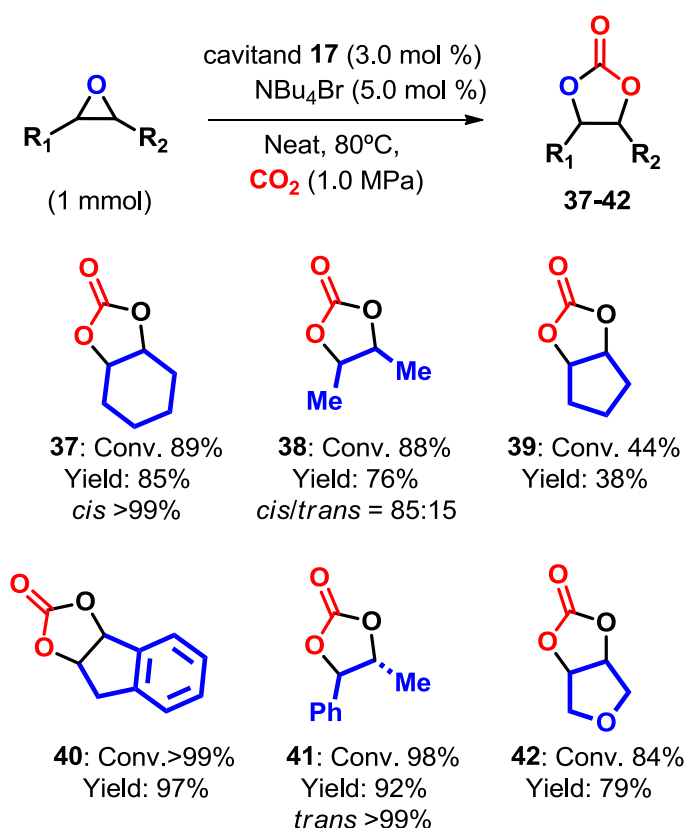
Scheme 3.8: Substrate scope in the conversion of internal epoxides into the targeted cyclic carbonates **37–42**.

Cavitand Scaffolds as active Organocatalysts for Carbon Dioxide Conversion

3.4 Conclusions and outlook

The use of easily accessible and modular cavitand structures such as resorcin[4]arenes and pyrogallol[4]arenes in combination with suitable ammonium halide salts constitute interesting hydrogen-bond donor binary catalysts for the conversion of CO_2 and oxiranes into cyclic organic carbonates. The preorganization of the phenolic units within the resorcin[4]arenes was beneficial for the catalytic efficiency in organic carbonate formation from epoxides and CO_2 and resulted in cooperative effects (for **17**) that led to significantly higher conversion rates compared to resorcinol **11**. Upon increasing the reaction temperature from 50 to 80 ºC, the overall reactivity was improved and the cavitand structures showed a higher chemical stability than pyrogallol **12**, which makes the former systems more suitable to achieve very high turnover numbers.

By modulating the upper and lower rims of the cavitand scaffolds, it was possible to minimize undesired/competitive self-assembly of the cavitand polyphenol and maximize the catalytic activity. This improved and unparalleled reactivity was shown to be beneficial in the formation of 19 different carbonates under relative mild reaction conditions (50–80 ºC, 1 MPa; 10 bar). Moreover, 6 disubstituted internal epoxides were also screened as reaction partners and were converted efficiently under neat conditions at 80 ºC to provide good to excellent isolated yields (38–97%). Compared with the state-of-the-art in organocatalytic CO_2/epoxide coupling chemistry, the cavitand-based binary organocatalysts are sustainable, versatile, and highly reactive alternatives to metal-based systems in the catalytic coupling of epoxides and CO_2.

3.5 Experimental section

MEK (Aldrich ACS reagent >99%) and CO_2 (purchased from PRAXAIR) were used as received without further purification or drying. All polyphenolic chemicals were commercially available from Aldrich and were used as received. ^{1}H and ^{13}C{1H} NMR spectra were recorded by using a Bruker Avance 500 NMR spectrometer at 297 K. Chemical shifts are reported in ppm relative to the residual

Chapter III

solvent peaks in CDCl$_3$ (δ=7.26 ppm), [D$_6$]Acetone (δ=2.05 ppm) and [D$_6$]DMSO (δ=2.50 ppm). MS studies were performed at the High Resolution Mass Spectrometry Unit at the ICIQ in Tarragona, Spain.

General procedure for the synthesis of the cavitand scaffolds:

All the resorcin[4]arenes and pyrogallol[4]arenes were synthesized following the classical condensation of aldehydes in the presence of a Brøndsted acid.[74-75,81] Typically, a solution of one equivalent of resorcinol/pyrogallol (6 mmol) in a solution of ethanol (95%, 75 mL) and concentrated HCl (25 mL) was cooled to 0 ºC. Then the aldehyde reagent (6 mmol, 1 equiv.) dissolved in ethanol (95% 50 mL) was added dropwise to the reaction mixture. The resulting solution was stirred at 75 ºC for 18–72 h and the reaction time depended on the aldehyde substrate used. Upon cooling to ambient temperature, the separated precipitate was washed repeatedly with cold water and methanol, and the compounds then dried *in vacuo*.

Resorcin[4]arene 14: White solid. Yield: 54%, ^{1}H NMR (500 MHz, Acetone-d_6): δ = 1.76 (d, J = 7.3 Hz, 12H), 4.52 (q, J = 7.3 Hz, 4H), 6.21 (s, 4H), 7.64 (s, 4H), 8.48 (s, 8H). ^{13}C NMR (125 MHz, Acetone-d_6): δ = 20.3, 28.7, 103.5, 125.2, 126.1, 152.2. MS (ESI−, MeOH): calcd for C$_{32}$H$_{31}$O$_8$ [M−H]$^-$: 543.2; found: 543.2.

Resorcin[4]arene 15: Yellow solid. Yield: 23%, ^{1}H NMR (500 MHz, Acetone-d_6): δ = 0.90 (t, J = 7.2 Hz, 12H), 2.19-2.38 (m, 8H), 4.18 (t, J = 7.9 Hz, 4H), 6.24 (s, 4H), 7.54 (s, 4H), 8.51 (s, 8H). ^{13}C NMR (125 MHz, Acetone-d_6): δ = 13.1, 27.2, 36.6, 103.7, 125.1, 125.4, 152.8. MS (ESI−, MeOH): calcd for C$_{36}$H$_{39}$O$_8$ [M−H]$^-$: 599.3; found: 599.3.

Resorcin[4]arene 16: Red solid. Yield: 84%, ^{1}H NMR (500 MHz, Acetone-d_6): δ = 0.89 (t, J = 7.2 Hz, 12H), 1.20-1.49 (m, 16H), 2.21-2.38 (m, 8H), 4.25-4.31 (m, 4H), 6.23 (s, 4H), 7.57 (s, 4H), 8.44 (s, 8H). ^{13}C NMR (125 MHz, Acetone-d_6): δ = 14.6, 23.4, 31.3, 34.0, 34.3, 103.7, 125.3, 125.5, 152.7. MS (ESI−, MeOH): calcd for C$_{44}$H$_{55}$O$_8$ [M−H]$^-$: 711.4; found: 711.4.

Cavitand Scaffolds as active Organocatalysts for Carbon Dioxide Conversion

Resorcin[4]arene 17: Yellow solid. Yield: 85%, ^{1}H NMR (500 MHz, Acetone-d_6): δ = 0.85-0.91 (m, 12H), 1.20-1.40 (m, 56H), 2.30 (q, J = 7.6 Hz, 8H) 4.31 (t, J = 7.9 Hz, 4H), 6.24 (s, 4H), 7.55 (s, 4H). ^{13}C NMR (125 MHz, Acetone-d_6): δ = 14.4, 23.4, 29.1, 29.9, 30.1, 30.3, 30.5, 30.6, 32.7, 34.3, 34.4, 103.7, 125.2, 125.4, 152.7. MS (ESI–, MeOH): calcd for $C_{64}H_{95}O_8$ [M–H]$^-$: 991.7; found: 991.7.

Resorcin[4]arene 18: Brown solid. Yield: 97%, ^{1}H NMR (500 MHz, DMSO-d_6): δ = 5.63 (s, 4H), 6.13 (s, 4H), 6.74 (d, J = 6.9 Hz, 8H), 6.96 (d, J = 6.9 Hz, 12H), 8.55 (s, 8H). ^{13}C NMR (125 MHz, DMSO-d_6): δ = 41.4, 102.0, 120.4, 124.5, 127.1, 128.6, 145.7, 152.6. MS (MALDI–, dctb): calcd for $C_{52}H_{39}O_8$ [M–H]$^-$: 791.3; found: 791.3.

Pyrogallol[4]arene 19: Purple solid. Yield: 52%, ^{1}H NMR (500 MHz, Acetone-d_6): δ = 1.74 (d, J = 7.3 Hz, 12H), 4.52 (q, J = 7.3 Hz, 4H), 6.21 (s, 4H), 7.63 (s, 4H), 8.51 (s, 8H). ^{13}C NMR (125 MHz, Acetone-d_6): δ = 20.3, 28.7, 103.6, 125.2, 126.1, 152.3. MS (ESI–, MeOH): calcd for $C_{32}H_{31}O_{12}$ [M–H]$^-$: 607.2; found: 607.2.

Pyrogallol[4]arene 20: Purple solid. Yield: 11%, ^{1}H NMR (500 MHz, Acetone-d_6): δ = 0.91 (t, J = 7.3 Hz, 12H), 2.20-2.44 (m, 8H), 4.23 (t, J = 8.0 Hz, 4H), 7.11 (s, 4H). ^{13}C NMR (125 MHz, Acetone-d_6): δ = 13.1, 26.8, 37.2, 114.4, 125.6, 133.5, 140.7. MS (MALDI+, dctb): calcd for $C_{36}H_{40}O_{12}$ [M–H]$^-$: 664.2520; found: 664.2523.

Pyrogallol[4]arene 21: Purple solid. Yield: 18%, ^{1}H NMR (500 MHz, Acetone-d_6): δ = 0.85-0.93 (m, 12H), 1.21-1.46 (m, 16H), 2.29 (q, J = 7.8 Hz, 8H), 4.35 (q, J = 7.9 Hz, 4H), 7.13 (s, 4H), 7.20 (s, 4H), 8.12 (s, 8H). ^{13}C NMR (125 MHz, Acetone-d_6): δ = 13.7, 22.5, 30.4, 32.7, 34.1, 113.5, 124.9, 132.8, 139.2. MS (ESI–, MeOH): calcd for $C_{44}H_{55}O_{12}$ [M–H]$^-$: 775.4; found: 775.4.

Pyrogallol[4]arene 22: Brown solid. Yield: 70%, ^{1}H NMR (500 MHz, Acetone-d_6): δ = 0.85-0.91 (m, 12H), 1.22-1.36 (m, 56H), 2.28 (q, J = 7.6 Hz, 8H), 4.35 (t, J = 7.9 Hz, 4H), 7.11 (s, 4H), 7.19 (s, 4H), 8.10 (s, 8H). ^{13}C NMR (125 MHz, Acetone-d_6): δ = 14.4, 23.4, 30.1, 30.3, 30.4, 30.5, 30.6, 32.7, 34.0, 35.0, 114.4, 125.7, 140.1. MS (ESI–, MeOH): calcd for $C_{64}H_{95}O_{12}$ [M–H]$^-$: 1055.7; found: 1155.7.

Chapter III

Octahydroxy-pyridine[4]arene 23: White solid. Yield: 46%, ^{1}H NMR (500 MHz, CDCl$_3$): δ = 0.88 (t, J = 6.8 Hz, 12H), 1.23-1.36 (m, 56H), 1.95-2.07 (m, 8H), 4.15 (t, J = 8.0 Hz, 4H), 7.09 (s, 4H), 11.17 (s, 4H), 12.8 (s, 4H). ^{13}C NMR (125 MHz, CDCl$_3$): δ = 14.3, 22.9, 29.5, 29.7, 29.8, 29.9, 32.1, 139.1, 148.6, 158.6. MS (ESI–, MeOH): calcd for C$_{60}$H$_{91}$O$_8$N$_4$ [M–H]$^-$: 995.6837; found: 995.6818.

General catalytic procedure in the synthesis of the cyclic carbonates:

A typical procedure for the synthesis of the cyclic carbonates from terminal epoxides and CO$_2$ was carried out in a 30 mL steel autoclave using 1,2-epoxyhexane (1 mmol, 1 equiv.), cavitand catalyst **17** (1.0-1.5mol %), NBu$_4$I (5 mol %) and MEK (2.5 mL). The autoclave was then subjected to three cycles of pressurization and depressurization with CO$_2$. Finally, the autoclave was charged with 1 MPa (10 bar) of CO$_2$, heated to 50ºC and the content stirred for 18 h. Hereafter, the autoclave was cooled to rt and carefully depressurized. The volatiles were removed under reduced pressure and the product was purified by flash column chromatography (1:1 hexane/ethyl acetate as eluent) to afford the pure cyclic carbonate.

Carbonate 24: Colorless oil. Yield: 94%, Selectivity: >99%. ^{1}H NMR (500 MHz, CDCl$_3$): δ = 0.92 (t, J = 7.0 Hz, 3H), 1.24-1.50 (m, 4H), 1.64-1.88 (m, 2H), 4.06 (t, J = 7.2; 8.4 Hz, 1H), 4.52 (dd, J = 7.8; 8.4 Hz, 1H), 4.67-4.72 (m, 1H). ^{13}C NMR (125 MHz, CDCl$_3$): δ = 13.9, 22.4, 26.6, 33.7, 69.5, 155.2. IR: 1785 cm^{-1} (C=O).

Carbonate 25: Colorless oil. Yield: 93%, Selectivity: >99%. ^{1}H NMR (500 MHz, CDCl$_3$): δ = 4.35 (dd, J = 7.8; 8.7 Hz, 1H), 4.80 (t, J = 8.4 Hz, 1H), 5.68 (t, J = 8.0 Hz, 1H), 7.33-7.49 (m, 5H). ^{13}C NMR (125 MHz, CDCl$_3$): δ = 71.3, 78.1, 126.0, 129.4, 129.9, 135.9, 155.2. IR: 1783 cm^{-1} (C=O).

Carbonate 26: Colorless oil. Yield: 97%, Selectivity: >99%. ^{1}H NMR (500 MHz, CDCl$_3$): δ = 3.62 (dd, J = 3.8; 11.0 Hz, 1H), 3.69 (dd, J = 4.1; 11.0 Hz, 1H), 3.91-4.15 (m, 2H), 4.40 (dd, J = 6.1; 8.3 Hz, 1H), 4.50 (t, J = 8.3 Hz, 1H), 4.82 (dd, J = 3.8; 8.1

Cavitand Scaffolds as active Organocatalysts for Carbon Dioxide Conversion

Hz, 1H), 5.06-5.30 (m, 2H), 5.78-5.84 (m, 1H). ^{13}C NMR (125 MHz, CDCl$_3$): δ = 66.4, 69.0, 72.8, 75.1, 118.1, 133.8, 155.0. IR: 1784 cm^{-1} (C=O).

Carbonate 27: Colorless oil. Yield: 98%, Selectivity: >99%. ^{1}H NMR (500 MHz, CDCl$_3$): δ = 3.66-3.88 (m, 2H), 3.41 (dd, J = 5.7; 8.9 Hz, 1H), 4.59 (dd, J = 8.2; 8.9 Hz, 1H), 4.93-4.97 (m, 1H). ^{13}C NMR (125 MHz, CDCl$_3$): δ = 43.6, 67.1, 74.3, 154.2. IR: 1778 cm^{-1} (C=O).

Carbonate 28: White solid. Yield: 92%, Selectivity: >99%. ^{1}H NMR (500 MHz, CDCl$_3$): δ = 4.40 (dd, J = 7.9; 8.7 Hz, 1H), 4.83 (dd, J = 8.2; 8.7 Hz, 1H), 5.73 (t, J = 8.0 Hz, 1H), 7.33-7.41 (m, 1H), 7.42-7.53 (m, 4H), 7.55-7.61 (m, 2H), 7.65-7.77 (m, 2H). ^{13}C NMR (125 MHz, CDCl$_3$): δ = 71.3, 78.0, 126.5, 127.3, 128.0, 128.1, 129.1, 134.7, 140.2, 143.0, 154.9. IR: 1770 cm^{-1} (C=O).

Carbonate 29: Colorless oil. Yield: 99%, Selectivity: >99%. ^{1}H NMR (500 MHz, CDCl$_3$): δ = 3.51-3.66 (m, 2H), 4.31-4.38 (m, 1H), 4.52-4.65 (m, 2H), 4.91-4.98 (m, 1H). ^{13}C NMR (125 MHz, CDCl$_3$): δ = 31.1, 68.3, 74.1, 154.1. IR: 1788 cm^{-1} (C=O).

Carbonate 30: Colorless oil. Yield: 83%, Selectivity: >99%. ^{1}H NMR (500 MHz, CDCl$_3$): δ = 3.43 (s, 3H), 3.52-3.60 (m, 2H), 4.37 (dd, J = 6.1; 8.4 Hz, 1H), 4.49 (t, J = 8.4 Hz, 1H), 4.74-4.81 (m, 1H). ^{13}C NMR (125 MHz, CDCl$_3$): δ = 59.8, 66.3, 71.6, 75.1, 155.0. IR: 1782 cm^{-1} (C=O).

Carbonate 31: Colorless oil. Yield: 93%, Selectivity: >99%. ^{1}H NMR (500 MHz, CDCl$_3$): δ = 1.19 (s, 9H), 3.50-3.55 (m, 1H), 3.58-3.63 (m, 1H), 4.38 (dd, J = 5.8; 8.3 Hz, 1H), 4.47 (t, J = 8.3 Hz, 1H), 4.70-4.82 (m, 1H). ^{13}C NMR (125 MHz, CDCl$_3$): δ = 27.4, 61.4, 66.7, 74.1, 75.3, 155.3. IR: 1787 cm^{-1} (C=O).

Carbonate 32: White solid. Yield: 81%, Selectivity: >99%. ^{1}H NMR (500 MHz, CDCl$_3$): δ = 4.32 (dd, J = 7.8; 8.7 Hz, 1H), 4.79 (dd, J = 8.1; 8.7 Hz, 1H), 5.66 (t, J = 8.1 Hz, 1H), 7.14 (d, J = 8.6 Hz, 2H), 7.36 (dd, J = 5.1; 8.6 Hz, 2H). ^{19}F NMR (500 MHz, CDCl$_3$): δ = −111.0. ^{13}C NMR (125 MHz, CDCl$_3$): δ = 71.2, 116.5 (d, J = 22.0 Hz), 128.1 (d, J = 8.6 Hz), 131.7 (d, J = 3.3 Hz), 154.7, 162.6, 164.5. IR: 1775 cm^{-1} (C=O).

Chapter III

Carbonate 33: Colorless oil. Yield: 96%, Selectivity: >99%. ^{1}H NMR (500 MHz, CDCl$_3$): δ = 0.84-0.90 (m, 3H), 1.20-150 (m, 16H), 1.63-1.85 (m, 2H), 4.03-4.10 (m, 1H), 4.52 (t, J = 8.0 Hz, 1H), 4.67-4.74 (m, 1H). ^{13}C NMR (125 MHz, CDCl$_3$): δ = 14.2, 22.8, 24.5, 29.3, 29.4, 29.5, 29.6, 29.7, 32.0, 34.0, 69.5, 155.2. IR: 1783 cm^{-1} (C=O).

Carbonate 34: Colorless oil. Yield: 88%, Selectivity: >99%. ^{1}H NMR (500 MHz, CDCl$_3$): δ = 1.48 (d, J = 6.3 Hz, 3H), 4.01 (dd, J = 7.2; 8.4 Hz, 1H), 4.54 (dd, J = 7.7; 8.4 Hz, 1H), 4.80-4.86 (m, 1H). ^{13}C NMR (125 MHz, CDCl$_3$): δ = 19.4, 70.8, 73.6, 155.1. IR: 1782 cm^{-1} (C=O).

Carbonate 35: Colorless oil. Yield: 94%, Selectivity: >99%. ^{1}H NMR (500 MHz, CDCl$_3$): δ = 1.53 (s, 6H), 4.15 (s, 2H). ^{13}C NMR (125 MHz, CDCl$_3$): δ = 26.3, 75.5, 76.4, 154.6. IR: 1794 cm^{-1} (C=O).

Carbonate 36: Colorless oil. Yield: 95%, Selectivity: >99%. ^{1}H NMR (500 MHz, CDCl$_3$): δ = 3.63 (dd, J = 3.7; 10.9 Hz, 1H), 3.71 (dd, J = 4.1; 10.9 Hz, 1H), 4.39 (dd, J = 6.0; 8.4 Hz, 1H), 4.61 (q, J = 10.5 Hz, 2H), 4.50 (t, J = 8.3 Hz, 1H), 4.70-4.89 (m, 1H), 7.28-7.48 (m, 5H). ^{13}C NMR (125 MHz, CDCl$_3$): δ = 66.5, 69.0, 73.9, 75.1, 127.9, 128.3, 128.7, 137.2, 155.0. IR: 1786 cm^{-1} (C=O).

A typical procedure for the synthesis of the cyclic carbonates from internal epoxides and CO$_2$ was carried out in a 30 mL steel autoclave using cyclohexene oxide (1 mmol, 1 equiv.), cavitand catalyst **17** (3.0 mol%), NBu$_4$Br (5 mol %) under neat conditions. The autoclave was then subjected to three cycles of pressurization and depressurization with CO$_2$. Finally, the autoclave was charged with 1 MPa (10 bar) of CO$_2$, heated to 80ºC and the mixture stirred for 18 h. Hereafter, the autoclave was cooled to rt and carefully depressurized. The volatiles were removed under reduced pressure and the product was purified by flash column chromatography (1:1 hexane/ethyl acetate as eluent) to afford the pure cyclic carbonate.

Cavitand Scaffolds as active Organocatalysts for Carbon Dioxide Conversion

Carbonate 37: Yellow oil. Yield: 85%, Selectivity: >99%. ^{1}H NMR (500 MHz, CDCl$_3$): δ = 1.38-1.48 (m, 2H), 1.58-1.70 (m, 2H), 1.86-1.93 (m, 4H), 4.65-4.71 (m, 2H). ^{13}C NMR (125 MHz, CDCl$_3$): δ = 19.3, 26.9, 75.9, 155.5. IR: 1783 cm^{-1} (C=O).

Carbonate 38: Colorless oil. Yield: 76%, Selectivity: >99% with a *cis/trans* ratio of 85:15. ^{1}H NMR (500 MHz, CDCl$_3$, major isomer): δ = 1.33 (d, *J* = 6.3 Hz, 6H), 4.79-4.85 (m, 2H). ^{13}C NMR (125 MHz, CDCl$_3$, major isomer): δ = 14.4, 73.0, 154.6. IR: 1784 cm^{-1} (C=O).

Carbonate 39: Yellow solid. Yield: 38%, Selectivity: >99%. ^{1}H NMR (500 MHz, CDCl$_3$): δ = 1.56-1.86 (m, 4H), 2.08-2.24 (m, 2H), 5.09-5.13 (m, 2H). ^{13}C NMR (125 MHz, CDCl$_3$): δ = 21.7, 33.3, 81.9, 155.6. IR: 1783 cm^{-1} (C=O).

Carbonate 40: White solid. Yield: 97%, Selectivity: >99%. ^{1}H NMR (500 MHz, CDCl$_3$): δ = 3.38-3.43 (m, 2H), 5.42-5.49 (m, 1H), 6.00 (d, *J* = 6.7 Hz, 1H), 7.30-7.38 (m, 2H), 7.43 (t, *J* = 7.5 Hz, 1H), 7.52 (d, *J* = 7.6 Hz, 1H). ^{13}C NMR (125 MHz, CDCl$_3$): δ = 38.2, 79.9, 83.7, 125.8, 126.7, 128.4, 131.3, 136.6, 140.2, 154.8. IR: 1780 cm^{-1} (C=O).

Carbonate 41: Yellow oil. Yield: 92%, Selectivity: >99%. ^{1}H NMR (500 MHz, CDCl$_3$): δ = 1.55 (d, *J* = 6.2 Hz, 3H), 4.57-4.62 (m, 1H), 5.13 (d, *J* = 8.0 Hz, 1H), 7.30-7.57 (m, 5H). ^{13}C NMR (125 MHz, CDCl$_3$): δ = 18.5, 80.9, 85.0, 126.1, 129.4, 129.9, 135.2, 154.4. IR: 1799 cm^{-1} (C=O).

Carbonate 42: Yellow oil. Yield: 79%, Selectivity: >99%. ^{1}H NMR (500 MHz, CDCl$_3$): δ = 3.51-3.60 (m, 2H), 4.21-4.32 (m, 2H), 5.20 (d, *J* = 2.0 Hz, 2H). ^{13}C NMR (125 MHz, CDCl$_3$): δ = 73.2, 80.1, 154.4. IR: 1779 cm^{-1} (C=O).

General procedure for the determination of the kinetic profiles:

A typical procedure was carried out in a 30 mL steel autoclave using 1,2-epoxyhexane (1 mmol, 1 equiv.), polyphenol catalyst (1.0-1.5mol %), NBu$_4$I (5 mol %) and MEK (2.5 mL) applying different reaction times (1, 2, 3, 4, 6, 10, 14 and 18

Chapter III

h). The autoclave was then subjected to three cycles of pressurization and depressurization with CO_2. Finally, the autoclave was charged with 1 MPa (10 bars) of CO_2, heated to 50ºC or 80ºC and the content stirred for the corresponding time. Hereafter, the autoclave was cooled to rt and carefully depressurized. An exact amount of mesitylene (around 0.100 mmol) was added to the reaction mixture to calculate the conversion of the substrate by ^1H NMR ($CDCl_3$).

Data Points relating to Figure 3.2:

Time/h	12	17	22	11
1	34%	15%	12%	6%
2	50%	21%	20%	11%
3	57%	31%	27%	20%
4	65%	42%	33%	25%
6	75%	61%	48%	32%
10	90%	85%	61%	42%
14	99%	91%	73%	45%
18	99%	98%	80%	47%

Data Points relating to Figure 3.4:

Time/h	12	17	22
1	32%	18%	15%
2	41%	34%	32%
3	48%	42%	39%
4	58%	58%	48%
6	69%	68%	65%
10	73%	81%	78%
14	74%	91%	93%
18	77%	99%	93%

3.6 References and notes:

[1]   M. Aresta, A. Dibenedetto, A. Angelini, *Chem. Rev.*, **2014**, *114*, 1709.
[2]   Q. Liu, L. Wu, R. Jackstell, M. Beller, *Nat. Commun.*, **2015**, *6*, 5933.
[3]   M. Cokoja, C. Bruckmeier, B. Rieger, W. A. Herrmann, F. E. Kühn, *Angew. Chem. Int. Ed.*, **2011**, *50*, 8510.

Cavitand Scaffolds as active Organocatalysts for Carbon Dioxide Conversion

[4]   M. Peters, B. Köhler, W. Kuckshinrichs, W. Leitner, P. Markewitz, T. E. Müller, *ChemSusChem,* **2011**, *4*, 1216.

[5]   M. H. Beyzavi, C. J. Stephenson, Y. Liu, O. Karagiaridi, J. T. Hupp, O. K. Farha, *Front. Energy Res.*, **2015**, *2*, 63.

[6]   R. Martín, A. W. Kleij, *ChemSusChem*, **2011**, *4*, 1259.

[7]   N. Kielland, C. J. Whiteoak, A. W. Kleij, *Adv. Synth. Catal.*, **2013**, *355*, 2115.

[8]   C. Martín, G. Fiorani, A. W. Kleij, *ACS Catal.*, **2015**, *5*, 1353.

[9]   Y. Tsuji, T. Fujihara, *Chem. Commun.*, **2012**, *48*, 9956.

[10]   B. Yu, L.-N. He, *ChemSusChem*, **2015**, *8*, 52.

[11]   J. W. Comerford, I. D. V. Ingram, M. North, X. Wu, *Green Chem.*, **2015**, *17*, 1966.

[12]   M. R. Kember, P. D. Knight, P. T. R. Reung, C. K. Williams, *Angew. Chem. Int. Ed.*, **2009**, *48*, 931.

[13]   M. A. Fuchs, C. Altesleben, S. C. Staudt, O. Walter, T. A. Zevaco, E. Dinjus, *Catal. Sci. Technol.*, **2014**, *4*, 1658.

[14]   A. Decortes, A. W. Kleij, *ChemCatChem*, **2011**, *3*, 831.

[15]   A. Decortes, M. Martínez Belmonte, J. Benet-Buchholz, A. W. Kleij, *Chem. Commun.*, **2010**, *46*, 4580.

[16]   R. Ma, L.-N. He, Y.-B. Zhou, *Green Chem.*, **2016**, *18*, 226.

[17]   O. Hauenstein, M. Reiter, S. Agarwal, B. Rieger, A. Greiner, *Green Chem.*, **2016**, *18*, 760.

[18]   S. Kissling, M. W. Lehenmeier, P. T. Altenbuchner, A. Kronast, M. Reiter, P. Deglmann, U. B. Seemann, B. Rieger, *Chem. Commun.*, **2015**, *51*, 4579.

[19]   C. M. Byrne, S. D. Allen, E. B. Lobkovsky, G. W. Coates, *J. Am. Chem. Soc.*, **2004**, *126*, 11404.

[20]   M. A. Fuchs, S. Staudt, C. Altesleben, O. Walter, T. A. Zevaco, E. Dinjus, *Dalton Trans.,* **2014**, *43*, 2344.

[21]   A. Buchard, M. R. Kember, K. G. Sandeman, C. K. Williams, *Chem. Commun.*, **2011**, *47*, 212.

[22]   A. Buonerba, A. De Nisi, A. Grassi, S. Milione, C. Capacchione, S. Vagin, B. Rieger, *Catal. Sci. Technol.*, **2015**, *5*, 118.

[23]   M. A. Fuchs, T. A. Zevaco, E. Ember, O. Walter, I. Held, E. Dinjus, M. Döring, *Dalton Trans.*, **2013**, *42*, 5322.

[24]   C. J. Whiteoak, E. Martin, M. Martínez Belmonte, J. Benet-Buchholz, A. W. Kleij, *Adv. Synth. Catal.*, **2012**, *354*, 469.

[25]   M. Taherimehr, S. M. Al-Amsyar, C. J. Whiteoak, A. W. Kleij, P. P. Pescarmona, *Green Chem.*, **2013**, *15*, 3083.

[26]   C. J. Whiteoak, E. Martin, E. Escudero-Adán, A. W. Kleij, *Adv. Synth. Catal.*, **2013**, *355*, 2233.

[27]   X. Frogneux, O. Jacquet, T. Cantat, *Catal. Sci. Technol.*, **2014**, *50*, 1529.

[28]   T. A. Zevaco, A. Janssen, J. Sypien, E. Dinjus, *Green Chem.*, **2005**, *7*, 659.

[29]   W. Clegg, R. Harrington, M. North, R. Pasquale, *Chem. Eur. J.*, **2010**, *16*, 6828.

[30]   J. Martínez, J. A. Castro-Osma, A. Earlam, C. Alonso-Moreno, A. Otero, A. Lara-Sánchez, M. North, A. Rodríguez-Diéguez, *Chem. Eur. J.*, **2015**, *21*, 9850.

[31]   J. A. Castro-Osma, M. North, X. Wu, *Chem. Eur. J.*, **2014**, *20*, 15005.

[32]   L. Peña Carrodeguas, J. González-Fabra, F. Castro-Gómez, C. Bo, A. W. Kleij, *Chem. Eur. J.*, **2015**, *21*, 6115.

[33]   V. Laserna, G. Fiorani, C. J. Whiteoak, E. Martin, E. Escudero-Adán, A. W. Kleij, *Angew. Chem. Int. Ed.*, **2014**, *53*, 10416.

Chapter III

[34] C. J. Whiteoak, N. Kielland, V. Laserna, E. C. Escudero-Adán, E. Martin, A. W. Kleij, *J. Am. Chem. Soc.*, **2013**, *135*, 1228.

[35] Y. Qin, H. Guo, X. Sheng, X. Wang, F. Wang, *Green Chem.*, **2015**, *17*, 2853.

[36] C. T. Cohen, T. Chu, G. W. Coates, *J. Am. Chem. Soc.*, **2005**, *127*, 10869.

[37] G.-P. Wu, D. J. Darensbourg, X.-B. Lu, *J. Am. Chem. Soc.*, **2012**, *134*, 17739.

[38] D. J. Darensbourg, S. J. Wilson, *J. Am. Chem. Soc.*, **2011**, *133*, 18610.

[39] K. Nakano, S. Hashimoto, M. Nakamura, T. Kamada, K. Nozaki, *Angew. Chem. Int. Ed.*, **2011**, *50*, 4868.

[40] M. R. Kember, A. J. P. White, C. K. Williams, *Macromolecules,* **2010**, *43*, 2291.

[41] P. P. Pescarmona, M. Taherimehr, *Catal. Sci. Technol.*, **2012**, *2*, 2169.

[42] M. North, R. Pasquale, C. Young, *Green Chem.*, **2010**, *12*, 1514.

[43] A. Decortes, A. M. Castilla, A. W. Kleij, *Angew. Chem. Int. Ed.*, **2010**, *49*, 9822.

[44] K. Ohmatsu, N. Imagawa, T. Ooi, *Nat. Chem.*, **2014**, *6*, 47.

[45] A. Khan, L. Yang, J. Xu, L. Y. Jin, Y. J. Zhang, *Angew. Chem. Int. Ed.*, **2014**, *53*, 11257.

[46] W. Guo, J. González-Fabra, N. A. G. Bandeira, C. Bo, A. W. Kleij, *Angew. Chem. Int. Ed.*, **2015**, *54*, 11686.

[47] J. Rintjema, R. Epping, G. Fiorani, E. Martín, E. C. Escudero-Adán, A. W. Kleij, *Angew. Chem. Int. Ed.*, **2016**, *55*, 3972.

[48] D. J. Darensbourg, M. W. Holtcamp, *Coordin. Chem. Rev.*, **1996**, *153*, 155.

[49] H. Sun, D. Zhang, *J. Phys. Chem. A.*, **2007**,*111*, 8036.

[50] C.-H. Guo, H.-S. Wu, X.-M. Zhang, J.-Y. Song, X. Zhang, *J. Phys. Chem. A.*, **2009**, *113*, 6710.

[51] F. Castro-Gómez, G. Salassa, A. W. Kleij, C. Bo, *Chem. Eur. J.*, **2013**, *19*, 6289.

[52] C. J. Whiteoak, N. Kielland, V. Laserna, F. Castro-Gómez, E. Martin, E. C. Escudero-Adán, C. Bo, A. W. Kleij, *Chem. Eur. J.*, **2014**, *20*, 2264.

[53] M. Drees, M. Cokoja, F. E. Kühn, *ChemCatChem*, **2012**, *4*, 1703.

[54] M. North, R. Pasquale, *Angew. Chem. Int. Ed.*, **2009**, *48*, 2946.

[55] G. Fiorani, W. Guo, A. W. Kleij, *Green Chem.*, **2015**, *17*, 1375.

[56] M. Cokoja, M. E. Wilhelm, M. H. Anthofer, W. A. Herrmann, F. E. Kühn, *ChemSusChem*, **2015**, *8*, 2436.

[57] A. Tlili, E. Blondiaux, X. Frogneux, T. Cantat, *Green Chem.*, **2015**, *17*, 157.

[58] B. Chatelet, L. Joucla, J.-P. Dutasta, A. Martinez, K. C. Szeto, V. Dufaud, *J. Am. Chem. Soc.*, **2013**, *135*, 5348.

[59] B. Chatelet, L. Joucla, J.-P. Dutasta, A. Martinez, V. Dufaud, *Chem. Eur. J.*, **2014**, *20*, 8571.

[60] S. Sopeña, G. Fiorani, C. Martín, A. W. Kleij, *ChemSusChem*, **2015**, *8*, 3248.

[61] C. J. Whiteoak, A. H. Henseler, C. Ayats, A. W. Kleij, M. A. Pericàs, *Green Chem.*, **2014**, *16*, 1552.

[62] C. J. Whiteoak, A. Nova, F. Maseras, A. W. Kleij, *ChemSusChem*, **2012**, *5*, 2032.

[63] H. Büttner, J. Steinbauer, T. Werner, *ChemSusChem*, **2015**, *8*, 2655.

[64] C. Kohrt, T. Werner, *ChemSusChem*, **2015**, *8*, 2031.

[65] T. Werner, H. Büttner, *ChemSusChem*, **2014**, *7*, 3268.

[66] A. M. Hardman-Baldwin, A. E. Mattson, *ChemSusChem*, **2014**, *7*, 3275.

[67] S. Gennen, M. Alves, R. Méreau, T. Tassaing, B. Gilbert, C. Detrembleur, C. Jerome, B. Grignard, *ChemSusChem*, **2015**, *8*, 1845.

[68] M. Alves, B. Grignard, S. Gennen, R. Mereau, C. Detrembleur, C. Jerome, T. Tassaing, *Catal. Sci. Technol.*, **2015**, *5*, 4636.

92

Cavitand Scaffolds as active Organocatalysts for Carbon Dioxide Conversion

[69] A. Mirabaud, J.-C. Mulatier, A. Martinez, J.-P. Dutasta, V. Dufaud, *ACS Catal.*, **2015**, *5*, 6748.

[70] H. Zhou, G.-X. Wang, W.-Z. Zhang, X.-B. Lu, *ACS Catal.*, **2015**, *5*, 6773.

[71] M. H. Anthofer, M. E. Wilhelm, M. Cokoja, M. Drees, W. A. Herrmann, F. E. Kühn, *ChemCatChem*, **2015**, *7*, 94.

[72] A. Gissot, J. Rebek, Jr., *J. Am. Chem. Soc.*, **2004**, *126*, 7424.

[73] D. Ajami, J. Rebek, Jr., *Nat. Chem.*, **2009**, *1*, 87.

[74] A. G. S. Hoegberg, *J. Org. Chem.*, **1980**, 45, 4498.

[75] L. M. Tunstad, J. A. Tucker, E. Dalcanale, J. Weiser, J. A. Bryant, J. C. Sherman, R. C. Helgeson, C. B. Knobler, D. J. Cram, *J. Org. Chem.,* **1989**, *54*, 1305.

[76] K. Kobayashi, M. Yamanaka, *Chem. Soc. Rev.*, **2015**, *44*, 449.

[77] L. R. MacGillivray, J. L. Atwood, *Nature*, **1997**, *389*, 469.

[78] L. Avram, Y. Cohen, *J. Am. Chem. Soc.*, **2002**, *124*, 15148.

[79] The use of parent, non-functionalized cavitand structures in catalytic applications remains rare, see: Q. Zhang, K. Tiefenbacher, *J. Am. Chem. Soc.*, **2013**, *135*, 16213.

[80] L. Avram, Y. Cohen, *Org. Lett.*, **2003**, *5*, 3329.

[81] T. Gerkensmeier, J. Mattay, C. Näther, *Chem. Eur. J.*, **2001**, *7*, 465.

[82] S. E. Blanco, M. C. Almandoz, F. H. Ferretti, *Spectrochim. Acta: A,* **2005**, *61*, 93.

[83] Dissociation Constants of Organic Acids in Aqueous Solution, eds. G. Kortum and K. Andrussow, International Union of Pure and Applied Chemistry, Buttersworth, London (UK), **1961**.

[84] H.-S. Kim, T. D. Chung, H. Kim, *J. Electroanal. Chem.*, **2001**, *498*, 209.

[85] C. Martín, C. J. Whiteoak, E. Martin, M. Martínez Belmonte, E. C. Escudero-Adán, A. W. Kleij, *Catal. Sci. Technol.*, **2014**, *4*, 1615.

[86] J. Langanke, L. Greiner, W. Leitner, *Green Chem.*, **2013**, *15*, 1173.

Chapter IV

Stereoselective Formation of (*Z*)-1,4-but-2-ene Diols using Water as a Nucleophile

Using readily available vinyl cyclic carbonates as starting materials, the first general catalytic stereoselective formation of (*Z*)-1,4-but-2-ene diols is described using water as nucleophile. These scaffolds present exquisite selectivity for the formation of the (*Z*)-alkene configuration, high yields and excellent group tolerance. This methodology is characterized by its operational simplicity and does not require any (stoichiometric) additive or special precautions. Control experiments suggest that the excellent stereoselectivity is a result of stabilization of the Pd-intermediate through hyper-conjugation.

Chapter IV

4.1 Diols as building blocks

Asymmetric catalytic reactions have emerged as a powerful tool in the development of efficient and practical methodologies for the syntheses of target molecules with biological and pharmaceutical applications.[1] Asymmetric reactions provide a sustainable entry into a broad variety of chiral products due to an atom-economical use of asymmetric auxiliaries.[2] In the last decades the progress achieved in the area of asymmetric catalysis has had a huge impact at the industrial level. Among the most important examples of commercialized reactions are the asymmetric hydrogenation developed by Knowles and Noyori that was translated into an industrial process (Monsanto Process).[3-5] Apart from this seminal examples, dihydroxylation of olefins development by the Upjohn Company was initially explored by Sharpless using osmium tetroxide as active catalyst in order to obtain enantiopure 1,2-diols.[6-7] Diols are among the most ubiquitous scaffolds in organic chemistry being of eminent value in the total synthesis of natural compounds, in polymer chemistry and typically encompass a wide structural diversity.[8-12]
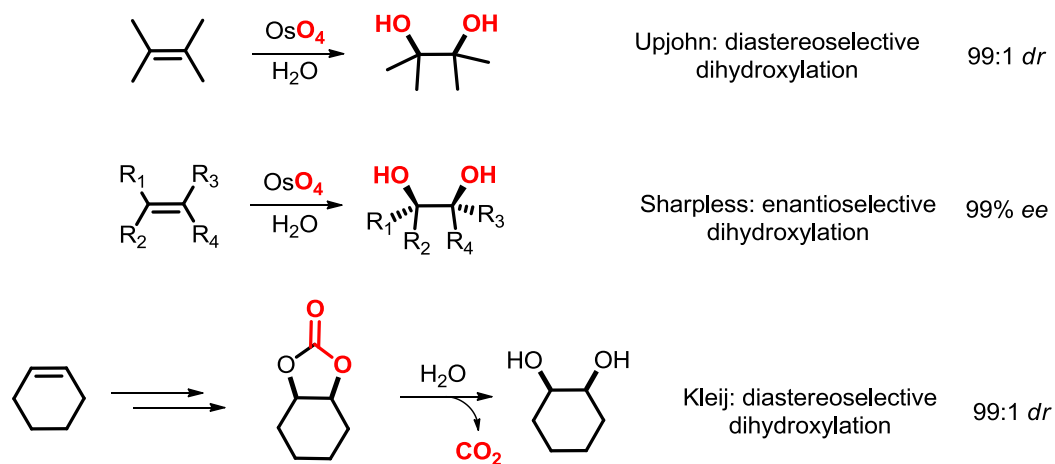
Scheme 4.1: Enantio- and diastereoselective methodologies to achieve 1,2-diol scaffolds.

The stereoselective and enantio-selective preparation of 1,2-diols presented in the **Scheme 4.1** has undoubtedly received most of the attention of the synthetic community. Regarding to safety, OsO₄ is not considered an ideal reagent and its

Stereoselective Formation of (*Z*)-1,4-but-2-ene Diols using Water as a Nucleophile

high toxicity (even at low concentrations) can lead to pulmonary edema; therefore new (more) sustainable processes have been developed to achieve 1,2-diols such as the hydrolytic kinetic resolution of epoxides[13] and the diastereoselective formation of 1,2-*cis*-diols using carbon dioxide as a protecting group representing important alternative of the use of osmium tetraoxide.[14]

On the other hand, other types of scaffolds like 1,3- and 1,4-diols still persist to challenge synthetic chemists in terms of stereocontrol and selectivity. In this respect, acyclic unsaturated (*Z*)-configured 1,4-diols have found important applications as transient scaffolds towards the stereo-controlled preparation of vinylcyclopropanes,[15] vinyl glycinols[16] and the formation of lactones.[17] A recent contribution from Hoveyda has exposed further growth potential of these 1,4-diol synthons in catalytic and stereoselective cross-metathesis furnishing valuable acyclic (*Z*)-allylic alcohols.[18] Up to now, the limited amount of available strategies for (*Z*)-1,4-but-2-ene diol synthesis have in common that they require stoichiometric chemistry and/or air-sensitive reagents such as DIBAL-H (diisobutylaluminum hydride).[15-16] Despite the increasing incentive of (*Z*)-1,4-but-2-ene diols in synthetic chemistry, the quest towards an efficient and mild catalytic protocol focusing on such (substituted) 1,4-diol scaffolds still continues.[19-20]

4.2 Screening studies and scope of 1,4-diol formation

Inspired by the dearth of catalytic solutions for the stereo-controlled construction of substituted (*Z*)-but-2-ene diols, the use of vinyl-substituted cyclic carbonates as key reaction partners was anticipated thus using CO_2 as temporary protecting group.[14] Previous success reported by Ooi and Zhang with these latter scaffolds demonstrated that decarboxylative functionalization with suitable electrophiles such as Michael acceptors is feasible under mild reaction conditions giving access to furans,[21] tertiary vinylglycols[22] and highly functional pyrrolidines.[23] As an intermediate in these Pd-mediated processes a zwitterionic structure was postulated (**Scheme 4.2**). Conceptually, such a charge-separated structure should possess ambivalent reactivity, with the Pd-allyl fragment being highly electrophilic and amenable to react with (very) weak nucleophiles such as

Chapter IV

water.[24-25] Examples of catalytic conversions that are based on the use of water as nucleophilic reagent are, however, extremely rare.[12-13,26-31] A successful development of new catalytic methodology towards selective (Z)-but-2-ene diol formation by nucleophilic hydration of *in situ* formed allyl surrogates would provide a highly attractive new route towards these synthetically useful scaffolds.

In this chapter is disclosed such a conceptually new and highly efficient approach for (Z)-but-2-ene diols that is based on a decarboxylative hydration of readily available vinyl-based cyclic carbonates under mild operating conditions (**Scheme 4.2**).
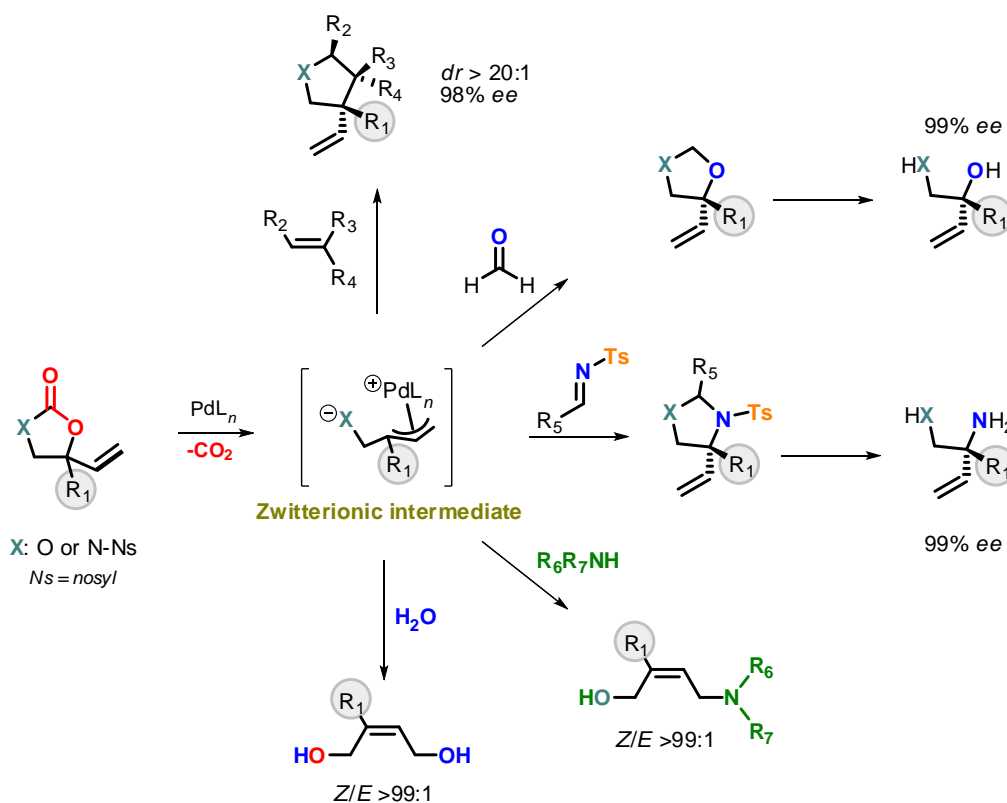
Scheme 4.2. Synthesis of various scaffolds based on the decarboxylative functionalization of vinyl cyclic carbonates; the 1,4-diol formation is subject of the present chapter.

The screening phase towards appropriate reaction conditions for the synthesis of unsaturated 1,4-diol compound **74** started off with the use of vinyl carbonate **43** and using various Pd precursors and phosphine ligands (**Table 4.1**). Various Pd precursors were tested including the well-known and reactive White catalyst, which is a (commercial) Pd(OAc)$_2$ precursor ligated by a bis-sulfoxide.[32-33] We first screened various mono- and bidentate ligands (**L1–L8**) combined with

Stereoselective Formation of (*Z*)-1,4-but-2-ene Diols using Water as a Nucleophile

this precursor using DMF as solvent.[34] Whereas the use of mono-dentate phosphine ligands **L1–L5** (entries 1–5) did not result in any observable formation of **74**, to our delight the presence of bidentate phosphines **L6–L8** (entries 6–8) proved to be highly beneficial for the formation of the desired 1,4-but-2-ene diol under ambient conditions.

Table 4.1: Optimization of conditions in the synthesis of (*Z*)-1,4-but-2-ene diol **74** from vinyl carbonate **43** varying the Pd precursor, phosphine ligand **L**, and the solvent.
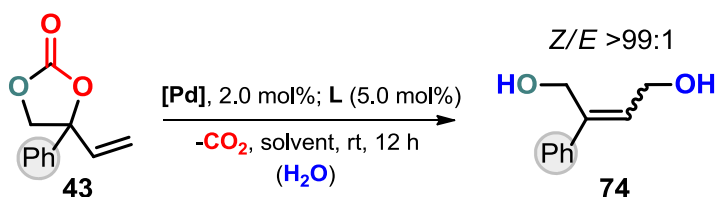
Entry	Pd precursor	Ligand	Solvent	Yield[35]
1	White catalyst	L1	DMF	0
2	White catalyst	L2	DMF	0
3	White catalyst	L3	DMF	0
4	White catalyst	L4	DMF	0
5	White catalyst	L5	DMF	0
6	White catalyst	L6	DMF	90
7	White catalyst	L7	DMF	95
8	White catalyst	L8	DMF	98
9	Pd₂(dba)₃·CHCl₃	L8	DMF	97
10	Pd(dba)₂	L8	DMF	99
11	Pd(OAc)₂	L8	DMF	94
12	Pd(PPh₃)₂Cl	L8	DMF	70
13	White catalyst	L8	CH₃CN	40
14	White catalyst	L8	MeOH	<1
15	White catalyst	L8	CH₂Cl₂	0
16	White catalyst	L8	THF	0
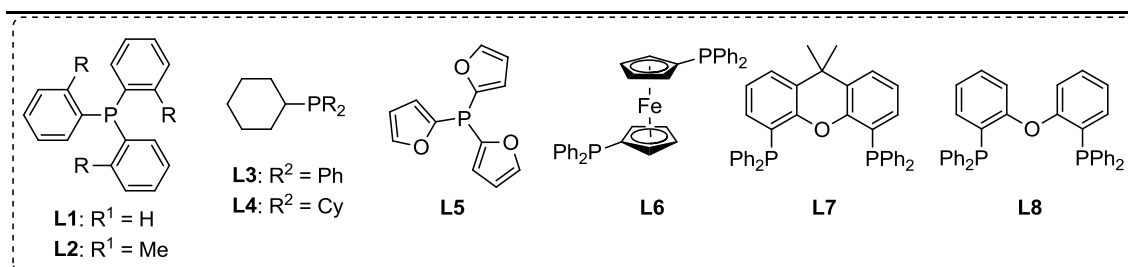
Chapter IV

Moreover, ^{1}H NMR analysis supported the exclusive formation of the (*Z*)-configured product (*Z/E* >99:1). Further screening (entries 8–12) of other Pd precursors in the presence of **L8** showed Pd(dba)$_2$ and [Pd$_2$(dba)$_3$·CHCl$_3$] (dba = dibenzylideneacetone) to be excellent precursors, but the use of Pd(PPh$_3$)$_2$Cl gave significantly lower yield likely due competition between the two types of phosphine ligands. Other solvents than DMF were probed (entries 13–16) but these showed inferior yields of **74** underlining the crucial importance of the polarity of the medium. Finally, it was considered that the use of the White catalyst is more practical as it is easier to handle and more stable than Pd(dba)$_2$ and Pd$_2$(dba)$_3$·CHCl$_3$, and therefore it was used to investigate the product scope of this catalytic reaction.

Thus, the optimized conditions reported in entry 8 of **Table 4.1** were then used to investigate the product scope in detail (**Scheme 4.3**). The substituents of the vinyl carbonate reagent were systematically varied and provided an entry into a series of substituted (*Z*)-but-2-ene diols **74–101**. In most cases excellent isolated yields (up to 98%) and selectivity (>99:1) towards the (*Z*)-isomer were noted. This user-friendly procedure does not require any additive and can be operated in air at ambient temperature. The introduction of various aryl groups in the olefinic unit are tolerated including *para*- and *meta*-substituted (di)halo-aryls (**75**, **76**, **80**, **91**, **92**, **96** and **97**), benzoic ester (**82**) and even thioether (**85**) groups. The use of 2- and 3-furyl and thiophene-substituted cyclic carbonates smoothly leads to (*Z*)-1,4-diols **86–88** in high yield despite the potential of the heteroatoms to coordinate and deactivate the Pd-catalyst.

The use of vinyl carbonates with an *ortho*-substitution in the aryl substituent did not result in any observable formation of the corresponding 1,4-diols under the optimized conditions (Entry 8, **Table 4.1**). For the conversion of these more challenging substrates harsher conditions were required, *i.e.* an increase in the reaction temperature to 60º C, the addition of higher amount of water to the medium (60 µL of H$_2$O to 200 µL of DMF), and increasing the catalyst loading (5.0 mol % White catalyst, 10.0 mol % **L8**). With these conditions in hand, the *ortho*-fluoro-aryl derived diol **93** was isolated in 55 % yield, and the *ortho*-Br-aryl derivative **94** in 63% yield with in both cases high selectivity for the (*Z*)-isomer (>99:1). The use of the vinyl carbonate equipped with a 3-pyridyl group

100

Stereoselective Formation of (*Z*)-1,4-but-2-ene Diols using Water as a Nucleophile

also required these modified conditions to be converted into the desired diol **89** (61% yield). Pyridine motifs are known to be excellent ligands in palladium mediated C-H activation and thus they may compete for coordination to the Pd precursor and slow down the decarboxylative functionalization reaction.[36]

Interestingly, the presence of other substitution patterns is also allowed producing for instance an *α*-functionalized diol (**100**) and an elusive tetra-substituted olefin derivative with complete control of the stereoselectivity towards the formation of the (*Z*) stereoisomer (**101**). The straightforward formation of **101** demonstrates the potential to install substituents on the *β*-carbon of the allylic scaffolds thus further amplifying the generality of the protocol, and typically the stereo-controlled introduction of different substituents in the olefin unit represents a huge challenge.[37] Various methodologies based on allylic chemistry towards the formation of *γ*-disubstituted olefins have been developed with poor group tolerance and without stereocontrol.[38-43] The (*Z*)-configuration of all the compounds was deduced from 1D and 2D NMR analysis, whereas in the case of **81** further evidence for the preferred stereo-isomer formation was obtained from X-ray diffraction studies (**Figure 4.1**).[44]
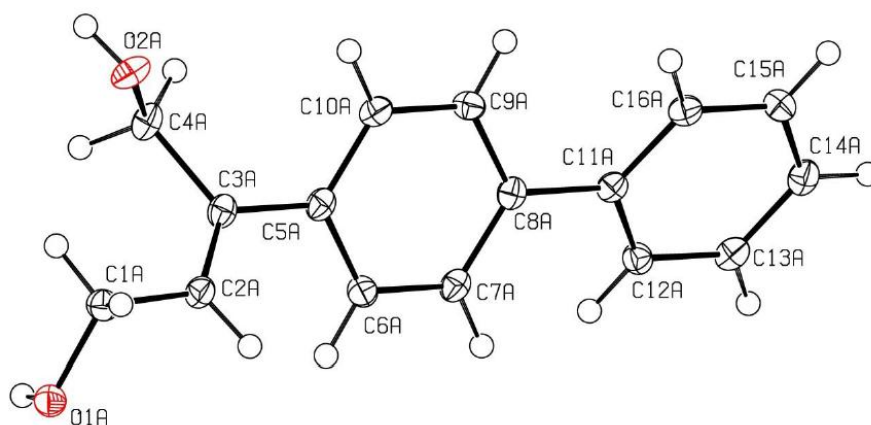
Figure 4.1: Displacement ellipsoid plot (50% probability level) of diol compound **81**.

Chapter IV

74-101: *Z/E* >99:1

74
Yield: 90%; *Z/E*>99:1

75
Yield: 90%; *Z/E*>99:1

76
Yield: 95%; *Z/E*>99:1

77
Yield: 74%; *Z/E*>99:1

78
Yield: 91%; *Z/E*>99:1

79
Yield: 80%; *Z/E*>99:1

80
Yield: 97%; *Z/E*>99:1

81
Yield: 78%; *Z/E*>99:1

82
Yield: 84%; *Z/E*>99:1

83
Yield: 91%; *Z/E*>99:1

84
Yield: 97%; *Z/E*>99:1

85
Yield: 50%; *Z/E*>99:1

86
Yield: 82%; *Z/E*>99:1

87
Yield: 98%; *Z/E*>99:1

88
Yield: 84%; *E/Z*>99:1

89
Yield: 61%; *Z/E*>99:1

90
Yield: 76%; *Z/E*>99:1

91
Yield: 81%; *Z/E*>99:1

92
Yield: 79%; *Z/E*>99:1

93
Yield: 55%; *Z/E*>99:1

94
Yield: 63%; *Z/E*>99:1

95
Yield: 85%; *Z/E*>99:1

96
Yield: 73%; *Z/E*>99:1

97
Yield: 83%; *Z/E*>99:1

98
Yield: 50%; *Z/E*>99:1

99
Yield: 73%; *Z/E*>99:1

100
Yield: 77%; *Z/E*>99:1

101
Yield: 48%; *Z/E*>99:1

Scheme 4.3: Product scope in the Pd-mediated formation of (*Z*)-but-2-ene diols **74-101**.

Stereoselective Formation of (*Z*)-1,4-but-2-ene Diols using Water as a Nucleophile

Highly functionalized olefin scaffolds have been found as various building blocks/reaction partners.[18,45-51] The presence of alcohol groups allows for an easy entry to unsaturated, nonsymmetrical 1,4-diamine scaffolds using standard nucleophilic displacements.[25] Other post-modifications of these (*Z*)-1,4-but-2-ene diols was investigated using **74** as starting material (**Scheme 4.4**). Simple oxidation of the double bond (after alcohol protection) in **74** by *meta*-chloroperoxybenzoic acid afforded **108** as a single diastereoisomer in 77% yield. Oxidative lactonization of 7**4** using a radical initiator (9-azabicyclo[3.3.1]nonane *N*-oxyl) under Cu-catalysis in the presence of *N*-methyl-imidazole produced the lactone **109** in 97% yield.[17] The cyclic ortho-ester **110** was prepared by combining **74** with trimethyl orthoformate under acid catalysis providing a well-known protection of this diol useful in synthetic chemistry.[52-53]
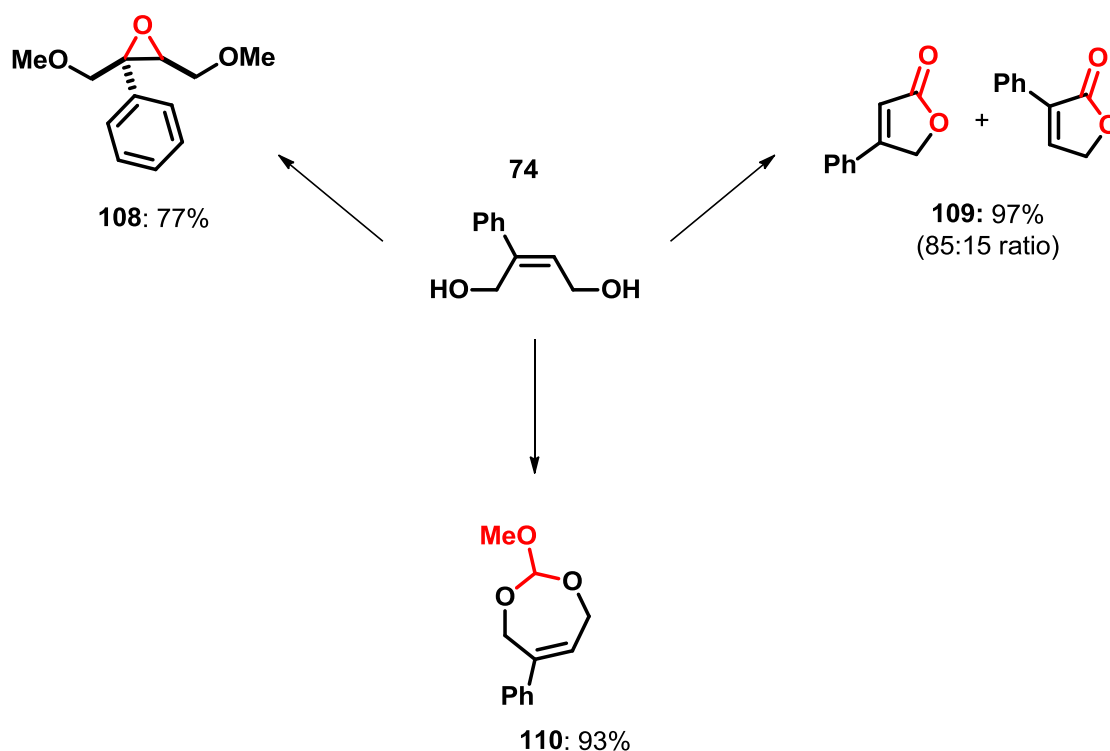
Scheme 4.4: Examples of post-modification reactions using (*Z*)-1,4-but-2-ene diol **74** in the synthesis of other interesting scaffolds **108–110**.

Chapter IV

4.3 Proposed catalytic cycle and control experiments

Intrigued by the highly stereo-selective nature of these conversions and in order to gain mechanistic insight, we performed a series of control experiments (**Scheme 4.5**). Vinyl carbonate **50** was subjected to the same reaction conditions as used for **74** using anhydrous DMF; no conversion to diol (*Z*)-**81** could be noted. Using a combination of anhydrous DMF with ^{18}O-labelled water (9:1 v/v) and treatment of vinyl carbonate **50** under these conditions afforded the labelled diol (confirmed by MS analysis) (*Z*)-**81** in 62% yield: these two combined results support the key role of water in the stereo-selective formation of the 1,4-diols. Further to this, when carbonate **50** is treated with H_2O under basic conditions in the absence of Pd catalyst the 1,2-diol **104** is produced that results from the hydrolysis of the carbonate unit; this confirms that the 1,4-diol **81** is not generated by a similar hydrolysis process known for cyclic carbonates under these basic conditions, and underlines the crucial role of the Pd-catalyst towards 1,4 diol formation.[14,54-56]
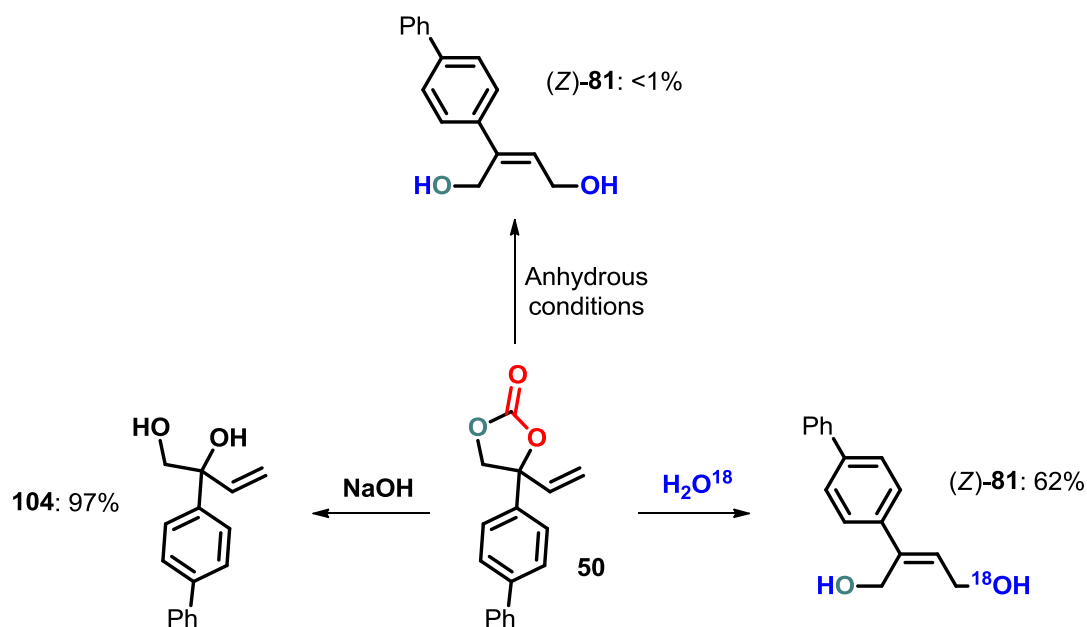
Scheme 4.5: Control experiments using vinyl carbonate **50** as substrate under different conditions.

104

Stereoselective Formation of (*Z*)-1,4-but-2-ene Diols using Water as a Nucleophile

Thus, the presence of a suitable Pd catalyst is essential to produce the 1,4-diol products, we then examined whether other vinyl-substituted carbonates (*i.e.*, **69**, **72** and **73**) would equally convert to their corresponding (*Z*)-but-2-ene diols using the optimized reaction conditions (**Scheme 4.6**). When *alkyl*-substituted carbonates (**72** and **73**) were probed no conversion to the targeted 1,4-diols **102** and **103** could be observed up to 60ºC. Interestingly, diol **105** derived from carbonate **69** that incorporates an additional vinyl substituent (less sterically demanding than the aryl groups present in the carbonates **74-101**) was obtained in 74% yield as a 72:28 mixture of both (*Z*) and (*E*) isomers. In the case of the non-substituted carbonate relatively slower conversion towards diol product **106** is observed. The low *Z/E* ratio (1:1) of this latter conversion is the result of a non-stereospecific nucleophilic attack governed by steric rather than electronic features.
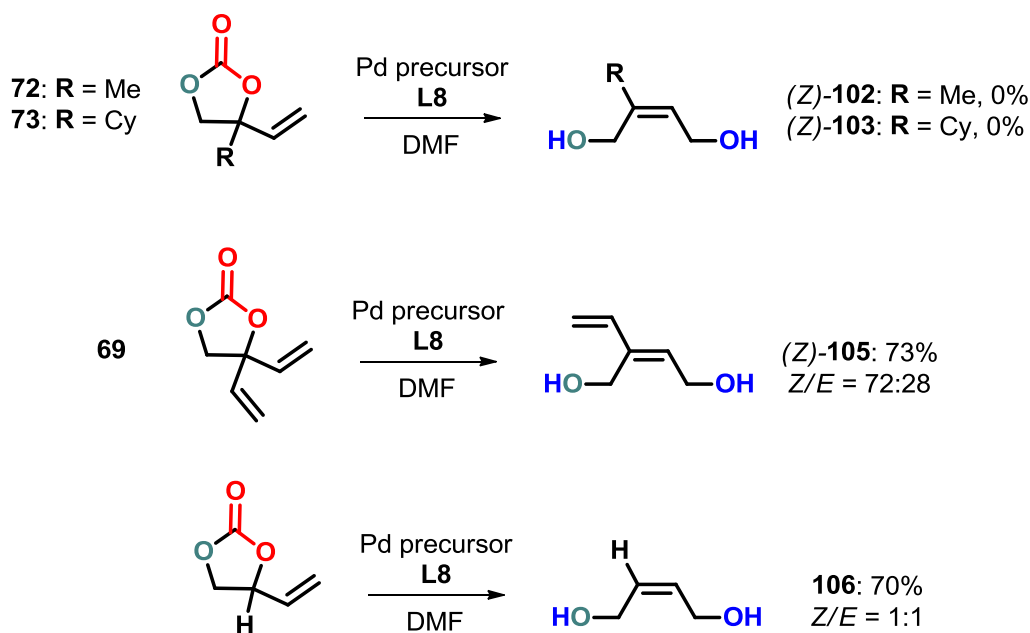
Scheme 4.6: Control experiments using non-aryl substituted vinyl carbonates.

From the results presented in the **Scheme 4.5** and **4.6** in combination with detailed DFT studies reported recently for a rather similar process that involved amines as nucleophiles,[25] a mechanistic rationale is proposed taking into count the previously postulated zwitterionic Pd-allyl intermediate **I** generated after the decarboxylative step (**Scheme 4.7**).[21-23]

105

Chapter IV
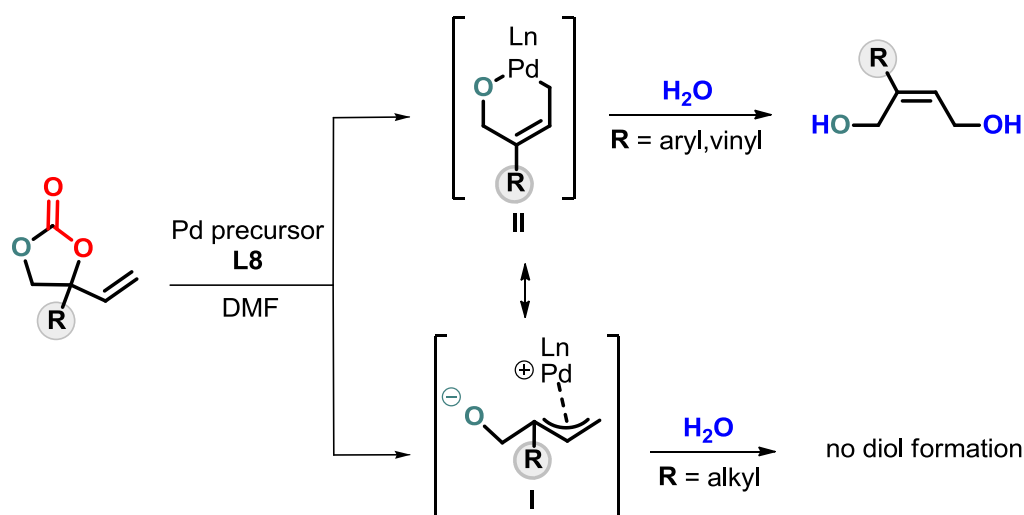
Scheme 4.7: Proposed mechanistic manifolds related to the Pd intermediates formed after decarboxylation.

Equilibration of η^3-allyl-Pd species **I** to η^1-palladacyclic intermediate **II** is electronically biased as the presence of an aryl/vinyl substituent allows for hyper-conjugation of the double bond: this in turn controls the (*Z*)-configuration of the palladacycle and thus the stereocontrol towards the 1,4-diol product. In turn, the lack of reactivity towards diol formation when R is an alkyl group is explained by a larger charge-delocalization in intermediate **I** onto which nucleophilic attack by water is disfavored for electronic reasons. Thus, clearly electron-donating groups are unable to mediate the formation of intermediate **II** and no conversion is observed as indeed noted experimentally.

Based on this, a catalytic cycle is showed in the **Scheme 4.8** where the key intermediates are represented to simplify and clarifies the mechanism of the reaction (note that similar intermediates of this reaction were determined by DFT analysis in a related amination process).[25] The initial step of the reaction starting from the White catalyst is the reduction of the Pd(II) precursor to Pd(0) in the presence of an excess of bidentate phosphine **L8** generating the catalytic active species **A** . Then the palladium complex coordinates the vinyl unit of the carbonate **43** to give intermediate **B** followed by an oxidative cleavage of the cyclic carbonate where there is a transfer of two electrons from the Pd center to the vinyl system. This leads the formation of intermediate **C** containing an η^3–allylic group attached to a linear carbonate, which is fast equilibrium by π–σ–π isomerization[57] with

Stereoselective Formation of (*Z*)-1,4-but-2-ene Diols using Water as a Nucleophile

intermediate **D**. Then, irreversible CO_2 extrusion takes place leading to the formation of the zwitterionic Pd-allyl intermediate **I**,[21-23] which due to hyper-conjugation stabilization (with carbonate substrates incorporating aryl groups) is favored over the formation of intermediate **II**, and consequently a six-membered palladacyclic ring is formed. The double bond in the final product is already formed in this intermediate, and it has to be necessarily in the (*Z*)-configuration as it is integrated into the six-membered ring.[25] The arrangement of the substituents in intermediate **II** is such that it can be subsequently attacked by the nucleophile resulting in the release of the 1,4-diol molecule **74** regenerating the Pd(0) species for further catalytic turnover.
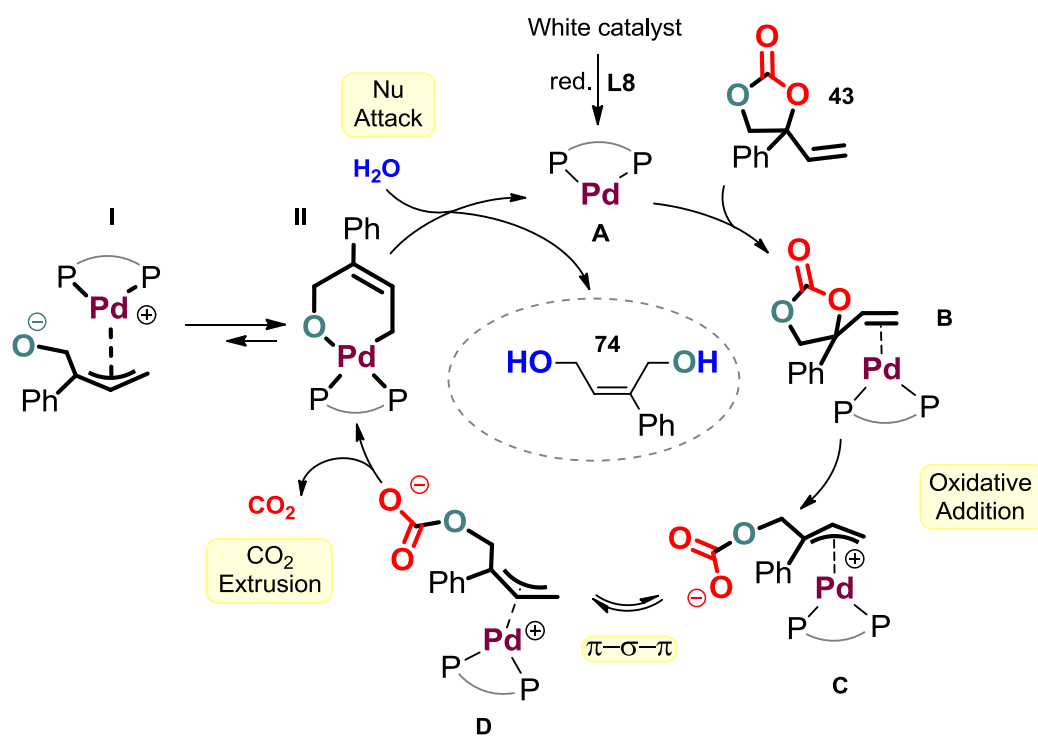
Scheme 4.8: Catalytic cycle for the formation of the (*Z*)-1,4-diol **74** through a decarboxylative hydration process catalyzed by Pd/**L8**.

4.4 Conclusions and outlook

A user-friendly, highly mild and stereo-selective methodology towards the formation of synthetically useful (*Z*)-1,4-but-2-ene diols in high yield and under exclusive stereocontrol has been developed. The results presented in this chapter

demonstrate wide scope in the reaction partners and functional group diversity allowing for the easy introduction of substituents in the α, β and γ-position of the allylic unit of the starting material. This procedure, that utilizes readily available and modular vinyl-based cyclic carbonates and simple water as reactants, can be operated in air and does not require any additive. Such privileged conditions may greatly advance the use of these diol synthons in preparative chemistry as demonstrated herein. Control experiments confirmed that water induces the formation of the 1,4-diol moiety. The exquisite stereoselectivity of the process is guided by the *in situ* formation of a six-membered palladacycle which is stabilized by hyper-conjugation with the aryl/vinyl groups of the carbonate substrate.

4.5 Experimental section

General methods and materials.

The White catalyst was purchased from Aldrich or TCI and was stored in the fridge (-20ºC) for use. ^{1}H NMR, ^{13}C{1H} NMR, ^{19}F NMR and related 2D NMR (COSY, HSQC, DEPTQ135, NOESY) spectra were recorded at room temperature on a Bruker AV-400 or AV-500 spectrometer and referenced to the residual deuterated solvent signals. All reported NMR values are given in parts per million (ppm). Chemical shifts are reported in ppm relative to the residual solvent peaks in CDCl$_3$ ($\delta = 7.26$ ppm), [D$_6$]Acetone ($\delta = 2.05$ ppm) and [D$_6$]DMSO ($\delta = 2.50$ ppm). FT-IR measurements were carried out on a Bruker Optics FTIR Alpha spectrometer. Mass spectrometric analyses and X-ray diffraction studies were performed by the Research Support Group at ICIQ and Universidade de Santiago de Compostela.

General procedure for the preparation of vinyl cyclic carbonates:

The α-hydroxylmethyl ketones were synthesized following a reported procedure when it was not commercial available.[58] The vinyl carbonates can be easily prepared according to a previous reported procedure using minor modifications (**Scheme 4.9**).[21-22]

Stereoselective Formation of (*Z*)-1,4-but-2-ene Diols using Water as a Nucleophile
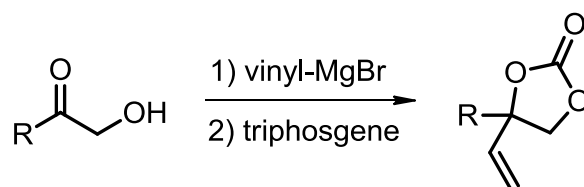
Scheme 4.9: General procedure for vinyl cyclic carbonates using α-hydroxymethyl ketones.

To a solution of the respective hydroxy methyl ketone (5 mmol, 1 eq) in THF (20 mL) was added vinylmagnesium bromide (1.0 M in THF, 2.5 eq) at 0 °C. The reaction was stirred under an N_2 atmosphere at room temperature for 2 h. The reaction mixture was then quenched with saturated aqueous NH_4Cl, and extracted with EtOAc. The combined organic layers were dried over anhydrous Na_2SO_4, filtered and concentrated affording a light yellow crude. To a solution of resultant crude mixture in CH_2Cl_2 (30 mL) added pyridine (20 mmol, 4 eq) and triphosgene (2.5 mmol, 0.5 eq) at 0 °C. The reaction was stirred under an N_2 atmosphere at room temperature for 2 h. The reaction mixture was then quenched with saturated aqueous NH_4Cl, washed with H_2O, and extracted with CH_2Cl_2. The combined organic layers were dried over anhydrous Na_2SO_4, filtered and concentrated. The residue was purified by flash chromatography on silica to afford the corresponding carbonate. Note that only for the previously unknown compounds a HRMS analysis was carried out.

The compound numbering can be found in the section "List of Relevant Compounds" on page 129.

4-Phenyl-4-vinyl-1,3-dioxolan-2-one, 43: Yellow oil. Yield: 80%, ^{1}H NMR (500 MHz, CDCl₃): δ = 4.58 (d, *J* = 8.4 Hz, 1H), 4.65 (d, *J* = 8.4 Hz, 1H), 5.41 (d, *J* = 6.8 Hz, 1H), 5.44 (s, 1H), 6.16 (dd, *J* = 10.8; 17.1 Hz, 2H), 7.34-7.45 (m, 5H). ^{13}C NMR (125 MHz, CDCl₃): δ = 74.5, 85.5, 117.6, 124.9, 128.9, 129.0, 136.5, 138.4, 154.1.

4-(4-Bromophenyl)-4-vinyl-1,3-dioxolan-2-one, 44: Yellow oil. Yield: 93%, ^{1}H NMR (500 MHz, CDCl₃): δ = 4.53 (d, *J* = 8.5 Hz, 1H), 4.64 (d, *J* = 8.5 Hz, 1H), 5.40 (dd, *J* = 10.7; 17.1 Hz, 2H), 6.12 (dd, *J* = 10.7; 17.1 Hz, 1H), 7.24 (d, *J* = 8.7 Hz, 2H), 7.57

Chapter IV

(d, J = 8.7 Hz, 2H). ^{13}C NMR (125 MHz, CDCl$_3$): δ = 74.5, 85.2, 118.3, 123.4, 126.8, 132.4, 136.2, 137.6, 153.9.

4-(4-Chlorophenyl)-4-vinyl-1,3-dioxolan-2-one, 45: Yellow oil. Yield: 76%, ^{1}H NMR (500 MHz, CDCl$_3$): δ = 4.53 (d, J = 8.5 Hz, 1H), 4.64 (d, J = 8.5 Hz, 1H), 5.36-5.50 (m, 2H), 6.13 (dd, J = 10.7; 17.1 Hz, 1H), 7.30 (d, J = 8.8 Hz, 2H), 7.41 (d, J = 8.8 Hz, 2H). ^{13}C NMR (125 MHz, CDCl$_3$): δ = 74.5, 85.2, 118.3, 126.6, 129.4, 135.2, 136.3, 137.1, 153.9.

4-(4-(Benzyloxy)phenyl)-4-vinyl-1,3-dioxolan-2-one, 46: White solid. Yield: 50%, ^{1}H NMR (500 MHz, CDCl$_3$): δ = 4.56 (d, J = 8.5 Hz, 1H), 4.60 (d, J = 8.5 Hz, 1H), 5.08 (s, 2H), 5.40 (d, J = 7.1 Hz, 1H), 5.43 (s, 1H), 6.14 (dd, J = 10.8; 17.1 Hz, 1H), 7.01 (d, J = 8.9 Hz, 2H), 7.23 (d, J = 8.9 Hz, 2H), 7.33-7.45 (m, 5H). ^{13}C NMR (125 MHz, CDCl$_3$): δ = 70.3, 74.7, 85.6, 115.4, 117.6, 126.7, 127.6, 128.3, 128.8, 130.6, 136.7, 136.8, 154.3, 159.3. IR: 1787 cm^{-1} (C=O). HRMS (ESI+, MeOH): calcd for C$_{18}$H$_{16}$O$_4$Na [M + Na]$^+$: 319.0941; found: 319.0938.

4-(4-Isocyanophenyl)-4-vinyl-1,3-dioxolan-2-one, 47: Yellow oil. Yield: 20%, ^{1}H NMR (500 MHz, CDCl$_3$): δ = 4.53 (d, J = 8.6 Hz, 1H), 4.70 (d, J = 8.6 Hz, 1H), 5.36-5.68 (m, 2H), 6.13 (dd, J = 10.7; 17.1 Hz, 1H), 7.50 (d, J = 8.5 Hz, 2H), 7.75 (d, J = 8.5 Hz, 2H). ^{13}C NMR (125 MHz, CDCl$_3$): δ = 74.3, 84.9, 113.3, 118.1, 118.9, 125.9, 133.0, 135.6, 143.6, 153.4.

4-(p-Tolyl)-4-vinyl-1,3-dioxolan-2-one, 48: Yellow oil. Yield: 71%, ^{1}H NMR (500 MHz, CDCl$_3$): δ = 2.37 (s, 3H), 4.56 (d, J = 8.4 Hz, 1H), 4.62 (d, J = 8.4 Hz, 1H), 5.40 (d, J = 4.0 Hz, 1H), 5.42 (d, J = 2.4 Hz, 1H), 6.15 (dd, J = 10.7; 17.2 Hz, 2H), 7.11-7.32 (m, 4H). ^{13}C NMR (125 MHz, CDCl$_3$): δ = 21.3, 74.7, 85.7, 117.6, 125.0, 129.8, 135.6, 136.8, 139.1, 154.3.

4-(4-Fluorophenyl)-4-vinyl-1,3-dioxolan-2-one, 49: Yellow oil. Yield: 91%, ^{1}H NMR (500 MHz, CDCl$_3$): δ = 4.55 (d, J = 8.5 Hz, 1H), 4.64 (d, J = 8.5 Hz, 1H), 5.41 (d, J = 17.2 Hz, 1H), 5.45 (d, J = 10.7 Hz, 1H), 6.14 (dd, J = 10.7; 17.2 Hz, 2H), 7.12 (t, J = 8.6 Hz, 2H), 7.35 (dd, J = 5.1; 8.9 Hz, 2H). ^{19}F NMR (500 MHz, CDCl$_3$): δ = -112.4. ^{13}C

110

Stereoselective Formation of (*Z*)-1,4-but-2-ene Diols using Water as a Nucleophile

NMR (125 MHz, CDCl$_3$): δ = 74.5, 85.1, 116.1 (d, *J* = 21.9 Hz), 118.0, 127.0 (d, *J* = 8.4 Hz), 134.1, 136.3, 153.8, 162.8 (d, *J* = 249.1 Hz). IR: 1797 cm^{-1} (C=O). HRMS (ESI+, MeOH): calcd for C$_{11}$H$_9$FO$_3$Na [M + Na]$^+$: 231.0428; found: 231.0419.

4-([1,1'-Biphenyl]-4-yl)-4-vinyl-1,3-dioxolan-2-one, 50: White solid. Yield: 84%, ^{1}H NMR (500 MHz, CDCl$_3$): δ = 4.62 (d, *J* = 8.5 Hz, 1H), 4.68 (d, *J* = 8.5 Hz, 1H), 5.35-5.58 (m, 2H), 6.20 (dd, *J* = 10.7; 17.2 Hz, 1H), 7.35-7.49 (m, 5H), 7.54-7.60 (m, 2H), 7.65 (d, *J* = 8.5 Hz, 2H). ^{13}C NMR (125 MHz, CDCl$_3$): δ = 74.7, 85.6, 117.9, 125.6, 127.3, 127.9, 128.0, 129.1, 130.5, 136.6, 137.4, 140.2, 142.1, 154.2. IR: 1781 cm^{-1} (C=O). HRMS (ESI+, MeOH): calcd for C$_{17}$H$_{14}$O$_3$Na [M + Na]$^+$: 289.0835; found: 289.0831.

4-Methyl-(2-oxo-4-vinyl-1,3-dioxolan-4-yl)benzoate, 51: Yellow oil. Yield: 87%, ^{1}H NMR (500 MHz, CDCl$_3$): δ = 3.94 (s, 3H), 4.56 (d, *J* = 8.5 Hz, 1H), 4.69 (d, *J* = 8.5 Hz, 1H), 5.42 (d, *J* = 15.6 Hz, 1H), 5.46 (d, *J* = 9.2 Hz, 1H), 6.15 (dd, *J* = 10.7; 17.1 Hz, 2H), 7.44 (d, *J* = 8.8 Hz, 2H), 8.10 (d, *J* = 8.8 Hz, 2H). ^{13}C NMR (125 MHz, CDCl$_3$): δ = 52.4, 74.3, 85.2, 118.2, 125.1, 130.4, 130.9, 136.0, 143.3, 153.8, 166.4. IR: 1776 cm^{-1}, 1716 cm^{-1} (C=O). HRMS (ESI+, MeOH): calcd for C$_{13}$H$_{12}$O$_5$Na [M + Na]$^+$: 271.0577; found: 271.0567.

4-(4-(tert-Butyl)phenyl)-4-vinyl-1,3-dioxolan-2-one, 52: White solid. Yield: 98%, ^{1}H NMR (500 MHz, CDCl$_3$): δ = 1.32 (s, 9H), 4.58 (d, *J* = 8.4 Hz, 1H), 4.63 (d, *J* = 8.4 Hz, 1H), 5.40 (d, *J* = 3.6 Hz, 1H), 5.44 (d, *J* = 10.0 Hz, 1H), 6.15 (dd, *J* = 10.7; 17.2 Hz, 1H), 7.29 (d, *J* = 8.5 Hz, 2H), 7.44 (d, *J* = 8.5 Hz, 2H). ^{13}C NMR (125 MHz, CDCl$_3$): δ = 31.4, 34.8, 74.7, 85.7, 117.5, 124.8, 126.1, 135.5, 136.8, 152.3, 154.3. IR: 1800 cm^{-1} (C=O). HRMS (ESI+, MeOH): calcd for C$_{15}$H$_{18}$O$_3$Na [M + Na]$^+$: 269.1148; found: 269.1159.

4-(4-Isopropylphenyl)-4-vinyl-1,3-dioxolan-2-one, 53: Yellow oil. Yield: 85%, ^{1}H NMR (500 MHz, CDCl$_3$): δ = 1.25 (d, *J* = 6.9 Hz, 6H), 2.93 (p, *J* = 6.9 Hz, 1H), 4.57 (d, *J* = 8.4 Hz, 1H), 4.63 (d, *J* = 8.4 Hz, 1H), 5.40 (d, *J* = 2.1 Hz, 1H), 5.44 (d, *J* = 8.4 Hz, 1H), 6.15 (dd, *J* = 10.8; 17.2 Hz, 1H), 7.28 (s, 4H). ^{13}C NMR (125 MHz, CDCl$_3$): δ = 24.0, 34.0, 74.7, 85.7, 117.5, 125.1, 127.2, 135.9, 136.8, 146.0, 154.3. IR: 1798 cm^{-1}

Chapter IV

(C=O). HRMS (ESI+, MeOH): calcd for $C_{14}H_{16}O_3Na$ [M + Na]$^+$: 255.0992; found: 255.0998.

4-(4-(Methylthio)phenyl)-4-vinyl-1,3-dioxolan-2-one, 54: Yellow oil. Yield: 52%, ^{1}H NMR (500 MHz, CDCl$_3$): δ = 2.49 (s, 3H), 4.55 (d, J = 8.5 Hz, 1H), 4.62 (d, J = 8.5 Hz, 1H), 5.41 (d, J = 11.5 Hz, 1H), 5.43 (d, J = 5.1 Hz, 1H), 6.14 (dd, J = 10.7; 17.1 Hz, 1H), 7.27-7.29 (m, 4H). ^{13}C NMR (125 MHz, CDCl$_3$): δ = 15.6, 74.6, 85.5, 117.9, 125.6, 126.7, 135.0, 136.5, 140.3, 154.1. IR: 1796 cm^{-1} (C=O). HRMS (ESI+, MeOH): calcd for $C_{12}H_{12}O_3SNa$ [M + Na]$^+$: 259.0399; found: 259.0408.

4-(Furan-2-yl)-4-vinyl-1,3-dioxolan-2-one, 55: Yellow oil. Yield: 56%, ^{1}H NMR (500 MHz, CDCl$_3$): δ = 4.48 (d, J = 8.5 Hz, 1H), 4.51 (d, J = 8.5 Hz, 1H), 5.33-5.59 (m, 2H), 6.13 (dd, J = 10.8; 17.2 Hz, 1H), 6.41 (dd, J = 1.2; 1.7 Hz, 1H), 7.40-7.61 (m, 2H). ^{13}C NMR (125 MHz, CDCl$_3$): δ = 74.2, 81.7, 108.4, 118.5, 124.3, 135.2, 140.7, 144.8, 154.1. IR: 1792 cm^{-1} (C=O). HRMS (ESI+, MeOH): calcd for $C_9H_8O_4Na$ [M + Na]$^+$: 203.0315; found: 203.0320.

4-(Thiophen-2-yl)-4-vinyl-1,3-dioxolan-2-one, 56: Yellow oil. Yield: 68%, ^{1}H NMR (500 MHz, CDCl$_3$): δ = 4.55 (d, J = 8.5 Hz, 1H), 4.59 (d, J = 8.5 Hz, 1H), 5.46 (dd, J = 3.2; 14.0 Hz, 2H), 6.17 (dd, J = 10.7; 17.1 Hz, 1H), 7.06 (dd, J = 1.4; 5.1 Hz, 1H), 7.35 (dd, J = 1.4; 3.0 Hz, 1H), 7.42 (dd, J = 3.0; 5.1 Hz, 1H). ^{13}C NMR (125 MHz, CDCl$_3$): δ = 74.5, 83.9, 118.1, 123.2, 125.2, 127.9, 135.9, 139.4, 154.2.

4-(Pyrrol-2-yl)-4-vinyl-1,3-dioxolan-2-one, 57: Yellow oil. Yield: 60%, ^{1}H NMR (500 MHz, CDCl$_3$): δ = 4.43 (d, J = 8.5 Hz, 1H), 4.49 (d, J = 8.5 Hz, 1H), 5.53-5.68 (m, 2H), 6.17 (dd, J = 10.8; 17.1 Hz, 1H), 6.43 (dd, J = 1.8; 3.4 Hz, 1H), 6.51 (dd, J = 0.9; 3.4 Hz, 1H), 7.53 (dd, J = 0.9; 1.8 Hz, 1H). ^{13}C NMR (125 MHz, CDCl$_3$): δ = 72.2, 80.8, 111.0, 111.4, 118.9, 133.5, 144.6, 149.3, 154.0.

4-(Pyridin-3-yl)-4-vinyl-1,3-dioxolan-2-one, 58: Brown oil. Yield: 23%, ^{1}H NMR (500 MHz, CDCl$_3$): δ = 4.60 (d, J = 8.6 Hz, 1H), 4.70 (d, J = 8.5 Hz, 1H), 5.40-5.55 (m, 2H), 6.17 (dd, J = 10.8; 17.1 Hz, 1H), 7.39 (ddd, J = 0.9; 4.8; 8.0 Hz, 1H), 7.75 (ddd, J = 1.6; 2.5; 8.0 Hz, 1H), 8.54-8.74 (m, 2H). ^{13}C NMR (125 MHz, CDCl$_3$): δ = 74.3, 84.1,

Stereoselective Formation of (*Z*)-1,4-but-2-ene Diols using Water as a Nucleophile

118.4, 123.9, 133.0, 135.9, 146.8, 150.5, 153.5. IR: 1798 cm^{-1} (C=O). HRMS (ESI+, MeOH): calcd for $C_{10}H_{10}NO_3$ [M + H]$^+$: 192.0656; found: 192.0655.

4-(m-Tolyl)-4-vinyl-1,3-dioxolan-2-one, 59: Yellow oil. Yield: 78%, ^{1}H NMR (500 MHz, CDCl$_3$): δ = 2.38 (s, 3H), 4.56 (d, *J* = 8.4 Hz, 1H), 4.64 (d, *J* = 8.4 Hz, 1H), 5.41 (d, *J* = 10.8 Hz, 1H), 5.42 (d, *J* = 17.2 Hz, 1H), 6.15 (dd, *J* = 10.8; 17.2 Hz, 1H), 7.10-7.23 (m, 3H), 7.28-7.33 (m, 1H). ^{13}C NMR (125 MHz, CDCl$_3$): δ = 21.7, 74.7, 85.7, 117.6, 122.0, 125.6, 129.0, 129.8, 136.8, 138.6, 139.1, 154.3. IR: 1798 cm^{-1} (C=O). HRMS (ESI+, MeOH): calcd for $C_{12}H_{12}O_3Na$ [M + Na]$^+$: 227.0679; found: 227.0680.

4-(3-Bromophenyl)-4-vinyl-1,3-dioxolan-2-one, 60: Yellow oil. Yield: 62%, ^{1}H NMR (500 MHz, CDCl$_3$): δ = 4.54 (d, *J* = 8.5 Hz, 1H), 4.65 (d, *J* = 8.5 Hz, 1H), 5.35-5.45 (m, 2H), 6.12 (dd, *J* = 10.7; 17.1 Hz, 1H), 7.27-7.36 (m, 2H), 7.49-7.52 (m, 2H). ^{13}C NMR (125 MHz, CDCl$_3$): δ = 74.5, 84.9, 118.4, 123.4, 123.6, 128.3, 130.8, 132.3, 136.1, 140.8, 153.8.

4-(3-Chlorophenyl)-4-vinyl-1,3-dioxolan-2-one, 61: Yellow oil. Yield: 70%, ^{1}H NMR (500 MHz, CDCl$_3$): δ = 4.55 (d, *J* = 8.5 Hz, 1H), 4.65 (d, *J* = 8.5 Hz, 1H), 5.40 (d, *J* = 14.5 Hz, 1H), 5.46 (d, *J* = 8.1 Hz, 1H), 6.13 (dd, *J* = 10.7; 17.1 Hz, 1H), 7.23-7.26 (m, 1H), 7.35-7.38 (m, 3H). ^{13}C NMR (125 MHz, CDCl$_3$): δ = 74.5, 85.0, 118.4, 123.2, 125.4, 129.3, 130.5, 135.3, 136.1, 140.6, 153.8. IR: 1798 cm^{-1} (C=O). HRMS (ESI+, MeOH): calcd for $C_{11}H_9ClO_3Na$ [M + Na]$^+$: 247.0132; found: 247.128.

4-(2-Fluorophenyl)-4-vinyl-1,3-dioxolan-2-one, 62: Yellow oil. Yield: 75%, ^{1}H NMR (500 MHz, CDCl$_3$): δ = 4.60 (dd, *J* = 1.7; 8.5 Hz, 1H), 4.75 (dd, *J* = 2.6; 8.8 Hz, 1H), 5.27-5.45 (m, 2H), 6.03-6.24 (m, 1H), 7.12 (ddd, *J* = 1.2; 8.3; 11.2 Hz, 1H), 7.23 (td, *J* = 1.2; 7.6 Hz, 1H), 7.35-7.42 (m, 1H), 7.56 (td, *J* = 1.8; 7.8 Hz, 1H). ^{19}F NMR (500 MHz, CDCl$_3$): δ = -115.1. ^{13}C NMR (125 MHz, CDCl$_3$): δ = 74.6 (d, *J* = 8.0 Hz), 83.4 (d, *J* = 2.5 Hz), 116.0 (d, *J* = 20.1 Hz), 117.1, 125.0 (d, *J* = 3.5 Hz), 126.3 (d, *J* = 3.5 Hz), 130.7 (d, *J* = 8.3 Hz), 135.3 (d, *J* = 1.9 Hz), 153.6, 158.5 (d, *J* = 245.1 Hz). IR: 1805 cm^{-1} (C=O). HRMS (ESI+, MeOH): calcd for $C_{11}H_9FO_3Na$ [M + Na]$^+$: 231.0428; found: 231.0427.

113

Chapter IV

4-(2-Bromophenyl)-4-vinyl-1,3-dioxolan-2-one, 63: Yellow oil. Yield: 50%, ^{1}H NMR (500 MHz, CDCl$_3$): δ = 4.74 (d, J = 8.9 Hz, 1H), 4.98 (d, J = 8.9 Hz, 1H), 5.40 (dd, J = 3.2; 13.8 Hz, 2H), 6.36 (dd, J = 10.6; 17.1 Hz, 1H), 7.22-7.30 (m, 1H), 7.42 (ddd, J = 1.3; 7.4; 7.9 Hz, 1H), 7.62 (dd, J = 1.3; 7.9 Hz, 1H), 7.70 (d, J = 1.7; 8.0 Hz, 1H). ^{13}C NMR (125 MHz, CDCl$_3$): δ = 74.6, 85.6, 118.6, 119.1, 127.5, 128.3, 130.5, 134.4, 135.1, 138.8, 153.6.

4-(3,5-Dimethylphenyl)-4-vinyl-1,3-dioxolan-2-one, 64: Yellow oil. Yield: 58%, ^{1}H NMR (500 MHz, CDCl$_3$): δ = 2.33 (d, J = 0.7 Hz, 6H), 4.55 (d, J = 8.4 Hz, 1H), 4.62 (d, J = 8.4 Hz, 1H), 5.36-5.46 (m, 1H), 6.13 (dd, J = 10.7; 17.2 Hz, 1H), 6.95 (dt, J = 0.7; 1.2 Hz, 2H), 7.00 (dt, J = 0.8; 1.5 Hz, 1H). ^{13}C NMR (125 MHz, CDCl$_3$): δ = 21.5, 74.7, 85.7, 117.3, 122.6, 130.6, 136.8, 138.6, 138.9, 154.3. IR: 1790 cm^{-1} (C=O). HRMS (ESI+, MeOH): calcd for C$_{13}$H$_{14}$O$_3$Na [M + Na]$^+$: 241.0835; found: 241.0831.

4-(3,4-Dichlorophenyl)-4-vinyl-1,3-dioxolan-2-one, 65: Yellow oil. Yield: 63%, ^{1}H NMR (500 MHz, CDCl$_3$): δ = 4.52 (d, J = 8.6 Hz, 1H), 4.65 (d, J = 8.6 Hz, 1H), 5.44 (d, J = 17.1 Hz, 1H), 5.48 (d, J = 10.7 Hz, 1H), 6.11 (dd, J = 10.7; 17.1 Hz, 1H), 7.21 (dd, J = 2.3; 8.4 Hz, 1H), 7.47 (d, J = 2.2 Hz, 1H), 7.52 (d, J = 8.4 Hz, 1H). ^{13}C NMR (125 MHz, CDCl$_3$): δ = 74.3, 84.6, 118.7, 124.4, 127.4, 131.3, 133.7, 135.7, 138.8, 153.6. IR: 1798 cm^{-1} (C=O). HRMS (ESI+, MeOH): calcd for C$_{11}$H$_8$Cl$_2$O$_3$Na [M + Na]$^+$: 280.9743; found: 280.9736.

4-(3-Bromo-4-fluorophenyl)-4-vinyl-1,3-dioxolan-2-one, 66: Brown oil. Yield: 60%, ^{1}H NMR (500 MHz, CDCl$_3$): δ = 4.53 (d, J = 8.6 Hz, 1H), 4.64 (d, J = 8.6 Hz, 1H), 5.34-5.62 (m, 2H), 6.11 (dd, J = 10.7; 17.1 Hz, 1H), 7.19 (ddd, J = 4.4; 8.0; 8.6 Hz, 1H), 7.30 (ddd, J = 2.4; 4.4; 8.6 Hz, 1H), 7.58 (dd, J = 2.4; 6.3 Hz, 1H). ^{19}F NMR (500 MHz, CDCl$_3$): δ = -106.2. ^{13}C NMR (125 MHz, CDCl$_3$): δ = 74.4, 84.6, 110.1 (d, J = 21.6 Hz), 117.2 (d, J = 22.9 Hz), 118.6, 125.9 (d, J = 7.5 Hz), 130.7, 135.9, 153.6, 159.4 (d, J = 250.5 Hz). IR: 1797 cm^{-1} (C=O).HRMS (ESI+, MeOH): calcd for C$_{11}$H$_8$BrFO$_3$Na [M + Na]$^+$: 308.9535; found: 308.9533.

4-(Naphthalen-2-yl)-4-vinyl-1,3-dioxolan-2-one, 67: White solid. Yield: 30%, ^{1}H NMR (500 MHz, CDCl$_3$): δ = 4.79 (d, J = 8.5 Hz, 1H), 5.00 (d, J = 8.5 Hz, 1H), 5.24-

114

Stereoselective Formation of (*Z*)-1,4-but-2-ene Diols using Water as a Nucleophile

5.55 (m, 2H), 6.40 (dd, *J* = 10.6; 17.1 Hz, 2H), 7.40-7.56 (m, 2H), 7.78 (dd, *J* = 1.2; 7.4 Hz, 1H), 7.84-8.05 (m, 1H). ^{13}C NMR (125 MHz, CDCl$_3$): δ = 74.9, 86.1, 120.1, 123.4, 124.5, 125.4, 126.1, 126.7, 128.8, 129.7, 130.1, 134.5, 136.8, 153.8.

4-(6-Methoxynaphthalen-2-yl)-4-vinyl-1,3-dioxolan-2-one, 68: White solid. Yield: 63%, ^{1}H NMR (500 MHz, CDCl$_3$): δ = 3.93 (s, 3H), 4.66-4.72 (m, 2H), 5.44 (d, *J* = 4.7 Hz, 1H), 5.48 (d, *J* = 1.7 Hz, 1H), 6.24 (dd, *J* = 10.7; 17.2 Hz, 1H), 7.19-7.22 (m, 1H), 7.14-7.15 (m, 1H), 7.35-7.38 (m, 1H), 7.74-7.81 (m, 3H). ^{13}C NMR (125 MHz, CDCl$_3$): δ = 55.5, 74.6, 85.9, 105.8, 118.0, 120.0, 123.1, 124.3, 128.0, 128.4, 129.9, 133.3, 134.6, 136.7, 154.3, 158.7. IR: 1795 cm^{-1} (C=O). HRMS (ESI+, MeOH): calcd for C$_{16}$H$_{14}$O$_4$Na [M + Na]$^+$: 293.0784, found: 293.0783.

4-Phenyl-4-(prop-1-en-1-yl)-1,3-dioxolan-2-one, 70: Yellow oil. Yield: 86%, (2 isomers 6:4). ^{1}H NMR (500 MHz, CDCl$_3$, major isomer): δ = 1.79 (d, *J* = 4.9 Hz, 3H), 4.54-4.65 (m, 2H), 5.73-5.93 (m, 2H), 7.35-7.47 (m, 5H). ^{13}C NMR (125 MHz, CDCl$_3$, major isomer): δ = 17.8, 75.0, 85.7, 124.9, 128.7, 128.9, 130.0, 132.8, 139.1, 154.3. IR: 1795 cm^{-1} (C=O). HRMS (ESI+, MeOH): calcd for C$_{12}$H$_{12}$O$_3$Na [M + Na]$^+$: 227.0679; found: 227.0687.

4-Phenyl-4-(prop-1-en-2-yl)-1,3-dioxolan-2-one, 71: Yellow oil. Yield: 35%, ^{1}H NMR (500 MHz, CDCl$_3$): δ = 1.73 (s, 3H), 4.63 (d, *J* = 8.6 Hz, 1H), 4.79 (d, *J* = 8.6 Hz, 1H), 5.03-5.25 (m, 2H), 7.31-7.53 (m, 5H). ^{13}C NMR (125 MHz, CDCl$_3$): δ = 18.4, 73.1, 88.0, 114.0, 125.0, 128.9, 138.4, 142.8, 154.0. IR: 1794 cm^{-1} (C=O). HRMS (ESI+, MeOH): calcd for C$_{12}$H$_{12}$O$_3$Na [M + Na]$^+$: 227.0679; found: 227.0677.

4-Methyl-4-vinyl-1,3-dioxolan-2-one, 72: Yellow oil. Yield: 32%, ^{1}H NMR (500 MHz, CDCl$_3$): δ = 1.60 (s, 3H), 4.18 (d, *J* = 8.3 Hz, 1H), 4.27 (d, *J* = 8.3 Hz, 1H), 5.33 (d, *J* = 10.9 Hz, 1H), 5.44 (d, *J* = 17.3 Hz, 1H), 5.94 (dd, *J* = 10.9; 17.3 Hz, 1H). ^{13}C NMR (125 MHz, CDCl$_3$): δ = 24.3, 74.5, 82.7, 116.7, 137.0, 154.5.

4-Cyclohexyl-4-vinyl-1,3-dioxolan-2-one, 73: Yellow oil. Yield: 62%, ^{1}H NMR (500 MHz, CDCl$_3$): δ = 0.93-1.40 (m, 4H), 1.61-1.91 (m, 7H), 4.22 (d, *J* = 8.4 Hz, 1H), 4.32 (d, *J* = 8.4 Hz, 1H), 5.27-5.61 (m, 2H), 5.85 (dd, *J* = 11.0; 17.3 Hz, 1H). ^{13}C NMR

Chapter IV

(125 MHz, CDCl$_3$): δ = 25.8, 26.1, 26.2, 26.5, 26.7, 45.6, 72.2, 87.3, 116.9, 134.8, 154.7.

Procedure for the preparation of bis-vinyl-carbonate 69:

To a solution of methyl glycolate (500 mg, 5.55 mmol) in dry THF (5 mL) was added vinylmagnesium bromide (1.0 M THF solution, 22.2 mL, 22.20 mmol) at 0 ºC under Ar. The solution was stirred at room temperature for 6 h. The reaction was then quenched with saturated solution of NH$_4$Cl. The organic phase was extracted with EtOAc (3 × 10 mL) and dried over anhydrous Na$_2$SO$_4$. The volatiles were removed under reduced pressure affording the crude diol. Hereafter, the crude diol was dissolved in CH$_2$Cl$_2$ (11 mL), followed by the addition of pyridine (1.8 mL, 22.20 mmol) and triphosgene (824 mg, 2.8 mmol) at 0 ºC. The resultant mixture was stirred at room temperature for 4 h and the reaction was quenched by addition of a saturated aqueous solution of NH$_4$Cl. The organic phase was extracted with DCM (3×10 mL) and dried over anhydrous Na$_2$SO$_4$. After removal of the volatiles, the reaction crude was purified by column chromatography (Hexane/EtOAc = 4:1 as eluent) to afford the bis-vinyl-carbonate **69**.

4,4-Divinyl-1,3-dioxolan-2-one, 69: Yellow oil. Yield: 44%, ^{1}H NMR (500 MHz, CDCl$_3$): δ = 4.33 (s, 2H), 5.43 (d, J = 10.8 Hz, 2H), 5.49 (d, J = 17.3 Hz, 2H), 5.97 (dd, J = 10.8; 17.3 Hz, 2H). ^{13}C NMR (125 MHz, CDCl$_3$): δ = 73.2, 84.2, 118.5, 134.8, 154.3. IR: 1791 cm^{-1} (C=O). HRMS (ESI+, MeOH): calcd for C$_7$H$_8$O$_3$Na [M + Na]$^+$: 163.0371; found: 163.0366.

General procedure for the formation of (Z)-1,4-But-2-ene diols:

A screw-capped vial was charged with the respective carbonate (0.2 mmol, 1 eq.), the White catalyst precursor (0.0020 g, 0.004 mmol, 2 mmol%), phosphine **L8** (0.0054 g, 0.01 mmol, 5 mmol%) and DMF (200 µL). The reaction mixture was stirred at rt for 12 h. Then, the product was purified by flash chromatography affording the corresponding product. To obtain the compounds **93**, **94**, **100** and **101** higher loading of catalyst was required (5.0 mol% of palladium precursor, 10

Stereoselective Formation of (*Z*)-1,4-but-2-ene Diols using Water as a Nucleophile

mol% of **L8**) and additionally 60 μl of H_2O was added; the reactions were carried at a temperature of 60 ºC. All purified products were fully characterized by ^1H and ^{13}C NMR and IR spectra, and HRMS analysis (in the case of newly reported compounds); ^{19}F NMR and 2D NMR (COSY, HSQC, DEPTQ135 and 2D ^1H-^1H NOESY) analyses were carried out when necessary to fully assign the proposed structures.

(*Z*)-2-Phenylbut-2-ene-1,4-diol, 74: Yellow oil. Yield: 90%, ^1H NMR (500 MHz, CDCl$_3$): δ = 4.34 (d, *J* = 6.9 Hz, 2H), 4.54 (s, 2H), 6.09 (t, *J* = 6.9 Hz, 1H), 7.27-7.30 (m, 1H), 7.32-7.36 (m, 2H), 7.42-7.45 (m, 2H). ^{13}C NMR (101 MHz, CDCl$_3$): δ = 58.9, 60.3, 126.5, 127.8, 128.7, 129.9, 140.6, 142.7.

(*Z*)-2-(4-Bromophenyl)-but-2-ene-1,4-diol, 75: Yellow oil. Yield: 90%, ^1H NMR (500 MHz, CDCl$_3$): δ = 2.61 (bs, 2H), 4.35 (d, *J* = 6.8 Hz, 2H), 4.52 (s, 2H), 6.08 (t, *J* = 6.8 Hz, 1H), 6.30 (d, *J* = 8.6 Hz, 2H), 7.44 (d, *J* = 8.6 Hz, 2H). ^{13}C NMR (125 MHz, CDCl$_3$): δ = 58.9, 60.2, 121.9, 128.1, 130.2, 131.8, 139.6, 141.8. HRMS (ESI+, MeOH): calcd for $C_{10}H_{11}BrO_2Na$ [M + Na]$^+$: 264.9835, found: 264.9839.

(*Z*)-2-(4-Chlorophenyl)-but-2-ene-1,4-diol, 76: Yellow oil. Yield: 95%, ^1H NMR (500 MHz, CDCl$_3$): δ = 3.24 (bs, 2H), 4.32 (d, *J* = 6.9 Hz, 2H), 4.49 (s, 2H), 6.06 (t, *J* = 6.9 Hz, 1H), 7.29 (d, *J* = 8.7 Hz, 2H), 7.36 (d, *J* = 8.7 Hz, 2H). ^{13}C NMR (125 MHz, CDCl$_3$): δ = 58.8, 59.9, 127.8, 128.8, 130.2, 133.7, 139.0, 141.4. HRMS (ESI+, MeOH): calcd for $C_{10}H_{11}ClO_2Na$ [M + Na]$^+$: 221.0340, found: 221.0334.

(*Z*)-2-(4-(Benzyloxy)phenyl)-but-2-ene-1,4-diol, 77: Yellow oil. Yield: 74%, ^1H NMR (500 MHz, CDCl$_3$): δ = 2.11 (bs, 2H), 4.36 (d, *J* = 7.0 Hz, 2H), 4.55 (s, 2H), 5.07 (s, 2H), 6.05 (t, *J* = 6.9 Hz, 1H), 6.95 (t, *J* = 8.8 Hz, 2H), 7.30-7.48 (m, 7H). ^{13}C NMR (125 MHz, CDCl$_3$): δ = 59.1, 60.4, 70.2, 115.0, 124.1, 127.6, 127.7, 128.1, 128.4, 128.7, 135.1, 137.0, 158.4. HRMS (ESI+, MeOH): calcd for $C_{17}H_{18}O_3Na$ [M + Na]$^+$: 293.1148, found: 293.1148.

(*Z*)-4-(1,4-Dihydroxybut-2-en-2-yl)-benzonitrile, 78: Yellow oil. Yield: 91%, ^1H NMR (500 MHz, CDCl$_3$): δ = 2.73 (bs, 2H), 4.46 (d, *J* = 6.7 Hz, 2H), 4.41 (s, 2H), 6.20 (t, *J* = 6.7 Hz, 1H), 7.50-7.65 (m, 4H). ^{13}C NMR (125 MHz, CDCl$_3$): δ = 59.0, 60.0,

Chapter IV

111.2, 119.0, 127.1, 132.4, 132.7, 141.2, 145.5. HRMS (ESI+, MeOH): calcd for $C_{11}H_{11}O_2NNa$ [M + Na]$^+$: 212.0682, found: 212.0682.

(Z)-2-(p-Tolyl)-but-2-ene-1,4-diol, 79: Yellow oil. Yield: 80%, ^{1}H NMR (500 MHz, CDCl$_3$): δ = 2.34 (s, 3H), 2.77 (bs, 2H), 4.33 (d, J = 7.0 Hz, 2H), 4.53 (s, 2H), 6.06 (t, J = 7.0 Hz, 1H), 7.14 (t, J = 7.9 Hz, 2H), 7.31-7.44 (m, 2H). ^{13}C NMR (125 MHz, CDCl$_3$): δ = 21.2, 58.9, 60.2, 126.4, 129.0, 129.4, 137.6, 137.7, 142.5. HRMS (ESI+, MeOH): calcd for $C_{11}H_{14}O_2Na$ [M + Na]$^+$: 201.0886, found: 201.0886.

(Z)-2-(4-Fluorophenyl)-but-2-ene-1,4-diol, 80: Yellow oil. Yield: 97%, ^{1}H NMR (500 MHz, CDCl$_3$): δ = 2.92 (bs, 2H), 4.33 (d, J = 6.9 Hz, 2H), 4.50 (s, 2H), 6.03 (t, J = 6.9 Hz, 1H), 7.00 (d, J = 8.7 Hz, 2H), 7.36-7.46 (m, 2H). ^{13}C NMR (125 MHz, CDCl$_3$): δ = 58.8, 60.2, 115.5 (d, J = 21.3 Hz), 128.2 (d, J = 8.0 Hz), 129.7, 136.7 (d, J = 3.3 Hz), 141.8, 162.2 (d, J = 247.2 Hz). ^{19}F NMR (500 MHz, CDCl$_3$): δ = -114.8. HRMS (ESI+, MeOH): calcd for $C_{10}H_{11}FO_2Na$ [M + Na]$^+$: 205.0635, found: 205.0634.

(Z)-2-([1,1'-Biphenyl]-4-yl)-but-2-ene-1,4-diol, 81: Yellow oil. Yield: 78%, ^{1}H NMR (500 MHz, Acetone-d_6): δ = 3.85-3.90 (m, 2H), 4.38-4.41 (m, 2H), 4.55 (d, J = 5.7 Hz, 2H), 6.11 (t, J = 6.4 Hz, 1H), 7.33-7.36 (m, 1H), 7.44-7.47 (m, 2H), 7.60-7.68 (m, 6H). ^{13}C NMR (125 MHz, Acetone-d_6): δ = 59.2, 59.8, 127.5, 127.6, 127.7, 128.1, 129.7, 132.0, 140.4, 141.0, 141.5. HRMS (ESI+, MeOH): calcd for $C_{16}H_{16}O_2Na$ [M + Na]$^+$: 263.1043, found: 263.1035. HRMS (ESI+, MeOH): ^{18}O labelled sample: calcd for $C_{16}H_{16}O_2Na$ [M + Na]$^+$: 265.1085, found: 265.1081.

(Z)-4-Methyl-(1,4-dihydroxybut-2-en-2-yl)-benzoate, 82: Yellow oil. Yield: 84%, ^{1}H NMR (500 MHz, CDCl$_3$): δ = 2.74 (bs, 2H), 3.90 (s, 3H), 4.37 (d, J = 6.8 Hz, 2H), 4.53 (s, 2H), 6.16 (t, J = 6.7 Hz, 1H), 7.48 (d, J = 8.5 Hz, 2H), 7.96 (d, J = 8.5 Hz, 2H). ^{13}C NMR (125 MHz, CDCl$_3$): δ = 52.3, 59.0, 60.0, 126.4, 126.6, 129.9, 131.8, 141.7, 145.3, 167.1. HRMS (ESI+, MeOH): calcd for $C_{12}H_{14}O_4Na$ [M + Na]$^+$: 245.0784, found: 245.0778.

(Z)-2-(4-(tert-Butyl)phenyl)-but-2-ene-1,4-diol, 83: Yellow oil. Yield: 91%, ^{1}H NMR (500 MHz, CDCl$_3$): δ = 1.32 (s, 9H), 2.75 (bs, 2H), 4.33 (d, J = 7.0 Hz, 2H), 4.53

118

Stereoselective Formation of (*Z*)-1,4-but-2-ene Diols using Water as a Nucleophile

(s, 2H), 6.08 (t, *J* = 7.0 Hz, 1H), 7.33-7.48 (m, 4H). ^{13}C NMR (125 MHz, CDCl$_3$): δ = 31.4, 34.7, 58.9, 60.2, 125.6, 126.2, 129.2, 137.5, 142.4, 150.9. HRMS (ESI+, MeOH): calcd for C$_{14}$H$_{20}$O$_2$Na [M + Na]$^+$: 243.1356, found: 243.1346.

(*Z*)-2-(4-Isopropylphenyl)-but-2-ene-1,4-diol, 84: Yellow oil. Yield: 97%, ^{1}H NMR (500 MHz, CDCl$_3$): δ = 1.25 (d, *J* = 6.9 Hz, 2H), 2.68 (bs, 2H), 2.90 (dt, 7.0; 14.2 Hz, 1H), 4.34 (d, *J* = 7.0 Hz, 2H), 4.54 (s, 2H), 6.08 (t, *J* = 7.0 Hz, 1H), 7.20 (d, *J* = 8.2 Hz, 2H), 7.37 (d, *J* = 8.2 Hz, 2H). ^{13}C NMR (125 MHz, CDCl$_3$): δ = 24.6, 33.9, 59.0, 60.3, 126.5, 126.8, 138.0, 142.6, 148.7. HRMS (ESI+, MeOH): calcd for C$_{13}$H$_{18}$O$_2$Na [M + Na]$^+$: 229.119, found: 229.119.

(*Z*)-2-(4-(Methylthio)phenyl)-but-2-ene-1,4-diol, 85: Yellow oil. Yield: 50%, ^{1}H NMR (500 MHz, CDCl$_3$): δ = 2.09 (bs, 2H), 2.51 (s, 3H), 4.41 (d, *J* = 6.8 Hz, 2H), 4.58 (s, 2H), 6.12 (t, *J* = 6.7 Hz, 1H), 7.19-7.31 (m, 2H), 7.30-7.46 (m, 2H). ^{13}C NMR (125 MHz, CDCl$_3$): δ = 15.9, 59.1, 60.4, 126.7, 126.9, 129.4, 137.3, 139.3, 142.4. HRMS (ESI+, MeOH): calcd for C$_{11}$H$_{14}$O$_2$SNa [M + Na]$^+$: 233.0607, found: 233.0597.

(*Z*)-2-(Furan-3-yl)-but-2-ene-1,4-diol, 86: Yellow oil. Yield: 82%, ^{1}H NMR (400 MHz, CDCl$_3$): δ = 2.49 (s, 2H), 4.32 (d, *J* = 7.1 Hz, 2H), 4.41 (s, 2H), 6.06 (t, *J* = 7.1 Hz, 1H), 6.53 (s, 1H), 7.54-760 (m, 1H), 8.37-8.38 (m, 1H). ^{13}C NMR (101 MHz, CDCl$_3$): δ = 58.5, 59.9, 108.1, 125.8, 126.9, 134.1, 139.8, 143.6. HRMS (ESI+, MeOH): calcd for C$_8$H$_{10}$O$_3$Na [M + Na]$^+$: 203.0315, found: 203.0320.

(*Z*)-2-(Thiophen-3-yl)-but-2-ene-1,4-diol, 87: Yellow oil. Yield: 98%, ^{1}H NMR (400 MHz, CDCl$_3$): δ = 2.80 (s, 2H), 4.30 (d, *J* = 7.1 Hz, 2H), 4.47 (s, 2H), 6.16 (t, *J* = 7.1 Hz, 1H), 7.21-7.22 (m, 1H), 7.26-7.28 (m, 1H), 7.32-7.33 (m, 1H). ^{13}C NMR (101 MHz, CDCl$_3$): δ = 58.6, 59.9, 121.4, 125.8, 126.1, 128.2, 137.1, 141.5. HRMS (ESI+, MeOH): calcd for C$_8$H$_9$OS [M - OH]$^+$: 153.0369, found: 153.0373.

(*E*)-2-(Furan-2-yl)-but-2-ene-1,4-diol, 88: Yellow oil. Yield: 84%, ^{1}H NMR (500 MHz, CDCl$_3$): δ = 2.34 (bs, 2H), 4.37 (d, *J* = 7.1 Hz, 2H), 4.47 (s, 2H), 6.32-6.53 (m, 3H), 7.38 (d, *J* = 1.8 Hz, 1H). ^{13}C NMR (125 MHz, CDCl$_3$): δ = 58.3, 58.5, 107.0, 111.6,

Chapter IV

126.0, 132.4, 142.4, 153.5. HRMS (ESI+, MeOH): calcd for $C_8H_{10}O_3Na$ [M + Na]⁺: 177.0522, found: 177.0514.

(Z)-2-(Pyridin-3-yl)-but-2-ene-1,4-diol, 89: Yellow oil. Yield: 61%, ¹H NMR (500 MHz, CDCl₃): δ = 4.36 (d, J = 6.7 Hz, 2H), 4.50 (s, 2H), 6.08 (t, J = 6.7 Hz, 1H), 7.22 (dd, J = 4.7; 7.9 Hz, 1H), 7.75 (dt, J = 1.9; 7.9 Hz, 1H), 8.41 (dd, J = 1.6; 5.0 Hz, 1H), 8.60 (d, J = 2.3 Hz, 1H). ¹³C NMR (125 MHz, CDCl₃): δ = 58.6, 59.5, 123.5, 132.1, 134.3, 136.8, 139.1, 147.5, 148.2. HRMS (ESI+, MeOH): calcd for $C_9H_{12}NO_2$ [M + H]⁺: 166.0855, found: 166.0863.

(Z)-2-(m-Tolyl)-but-2-ene-1,4-diol, 90: Yellow oil. Yield: 76%, ¹H NMR (500 MHz, CDCl₃): δ = 2.35 (s, 3H), 2.60 (bs, 2H), 4.36 (d, J = 6.9 Hz, 2H), 4.55 (s, 2H), 6.08 (t, J = 6.9 Hz, 1H), 7.08-7.13 (m, 1H), 7.21-7.27 (m, 2H). ¹³C NMR (125 MHz, CDCl₃): δ = 21.6, 59.0, 60.4, 123.6, 127.3, 128.5, 128.6, 129.7, 138.3, 140.6, 142.9. HRMS (ESI+, MeOH): calcd for $C_{11}H_{14}O_2Na$ [M + Na]⁺: 201.0886, found: 201.0889.

(Z)-2-(3-Bromophenyl)-but-2-ene-1,4-diol, 91: Yellow oil. Yield: 81%, ¹H NMR (500 MHz, CDCl₃): δ = 2.85 (bs, 2H), 4.35 (d, J = 6.8 Hz, 2H), 4.50 (s, 2H), 6.08 (t, J = 6.8 Hz, 1H), 7.19 (t, J = 8.0 Hz, 1H), 7.35 (dd, J = 8.0; 1.9 Hz, 1H), 7.40 (dd, J = 8.0; 1.9 Hz, 1H), 7.58 (t, J = 1.9 Hz, 1H). ¹³C NMR (125 MHz, CDCl₃): δ = 58.9, 60.1, 122.8, 125.1, 129.6, 130.1, 130.8, 131.1, 141.4, 142.9. HRMS (ESI+, MeOH): calcd for $C_{10}H_{11}BrO_2Na$ [M + Na]⁺: 264.9835, found: 264.9826.

(Z)-2-(3-Chlorophenyl)-but-2-ene-1,4-diol, 92: Yellow oil. Yield: 79%, ¹H NMR (500 MHz, CDCl₃): δ = 2.33 (bs, 2H), 4.38 (d, J = 6.8 Hz, 2H), 4.53 (s, 2H), 6.11 (t, J = 6.8 Hz, 1H), 7.24-7.50 (m, 3H). ¹³C NMR (125 MHz, CDCl₃): δ = 59.0, 60.4, 124.7, 126.7, 127.8, 129.9, 131.0, 134.6, 141.7, 142.6. HRMS (ESI+, MeOH): calcd for $C_{10}H_{11}O_2ClNa$ [M + Na]⁺: 221.0340, found: 221.0334.

(Z)-2-(2-Fluorophenyl)-but-2-ene-1,4-diol, 93: Yellow oil. Yield: 55%, ¹H NMR (500 MHz, CDCl₃): δ = 4.42 (d, J = 6.7 Hz, 2H), 4.52 (s, 2H), 6.05 (t, J = 6.7 Hz, 1H), 7.00-7.16 (m, 2H), 7.23-7.35 (m, 2H). ¹⁹F NMR (500 MHz, CDCl₃): δ = -115.9. ¹³C NMR (101 MHz, CDCl₃): δ = 55.9, 61.1 (d, J = 4.2 Hz), 115.8 (d, J = 23.4 Hz), 124.4 (d,

Stereoselective Formation of (*Z*)-1,4-but-2-ene Diols using Water as a Nucleophile

J = 3.1 Hz), 129.1 (d, J = 14.6 Hz), 129.4 (d, J = 8.0 Hz), 130.5 (d, J = 4.3 Hz), 133.4 (d, J = 2.6 Hz), 139.0 (d, J = 2.1 Hz), 160.0 (d, J = 246.5 Hz). HRMS (ESI+, MeOH): calcd for $C_{10}H_{11}FO_2Na$ [M + Na]$^+$: 205.0635, found: 205.0625.

(*Z*)-2-(2-Bromophenyl)-but-2-ene-1,4-diol, 94: Yellow oil. Yield: 63%, ^{1}H NMR (500 MHz, CDCl$_3$): δ = 4.38 (d, J = 6.8 Hz, 2H), 4.52 (s, 2H), 6.10 (t, J = 6.8 Hz, 1H), 7.20 (t, J = 7.9 Hz, 1H), 7.36 (ddd, J = 1.1; 1.8; 7.8 Hz, 1H), 7.41 (ddd, J = 1.0; 1.9; 7.8 Hz, 1H), 7.59 (t, J = 1.9 Hz, 1H). ^{13}C NMR (101 MHz, CDCl$_3$): δ = 59.0, 60.3, 122.8, 125.1, 129.6, 130.2, 130.8, 131.1, 141.6, 142.9. HRMS (ESI+, MeOH): calcd for $C_{10}H_{11}BrO_2Na$ [M + Na]$^+$: 264.9835, found: 264.9842.

(*Z*)-2-(3,5-Dimethylphenyl)-but-2-ene-1,4-diol, 95: Yellow oil. Yield: 85%, ^{1}H NMR (500 MHz, CDCl$_3$): δ = 2.32 (s, 6H), 4.40 (d, J = 6.8 Hz, 2H), 4.57 (s, 2H), 6.09 (t, J = 6.8 Hz, 1H), 6.95 (dt, J = 0.8; 1.6 Hz, 2H), 7.06 (dt, J = 0.8; 1.6 Hz, 2H). ^{13}C NMR (101 MHz, CDCl$_3$): δ = 21.5, 59.2, 60.7, 124.4, 129.5, 129.6, 138.3, 140.5, 143.4. HRMS (ESI+, MeOH): calcd for $C_{12}H_{16}O_2Na$ [M + Na]$^+$: 215.1043, found: 215.1040.

(*Z*)-2-(3,4-Dichlorophenyl)-but-2-ene-1,4-diol, 96: Yellow oil. Yield: 73%, ^{1}H NMR (500 MHz, CDCl$_3$): δ = 2.73 (bs, 2H), 4.36 (d, J = 6.7 Hz, 2H), 4.49 (s, 2H), 6.10 (t, J = 6.7 Hz, 1H), 7.22-7.30 (m, 1H), 7.39 (d, J = 8.4 Hz, 1H), 7.50-7.57 (m, 1H). ^{13}C NMR (125 MHz, CDCl$_3$): δ = 58.9, 60.0, 124.1, 125.8, 128.5, 130.5, 131.3, 132.7, 140.8, 140.8. HRMS (ESI+, MeOH): calcd for $C_{10}H_{10}O_2Cl_2Na$ [M + Na]$^+$: 254.9950, found: 254.9940.

(*Z*)-2-(3-Bromo-4-fluorophenyl)-but-2-ene-1,4-diol, 97: Yellow oil. Yield: 83%, ^{1}H NMR (500 MHz, CDCl$_3$): δ = 4.33 (d, J = 6.7 Hz, 2H), 4.47 (s, 2H), 6.03 (td, J = 1.4; 6.8 Hz, 1H), 7.06 (td, J = 09; 8.4 Hz, 1H), 7.29-7.35 (m, 1H), 7.63 (dd, J = 2.3; 6.6 Hz, 1H). ^{19}F NMR (500 MHz, CDCl$_3$): δ = -109.1. ^{13}C NMR (101 MHz, CDCl$_3$): δ = 58.8, 60.1, 109.2 (d, J = 21.0 Hz), 116.5 (d, J = 22.3 Hz), 127.1 (d, J = 7.1 Hz), 130.8 (d, J = 1.4 Hz), 131.6, 138.4 (d, J = 3.8 Hz), 140.6, 158.7 (d, J = 248.2 Hz). HRMS (ESI-, MeOH): calcd for $C_{11}H_{11}FBrO_4$ (M+HCOO)$^-$: 304.9825, found: 304.9815.

Chapter IV

(*Z*)-2-(Naphthalen-2-yl)-but-2-ene-1,4-diol, 98: Yellow oil. Yield: 50%, ^{1}H NMR (400 MHz, CDCl$_3$): δ = 4.51 (d, *J* = 6.7 Hz, 2H), 4.59 (s, 2H), 5.99 (t, *J* = 6.6 Hz, 1H), 7.33-7.35 (m, 1H), 7.43-7.46 (m, 1H), 7.47-7.54 (m, 2H), 7.80-7.82 (m, 1H), 7.85-7.88 (m, 1H), 7.97-8.00 (m, 1H). ^{13}C NMR (101 MHz, CDCl$_3$): δ = 59.3, 62.7, 125.5, 125.6, 126.0, 126.1, 126.4, 128.1, 125.6, 131.5, 132.4, 133.9, 139.6, 143.2. HRMS (ESI+, MeOH): calcd for C$_{14}$H$_{14}$O$_2$Na [M + Na]$^+$: 237.0873, found: 237.0877.

(*Z*)-2-(6-Methoxy-naphthalen-2-yl)-but-2-ene-1,4-diol, 99: White solid. Yield: 73%, ^{1}H NMR (500 MHz, CDCl$_3$): δ = 3.93 (s, 3H), 4.46 (d, *J* = 6.8 Hz, 2H), 4.69 (s, 2H), 6.24 (t, *J* = 6.8 Hz, 1H), 7.08-7.20 (m, 2H), 7.56 (dd, *J* = 1.9; 7.6 Hz, 1H), 7.71 (d, *J* = 4.8 Hz, 1H), 7.73 (d, *J* = 5.0 Hz, 1H), 7.84 (d, *J* = 1.8 Hz, 1H). ^{13}C NMR (101 MHz, CDCl$_3$): δ = 55.4, 59.3, 60.6, 105.8, 119.3, 125.1, 125.2, 127.2, 129.0, 129.6, 129.8, 134.2, 135.5, 143.1, 158.1. HRMS (ESI+, MeOH): calcd for C$_{15}$H$_{16}$O$_3$Na [M + Na]$^+$: 267.0992, found: 267.0992.

(*Z*)-2-Phenyl-pent-2-ene-1,4-diol, 100: Yellow oil. Yield: 77%, ^{1}H NMR (400 MHz, CDCl$_3$): δ = 1.36 (d, *J* = 6.3 Hz, 3H), 2.60 (bs, 2H), 4.47 (d, *J* = 12.3 Hz, 1H), 4.64 (d, *J* = 12.6 Hz, 1H), 4.75-4.81 (m, 1H), 5.88 (d, *J* = 8.1 Hz, 1H), 7.26-7.36 (m, 3H), 7.41-7.44 (m, 2H). ^{13}C NMR (101 MHz, CDCl$_3$): δ = 23.9, 60.5, 64.5, 126.5, 127.8, 128.7, 135.5, 140.7, 141.0. HRMS (ESI+, MeOH): calcd for C$_{11}$H$_{14}$O$_2$Na [M + Na]$^+$: 201.0886, found: 201.0889.

(*Z*)-2-Methyl-3-phenyl-but-2-ene-1,4-diol, 101: Yellow oil. Yield: 48%, ^{1}H NMR (500 MHz, CDCl$_3$): δ = 1.74 (s, 3H), 4.32 (s, 2H), 4.43 (s, 2H), 7.19-7.21 (m, 2H), 7.25-7.28 (m, 1H), 7.34-7.37 (m, 2H). ^{13}C NMR (126 MHz, CDCl$_3$): δ = 19.4, 63.6, 63.8, 127.0, 128.5, 128.7, 136.4, 138.9, 141.4. HRMS (ESI+, MeOH): calcd for C$_{11}$H$_{14}$O$_2$Na [M + Na]$^+$: 201.0886, found: 201.0886.

2-Vinyl-but-2-ene-1,4-diol, 105: Yellow oil. Yield: 73%, mixture of isomers in a 72:28 *Z/E* ratio. ^{1}H NMR (500 MHz, CDCl$_3$, major isomer): δ = 2.96 (bs, 2H). 4.29 (d, *J* = 6.8 Hz, 2H), 4.34 (s, 2H), 5.14 (d, *J* = 10.9 Hz, 1H), 5.40 (d, *J* = 17.6 Hz, 1H), 5.84 (t, *J* = 7.0 Hz, 1H), 6.31 (dd, *J* = 10.9; 17.7 Hz, 1H). ^{13}C NMR (125 MHz, CDCl$_3$, major

Stereoselective Formation of (Z)-1,4-but-2-ene Diols using Water as a Nucleophile

isomer): δ = 56.9, 58.6, 114.3, 132.8, 138.1, 140.2. HRMS (ESI+, MeOH): calcd for $C_6H_{10}O_2Na$ [M + Na]$^+$: 137.0578, found: 137.0573.

Preparation and characterization of the compounds obtained in the control experiments and post-modification experiments.
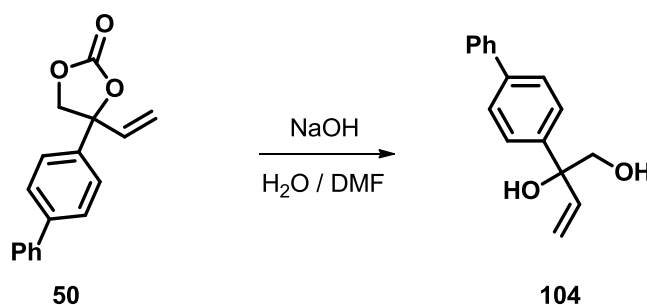
Scheme 4.10: Hydrolysis of carbonate **50** under basic conditions to obtain the 1,2-diol **104**.

The carbonate **50** was dissolved into a NaOH (5 equiv.) solution in H_2O/DMF. The mixture was left stirring for 8 h at room temperature. Thereafter the crude mixture was extracted with EtOAc (50 mL). Drying of the organic layer over sodium sulphate and concentration *in vacuo* afforded the 1,2-diol **104**.

2-([1,1'-Biphenyl]-4-yl)-but-3-ene-1,2-diol, 104: Yellow oil, Yield: 97%, ^{1}H NMR (500 MHz, CDCl$_3$): δ = 2.17 (bs, 1H), 3.01 (bs, 1H), 3.82-3.88 (m, 2H), 5.33 (dd, J = 1.1; 10.7 Hz, 1H), 5.45 (dd, J = 1.2; 17.3 Hz, 1H), 6.20 (dd, J = 10.7; 17.3 Hz, 1H), 7.58-7.61 (m, 4H), 7.34-7.37 (m, 1H), 7.43-7.46 (m, 2H), 7.53-7.55 (m, 2H). ^{13}C NMR (101 MHz, CDCl$_3$): δ = 69.5, 77.4, 115.8, 126.2, 127.2, 127.3, 127.5, 128.9, 140.5, 140.6, 140.7, 141.5. HRMS (ESI+, MeOH): calcd for $C_{16}H_{16}O_2Na$ [M + Na]$^+$: 263.1043, found: 263.1049.
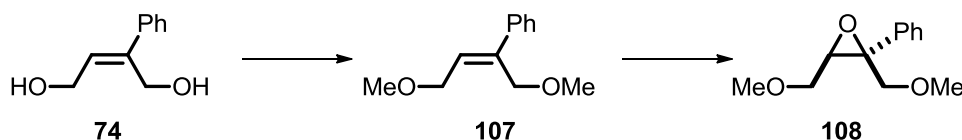
Scheme 4.11: General procedure to obtain the highly substituted *cis*-epoxide **108**.

Chapter IV

To a solution of compound **74** (60 mg, 0.36 mmol, 1 eq.) in dry DMF (2 mL) was added NaH (45 mg, 1.1 mmol, 3 eq.) at 0 ºC under Ar and stirred for 30 min. After that MeI (0.1 mL, 1.46 mmol, 4 eq.) was added dropwise and the reaction was stirred for another 18 h. The reaction was then quenched with a saturated solution of NH_4Cl and the organic phase was extracted with EtOAc (3 × 10 mL). The combined organic phases were dried over Na_2SO_4, concentrated under reduced pressure and purified by column chromatography (Hexane/EtOAc = 4:1 as eluent) to afford the protected compound **107** (68 mg, 98% yield) as a brown oil. The pure product **107** (40 mg, 0.208 mmol, 1 eq.) was dissolved in CH_2Cl_2 (2 mL) and *m*-CPBA (56 mg, 0.229 mmol, 1.1 eq) was added at 0 ºC. The resultant reaction mixture was stirred for 16 h and quenched by addition of a saturated aqueous solution of thiosulfate. The organic phase was extracted with CH_2Cl_2 (3 × 10 mL), and washed with saturated aqueous solution of sodium bicarbonate, and dried over anhydrous Na_2SO_4. Upon the removal of the solvent under reduced pressure, the crude of the desired product was afforded, which was purified by column chromatography (Hexane/EtOAc = 5:1 as eluent) to give the epoxide **108**.

(*Z*)-(1,4-Dimethoxybut-2-en-2-yl)-benzene, 107: Brown oil. Yield: 98%, ^{1}H NMR (400 MHz, $CDCl_3$): δ = 3.35 (s, 3H), 3.41 (s, 3H), 4.22 (d, *J* = 6.4 Hz, 2H), 4.35 (s, 2H), 6.09 (t, *J* = 6.4 Hz, 1H), 7.24-7.36 (m, 3H), 7.41-7.46 (m, 2H). ^{13}C NMR (101 MHz, $CDCl_3$): δ = 58.1, 58.4, 69.1, 69.6, 126.5, 127.6, 128.5, 129.6, 139.2, 140.8. HRMS (ESI+, MeOH): calcd for $C_{12}H_{16}O_2Na$ [M + Na]+: 215.1043, found: 215.1049.

(*cis*)-2,3-Bis(methoxymethyl)-2-phenyloxirane, 108: Yellow oil. Yield: 77%, ^{1}H NMR (400 MHz, $CDCl_3$): δ = 3.11 (dd, *J* = 3.8; 6.5 Hz, 1H), 3.38 (s, 3H), 3.45 (s, 3H), 3.60 (dd, *J* = 6.5; 11.5 Hz, 1H), 3.78 (d, *J* = 11.0 Hz, 1H), 3.85 (dd, *J* = 3.8; 11.5 Hz, 1H), 3.96 (d, *J* = 11.0 Hz, 1H), 3.27-3.47 (m, 5H). ^{13}C NMR (101 MHz, $CDCl_3$): δ = 59.2, 59.3, 61.4, 60.1, 70.7, 73.7, 125.8, 127.9, 128.4, 139.2. HRMS (ESI+, MeOH): calcd for $C_{12}H_{16}O_3Na$ [M + Na]+: 231.0997, found: 231.1002.

124

Stereoselective Formation of (*Z*)-1,4-but-2-ene Diols using Water as a Nucleophile
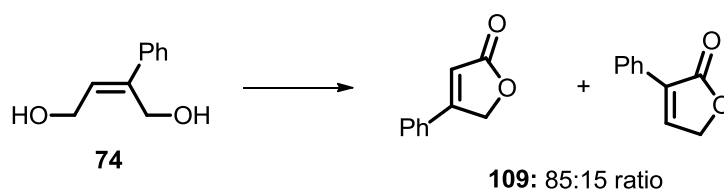
Scheme 4.12: General procedure to obtain functionalized lactone **109** starting from 1,4-diol **74**.

To a solution of diol **74** (33 mg, 0.2 mmol, 1 eq.) in CH$_3$CN (0.5 mL) were added CuI (4 mL, 0.01 mmol, 5.0 mol %), 2,2′-bipyridine (2 mg, 0.01 mmol, 5.0 mol %), *N*-methyl imidazole (2.0 mg, 0.020 mmol, 10 mol %) and 9-azabicyclo[3.3.1]nonane *N*-oxyl (0.28 mg, 0.0020 mmol, 1.0 mol %). The mixture was stirred for 2 h (the color of reaction changed to green when the reaction was finished). Water was added (1 mL) and the organic phase was extracted with CH$_2$Cl$_2$ (3 × 5 mL) and dried over anhydrous Na$_2$SO$_4$. The volatiles were removed under reduced pressure to give the desired lactone **109**.

4-Phenylfuranone, 109: Yellow oil. Yield: 97%, mixture of isomers in 85:15 ratio.
^{1}H NMR (500 MHz, CDCl$_3$ major isomer): δ = 5.23 (d, *J* = 1.8 Hz, 2H), 6.39 (t, *J* = 1.8 Hz, 1H), 7.47-7.54 (m, 5H). ^{13}C NMR (101 MHz, CDCl$_3$, major isomer): δ = 71.2, 113.3, 126.6, 129.5, 131.9, 144.3, 164.0, 174.0.
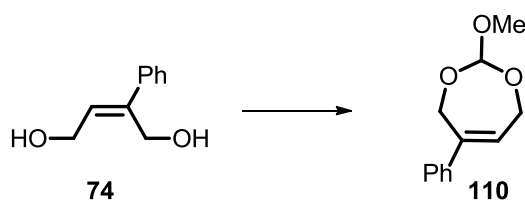
Scheme 4.13: Procedure to protect the (*Z*)-1,4-diol **74** with trimethyl orthoformate.

To a solution of diol **74** (33 mg, 0.2 mmol, 1 eq.) in DCM (1 mL) were added trimethyl orthoformate (44 μL, 0.40 mmol, 2.0 eq.) and racemic camphorsulfonic acid catalyst (0.46 mg, 0.0020 mmol, 1.0 mol %), and the mixture was stirred for 3 h. After that, the volatiles were removed under reduced pressure to afford the pure product **110**.

125

Chapter IV

2-Methoxy-5-phenyl-4,7-dihydro-1,3-dioxepine, 110: Brown oil. Yield: 93%, ^{1}H NMR (500 MHz, $CDCl_3$): δ = 3.45 (s, 3H), 4.23-4.32 (m, 1H), 4.50 (dd, *J* = 2.1; 15.8 Hz, 1H), 4.57-4.65 (m, 1H), 4.88 (dd, *J* = 2.1; 15.8 Hz, 1H), 5.47 (s, 1H), 5.72-5.95 (m, 1H), 7.26-7.34 (m, 5H). ^{13}C NMR (101 MHz, $CDCl_3$): δ = 53.8, 61.4, 64.1, 113.9, 126.2, 126.4, 127.7, 128.6, 139.7, 141.3.

Single crystal X-ray analysis of compound 81:

Single crystals of compound **81** (**Figure 4.1**) were obtained after slow evaporation of the solvent (mixture of $CHCl_3$ and hexane) in a vial. These were immersed under inert conditions in perfluoro-polyhether as protecting oil for further manipulation. Data Collection: measurements were made on a Bruker-Nonius diffractometer equipped with an APPEX II 4 K CCD area detector, a FR591 rotating anode with Mo Kα radiation, Montel mirrors and a Kryoflex low temperature device (*T* = −173ºC). Full-sphere data collection was used with ω and φ scans. Programs used: Data collection Apex2V2011.3 (Bruker-Nonius 2008), data reduction Saint+Version 7.60 A (Bruker AXS 2008) and absorption correction SADABS V. 2008−1 (2008). Structure Solution: SHELXTL Version 6.10 (Sheldrick, 2000) was used.[59] Structure Refinement: SHELXTL−97−UNIX VERSION. The supplementary crystallographic data for this crystal be obtained free of charge from The Cambridge Crystallographic Data Centre *via* www.ccdc.cam.ac.uk/ data_request/cif. CCDC-1465246.

4.6 References and notes

[1]   J. Hagen, *Industrial Catalysis: A Practical Approach*. Weinheim, Germany, Wiley-VCH, **2006**.
[2]   R. Noyori, *Angew. Chem. Int. Ed.*, **2002**, *41*, 2008.
[3]   W. S. Knowles, *Acc. Chem. Res.*, **1983**, *16*, 106.
[4]   R. Noyori, S. Hashiguchi, *Acc. Chem. Res.*, **1997**, *30*, 97.
[5]   D. Forster, Monsanto Company, *Adv. Organomet. Chem.,* **1979**, *17*, 255.
[6]   V. VanRheenen, R. C. Kelly, D. Y. Cha, Upjohn Company, *Tetrahedron. Lett.*, **1976**, *17*, 1973.
[7]   H. C. Kolb, M. S. VanNieuwenhze, K. B. Sharpless, *Chem. Rev.*, **1994**, *94*, 2483.
[8]   E. Bode, M. Wolberg, M. Müller, *Synthesis*, **2006**, 557.

126

Stereoselective Formation of (*Z*)-1,4-but-2-ene Diols using Water as a Nucleophile

[9]   H. R. Kricheldorf, J. Macromol. *Sci., Part C: Polym. Rev.*, **1997**, *37*, 599.

[10]   C. J. R. Bataille, T. J. Donohoe, *Chem. Soc. Rev.*, **2011**, *40*, 114.

[11]   H.-W. Engels, H.-G. Pirkl, R. Albers, R. W. Albach, J. Krause, A. Hoffmann, H. Casselmann, J. Dormish, *Angew. Chem. Int. Ed.*, **2013**, *52*, 9422.

[12]   E. N. Jacobsen, *Acc. Chem. Res.*, **2000**, *33*, 421.

[13]   M. Tokunaga, J. F. Larrow, F. Kakiuchi, E. N. Jacobsen, *Science*, **1997**, *277*, 936.

[14]   V. Laserna, G. Fiorani, C. J. Whiteoak, E. Martin, E. Escudero-Adán, A. W. Kleij, *Angew. Chem. Int. Ed.*, **2014**, *53*, 10416.

[15]   D. Craig, S. J. Gore, M. I. Lansdell, S. E. Lewis, A. V. W. Mayweg, A. J. P. White, *Chem. Commun.*, **2010**, *46*, 4991.

[16]   K. Klimovica, L. Grigorjeva, A. Maleckis, J. Popelis, A. Jirgensons, *Synlett.*, **2011**, 2849.

[17]   X. Xie, S. S. Stahl, *J. Am. Chem. Soc.*, **2015**, *137*, 3767.

[18]   M. J. Koh, R. K. M. Khan, S. Torker, M. Yu, M. S. Mikus, A. H. Hoveyda, *Nature,* **2015**, *517*, 181.

[19]   C. H. Oh, H. H. Jung, K. S. Kim, N. Kim, *Angew. Chem. Int. Ed.*, **2003**, *42*, 805.

[20]   A. K. Gupta, K. S. Kim; C. H. Oh, *Synlett.*, **2005**, 457.

[21]   A. Khan, L. Yang, J. Xu, L. Y. Jin, Y. J. Zhang, *Angew. Chem. Int. Ed.*, **2014**, *53*, 11257.

[22]   A. Khan, R. Zheng, Y. Kan, J. Ye, J. Xing, Y. J. Zhang, *Angew. Chem. Int. Ed.*, **2014**, *53*, 6439.

[23]   K. Ohmatsu, N. Imagawa, T. Ooi, *Nat. Chem.*, **2014**, *6*, 47.

[24]   T.-R. Li, F. Tan, L.-Q. Lu, Y. Wei, Y.-N. Wang, Y.-Y. Liu, Q.-Q. Yang, J.-R. Chen, D.-Q. Shi, W.-J. Xiao, *Nat. Commun.* **2014**, *5*, 5500.

[25]   W. Guo, L. Martínez-Rodríguez, R. Kuniyil, E. Martin, E. C. Escudero-Adán , F. Maseras, A. W. Kleij. *J. Am. Chem. Soc.*, **2016**, *138*, 11970.

[26]   G. Dong, P. Teo, Z. K. Wickens, R. H. Grubbs, *Science*, **2011**, *333*, 1609.

[27]   Q.-K. Kang, L. Wang, Q.-J. Liu, J.-F. Li, Y. Tang. *J. Am. Chem. Soc.*, **2015**, *137*, 14594.

[28]   M. Lee, M. S. Sanford, *J. Am. Chem. Soc.*, **2015**, *137*, 12796.

[29]   B. J. Lüssem, H. J. Gais, *J. Am. Chem. Soc.*, **2003**, *125*, 6066.

[30]   N. Kanbayashi, K. Onitsuka, *Angew. Chem. Int. Ed.*, **2011**, *50*, 5197.

[31]   M. Gärtner, S. Mader, K. Seehafer, G. Helmchen, *J. Am. Chem. Soc.*, **2011**, *133*, 2072.

[32]   C. C. Pattillo, I. I. Strambeanu, P. Calleja, N. A. Vermeulen, T. Mizuno, M. C. White, *J. Am. Chem. Soc.*, **2016**, *138*, 1265.

[33]   E. M. Stang, M. C. White, *Nat. Chem.*, **2009**, *1*, 547.

[34]   Note that if larger excess of H_2O was used, the reaction was completely shut down.

[35]   The yield for the screening studies was calculated by ^{1}H NMR yield using toluene (1 eq.) as internal standard.

[36]   F. Shibahara, T. Murai, *Asian J. Org. Chem.*, **2013**, *2*, 624.

[37]   A. B. Flynn, W. W. Ogilvie, *Chem. Rev.*, **2007**, *107*, 4698

[38]   B. M. Trost, S. Malhotra, W. H. Chan, *J. Am. Chem. Soc.*, **2011**, *133*, 7328.

[39]   X. Fang, H. Li, R. Jackstell, M. Beller, *J. Am. Chem. Soc.*, **2014**, *136*, 16039.

[40]   D. Banerjee, K. Junge, M. Beller, *Angew. Chem. Int. Ed.*, **2014**, *53*, 1630.

[41]   D. Banerjee, K. Junge, M. Beller, *Org. Chem. Front.*, **2014**, *1*, 368.

Chapter IV

[42] T. Ohshima, Y. Miyamoto, J. Ipposhi, Y. Nakahara, M. Utsunomiya, K. Mashima, *J. Am. Chem. Soc.*, **2009**, *131*, 14317.

[43] V. Pace, F. Martínez, M. Fernádez, J. V. Sinisterra, A. R. Alcántara, *Org. Lett.*, **2007**, *9*, 2661.

[44] For more details see: CCDC-1465246.

[45] C. Zhang, C. B. Santiago, J. M. Crawford, M. S. Sigman, *J. Am. Chem. Soc.*, **2015**, *137*, 15668.

[46] S. Zhu, N. Niljianskul, S. L. Buchwald, *Nat. Chem.*, **2016**, *8*, 144.

[47] M. Dischmann, T. Frassetto, M. A. Breuning, U. Koert, *Chem. Eur. J.*, **2014**, *20*, 11300.

[48] A. C. Fonseca, J. F. J. Coelho, M. H. Gil, P. N. Simoes, *Polym. Bull.*, **2014**, *71*, 3085.

[49] B. Gockel, S. S. Goh, E. J. Puttock, H. Baars, G. Chaubet, E. A. Anderson, *Org. Lett.*, **2014**, *16*, 4480.

[50] S. Taillemaud, N. Diercxsens, A. Gagnon, A. B. Charette, *Angew. Chem. Int. Ed.*, **2015**, *54*, 14108.

[51] Z. He, S. Kirchberg, R. Fröhlich, A. Studer, *Angew. Chem. Int. Ed.*, **2012**, *51*, 3699.

[52] M. Sekine, T, Hata, *J. Am. Chem. Soc.*, **1983**, *105*, 2044.

[53] J. J. Bozell, D. Miller, B. R. Hames, C. Loveless, *J. Org. Chem.*, **2001**, *66*, 3084.

[54] P. Le Gendre, T. Braun, C. Bruneau, P. H. Dixneuf, *J. Org. Chem.*, **1996**, *61*, 8453.

[55] C. Beattie, M. North, P. Villuendas, C. Young, *J. Org. Chem.*, **2013**, *78*, 419.

[56] S. Sarel, I. Levin, L. A. Pohoryles, *J. Chem. Soc.*, **1960**, 3079.

[57] B. M. Trost, M. L Crawley, *Chem. Rev.*, **2003**, *103*, 2921.

[58] N. Kuhl, F. Glorius, *Chem. Commun.*, **2011**, *47*, 573.

[59] G. M. Sheldrick, *SHELXTL Crystallographic System*, version 6.10; Bruker AXS, Inc.: Madison, WI, **2000**.

List of Relevant Compounds
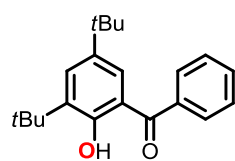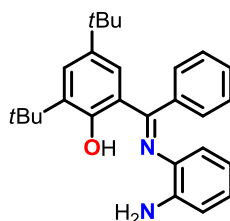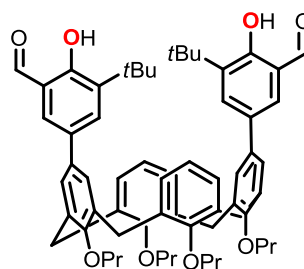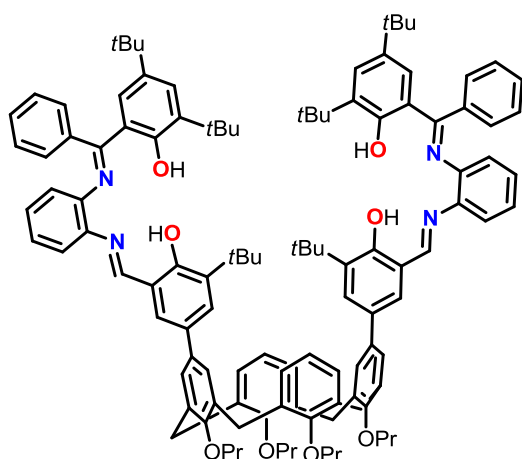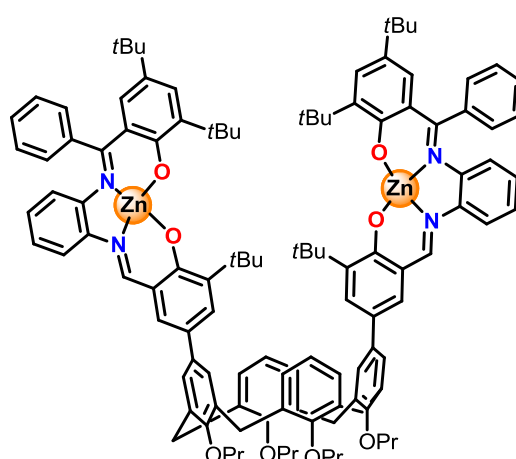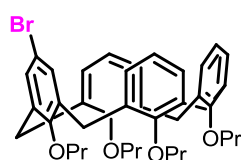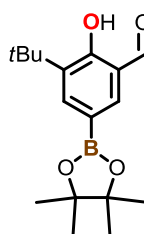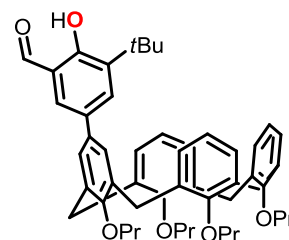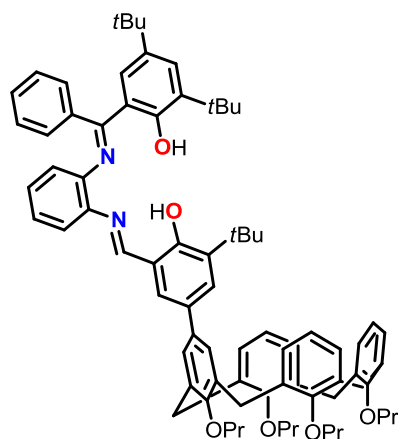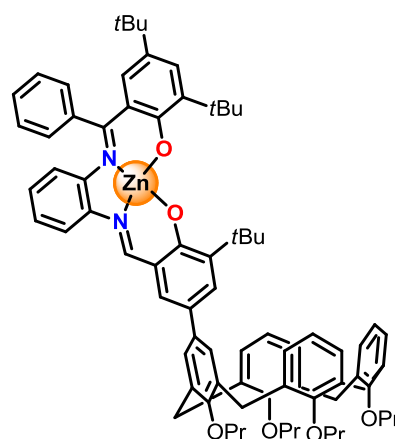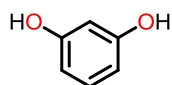
11
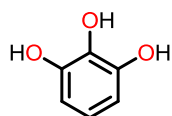
12
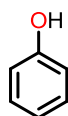
13

14

15

16

17

18

19

20

21

22

23

130

24

25

26

27

28

29

30

31

32

33

34

35

36

37

38

39

40

41

42

43

44

45

46

47
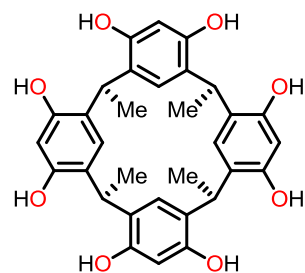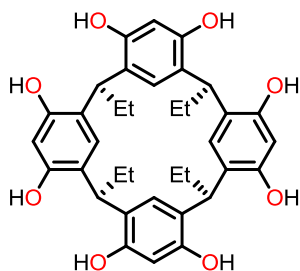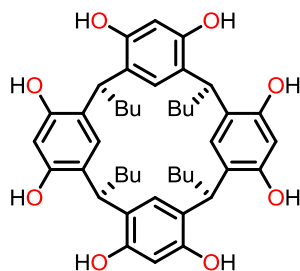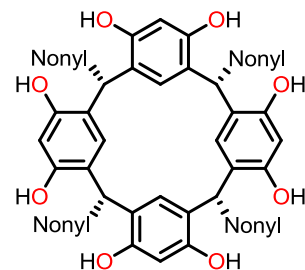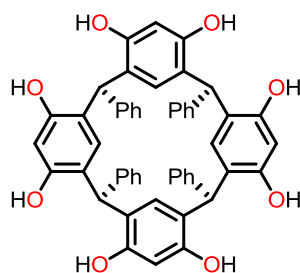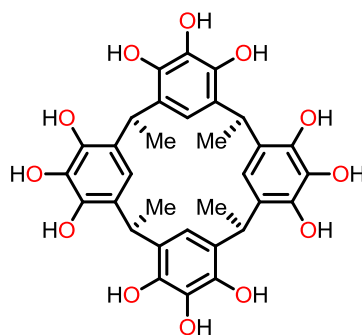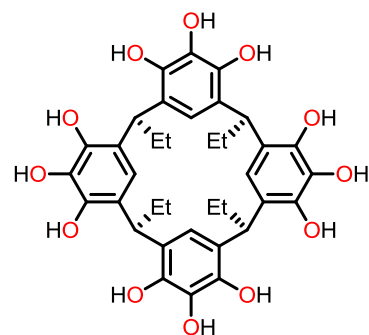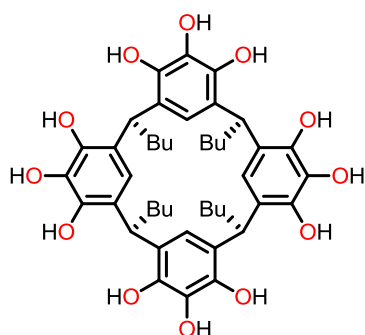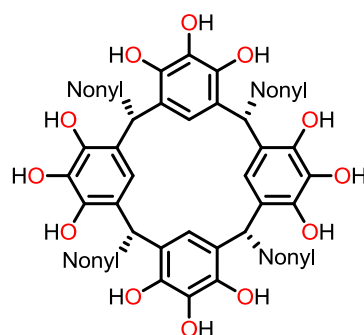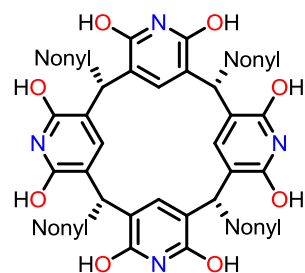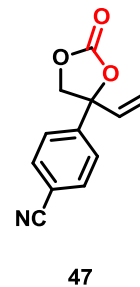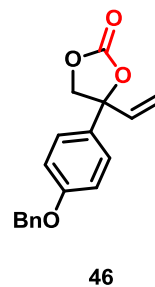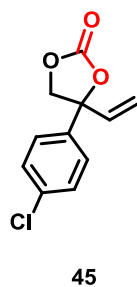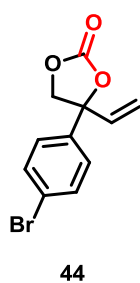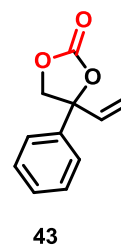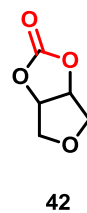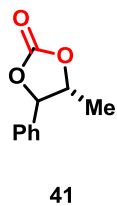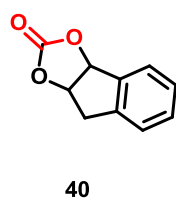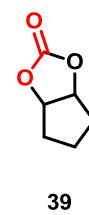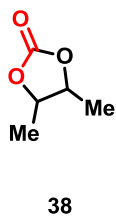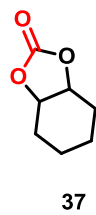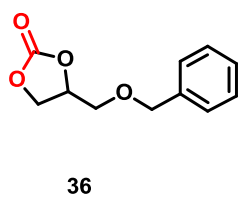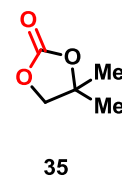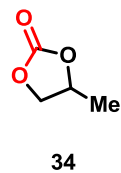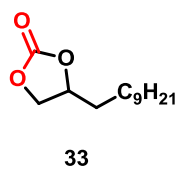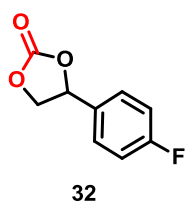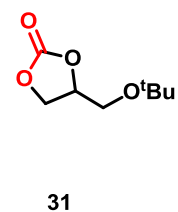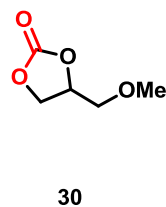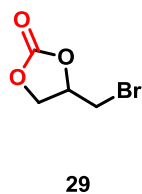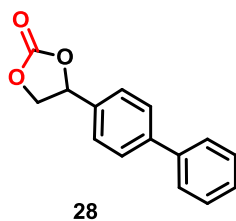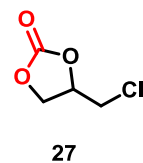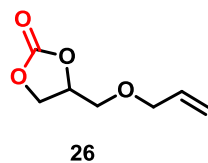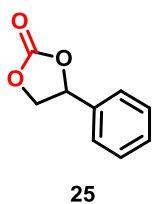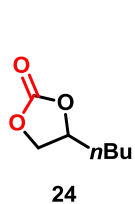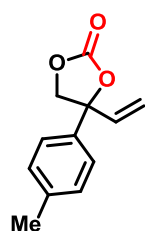
48
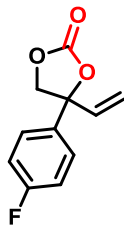
49
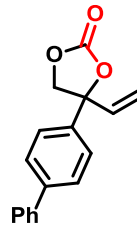
50
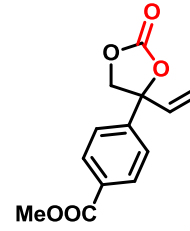
51
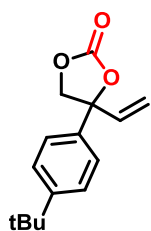
52
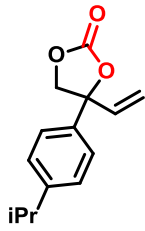
53
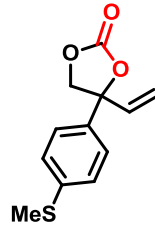
54
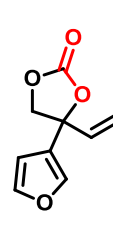
55
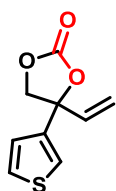
56
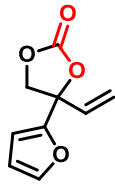
57

58

59

60

61

62

63

64

65

66

67

132

68

69

70

71

72

73

74

75

76

77

78

79

80

81

82

83

84

85

86

87

133

88

89

90

91

92

93

94

95

96

97

98

99

100

101

102

103

104

105

106

107

108

109

110

134
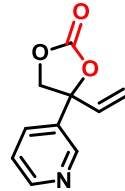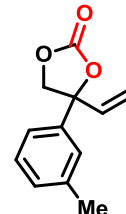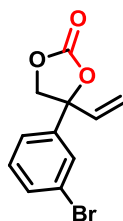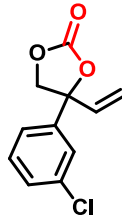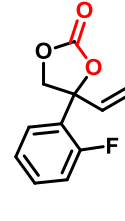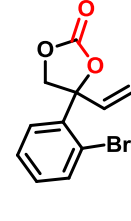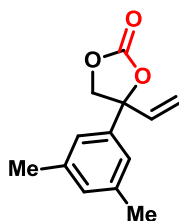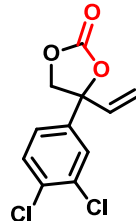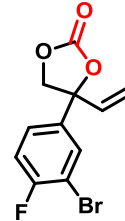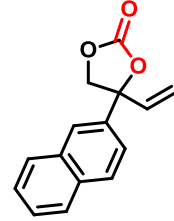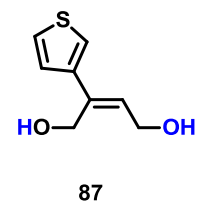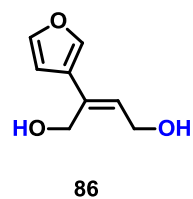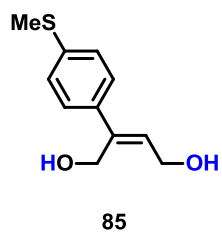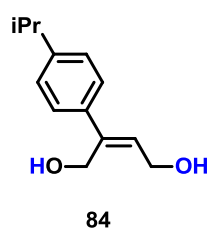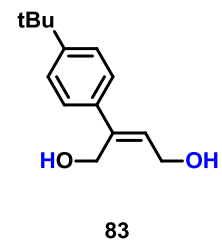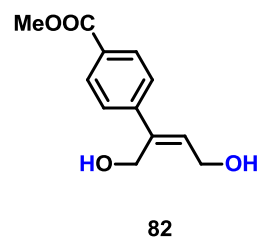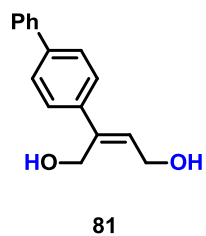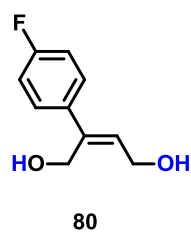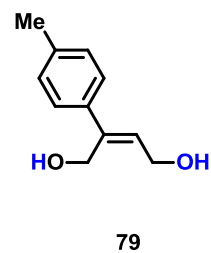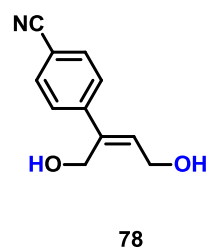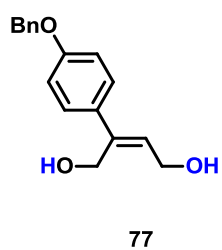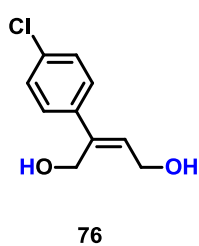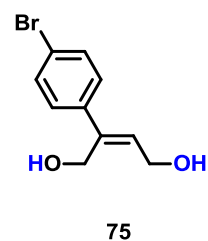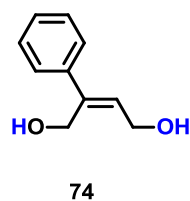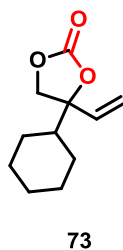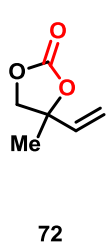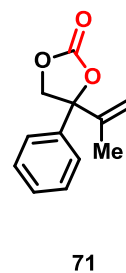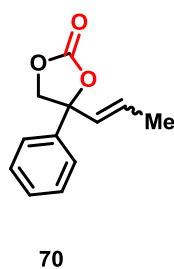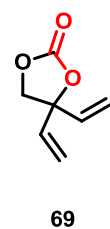
Conclusions

Supramolecular scaffolds with *inner* cavities, also called cavitands, can be used in material science for molecular recognition, and in organic synthesis as powerful catalysts. The cavitand scaffold can be easily accessed and modulated by a condensation reaction of simple starting materials. After functionalization of the *upper* and *lower* rims of the cavitand, the affinity constant can be tuned in order to bind a specific substrate. These processes are controlled by weak supramolecular interactions (such as metal coordination or hydrogen bonds), and the cavitand scaffolds often form aggregates through self-assembly processes.
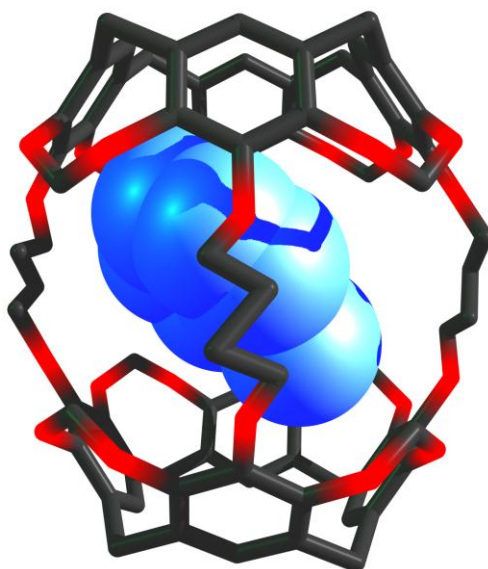
Figure 1: A carcerand scaffold encapsulating a solvent (toluene) molecule.

Interested by the use of molecular containers as hosts towards enantio-selective molecular recognition, a calix[4]arene (**5**; chapter 2, see also **Figure 2**) was designed having two co-facial zinc(salphen) units which have high affinit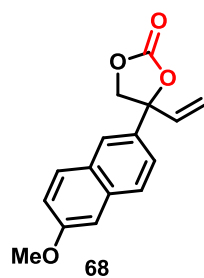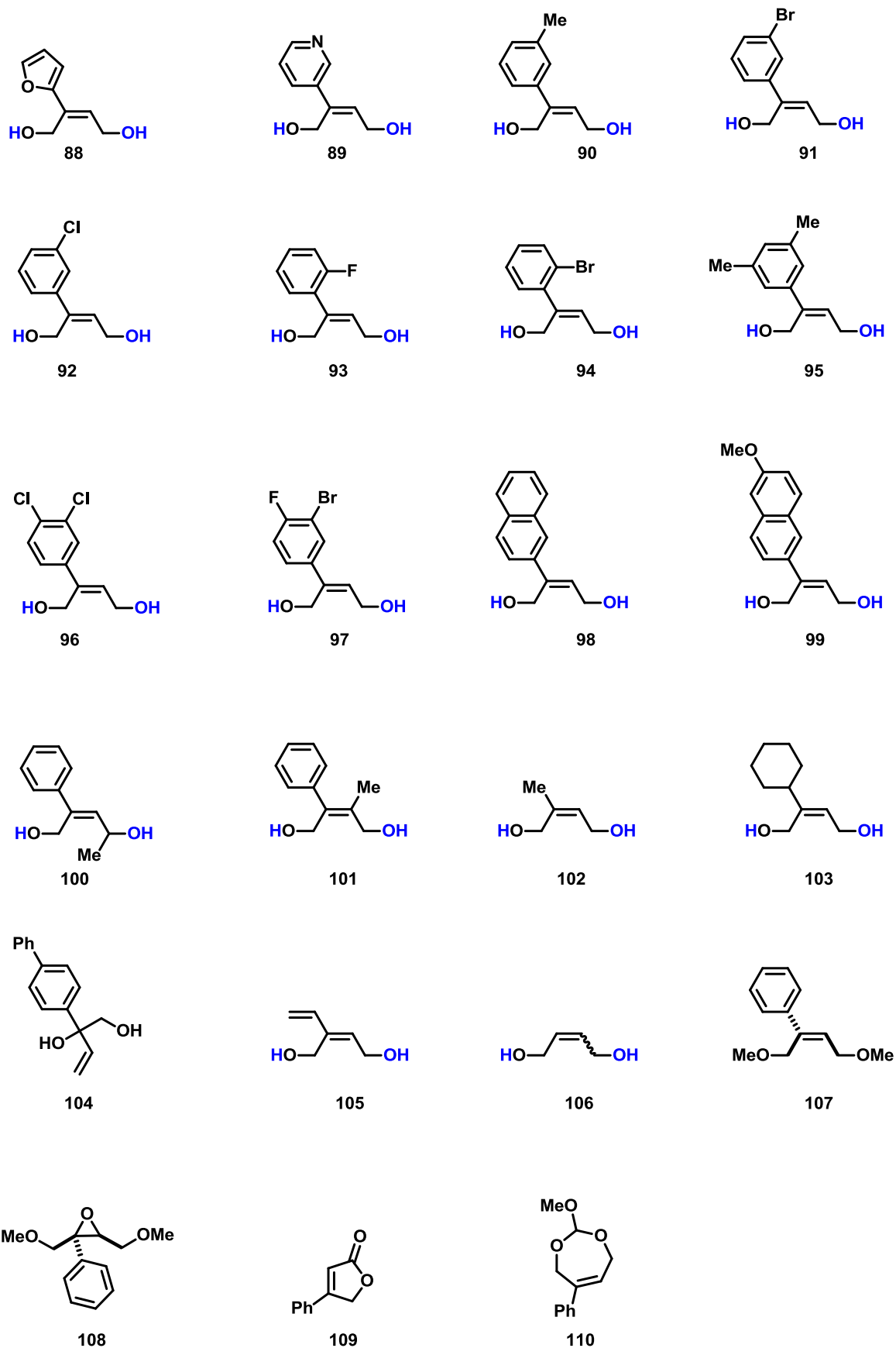y to bind small molecules containing nitrogen donor atoms. The structure was designed in such a way to avoid undesired competitive self-assembly processes that could compete with the interaction of the desired guest in the *inner* cavity. This host–guest system presents a unique and unexpected binding motif where two molecules of the calix[4]arene host bind one diamine guest molecule to form

an encapsulated system with effective chirality transfer from the chiral diamine to the pro-chiral calix[4]arene structure, as was confirmed by CD spectroscopy. This host–guest system presents high stability (more than 40 equivalents of the chiral diamine are required to break the capsule; the 2:1 binding $K_{2,1}$ constant was determined at $1.59 \pm 0.14 \times 10^{11}$ M^{-2}) and prospectively allows for the recognition of a series of chiral diamines, their absolute configuration and their enantiomeric excess at low concentration.
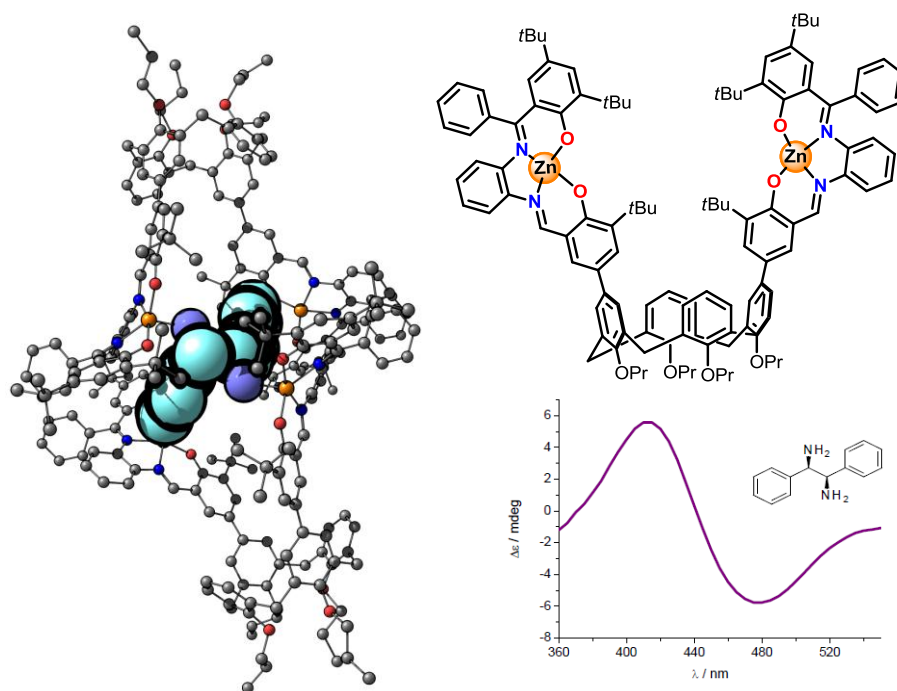
Figure 2: (Left) Encapsulation of the diamine by two calix[4]arenes **5**; (right) design of the calix[4]arene **5** host and the CD spectra recorded combining the calix[4]arene **5** and the chiral diamine (R,R)-(+)-1,2-diphenylethylenediamine.

The resorcin[4]arene scaffolds are based on the combination of polyphenol units forming a cavitand molecule. They can be easily obtained by a simple condensation reaction of the polyphenol and an aldehyde under acidic conditions. These molecules often form hexamers as a consequence of a self-assembly process through intermolecular hydrogen bonding interactions (**Figure 3**).
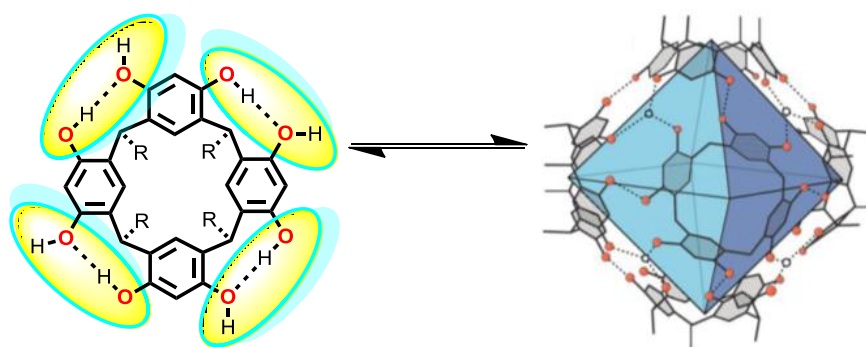
Figure 3: *Intra-* and *inter*-molecular hydrogen-bonding networks in the cavitand structures.

Polyphenols are known to catalyze the coupling of epoxides and CO_2 to obtain organic cyclic carbonates. The development of sustainable catalysts is an important factor in the field of CO_2 valorization, where useful organic molecules are formed using an industrial waste. By modifying the upper and the lower rims of the resorcin[4]arene moiety it was possible to optimize the catalytic activity for this CO_2 conversion reaction, and minimizing undesired and competitive cavitand self-assembly. Different organocatalysts based on such polyphenols were screened and compared with each other and their kinetic profiles showed that the resorcin[4]arene based polyphenols constitute the highest activity and thermal stability (at elevated temperatures; *cf.*, 50–80ºC) , which allows to obtain high TON and TOF values; apart from the attractive kinetic features, also an unusual scope in disubstituted carbonate products derived from internal epoxides was accomplished.
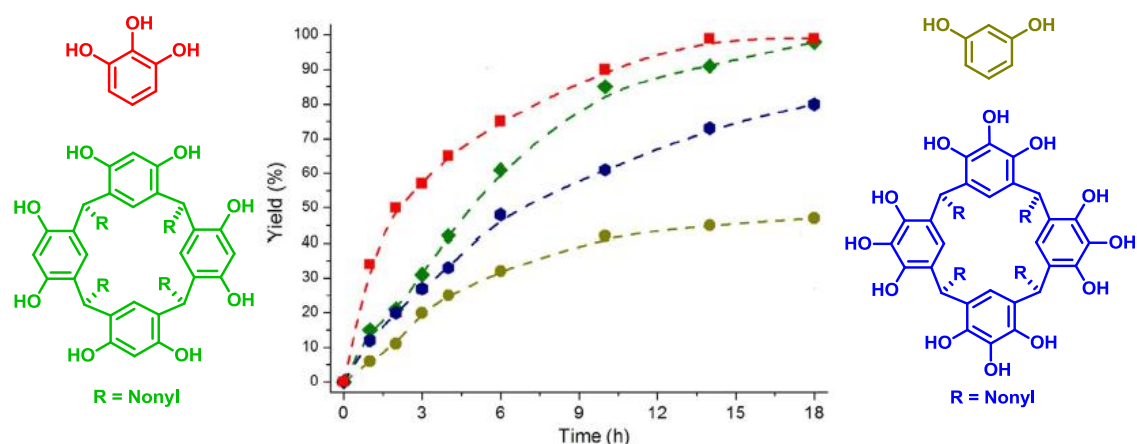
Figure 4: Kinetic profiles of pyrogallol **12** (**red**), resorcin[4]arene **17** (**green**), pyrogallol[4]arene **22** (**blue**) and resorcinol **11** (**gold**) at 50 ºC.

137

An interesting application of organic cyclic carbonates is the stereoselective formation of 1,4-but-2-ene-diols *via* a decarboxylative functionalization process. The synthesis of these 1,4-diols under excellent stereocontrol opens up a new opportunity in the field of polymer chemistry or total synthesis, where these kind of compounds are important building blocks. The reaction is catalyzed by a palladium precursor combined with a suitable diphosphine ligand (**DPEPhos**) using DMF as solvent, and no special precautions or additives are required. This reaction presents excellent functional group tolerance and exquisite stereocontrol (28 examples with *Z/E* ratios >99:1 in all cases). Control experiments confirm that the diol formation is indeed mediated by water present in the solvent. The excellent stereocontrol is ascribed to hyper-conjugation in a key intermediate forming a six-membered palladacycle, where the final stereo-information is already determined.
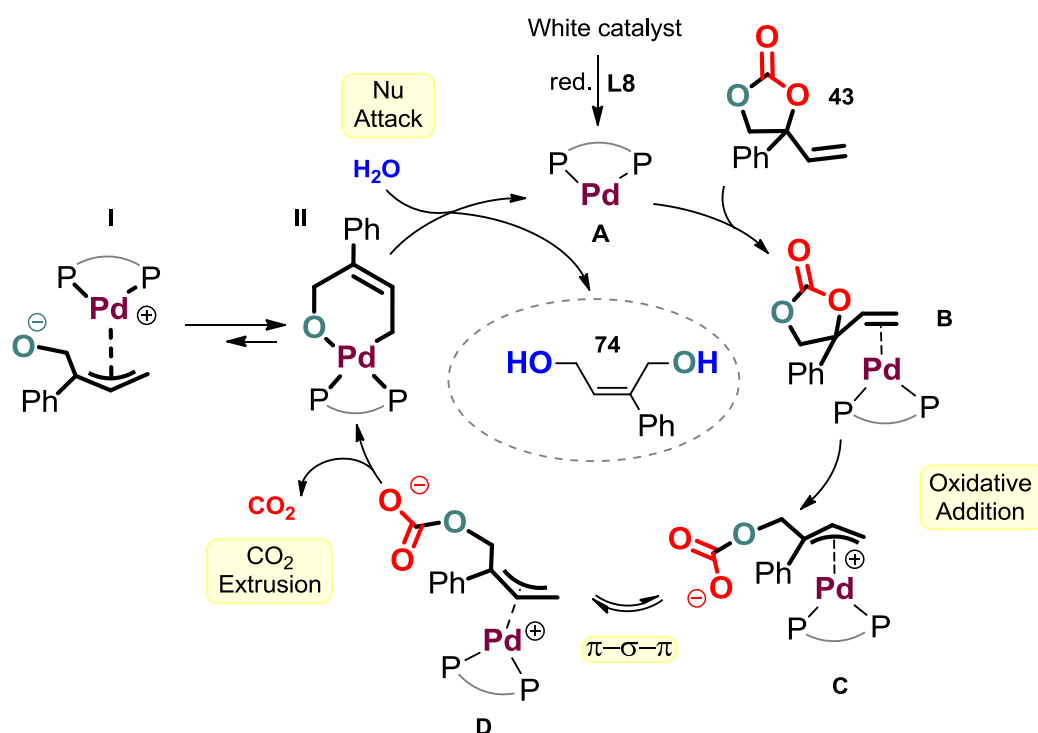
Figure 5: Proposed catalytic cycle for the formation of the (*Z*)-1,4-diol **74** through a palladium catalyzed decarboxylation of the carbonate following stereoselective hydration.

138

Acknowledgements

This is last part of the thesis and probably the most difficult to write. After four years working in ICIQ, I don´t know how many people and fantastic (surreal) moments I have lived. First of all, I want to thank Arjan for giving me the opportunity to do my PhD in his group, for all the chemistry support and for the (not related to chemistry) jokes that we shared. It was a pleasure being part of his group and I think that now a small piece of me is a little bit Dutch.

The *Lab 2.6* would not be the same without all the people who are or were working there with me. When I arrived in the lab only three people were there (Chris, Carmen and Leti) and after these years I had the opportunity to meet more than 20 excellent colleagues. Probably I will miss one or two of them, but please don´t be mad with me. I would like to thank Chris, Carmen, Giulia, Moritz, Kike, Aijie, Nicole, Rui, Tharun, Alex, and Claudia for making my days in the laboratory more relaxed, sometimes I felt like I was not working at all. I also want to thank "Tormenta", who during his internship pushed my patience until limits that I did not know that I had. I also would like to acknowledge Prof. Carles Bo and Dr. Nuno Bandeira for the nice collaboration we had that eventually led to a joint publication (chapter 2 of this thesis).

I think that there are people who deserve a distinctive mention, especially the four PhD students who started their thesis in the group (more or less) at the same time as me. Leti, Victor, Jeroen, Sergio and I shared uncountable problematic, funny and alcoholic experiences/dramas. I would say that during the last 4 years 20% of the time I hated all of you, especially Sergio (living together increases the hate ratio) but the other 80% of the time I loved you. Leti, as I know that your most favorite singer in the entire world is Taylor Swift, I selected this piece of one of her famous songs that I´m sure, you will recognize: "You are the best thing that's ever been mine". Sergio, I will remember you for all our awkward moments and I wish you the best for your future. Good luck in your next marathon race and take care of our home. Victor, right now you are not here, but we miss you every day, especially me, because fighting with you was more funny and enriching than with the others. Your value as a colleague and your capacity to organize our free-time are only

comparable with your ego. Jeroen, I have to thank you two important things: first of all, you were the chosen one who introduced the word "roundabout" into my deficient English vocabulary; and the second one and more important, you were the only one who read and checked all the mistakes of my first thesis draft. Thanks for all the effort, I think I cannot pay you back the same way. I hope all of you continue with our old traditions ("fideos night", making fun of stupid mistakes, "merienda time", sport training, trips) and you should create a new one in my honor.

The biggest achievements that I got from a chemistry point of view are due to the enormous contribution, help and guidance of Wusheng, who with his sacrifice, effort and ambition achieved all the objectives proposed, and this has led, inter alia, to the results presented in chapter 4.

Another person who contributed to the graphic design of the cover and figures was Pablo. Your help increased the artistic value of this research. I also want thank the people who don´t belong to the Kleij lab, but with whom I shared laughs and tears during these four years. Claudio, Noemi, Martin, Laura, Tania, Alba and Yolanda are the people responsible for my liver "disease", for the improvements in my personal relationships and also the chemistry tricks. I also would like to thank my previous research supervisors for sharing with me their time and enormous knowledge, especially Prof. Jesus Sanmartín and Prof. Kilian Muñiz who showed me the two sides of the same coin.

Por último pero no menos importante, quiero que agradecer a toda mi familia ya se encuentren arriba o abajo, a la izquierda o a la derecha del atlántico por todo el apoyo en los buenos y en los malos momentos. Sé que por muchas veces que os explique lo que hago os seguirá sonando a chino. Digna mención final, para todos mis amigos de La Guardia. La distancia es dura, pero por muy chungo-crudas que estén nuestras vidas, la culpa siempre será de Zidane. Espero que nunca os caséis.

- Luis -

140

Curriculum Vitae

Luis Martínez Rodríguez was born on June 18, **1987** in La Guardia (Galicia). He started studying chemistry at the University of Santiago de Compostela in October **2005** obtaining his BSc degree in June **2010** presenting his final research project in the field of organometallic chemistry in the group of Professor Vila. In July of **2011** he got his MSc degree in "*Advanced Chemistry*" at the same university. After that, he worked in different research groups under the supervision of Professor Jesus Sanmartin, Manuel Bermejo, Ana Maria Gonzalez and Kilian Muñiz to improve his synthetic experience. Finally he stared his PhD at the Institute of Chemical Research of Catalonia (ICIQ) in Tarragona under the supervision of Professor Arjan W. Kleij in **2013** where he performed the research that is described in this thesis. His PhD research was financially supported with a pre-doctoral fellowship from the ICIQ Foundation, and results described in this thesis have been communicated at 13th International Conference on Calixarenes (Giardini-Naxos, **2015**) and at Zing conferences "*Carbon Dioxide Catalysis*" (Albufeira, **2016**).

List of Publications

- *"Palladium-Catalyzed Regio- and Enantio-Selective Synthesis of Allylic Amines Featuring Quaternary Centers"*: A. Cai, W. Guo, L. Martínez-Rodríguez, A. W. Kleij. **2016**, *under evaluation*.

- "*N-Aryl Amide Formation via Organocatalytic Ring-Opening of Non-Strained Lactones using Aromatic Amines*": W. Guo, J. Enrique Gómez, L. Martínez-Rodríguez, A. W. Kleij. **2016**, *under evaluation*.

- "*Stereoselective and Versatile Preparation of Tri- and Tetra-Substituted Allylic Amine Scaffolds under Ambient Conditions*": W. Guo, L. Martínez-Rodríguez, R. Kuniyil, E. Martin, E. C. Escudero-Adán, F. Maseras, A. W. Kleij. *J. Am. Chem. Soc.*, **2016**, *138*, 11970-11978.

- "*Highly Efficient Catalytic Formation of (Z)-1,4-But-2-ene Diols using Water as a Nucleophile*": W. Guo,* L. Martínez-Rodríguez,* E. Martin, E. C. Escudero-Adán, A. W. Kleij. *Angew. Chem. Int. Ed.,* **2016**, *55*, 11037–11040. (*contributed equally). **Chapter 4** of this thesis.

- "*Iron Complex Based catalysts*: in Sustainable Catalysis: Volume 1: Catalysis by Non-Endangered Metals". L. Martínez-Rodríguez, G. Fiorani, C. Martín, A. W. Kleij, Ed. Michael North, Royal Society of Chemistry, **2016**, *13*, 373–406.

- "*Cavitand based Polyphenols as Highly Reactive Organocatalysts for the Coupling of Carbon Dioxide and Oxiranes*": L. Martínez-Rodríguez, J. Otalora Garmilla, A. W. Kleij, *ChemSusChem,* **2016**, *9*, 749–755. **Chapter 3** of this thesis.

- "*Highly Efficient Chirality Transfer from Diamines Encapsulated within a Self-Assembled Calixarene-Salen Host*": <u>L. Martínez-Rodríguez</u>, N. A. G. Bandeira, C. Bo, A. W. Kleij, *Chem. Eur. J.*, **2015**, *21*, 7144–7150. **Chapter 2** of this thesis.

- "*Copper-Mediated 1,4-Diamination of 1,3-Butadienes*": C. Martínez, <u>L. Martínez-Rodríguez</u>, J. Kirsch, E. C. Escudero-Adán, E. Martín, K. Muñiz, *Eur. J. Org. Chem.*, **2014**, *10*, 2017–2021.

- "*Structural Variety of Zinc and Copper Complexes based on a 2,3-disubstituted 1,2,3,4-tetrahydroquinazoline Ligand*": J. Sanmartin-Matalobos, C. Portela-Garcia, <u>L. Martínez-Rodríguez</u>, C. Gonzalez-Bello, E. Lence, A. M. Garcia-Deibe, M. Fondo, *Dalton Trans.*, **2012**, *41*, 6998–7004.

- "*Metal-Assisted Ring-Closing/Opening Process of a Chiral Tetrahydroquinazoline*": A. M. Garcia-Deibe, J. Sanmartin-Matalobos, C. Gonzalez-Bello, E. Lence, C. Portela-Garcia, <u>L. Martínez-Rodríguez</u>, M. Fondo, *Inorg. Chem.*, **2012**, *51*, 1278–1293.